

**Surface Functionalized Solid Waste Supported Catalysis:
Applications in Conventional and Microwave assisted
Acylation and Esterification Reactions**

A Thesis

Submitted for award of Ph.D. degree of
UNIVERSITY OF KOTA, KOTA

in the

Faculty of science

By

Priyanka Rajoriya



Under the supervision of

Prof. Ashu Rani

**Department of Pure and Applied Chemistry
UNIVERSITY OF KOTA, KOTA
KOTA (RAJ.)**

2017

Candidate's Declaration

I hereby certified that the work, which is being presented in the thesis entitled **“Surface Functionalized Solid Waste Supported Catalysis: Applications in Conventional and Microwave assisted Acylation and Esterification Reactions”** in partial fulfillment of the requirement for the award of the Degree of Doctor of Philosophy, carried under the supervision of **Professor Ashu Rani** and submitted to the **Department of Pure & Applied Chemistry, University of Kota, Kota** represent my idea in my own words and where others ideas or words have been included, have adequately cited and referenced the original sources. The work presented in this thesis has not been submitted elsewhere for the award of any other degree or diploma from any Institutions. I also declare that I have adhered to all principles of academic honesty and integrity and have not misrepresented or fabricated or falsified any idea/data/fact/source in my submission. I understand that any violation of the above will be cause for disciplinary action by the University and can also evoke penal action from the sources which have thus not been properly cited or from whom proper permission has not been taken when needed.

Date:

Priyanka Rajoriya

This is to certify that the above statement made by **Priyanka Rajoriya** (Enrolment No. **F-6 ()/Res/UOK/2013/18132-33**) is correct to the best of my knowledge.

Date:

Prof. Ashu Rani

Dean, Faculty of Science

Department of Pure & Applied Chemistry,

University of Kota, Kota

CERTIFICATE

I feel great pleasure in certifying that the thesis entitled “**Surface Functionalized Solid Waste Supported Catalysis: Applications in Conventional and Microwave assisted Acylation and Esterification Reactions**” by **Priyanka Rajoriya** under my guidance.

She has completed the following requirement as per Ph.D. regulations of the University:

- a) Course work as per the university rules.
- b) Residential requirement of the university (200 days).
- c) Regularly submitted annual progress reports.
- d) Presented his work in the departmental committee.
- e) Published/accepted minimum of one research paper in a referred research journal.

I recommend the submission of thesis.

Date:

Prof. Ashu Rani

Dean, P.G. Studies

**Department of Pure & Applied Chemistry,
University of Kota, Kota**



*Dedicated
To
My wonderful, supportive
supervisor and my loving
family*

ACKNOWLEDGMENT

Writing this thesis has been fascinating and extremely rewarding. I would like to thank a number of people who have contributed to the final result in many different ways:

*To commence with, I pay my obeisance to **GOD**, the almighty to have bestowed upon me good health, courage, inspiration, zeal and the light.*

*I avail myself of this pleasant opportunity in expressing profound gratitude to my research supervisor with respect and appreciation, **Prof. Ashu Rani** (Professor, Department of Pure and Applied Chemistry and Dean, P.G. Studies) for her constructive criticism, invaluable and simulating suggestions. Her remarkable scientific ability, hardworking, affectionate and amicable nature is always an inspiration for me towards achieving a good career. Without her untiring patience, constant encouragement, guidance and knowledge, this work would not have been possible. Not only did she direct my learning and research as a student, but she also played the very important role of a mentor. I want to thank her for the support, she has provided me, and for all the opportunities she has created during the last five years for me to grow as a professional and as a person. She has proved herself as a successful woman chemist and professor. I am sure that I will pass on the research values and the dreams that she had given to me.*

*I am grateful to **Prof. P.K. Dashora**, Vice Chancellor, **Sh. Omkar Singh**, **Prof. Madhusudhan Sharma**, former Vice Chancellor, **Dr. O.P. Rishi**, Director (Research), University of Kota, Kota for allowing me to carry on my research work in his respective institute.*

*With the deepest sense of gratitude, I would like to thank **Dr. Arun Kumar** (Lecturers, Government Collage, Kota) for her generous support, friendly nature, pleasant behavior. They inspired me in all the stages of my research work.*

*I would like to thank faculty members of Department of Pure & Applied Chemistry, University of Kota, **Dr. Niloo Chauhan, Dr. Bhawani Singh, Dr. Sweta Vyas, Mr. Ankit Sharma, Dr. Sushil Sharma, Dr. Shweta Saxena, Dr. Bhartiya Sharma** and official staff of department, Research section and Accounts section of University of Kota, for immediate help and timely cooperation.*

*I would like to acknowledge **Dr. Mukul Gupta, Dr. D.M. Phase, Er. V.K. Ahire** of **UGE-DAE Consortium for scientific Research**, Indore, CSMCRI, Bhavnagar, Gujarat and **MRC, MNIT**, Jaipur for providing instrumentation facilities for sample analysis. I would like to express my sincere thanks to UGC for giving me Junior and Senior Research Fellowship and Fly ash Mission Project, sanctioned to Prof. Ashu Rani for providing me analytical support in my department.*

*I am grateful to my ex-colleagues **Dr. Deepti, Dr. Anita, Dr. Shefali, Sakshi, Renu, Khushboo, Niharika** my lab-mates **Hariom, Swarnima, Niranjan, Rajesh, Kiran, Deepak and Honey** for their unconditional support and friendly atmosphere in the lab throughout my research career.*

My deepest love to my son Pralaksh who have been marooned of all my care & attention during my research, and motivated me and recharged me by the divine touch of her tender fingers whenever I had felt low.

*My biggest source of strength has been my family: My Parents, **Mr. O. P. Rajoriya and Mrs. Uma Rajoriya**. They are the one who really stood by me, bear my all mood swings, encouraged me and sustained my will power. Their love, care, affection and moral support have helped me to achieve this dream. They are always being there when I needed them most. Completion of Ph.D would have been not possible without their support. The encouragement and support of my loving brother and mentor, **Kapil Rajoriya and bhabhi Renu Rajoriya** have always been a powerful source of inspiration and energy. I am extremely indebted towards my respected **Dadiji and Naniji** for their endless love and blessings. . I would also like to express a debt of*

*gratitude to my badepapa **Mr. Mahesh Sharma** and badymummy **Mrs. Kunti Sharma** for their kind support, love and wishes.*

*I consider myself to be fortunate enough to have a caring and understanding husband **Rahul Sharma**, who always stood by my decisions, realize my dreams, encourage me to achieve my goals and helped me in resolving difficulties during thesis preparation. I also extend my thanks to my in-laws, **Mr. Devendra Sharma, Mrs. Gaytri Sharma** and my loving sister in-laws, **Monika and Meenakshi** for their moral support, constant encouragement and patience throughout the work.*

*Finally, I would like to thank everybody who was important to the realization of this thesis, as well as expressing my apology that I could not mention personally one by one. To all of them I say “**THANKS**” from the core of my heart.*

Priyanka Rajoriya

INDEX

Chapters	Page No.
Chapter 1: Introduction	1-55
1.1 Surface functionalization	1
1.2 Ionic liquids	18
1.3 Supported Ionic Liquid phase catalysis	22
1.4 Conventional and microwave heating	43
1.5 Scope of the work	46
1.6 References	47
Chapter2: Fly supported ionic liquid 1-methyl-3 -[(triethoxysilyl)propyl] imidazolium chloride: a heterogenized organocatalyst for a series of esterification reactions under microwave irradiations	56-93
Abstract	56
2.1 Introduction	57
2.2 Experimental	59
2.3 Results and Discussion	70
2.4 Catalytic activity	81
2.5 Proposed mechanism of ester formation over an acidic site	87
2.6 Catalyst Regeneration and Reusability	89
2.7 Conclusion	90
References	91
Chapter 3: Fly supported ionic liquid 1-butyl-3-methyl imidazolium chloride: a heterogenized organocatalyst for a series of esterification reactions under microwave irradiations	94-128
Abstract	94
3.1 Introduction	95
3.2 Experimental	97

3.3	Result and discussion	102
3.4	Catalytic activity	111
3.5	Proposed mechanism of ester formation	119
3.6	Regeneration and reusability of catalyst	121
3.7	Conclusion	122
	References	123

Chapter 4: Fly ash supported ionic liquid [bmim]PF₆: a heterogenized organocatalyst for a series of benzoylation reactions under microwave irradiations

129-158

Abstract		129
4.1	Introduction	130
4.2	Experimental	133
4.3	Result and discussion	137
4.4	Catalyst selection	144
4.5	Catalytic activity	145
4.6	Proposed mechanism	154
4.7	Regeneration and reusability of catalyst	155
4.8	Identification of products	156
4.9	Conclusion	156
4.10	References	157

Chapter 5: Fly ash supported ionic 3-sulfopropyl-1-(3-Propyl triethoxysilane) imidazolium hydrogen sulfate: a heterogenized organocatalyst for a series of Friedel Craft Acylation reactions under microwave irradiations

159-189

Abstract		159
5.1	Introduction	160
5.2	Experimental	163
5.3	Result and discussion	168
5.4	Catalytic activity	174
5.5	Mechanistic aspects	183
5.6	Regeneration and reusability of catalyst	184
5.7	Identification of products	185
5.8	Conclusion	186

Chapter 6: Fly ash supported ionic liquid N-(3-(trimethoxysilyl)propyl)-N-(propyl-3-sulfonate) ammonium hydrosulfate: a heterogenized organocatalyst for Friedel Craft Acylation reaction under microwave irradiations

		190-216
Abstract		190
6.1	Introduction	191
6.2	Experimental	193
6.3	Result and discussion	198
6.4	Catalytic performance	205
6.5	Mechanistic aspects	210
6.6	Regeneration and reusability of catalyst	211
6.7	Identification of product	213
6.8	Conclusion	214
6.9	References	214
	Annexure-I	217
	Annexure-II	220
	Publications	

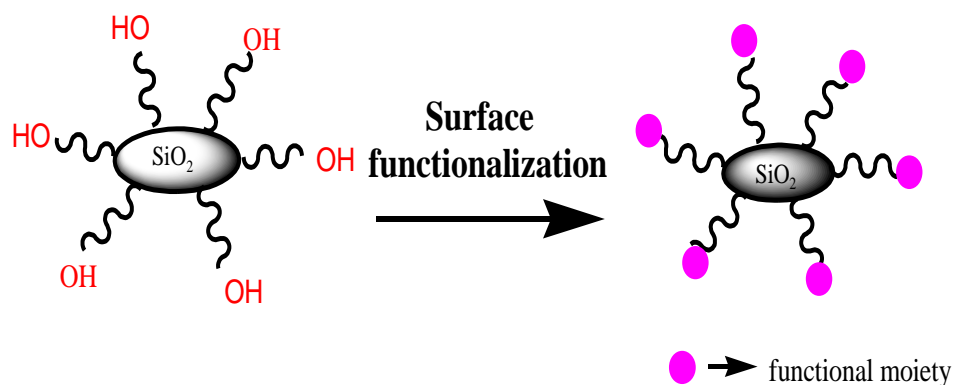


CHAPTER-1

Introduction

1.1 Surface functionalization

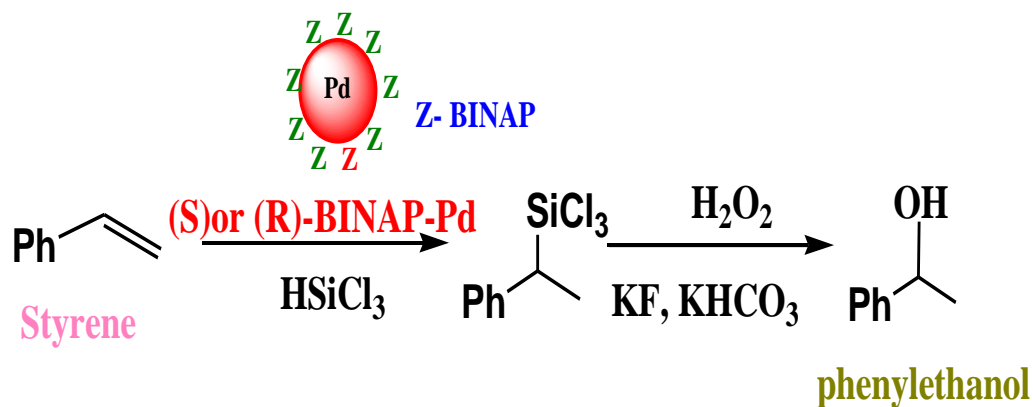
Surface functionalization of support materials is one of the innovative and effective concept of catalysis that can endow these materials with novel properties and transform them into valuable finished products. Functionalization is the process of adding new functions, features, capabilities, or properties to a material by changing the surface chemistry of the material. It is a fundamental technique used in chemical and material science, biological engineering, textile engineering, and nanotechnology. Functionalization is performed by attaching both inorganic and organic functional species to the surface of a material through chemical bonds or physical adsorption. Surface modification and functionalization can also be applied to a variety of different support materials for their target properties by designing appropriate chemical reactions. Various materials viz. nanoparticles[1-2], carbon nanotube[3-4], metal oxides[5-6], zeolites[7-8], polymers[9-10], rice husk[11] and fly ash[12-13] etc. have been reported as a catalytic system after suitable functionalization for industrially important organic synthesis. Scheme 1.1 represents the process of functionalization on silica silanols.



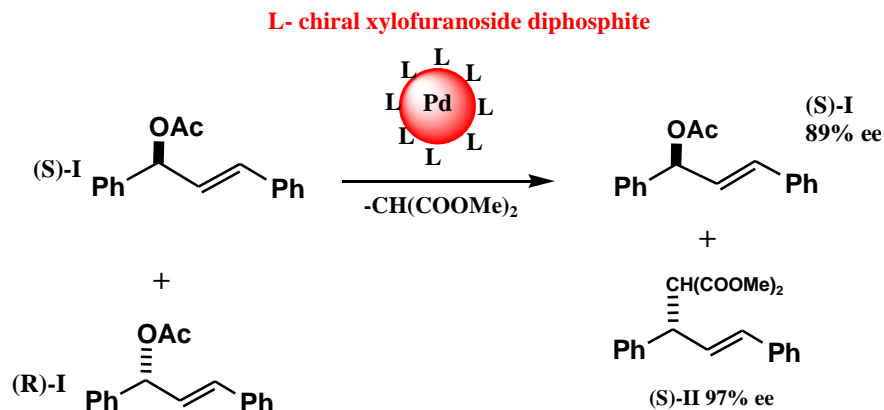
Below a brief overview of several functionalized materials and their applications are discussed.

1.1.1 Metal nanoparticles

Functionalized nanoparticles catalytic systems have been developed for various catalytic applications. Large number of functionalized nanoparticles have been reported as catalysts for organic synthesis in the recently literature. A facile synthesis of chiral palladium nanoparticles functionalized by BINAP(2,2'-bis(diphenylphosphino)-1,1'-binaphthyl ligands) was reported by Fujihara and Tamura[14]. These functionalized palladium nanoparticles were employed in different organic reactions such as Hydrosilylation of olefin, Suzuki–Miyaura coupling, Allylic alkylation(Scheme 1.2 and 1.3).



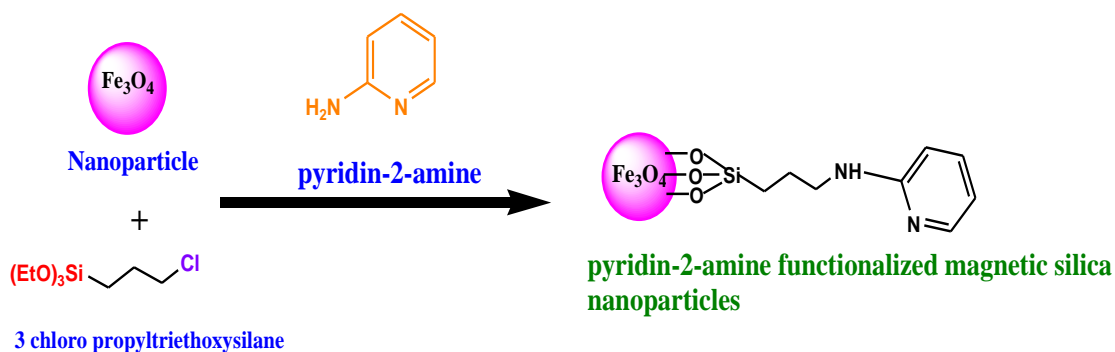
Scheme 1.2: Application of chirally modified Pd nanoparticles in the asymmetric hydrosilylation of styrene.



rac-3-acetoxy-1,3-diphenyl-1-propene

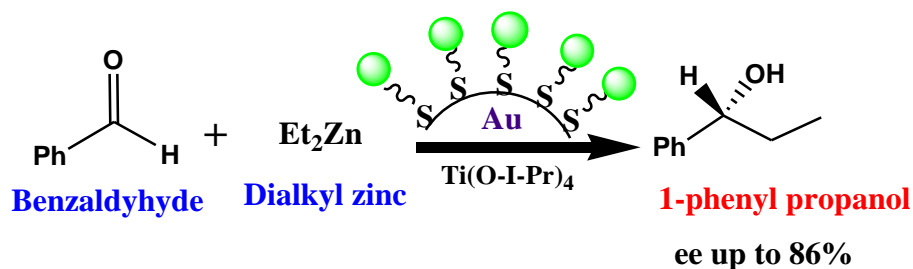
Scheme 1.3: Chiral Pd nanoparticle catalyzed asymmetric allylic alkylation

Pyridin-2-amine functionalized magnetic silica nanoparticles are used as the catalyst for synthesis of chromones under MW irradiation conditions as shown in Scheme 1.4 [15].



Scheme 1.4: Synthesis of pyridin-2-amine functionalized magnetic silica nanoparticles (MSN-AP)

Gold nanoparticle-supported 1,1'-bi-2-naphthol (BINOL) efficiently employed for the asymmetric alkylation of aldehydes with diethylzinc as given in Scheme 1.5[16].

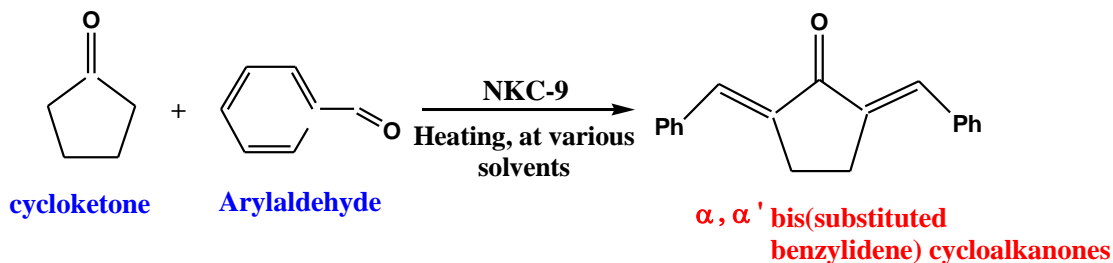


Scheme 1.5: Gold nanoparticle-supported BINOL catalyzed asymmetric alkylation of aldehydes with diethylzinc

1.1.2 Polymers

Polymeric materials have numerous applications due to their versatile characteristics such as high surface area, ability to uptake various solvents with different polarity, cost-effectiveness, and highly tailored production. A polymeric material can be functionalized by the addition of small moieties, oligomers, and even other polymers (grafting copolymers) onto the surface or interface and utilized as catalyst in heterogeneous catalysis.

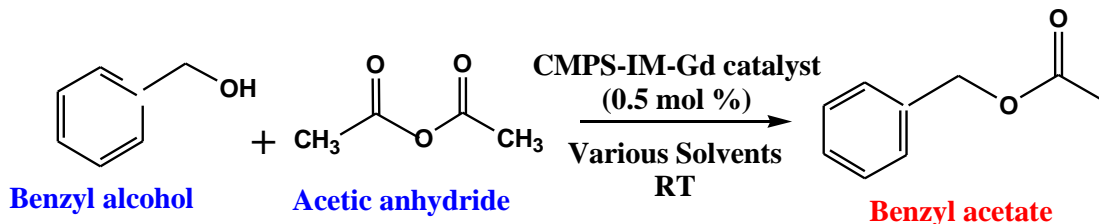
Polystyrene-divinyl benzene functionalized with sulphanilic acid efficiently was used as catalyst in microwave assisted synthesis of 4,5- dihydropyrano [3,2-c]chromenes under acidic conditions.[17]. Polymer-supported sulphonic acid (NKC-9) efficiently catalyzed the cross-aldol condensation of arylaldehydes and cycloketones to afford α, α' -bis(substituted benzylidene) cycloalkanones in good yields (Scheme 1.6) [18].



Scheme 1.6: reaction of cyclopentanone with benzaldehyde over NKC-9

New materials have been obtained from aluminium or copper salts of tungstophosphoric and tungstosilicic acids immobilized in a polymeric blend prepared with polyvinyl alcohol and polyethylene glycol by the freeze-thawing

method. Their catalytic activities were investigated for acylation of anisole [19]. A polymer-supported gadolinium triflate (CMPS-IM-Gd) catalyst was synthesized from chloromethyl polystyrene (CMPS) resin using a simple and convenient procedure. This catalyst was used as an efficient Lewis acid catalyst for the acetylation of various alcohols and phenols with acetic anhydride, affording high yields under mild conditions as shown in Scheme 1.7[20].

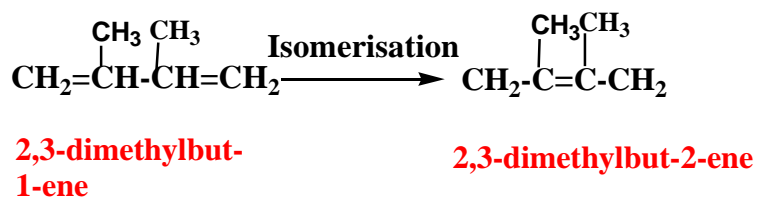


Scheme 1.7: Acetylation of benzyl alcohol with acetic anhydride over CMPS-IM-Gd catalyst

1.1.3 Metal oxides

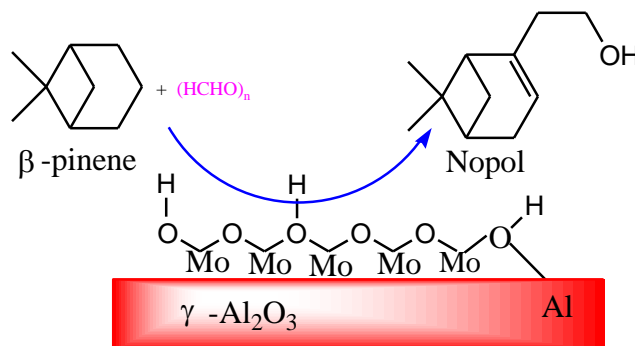
Different functionalized metal oxides are recognized as industrially important catalysts for numerous chemical processes. These catalysts consist of highly dispersed surface metal oxide species, catalytic active sites- anchored to the underlying oxide support.

Alumina (Al_2O_3) is a commonly-used ceramic support, and its hydroxylated surface is attractive for anchoring or grafting active species for either gas separation or heterogeneous catalysis [21]. KF loaded on alumina heated under vacuum at 673 K ($\text{KF}/\text{Al}_2\text{O}_3$) quantitatively gave benzyloxytriethylsilane by addition of triethylsilane to benzaldehyde at 303 K in *N,N*-dimethylformamide (DMF)[22]. The isomerisation olefinic amines were carried out in a quartz reactor using $\text{KNH}_2/\text{Al}_2\text{O}_3$ as the catalyst. Alumina/ NaOH/Na shows also a very high catalytic activity for the isomerization of 2,3-dimethylbut-1-ene to 2,3-dimethylbut-2-ene, which is usable as an intermediate material for synthetic parathyroid(Scheme 1.8). A 94% yield was obtained in 3 h at 293 K[23].



Scheme 1.8: Isomerization of 2,3-dimethylbut-1-ene to 2,3-dimethylbut-2-ene

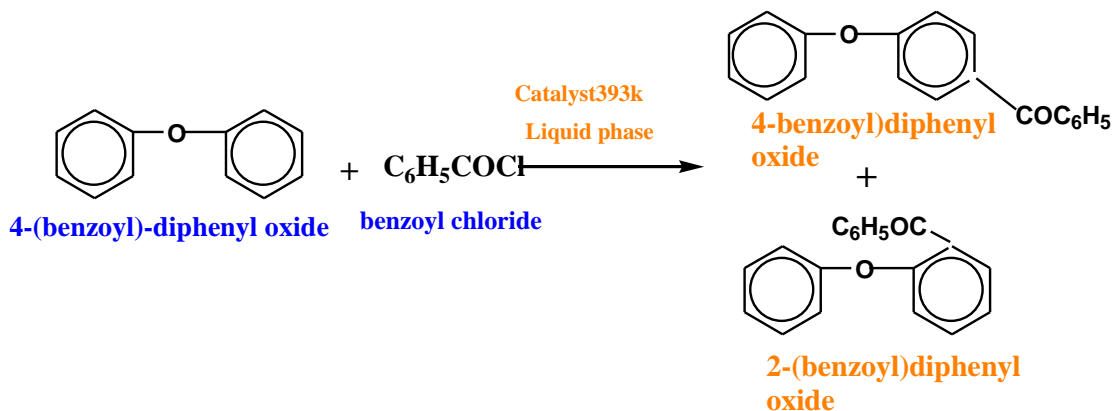
Phosphoric acid supported on alumina ($\text{H}_3\text{PO}_4/\text{Al}_2\text{O}_3$) is found to be an efficient catalyst for the three-component condensation reaction of β -naphthol, aromatic aldehydes and amides or carbamates to afford the corresponding α -amidoalkyl- β -naphthols, α -carbamato-alkyl- β -naphthols under solvent-free conditions as shown in Scheme[24]. The acidic properties of alumina-supported niobium oxide ($\text{Nb}_2\text{O}_5/\text{Al}_2\text{O}_3$) calcined at high temperatures, with Nb_2O_5 loadings of 5–30 wt % as Nb_2O_5 , were investigated for acid-catalyzed reactions (benzylation of anisole, cumene cracking, and isomerization of α -pinene) Prins condensation of β -pinene with paraformaldehyde was carried out over $\text{MoO}_x/\gamma\text{-Al}_2\text{O}_3$ catalyst in liquid phase. $\text{MoO}_x/\gamma\text{-Al}_2\text{O}_3$ catalysts were synthesized by impregnation method as given in Scheme 1.9[25].



Scheme 1.9: $\text{MoO}_x/\gamma\text{-Al}_2\text{O}_3$ catalysts catalyzed Prins condensation of β -pinene with paraformaldehyde

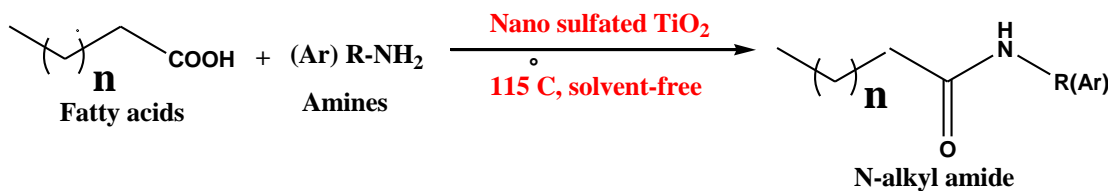
Functionalization of alumina surface with alkaline earth metal oxides was carried out, using the polymeric precursor method. the transesterification reaction of babassu oil with methanol was successfully carried out using the modified alumina as a catalyst.[26]. Ni catalysts supported on La, Sm and Ce oxides were utilized in oxidative transformation of methane.[27]. Heterogeneous base catalysts

(NaOH/Al₂O₃, K/ TiO₂, CaMgO and CaZnO) were used as catalysts for the production of biodiesel from edible palm and non-edible Jatropha oils.[28]. Liquid phase benzoylation of diphenyl oxide (DPO) to 4-(benzoyl)-diphenyl oxide (p-isomer) with benzoyl chloride (BC) is reported with 12-tungstophosphoric acid supported on zirconia (TPA/ZrO₂) as the catalyst(Scheme 1.10)[29].



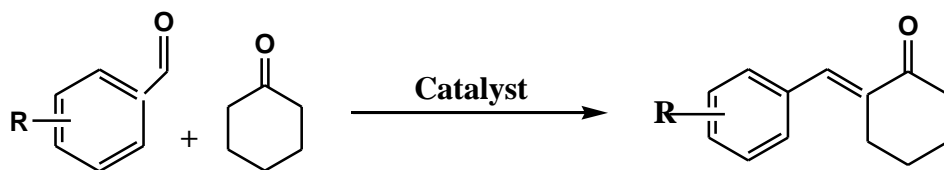
Scheme 1.10: Prins condensation of β -pinene with paraformaldehyde over zirconia (TPA/ZrO₂) with 12-tungstophosphoric acid catalyst

Nanoparticles showed high catalytic activity in direct amidation of fatty acids as well as benzoic acids with various amines under solvent-free conditions(Scheme 1.11)[30].



Scheme 1.11: Nanosulphated TiO₂ catalyzed amidation of fatty acids

A highly efficient and stable solid-base catalyst for Aldol condensation was prepared by modifying commercial CaO with benzyl bromide in a simple way. It was found that modified CaO can effectively catalyse the Aldol condensation of cyclohexanone and benzaldehyde, as well as various benzaldehydes, to produce 2-benzylidenecyclohexanone with a good selectivity and high yield as shown in Scheme 1.12 [31].



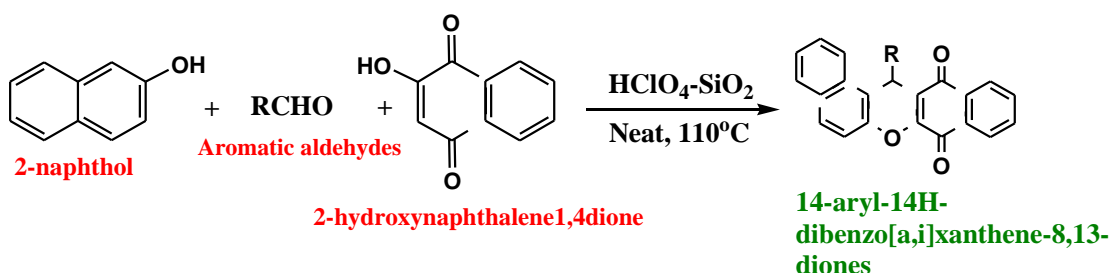
Benzaldehyde Cyclohexanone

2-benzylidenecyclohexanone

Scheme 1.12: Modified CaO catalyzed Aldol condensation of cyclohexanone and benzaldehyde

Many solid super base catalyst such as $\text{KNO}_3/\text{Al}_2\text{O}_3$ [32], $\text{KNO}_3/\text{ZrO}_2$ [33], $\text{KF}/\text{Al}_2\text{O}_3$ [34], $\text{K}_2\text{CO}_3/\text{Al}_2\text{O}_3$ [35] have become highly important as they catalyze a number of organic reactions under mild conditions.

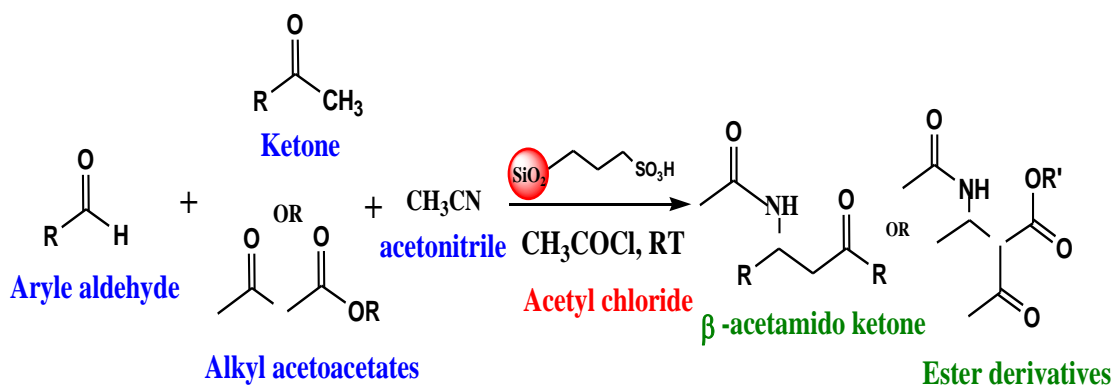
In recent years functionalized silica materials are gaining considerable interest due to their specific characteristic viz. high surface area, better selectivity, low toxicity, chemical inertness and unique pore system. Alkali metal (Li, Na, K and Cs) loaded silica has efficiently catalyzed vapour phase O-alkylation of phenol with methanol, ethanol, n-propanol and n-butanol.[36]. Silica supported perchloric acid as a highly efficient catalyst has been reported for condensation of β -naphthol with aromatic aldehydes and 2-hydroxynaphthalene-1,4-dione to afford the corresponding 14-aryl-14H-dibenzo[a,i]xanthene-8,13-diones in excellent yields under solvent free conditions(scheme 1.13).[37]



Scheme 1.13: Condensation of β -naphthol with aromatic aldehydes and 2-hydroxynaphthalene-1,4-dione over Silica supported perchloric acid

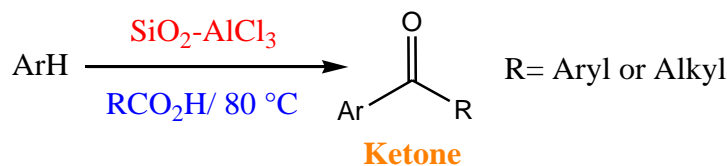
Silica-supported 12-molybdophosphoric acid catalysts have been proved to be a good catalyst for partial oxidation of methane to formaldehyde[38]. Silica supported

sulphonic acids have been efficiently catalyzed Friedel-Crafts acylation of anisole with acetic anhydride[39]. Silica-functionalized sulfonic acid (SFSA) efficiently catalysed one-pot multi-component condensation of enolizable ketones or alkyl acetoacetates with arylaldehydes, acetonitrile and acetyl chloride to afford the corresponding β -acetamido ketone or ester derivatives in high to excellent yields(scheme 1.14)[40].



Scheme 1.14: The synthesis of β -acetamido ketones/esters from enolizable ketones/alkyl acetoacetates, aldehydes, acetonitrile and acetyl chloride using SFSA

SiO_2 - AlCl_3 is also an effective and highly chemoselective catalyst for the acylation of aromatic compounds with carboxylic acids under mild reaction conditions (Scheme 1.15). [41]



Scheme 1.15: Acylation of arenes with carboxylic acids using SiO_2 - AlCl_3 .

1.1.4 Carbon nano tubes

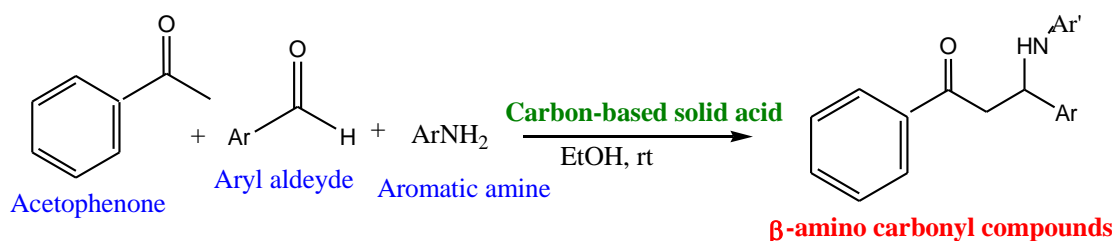
Carbon nanotubes (CNTs) have become the most attractive due to their unique physico-chemical and textural properties [42-44]. Oxidation treatments can introduce a variety of oxygenated functional groups upon the surface, which can subsequently

affect the interactions between CNTs and the active metal particles and thus perform the catalysis in reactions [45-47]. We prepared surface functionalized pristine CNTs with oxygen containing groups were synthesized by refluxing and oxidizing in concentrated HNO₃. This prepared high performance catalyst was used for oxidative dehydrogenation of butane.[48].

1.1.5 Activated carbon

Carbon materials as such are inert but certain functionality can exist or can be created on the surface. Active sites on the surface can be defects on the surface; surface groups containing heteroatoms (for example oxygen-, sulphur-, or nitrogen-containing surface sites); or metal particles added on the surface.

Sulfonated carbonaceous material useful as solid acid catalyst was prepared from lignosulfonate, a waste of the paper-making industry sulfite pulping. AC-SO₃H exhibited high catalytic activity in the esterification of cyclohexanecarboxylic acid with anhydrous ethanol.[49] Carbon based solid acid (CBSA), prepared by sulfation of naphthalene proved to be an effective and reusable catalyst [50] for synthesis of β-amino carbonyl compounds by one-pot three-component Mannich reaction of acetophenone, aromatic aldehydes and aromatic amines as described in Scheme[1.16]

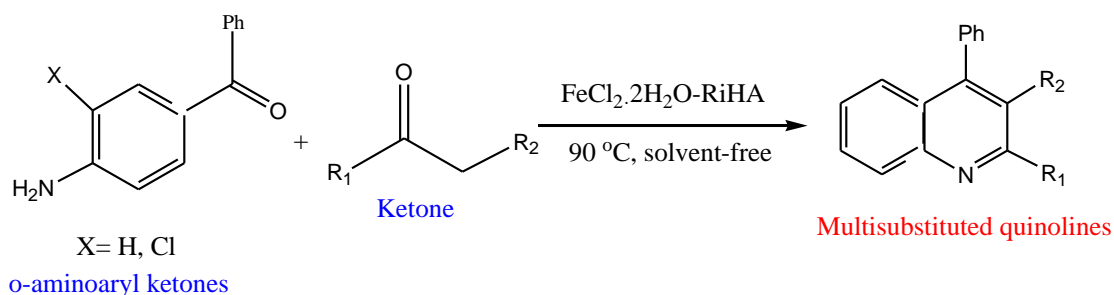


Scheme 1.16: Mannich reaction of acetophenone, aromatic aldehydes and aromatic amines over CBSA catalyst

Tungstophosphoric (TPA) and tungstosilicic acid (TSA) catalysts supported on carbon were studied. They were prepared by equilibrium and incipient wetness impregnation for isopropanol dehydration[51]

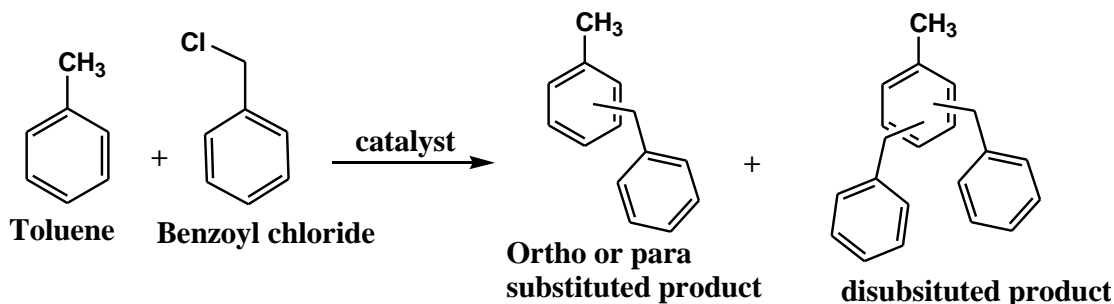
1.1.6 Rice husk

Rice husk (RH) is an agro-biomass removed during the refining of rice. RHA contains considerable amount of amorphous silica (up to 80%) and a small proportion of other metal oxide such as K_2O , Na_2O , and Fe_2O_3 [52]. The synthesis of the desired RH grafted oxo-vanadium complex involves prior functionalization of the RH support with amino-propyltrimethoxysilane (APTMS) followed by its reaction with salicylaldehyde to get an RH-functionalized Schiff base which subsequently reacted with vanadyl sulphate to get the targeted oxo-vanadium catalyst. The synthesized catalyst was found to be an efficient heterogeneous catalyst and afforded an excellent yield of corresponding N-oxides via oxidation of tertiary amines with hydrogen peroxide as an oxidant.[53]. RHA functionalized with $FeCl_2 \cdot 2H_2O$ have been efficiently used for catalyzing the synthesis of multisubstituted quinolines by the Friedländer heteroannulation of o-aminoaryl ketones with ketones or β -diketones under mild reaction conditions(Scheme 1.17).[54]



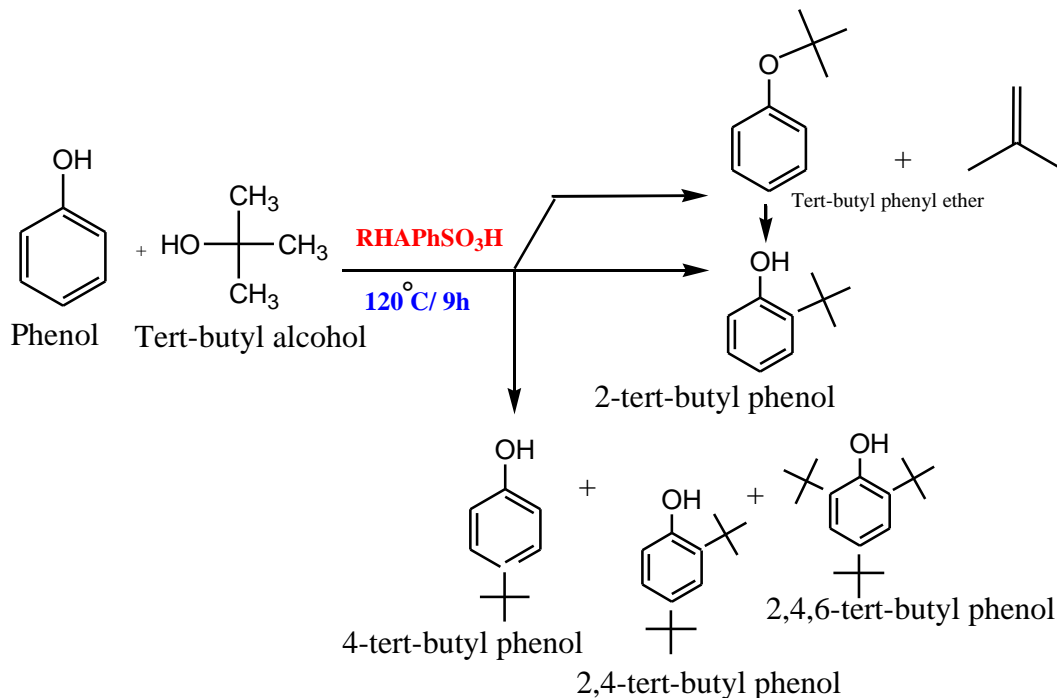
Scheme 1.17: Friedländer reaction catalyzed by $FeCl_2 \cdot 2H_2O$ -RHA.

Iron and 4-(methylamino)benzoic acid/RH-silica have been successfully investigated for benzylation reaction with toluene as given by Scheme 1.18 [55].



Scheme 1.18: Friedel-Craft reaction between toluene and benzyl chloride

Sulfanilic acid was immobilized onto rice husk ash via 3-(chloropropyl)triethoxy-silane to form an acidic solid catalyst denoted as RHAPhSO₃H. Bronsted acid sites of catalyst have been utilized in t-butylation of phenol(Scheme 1.19).[56]



Scheme 1.19 : Tert-butylation of phenol over RHAPhSO₃H.

The p-phenylenediamine (PDA) and dithiooxamide (DTO) were immobilized onto silica from rice husk ash (RHA) using 3-chloropropyltriethoxysilane (CPTES) to form a solid catalyst denoted as RHAPDA and RHADTO, respectively. The catalytic performance of RHAPDA and RHADTO was tested in the esterification of ethyl alcohol with acetic acid[57].

1.1.7 Fly ash

Fly ash (FA) comprised of the non-combustible mineral portion of coal consumed in a coal fueled power plant. Fly ash particles are glassy, spherical shaped “ball bearings” typically finer than cement particles that are collected from the combustion air-stream exiting the power plant. Fly ash is one of the residues generated in coal combustion facilities, and comprises the fine particles that rise with the flue gases. Fly ash is collected from the flue gases by using electrostatic precipitators (ESP) or in filter fabric collectors[58]. According to ASTM C618 12a [59], Standard chemical

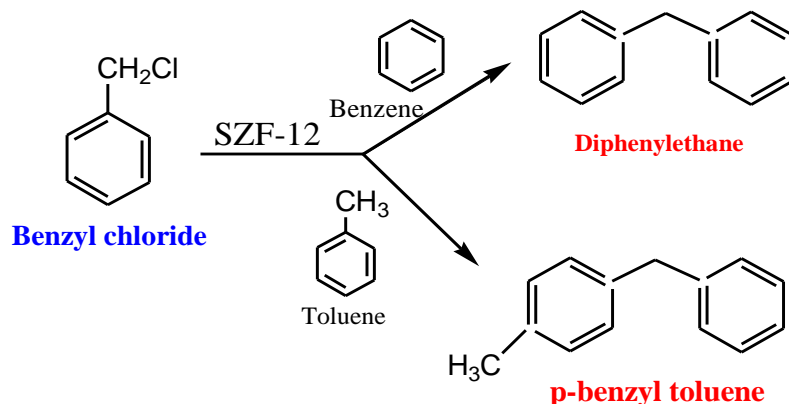
requirements there are two classes of fly ash determined by the content by mass of lime:

Class F: ash is generally derived from sub-bituminous coals and consist primarily of calcium alumino-sulfate glass, as well as quartz, tricalcium aluminate, and free lime (CaO). . Class F, or low calcium fly ash has less than 10 percent CaO.

Class C: ashes are typically derived from bituminous and anthracite coals and consist primarily of an alumino-silicate glass, with quartz, mullite, and magnetite etc. Class C ash is also referred to as high calcium fly ash because it typically contains more than 20 percent CaO.

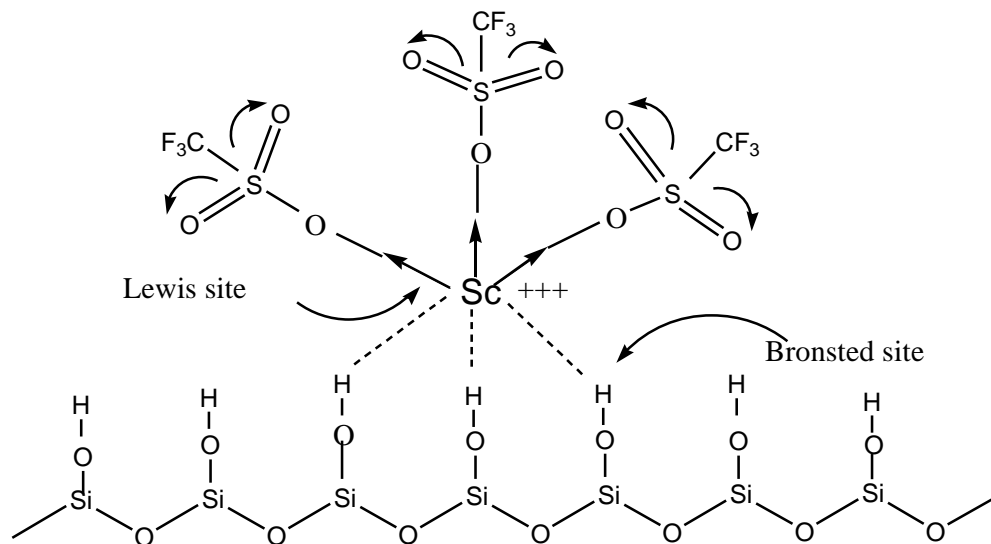
Fly ash having higher degree of fineness corresponds to larger specific area, higher surface energy and more acting faces which illustrate higher activity on its surface. This feature of FA makes it promising support material for loading of different organic or inorganic species. In the present work, focus is on synthesis of functionalized class F fly ash and their application in modern synthetic chemistry. Literature also reports several studies on functionalized FA.

Coal fly ash modified with a mesoporous siliceous material and functionalized with 3-aminopropyl-triethoxysilane was reported as a promising material to evaluate the adsorption capacity of the new matrix for Cu^{2+} ions under different pH, initial metal concentrations, number of contacts and times for different adsorbent masses[60]. Fly ash supported zirconia was reported as solid acid catalyst in benzylation of benzene and toluene with benzyl chloride(Scheme 1.20)[61].



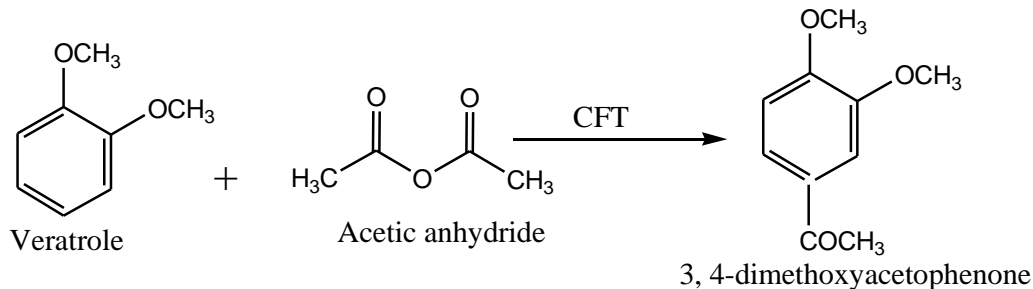
Scheme 1.20: Benzylation of benzene and toluene with benzyl chloride over SZF-12 catalyst.

Novel Ni-Fe solid acid catalyst was prepared through co-wet impregnation of $\text{Fe}_2(\text{SO}_4)_3 \cdot \text{H}_2\text{O}$ and $\text{Ni}(\text{NO}_3)_2 \cdot 6\text{H}_2\text{O}$ on fly ash (FA) support and employed in the production of methyl oleate[62]. A novel fly ash supported solid base catalyst ($\text{MgO}/\text{fly ash}$) possessed stable Si-O-Mg phase with sufficient hydroxyl group to catalyze liquid phase, solvent free and single step condensation of 4-methoxybenzaldehyde with 2-hydroxyacetophenone giving higher conversion (86%) of desired product (4-methoxy-2-hydroxychalcone) with 93% yield[63]. Recently FA has been used for developing several solid acid catalyst by functionalization with various acids, super acids etc. FA functionalized with scandium triflate has been used for solvent free single pot Friedel–Crafts acylation of 2-methoxynaphthalene (2-MN) using acetic anhydride to give 2-acetyl-6-methoxynaphthalene. The proposed model structure of FA supported scandium triflate is shown in Scheme 1.21 [64]



Scheme 1.21: The proposed structure for active site of the catalyst FST.

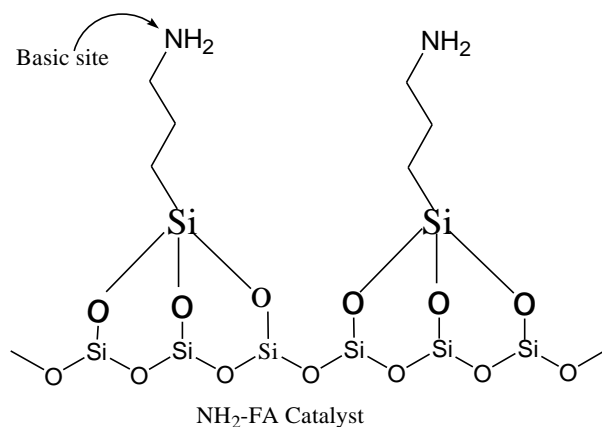
Fly ash-supported cerium triflate catalyst (CFT) possessed stable Lewis acid sites for catalyzing acylation of veratrole by acetic anhydride to synthesize 3,4-dimethoxyacetophenone, a chemical widely used as antineoplastic (Scheme 1.22) [65].



Scheme 1.22. Acylation of veratrole with acetic anhydride over CFT.

Fly ash supported vanadia catalyst was used for catalyzing solvent free selective oxidation of toluene using molecular oxygen as oxidant in a vapor phase micro-reactor under normal atmospheric pressure [66]. FA functionalized with aminopropyltrimethoxysilane (NH₂-FA) has been developed for catalyzing condensation of ethyl cyanoacetate and cyclohexanone to give Ethyl (cyclohexylidene) cyanoacetate an important intermediate of gabapentin (Neurontin),

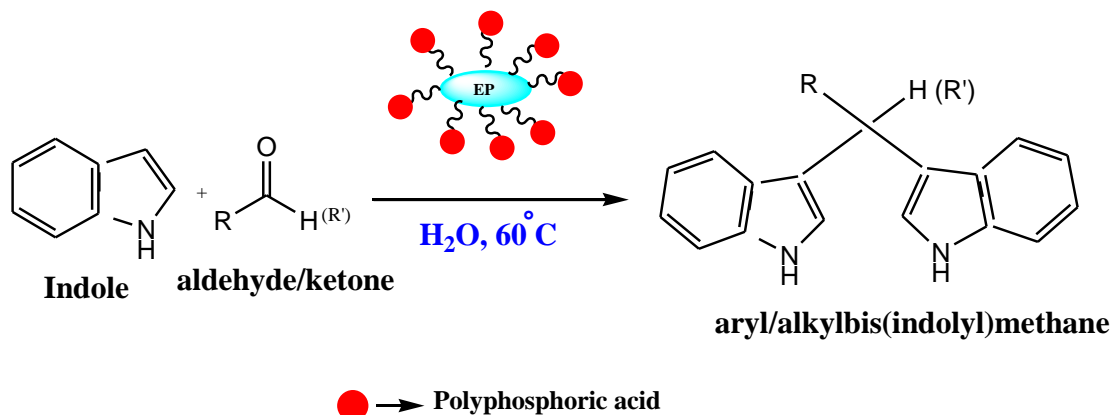
widely used in the treatment of epilepsy to relieve neuropathic pain[67]. the proposed model structure of NH_2 -FA catalyst is shown in Scheme 1.23.



Scheme 1.23: The proposed structure of NH_2 FA catalyst.

1.1.8 Perlite

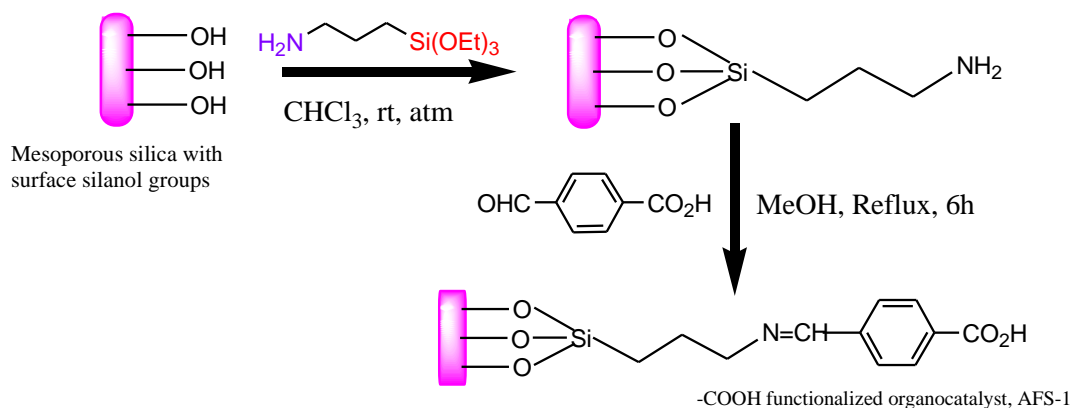
Perlite is an amorphous light gray volcanic glass, with SiO_2 content higher than 70 % and 2 to 5 wt % of bound water. Perlite can be unusually expanded up to 20 times of its volume, when heated quickly, forming a lightweight frothy material [68]. its high activity, availability and low cost make it suitable support material for catalytic applications[69] Perlite sulfonic acid (Perlite- SO_3H (PeSA)) has been synthesized by grafting the sulfonic groups on the perlite surface to produce novel heterogeneous reusable solid acid catalysts for catalyzing heterocyclic multicomponent reaction.[70]. Expanded Perlite-Polyphosphoric acid (EP-PPA) as a novel, efficient, recyclable and eco-benign heterogeneous catalyst has been applied for the green and rapid synthesis of aryl/alkylbis(indolyl)methanes, in water, in good to excellent yields[71].



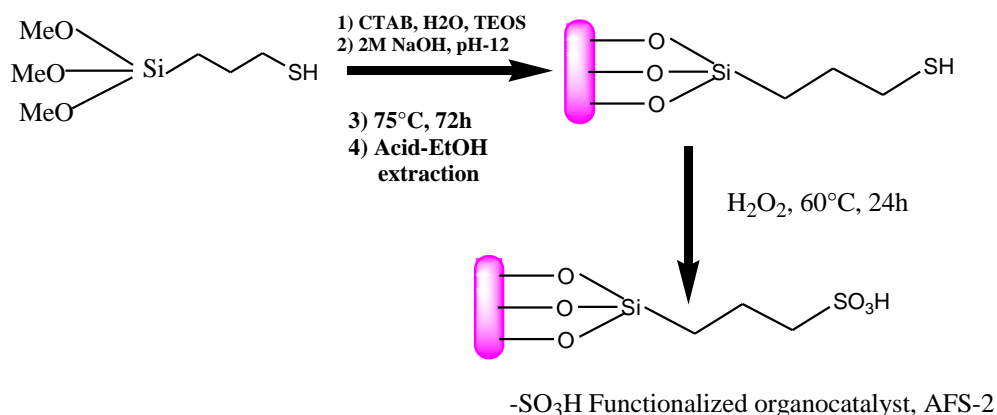
Scheme 1.24: Synthesis of aryl/alkylbis(indolyl)methane derivatives in the presence of EP-PPA.

1.1.9 Mesoporous materials

Mesoporous materials have defined pore sizes in the 2 to 50nm regime. Mesoporous materials with high surface area, controllable pore size and narrow pore size distribution are interesting in a great variety of real and potential applications such as shape selective catalysis and selective adsorption. The advent of mesoporous silicas such as MCM-41 and SBA-15 has provided new opportunities for research into supported metal catalysis. Interestingly, the surface functionalization of mesoporous silica using organosilane compounds has opened new possibilities in the field of green catalysis. The surface functionalized SBA-15 catalysts with $-\text{SO}_3\text{H}$ and $-\text{COOH}$ groups were prepared by co-condensation method as shown in Scheme 1.25 and 1.26. These catalysts have been used as heterogeneous catalysts for the condensation of aromatic aldehyde with 2-naphthol under mild conditions[72]. SBA-15 functionalized with phosphoric acid group was prepared by immersion method and utilized in esterification reaction of acrylic acid and butyl alcohol[73].



Scheme 1.25: Schematic diagram for the preparation of $-\text{CO}_2\text{H}$ functionalized SBA-15



Scheme 1.26: Schematic diagram for the preparation of $-\text{SO}_3\text{H}$ functionalized MCM-41

1.2 Ionic liquids

Recently Ionic liquids have attracted increasing interest in the area of green chemistry. Ionic liquids are defined as pure compounds, consisting only of cations and anions (i. e. salts), which melt at or below 100 °C and can be designed to possess a definite set of properties. ILs have magical properties, including undetectable vapor pressure, reusability and able to dissolve many organic and inorganic substrates. Free

flowing ionic liquid at room temperature are called room temperature ionic liquids (RTILs). There are a great number of different cation and anion combinations to synthesize IL and give an opportunity to modify the physical and chemical properties of the Different types of ILs. The properties of ILs are determined by mutual fit of cation and anion, size, geometry, and charge distribution. Usually, the anion controls the water miscibility, but the cation also has an influence on the hydrophobicity or hydrogen bonding ability [74]. The structures of most commonly used cations and some possible anion types are summarized in Figure 1.1 [75].

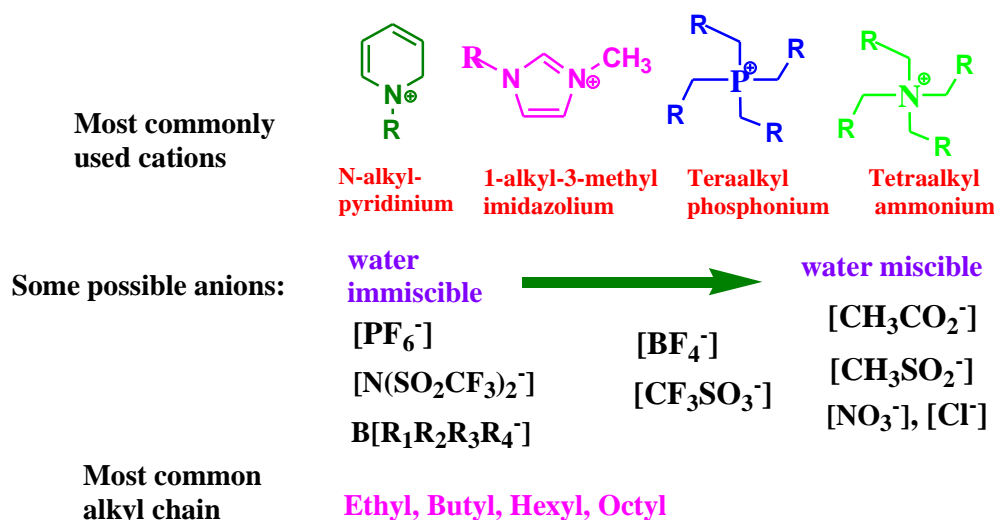


Figure 1.1: Most commonly used cation structures and possible anion types .

ILs possess several magical properties which make them environmentally compatible [76-78]:

- ILs have the ability to dissolve many different organic, inorganic and organometallic materials.
- ILs are highly polar.
- ILs consist of loosely coordinating bulky ions.
- ILs do not evaporate since they have very low vapor pressures.
- ILs are thermally stable, approximately up to 300 °C.
- Most of ILs have a liquid window of up to 200 °C which enables wide kinetic control.

- ILs have high thermal conductivity and a large electrochemical window.
- ILs are immiscible with many organic solvents.
- ILs are nonaqueous polar alternatives for phase transfer processes.
- The solvent properties of ILs can be tuned for a specific application by varying the anion cation combinations.

Taking the commonly used dialkylimidazolium type IL as an example (Figure 1.2). It can be seen that multiple intermolecular forces are possible, including π - π stacking hydrogen-bond donation by the protons of the cation and acceptance by the anion, the aromatic ring of the imidazolium unit and possible Vander Waals interactions[79].

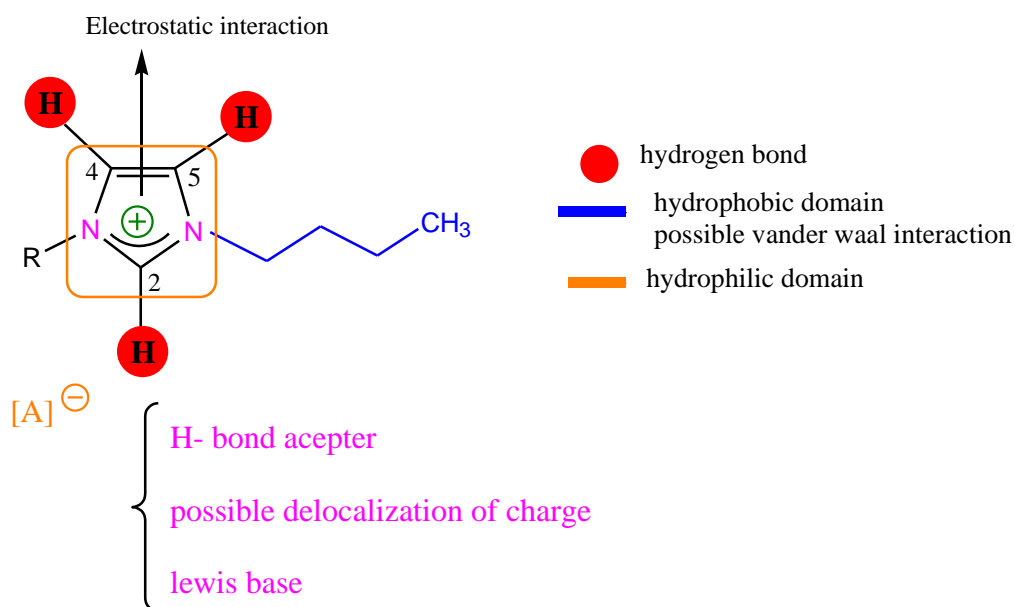
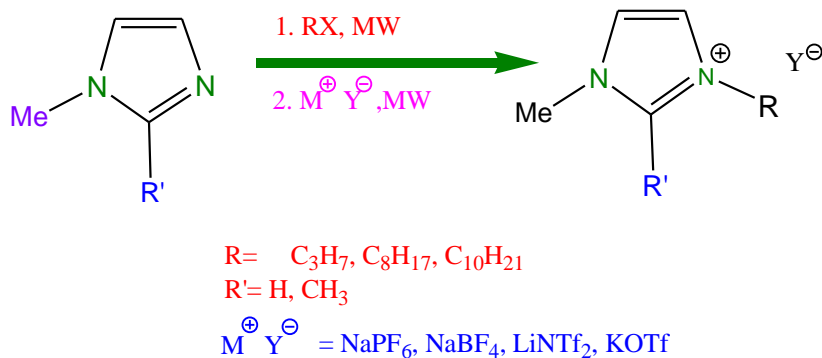


Figure 1.2: Representation of the different types of interactions present in imidazolium-based ILs .

The combination and functionalization of both anion and cation in ILs leads to an incredibly broad variation in their properties, possibly the most notable and important of which is polarity. The high polarizability of ILs provides efficient coupling with microwaves. Microwave (MW) activation, a non-conventional energy source, has emerged as a powerful technique for promoting a variety of chemical reactions and has become a useful technology in organic chemistry[80]. The combination of

solvent-free conditions and MW irradiation considerably reduces reaction time, enhances conversions as well as selectivity as compared to conventional heating and presents certain environmental advantages[81] Microwave flash heating has successfully been used for synthesis of imidazolium based ILs involve a consecutive quaternisation-anion metathesis procedure as given in Scheme 1.27. [82].



Scheme 1.27: microwave assisted synthesis of imidazolium based ILs

Several functionalized imidazolium-based ILs have been reported in the literature with functional groups, such as trimethoxysilyl, thiol-, ether-, sulphonic, carboxylic acid, amino- and hydroxyl-groups [83]. ILs possess unique properties and scope in the usage of catalytic processes, allowing for improvement in catalyst performance as well as its recycle and reuse, while their diverse, tuneable nature allows for optimisation for almost any conceivable system. Sometimes severe drawbacks of ILs, in particular their high viscosity and high cost, has led to considerable drive within the chemical community to develop new, environmentally friendly and highly efficient methodologies for their usage.

1.3 Supported Ionic Liquid phase catalysis

The major concern evidents when using ILs in homogeneous catalysis most predominantly product isolation as well as the large quantities required, particularly when processes are conducted on a large scale. As such there has been a considerable drive to reduce the amount of IL used whilst still maintaining the positive influences in homogeneous catalysis; this led to the new concept of the Supported Ionic Liquid Phase (SILP). In supported ionic liquids phase (SILP) catalyst system, a thin film of ionic liquid is immobilized on high surface area porous solid and a homogeneous catalyst is dissolved in this supported IL layer. This catalyst system, capable to restrict negative effects of the conventional ILs have successfully used in different catalytic area affording high catalytic activity and selectivity. There are several different synthetic methods to perform the immobilization or supporting of ionic liquids, such as simple impregnation, grafting, polymerization, sol-gel method, encapsulation, or pore trapping[84-88]. A novel, synthesis method involves impregnation of the support material with an ionic liquid, diluted with a molecular solvent such as acetone etc. The dilution followed by evaporation of the co-solvent results in a uniform and thin ionic liquid layer on the support material[89]. SILPs allow a more efficient utilization of the IL and the catalyst since the IL's surface area is increased relative to its volume and the substrate can readily diffuse to the catalyst. In a supported ionic liquid phase (SILP) catalyst system, an IL film is immobilized on a high-surface area porous solid and the homogeneous catalyst is dissolved in the IL layer. The resulting catalyst is a solid, with the active species being solubilized in the

IL phase and behaving as a homogeneous catalyst. SILP catalysis combines the most attractive features of homogeneous catalysis like high activity and selectivity with benefits of heterogeneous catalysts such as large interfacial reaction areas and ease of product separation. Indeed, the reaction products can be recovered from the organic phase, while the catalyst remains immobilized in the SILP[90]. Catalysts with immobilized ionic liquids were successfully used in various catalytic reactions like hydroformylation of olefins[91] achiral hydrogenation[92] Heck reaction[93] and hydroamination[94]. Friedel–Crafts reactions[95] Rh-catalyzed hydroformylations[96] and hydrogenations[96] Pd-catalyzed Heck reactions[97] and Rh-, Pd-, and Zn-catalyzed hydroaminations[98]. Mizoroki–Heck reaction[99], chemical fixation of carbon dioxide [100], aldol reaction [101], epoxidation [102].

SILP thus can be used in the following ways:

- *To generate novel catalytic species*
- To improve the stability of the catalyst
- To optimize immobilization and recyclability
- To assist the activation of the catalyst
- To facilitate product isolation
- To influence the selectivity of the reaction, which are some of the essential roles of conventional solvents.

1.3.1 Pathways of immobilization of IL

There are three different synthetic pathways have been developed for the preparation of the ionic liquid functionalized materials[103]. The pre- or post-functionalized ILs

can be bound to a surface either by covalent bonds between silanol groups and the anion or the cation of the liquid, or without covalent bonds in the form of supported liquid phases. The general synthetic methodologies are given below.

Immobilization via anion

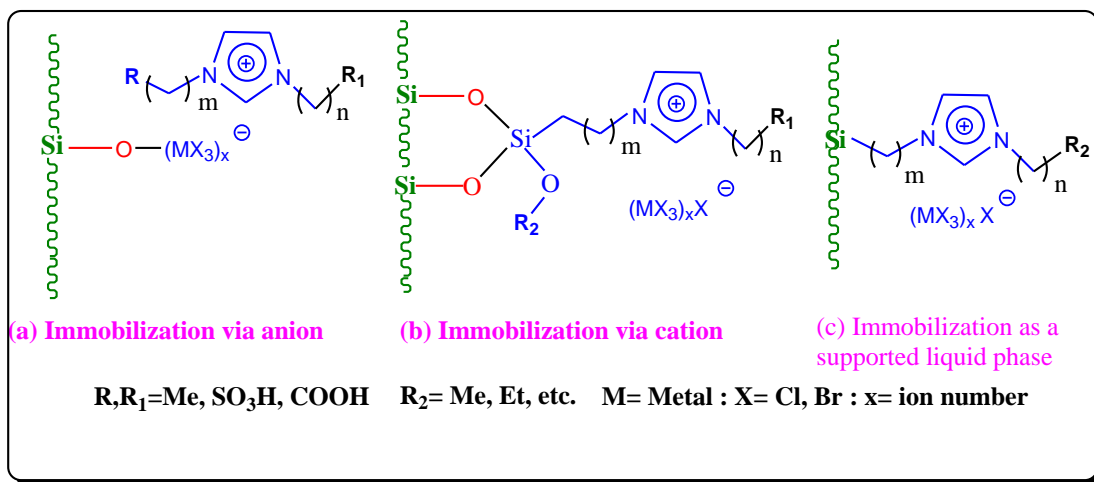
In this method, a solid support material is impregnated with a pre-formed functional ionic liquid containing active group (such as AlCl_4), and the anion group is usually covalently anchored to the support surface via chloroaluminate-based anion, which could further interact with the cation of IL to achieve the aim of immobilization (Scheme 1.28 (a)).

Immobilization via cation

In this approach an organic anchor group is covalently attached to the surface and is used as the cation in the formation of the ionic liquid. A thin film of ILs can be formed on the surface of the support, which may be beneficial for further introducing catalytically active species to functionalize the immobilized ILs (Scheme 1.28(b)).

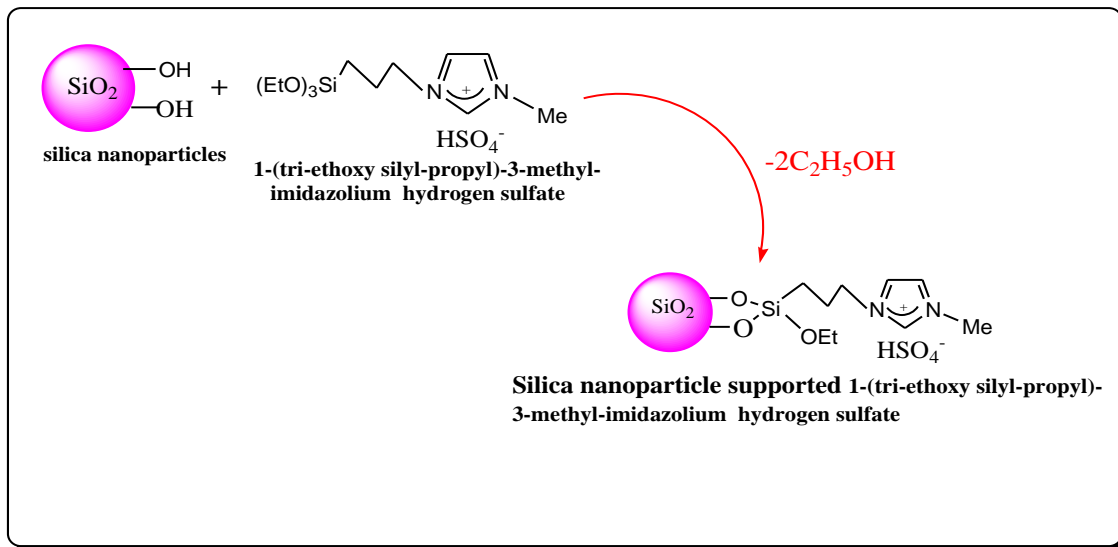
Immobilization via solid support

In this method, the ILs, either with or without the catalysts, can be physically confined or encapsulated into the pores of solid supports (Scheme 1.28(c)).

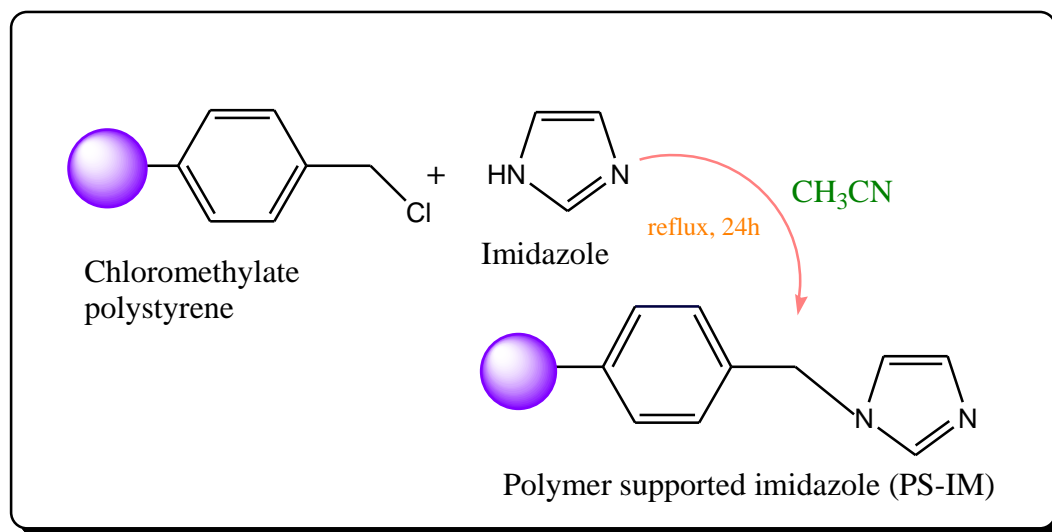


Scheme 1.28: Immobilisation of ionic liquids via the anion, the cation or supported liquid phase

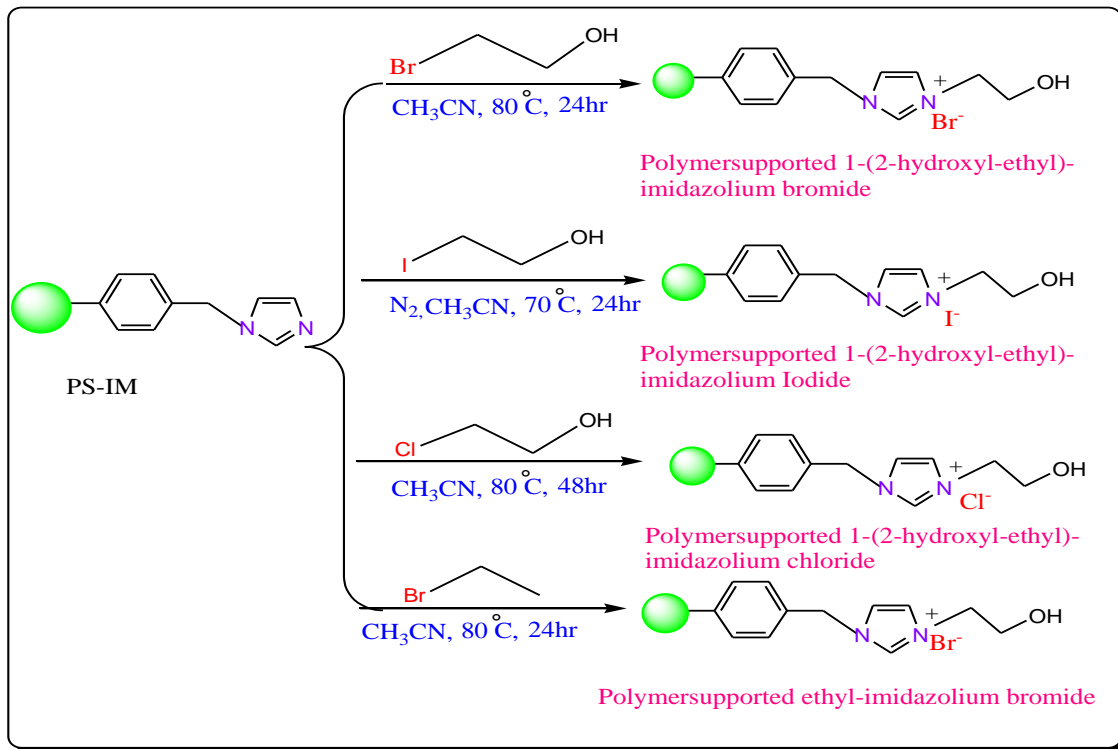
Various mesoporous materials viz. silica[104], polymers[105] and magnetic materials[106] are extensively used as support materials for immobilizing different ionic liquids. Some examples of immobilized ionic liquids on different support materials are given below.



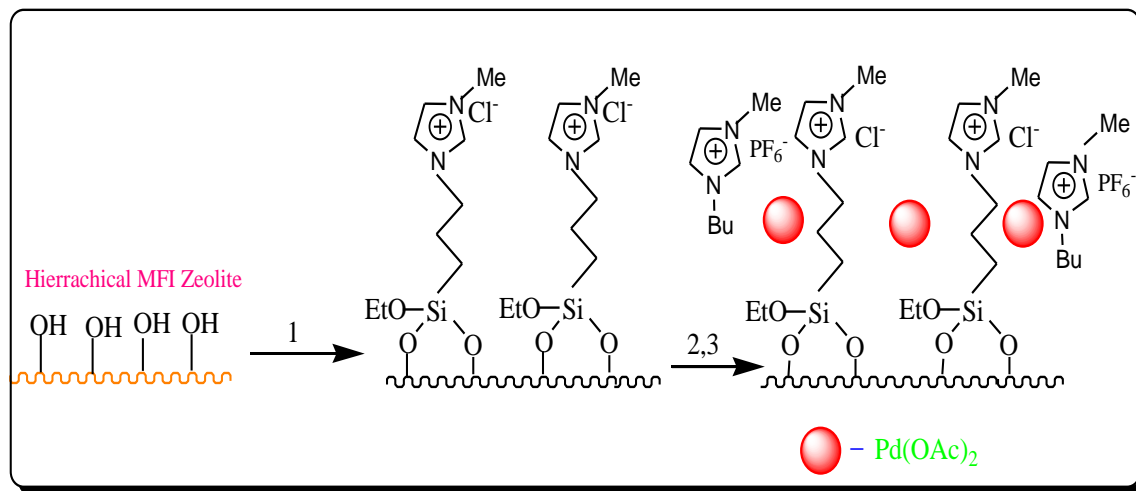
Scheme 1.29: Schematic representation of 1-(tri-ethoxy silyl-propyl)-3-methyl-imidazolium hydrogen sulfate (IL-HSO₄) immobilization on silica nanoparticles[107].



Scheme 1.30: Synthesis of polymer-supported imidazole[108]

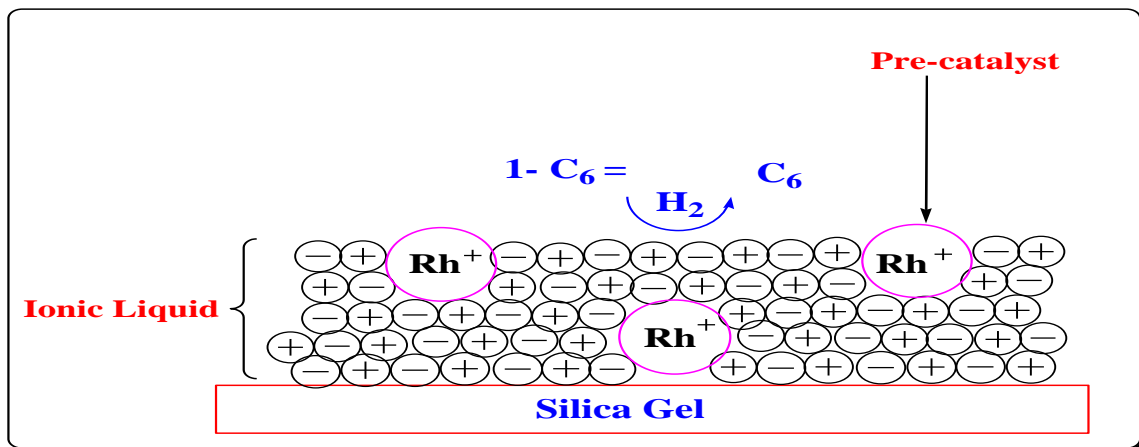


Scheme 1.31: Synthesis of polymer-supported ionic liquids[108]

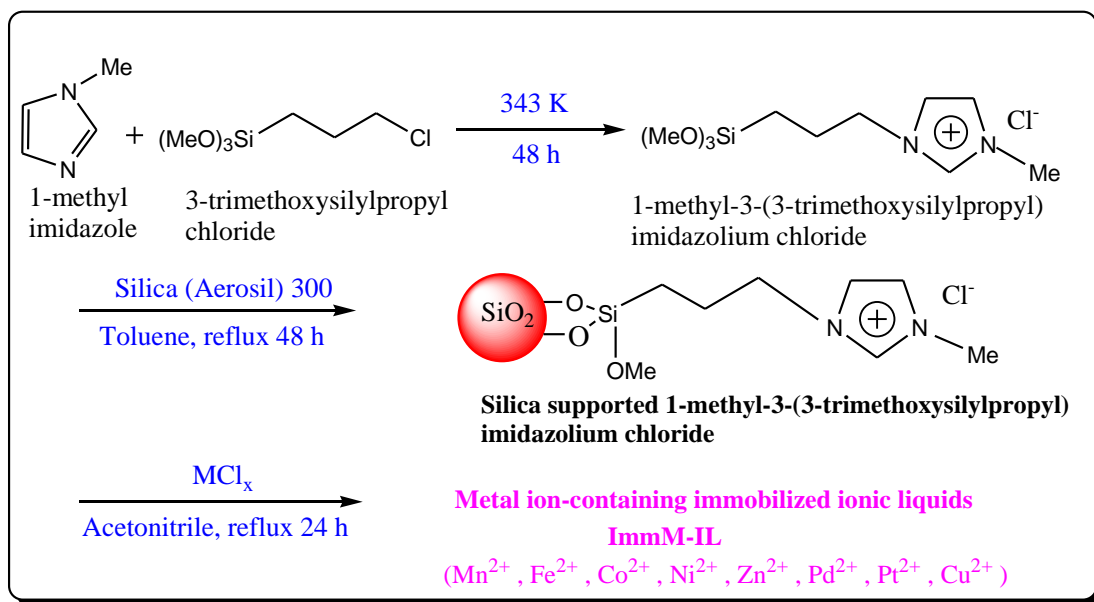


1. [tpim][Cl]/toluene, 100°C; 2. [bmim]-Pd(OAc)₂/THF, RT, 1h; 3. Removal of THF

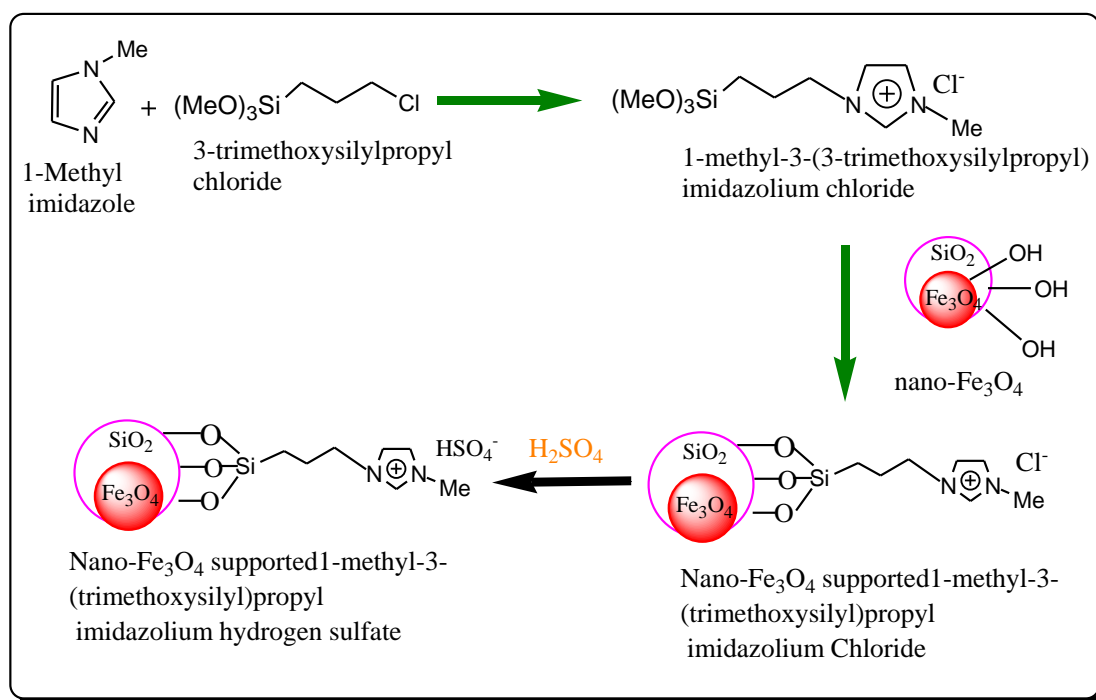
Scheme 1.32: Preparation of MFI-supported Pd(OAc)₂-ionic liquid 1-butyl-3-methylimidazolium hexafluorophosphate[109]



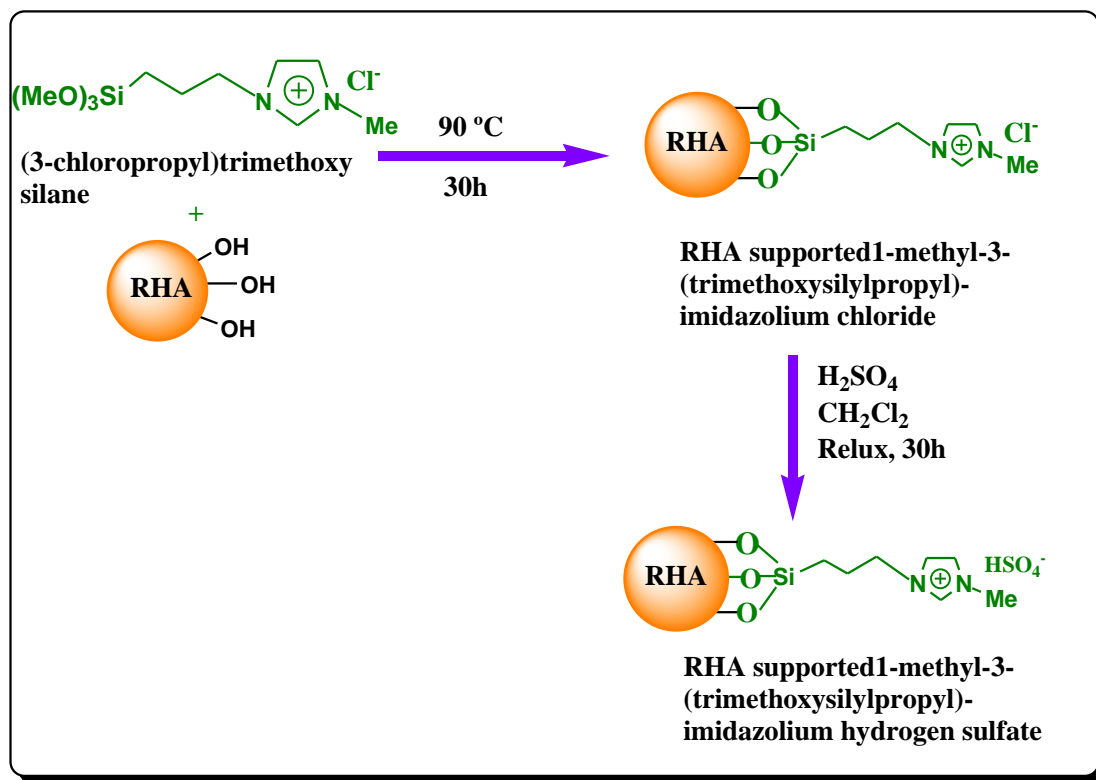
Scheme 1.33: Confined ionic liquid phase containing the Rhodium complex 1 on the surface of a silica gel support material[110]



Scheme 1.34: Preparation of metal ion-containing immobilized ionic liquid[111]



Scheme 1.35: Preparation steps for fabricating 1- methyl -3-(3-trimethoxysilylpropyl)-1H-imidazol-3-ium chloride -functionalized magnetic Fe₃O₄[112]



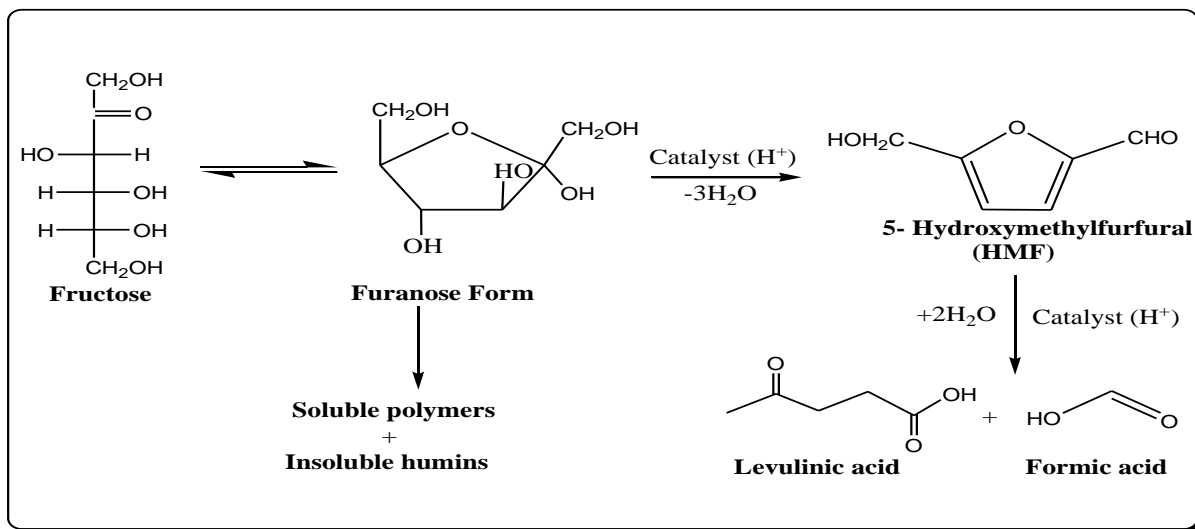
Scheme 1.36: Preparation of the acidic ionic liquid supported on rice husk ash[113]

1.3.2 Applications of immobilized ionic liquid in organic synthesis

Examples of organic reactions catalyzed by various immobilized ionic liquids are given below.

Dehydration reaction

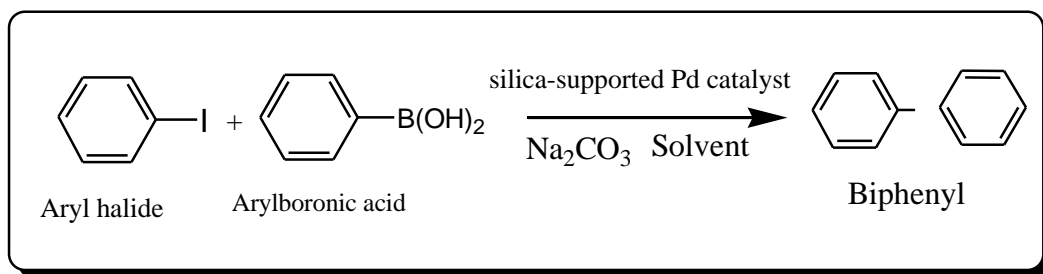
Supported ionic liquid nanoparticles (SILnPs) have been prepared by immobilization of ionic liquid, 1-(tri-ethoxy silyl-propyl)-3-methyl-imidazolium hydrogen sulfate (IL-HSO₄) on the surface of silica nanoparticles. The catalytic activity of the prepared SILnPs was investigated for the dehydration of fructose to 5-hydroxymethylfurfural (HMF) in the presence of dimethylsulfoxide (DMSO) as a solvent. At optimized reaction conditions, 99.9% fructose conversion and 63% HMF yield was achieved(Scheme 1.37)[107].



Scheme 1.37: Supported ionic liquid nanoparticles(SILnPs) catalyzed the dehydration of fructose to 5-hydroxymethylfurfural (HMF)

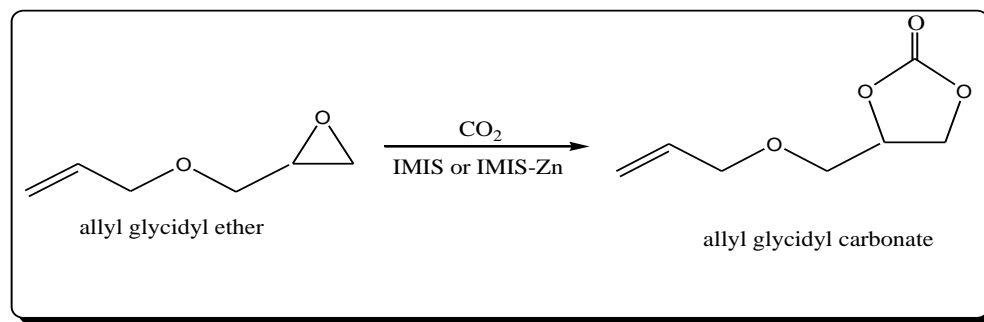
Coupling reactions

- Suzuki-Miyaura coupling reaction:** The immobilized N-heterocyclic carbene-Pd complex was synthesized by reaction of silica gel-supported imidazolium chloride with Pd(OAc)₂. The Pd complex showed excellent catalytic activity in the coupling reaction of aryl halides with arylboronic acid as shown in Scheme 1.38. This heterogeneous Pd catalyst was reusable as well as air-stable to allow easy use[114].



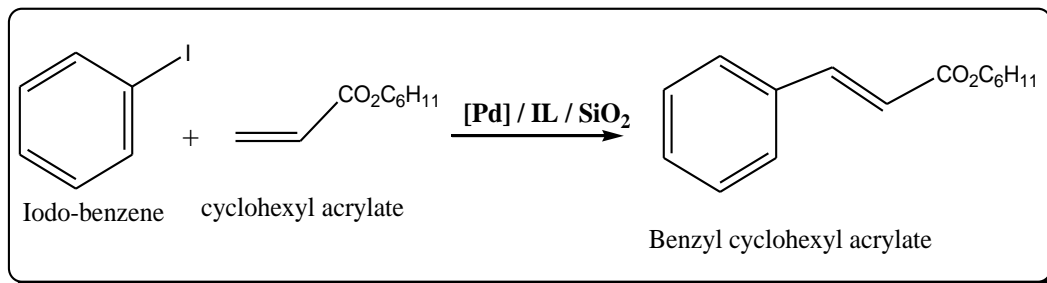
Scheme 1.38: Silica-supported NHC-Pd catalyzed Suzuki-Miyaura coupling reaction

- Imidazolium-based ionic liquids with varied alkyl chain lengths bearing different anions (Cl^- , Br^- and I^-) were synthesized and immobilized onto the commercial silica surface (IMIS). These heterogeneous catalysts showed high catalytic activities and selectivities in the cycloaddition of carbon dioxide to allyl glycidyl ether (AGE) as given in Scheme 1.39. The immobilized ionic liquids with longer alkyl chain length and more nucleophilic anion showed higher activity. In particular, compared with pristine IMIS, zinc halide combined IMIS (IMIS-Zn) with Cl^- exhibited an increased activity, while the IMIS-Zn with Br^- and I^- showed lower activity than IMIS itself [115].



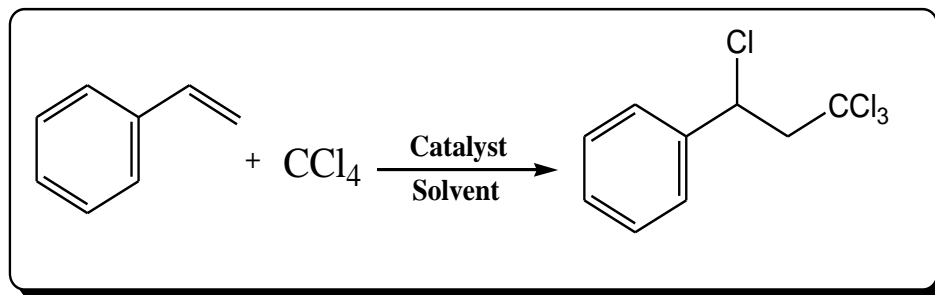
Scheme 1.39: Synthesis of Allyl glycidyl carbonate over IMIS-Zn catalyst

- C-C coupling reaction-** $\text{Pd}(\text{OAc})_2$ and $[\text{bmim}][\text{PF}_6]$ were impregnated on amorphous silica. The prepared catalyst was used for Mizoroki-Heck reaction between iodo-benzene and cyclohexyl acrylate with tri-*n*-butyl amine as the base (Scheme 1.40)[116].



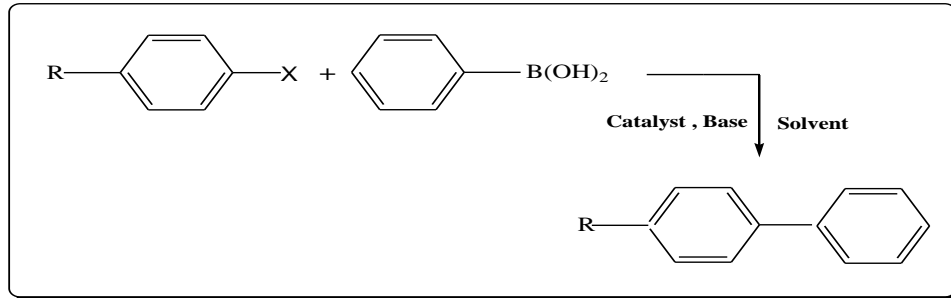
Scheme 1.40: Mizoroki-Heck reaction over Pd/IL/SiO₂ catalyst

- **Kharasch addition reaction-** A chlorine ion containing ionic liquid $[\text{Bmim}]_2\text{CuCl}_4$ immobilized on silica surface. The prepared ImimCu^{2+} -IL was used for Kharasch addition reaction between CCl_4 and styrene as given in Scheme 1.41[111].



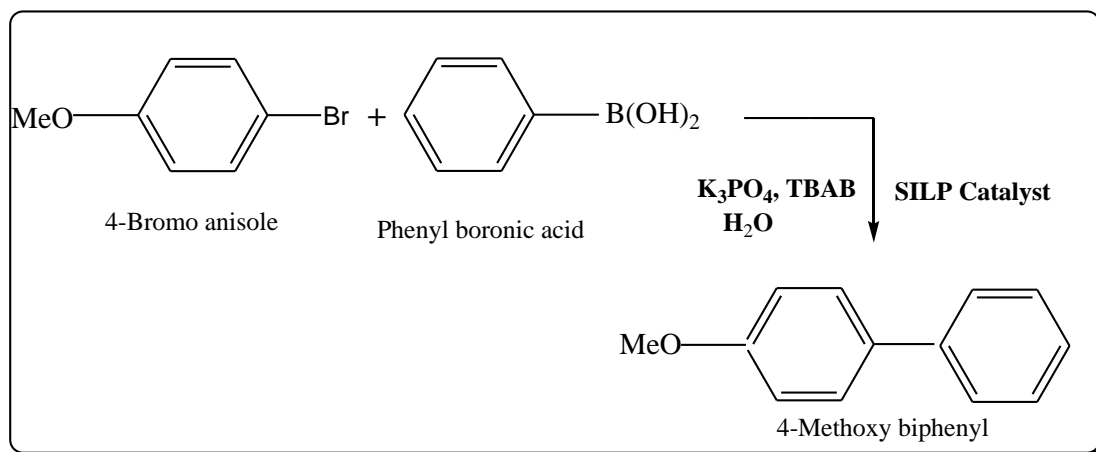
Scheme 1.41: $[\text{Bmim}]_2\text{CuCl}_4/\text{SiO}_2$ catalyzed Kharasch addition reaction

- **Suzuki cross-coupling reaction-** Ionic liquid $[\text{Bmim}]_2[\text{PdCl}_4]$ immobilized on silica surface. ImimPd^{2+} -IL was used as a catalyst for Suzuki cross coupling reaction between phenyleboronic acid and aryl halide Scheme 1.42 [111]



Scheme 1.42: $[\text{Bmim}]_2[\text{PdCl}_4]/\text{SiO}_2$ catalyzed Suzuki cross-coupling reaction

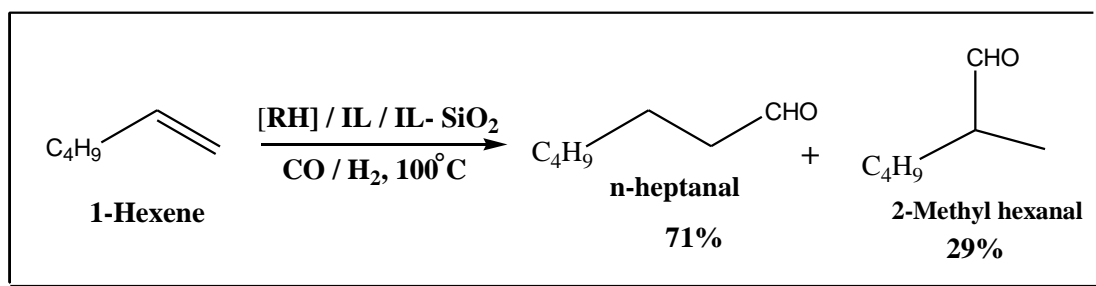
- Palladium acetate was immobilized in thin ionic liquid 1-(3-triethoxysilylpropyl)-3-methylimidazolium chloride ($[\text{tpim}] [\text{Cl}]$) layers on the mesopore wall of hierarchical MFI zeolite, and the prepared catalyst was used for Suzuki coupling reaction between aryl bromides and arylboronic acids (Scheme 1.43)[109].



Scheme 1.43: [tpim] [Cl]/ MFI zeolite catalyzed Suzuki coupling reaction between aryl bromides and arylboronic acids.

Hydroformylation reaction:

- A Rh-monophosphine based system was prepared using a MCM-41 silica as the support and [bmim][BF₄], [bmim][PF₆], [1,1,3,3-tetramethylguanidinium] [acetate] (TMGL) as ILs. The resulting supported ionic liquid phase catalyst [Rh/IL/IL-SiO₂] was used for the hydroformylation of 1-hexene (Scheme 1.44) [117].



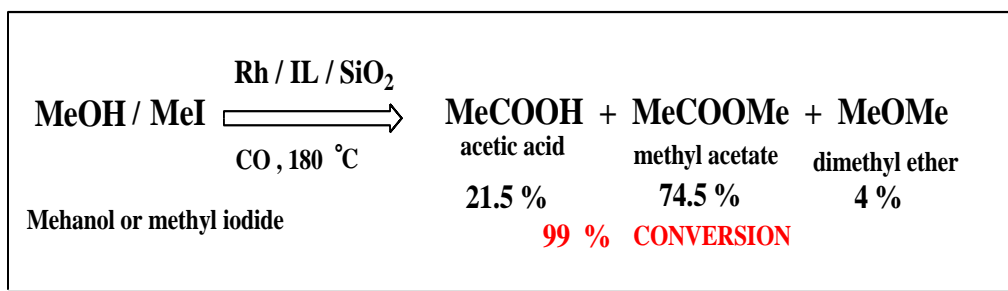
Scheme 1.44: [Rh/IL/IL-SiO₂]catalyzed hydroformylation of 1-hexene

Olefin Metathesis:

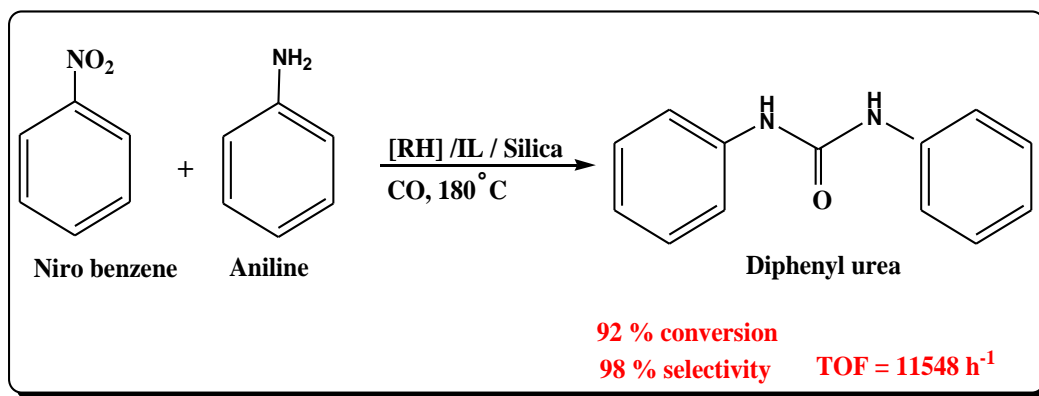
- A solution of the Grubbs Ru catalyst and 1-hexyl-3-methyl imidazolium hexafluorophosphate [hmim][PF₆] was impregnated on amorphous alumina. The Ru-SILP catalyst (0.03 mmol Ru g⁻¹) was used for multiple olefin metathesis reactions like macrocyclizations and dimerizations[90]

Carbonylation reaction:

- **Methanol carbonylation-** The [bmim][Rh(CO)₂I₂] IL was prepared by stirring the dimeric catalyst precursor [Rh(CO)₂I]₂ with an excess of 1-butyl-3-methylimidazolium iodide [bmim][I] in methanol. Then resulting [bmim][Rh(CO)₂I₂] IL was impregnated on silica gel. The prepared catalyst was used for the continuous gas-phase carbonylation of a mixture of methanol and methyl iodide (75:25 wt%) with CO at 180 °C(Scheme 1.45)[90]

**Scheme 1.45: [bmim][Rh(CO)₂I₂]/SiO₂ catalyzed carbonylation**

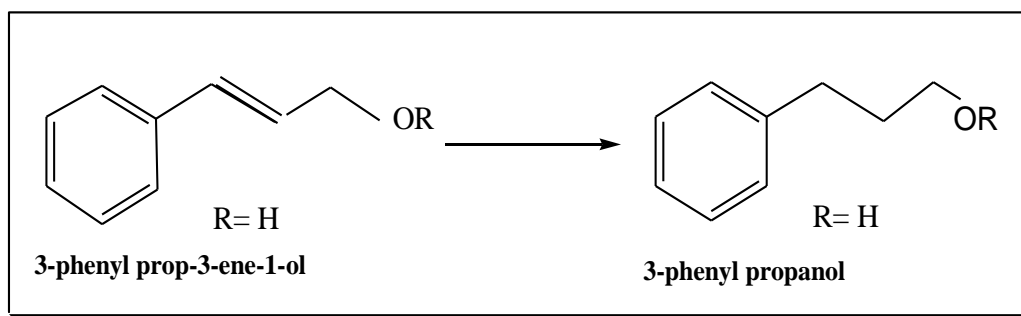
- **Carbonylation of amines and nitrobenzene to ureas-** The Rh(PPh₃)₃Cl catalyst immobilized in [1-decyl-3-methylimidazolium][BF₄] on silica using sol-gel method. The prepared catalyst was used in the carbonylation of aniline and nitrobenzene as shown in Scheme 1.46 [90].



Scheme 1.46: RH/IL/Silica catalyzed Carbonylation of amines and nitrobenzene to ureas

Hydrogenation reaction:

- The Rh complex [Rh(norboradiene)(PPh₃)](PF₆) and 1-butyl-3-methyl imidazolium hexafluorophosphate [bmim][PF₆] were impregnated on silica gel. The prepared catalyst was used for the hydrogenation of alkenes like 1-hexene, cyclohexene and 2,3-methyl-2-butene at room temperature and 41 bars of H₂ in n-heptanes as the solvent[90].
- Palladium acetate was immobilized in the pores of amorphous mercaptopropyl silica gel with an ionic liquid 1-butyl-3-methyl imidazolium tetrafluoroborate [bmim][BF₄]. The heterogeneous Pd-SH-SILC (Pd supported ionic liquid catalyst) was used for catalytic hydrogenation of a variety of olefins at atmospheric pressure and room temperature (scheme 1.47)[118]

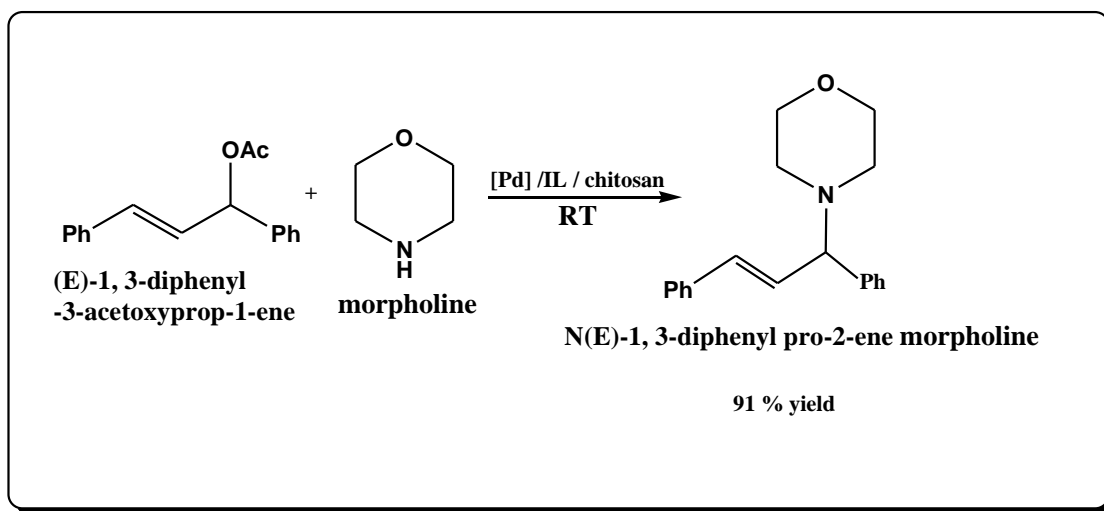


Scheme 1.47: Hydrogenation of a variety of olefins Pd-SH-SILC

- Silica supported platinum catalysts coated with a thin film of 1-butyl-2,3-dimethyl-imidazolium trifluoromethane sulfonate (BDiMIm) was used as catalyst for hydrogenation of ethane[119].

Allylic substitution reaction:

- Pd (OAc)₂ and [bmim] [BF₄] or [bmim] [BF₆] were immobilized on chitosan. The SILP catalyst was used for the allylic substitution between morpholine and (E)-1, 3-diphenyl-3-acetoxyprop-1-ene at room temperature as shown in Scheme 1.48)[90].



Scheme 1.48: Allylic substitution between morpholine and (E)-1, 3-diphenyl-3-acetoxyprop-1-ene using Pd/IL/Chitosan

Asymmetric reactions:

- **Asymmetric Mukaiyama aldol condensation-** A SILPC was prepared by impregnation of Copper(II) trifluoromethanesulfonate(Cu(OTf)₂), an imidazolium tagged bis(oxazoline) ligand and 1-Ethyl-3-methylimidazoliumbis(trifluoromethylsulfonyl)imide [emim][NTf₂] on silica(20m² g⁻¹). The prepared catalysts were applied in the asymmetric

Mukaiyama aldol condensation of 1-phenyl-1-trimethylsiloxyethene and methyl pyruvate in diethyl ether as the co-solvent[120].

- **Asymmetric ring opening of epoxies-** A dimeric (R,R)-Cr(III)salen complex and 1-butyl-3-methyl imidazolium hexafluorophosphate were impregnated on silica and the prepared catalyst was applied in the asymmetric ring opening of 1,2-epoxyhexane with trimethylsilylazide (TMSN_3) in n-hexane in batch and fixed-bed reactor[121].

Condensation reaction:

- 3-sulfobutyl-1-(3-propyltriethoxysilane)-imidazolium hydrogen sulfate immobilized on silica gel with covalent bonds. The prepared catalyst can catalyze the one-spot synthesis of amidoalkyl naphthols by the multicomponent condensation of aldehydes with 2-naphthol amide under solvent free conditions[122].
- Rice husk ash (RHA) was used as a support material for the immobilization of 1-methyl-3-(trimethoxysilylpropyl)-imidazolium hydrogen sulfate. The immobilized acidic ionic liquid was tested for the preparation of 1-(benzothiazolylamino)phenylmethyl-2-naphthols from the one-pot condensation of an aldehyde, 2-aminobenzothiazole and 2-naphthol, at 100 °C under solvent-free conditions.[113]

Cycloaddition of CO_2 :

- An ionic liquid 1-(triethoxysilyl) propyl-3-methylimidazolium hydroxide ($[\text{Smim}] \text{OH}$) was grafted on silica gel. The grafted ionic liquids (GILs) could be used as highly effective heterogeneous catalysts toward propylene carbonate synthesis through cycloaddition of CO_2 with propylene oxide under solvent less and mild conditions[123].
- 1-(2-Hydroxyl-ethyl)-imidazolium-based ionic liquid chemically immobilized on polystyrene resin through covalent bonds. The prepared heterogeneous catalyst was used for the synthesis of cyclic carbonates via cycloaddition reaction of CO_2 with epoxies[124].

Acylal Formation reaction:

- A silica-supported functional ionic liquid, Si-3-sulfobutyl-1-(3-propyltriethoxysilane) imidazolium hexafluorophosphate [SbSipim][PF₆] was used for the acylalformation from aldehydes and acetic anhydride, under solvent free conditions[125].

Streker reaction:

- Yb(OTf)₃-pybox is immobilized in a novel self-assembled ionic liquid hybrid silica and the prepared catalyst was used for the asymmetric Strecker hydrocyanation of aldimines[126].

Scavenging reaction:

- A scavenging system of silica-supported sulfonic acid-functional ionic liquid (Si-[SbSipim][PF₆]) coated with a conventional ionic liquid, 1-butyl-3-methylimidazolium hexafluorophosphate ([bmim][PF₆]) (Si-[SbSipim][PF₆]-[bmim][PF₆]) which combines the advantages of solid-supported and solution-phase scavengers. The prepared scavenging system was used as a scavenger in the removal of excess amine in the parallel synthesis of amides[127].

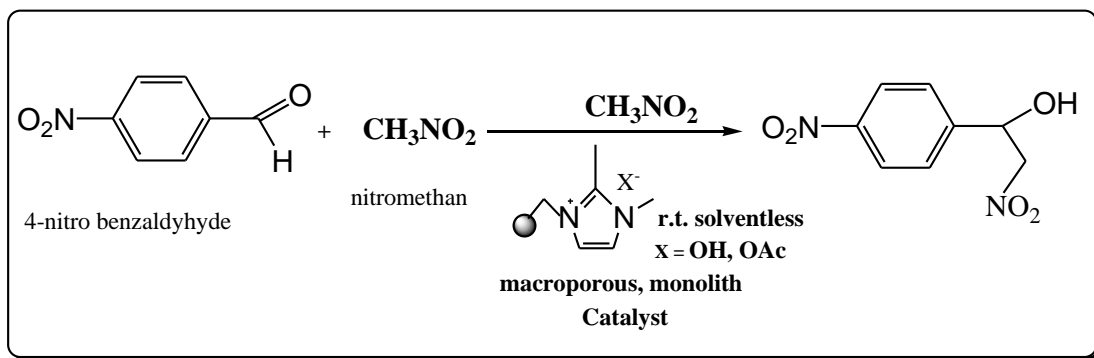
Oxidation reaction:

- A magnetic silica supported bifunctional hybrid-type ionic liquid catalyst (IL/SMNP) bearing two catalyst sites, TEMPO and polyoxometalate moieties was used for selective oxidation of a wide set of aliphatic, allylic, heterocyclic and benzylic alcohols[128].
- 1-Butyl-3-methylimidazolium Methanesulfonate impregnated on a commercial gamma aluminium oxide. The gold nanoparticles dispersed on ionic liquid layer supported on a commercial gamma aluminium oxide. The

prepared catalyst was applied in the reaction of oxidation of carbon monoxide[129].

Henry reaction:

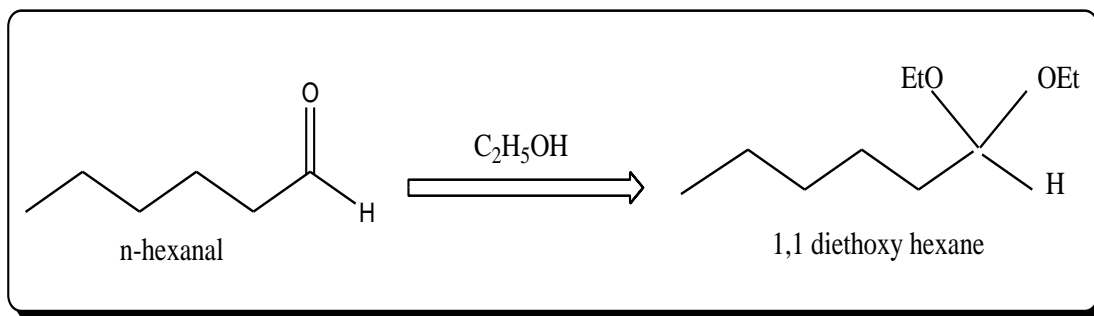
1. The base supported ionic liquid like phase(SILLPs) catalyst were prepared by the reaction of 1,2-dimethylimidazole(1,2-DMIM) with the different chloromethylated resins at a constant concentration of 1M of 1,2 DMIM in DMF. The Henry reaction between p-nitrobenzaldehyde and nitromethane under solvent less condition catalyzed by base SILPs catalyst(Scheme 1.49) [130].



Scheme 1.49: Continuous-flow solvent less Henry reaction catalyzed by basic-SILPs.

Acetalization Reaction:

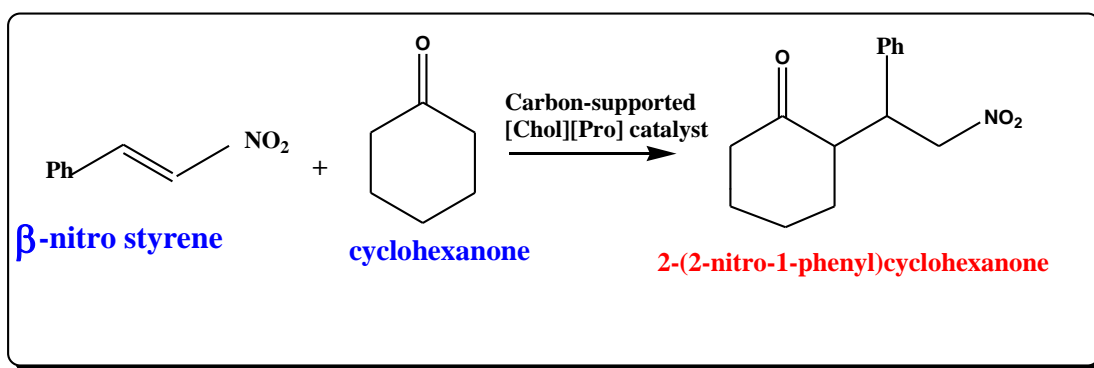
2. 1,1-vinylimidazolium based bronsted ionic liquid immobilized on solid support by copolymerization with styrene. The prepared catalyst was used for acetalization of n-hexanal with ethanol as shown in Scheme 1.50[131].



Scheme 1.50: Bronsted acid catalyzed acetalization of n-hexanal with ethanol

Michael reaction:

3. [Chol][Pro] choline based ionic liquid (2-hydroxyethyl)trimethylammonium DL-prolinate) was supported on porous carbon materials with highly pure carbon surface. Carbon-supported [Chol][Pro] catalyst was used for Michael reaction between cyclohexanone and β -nitro styrene to produce 2-(2-nitro-1-phenyl)cyclohexanone is given in Scheme 1.51[132].

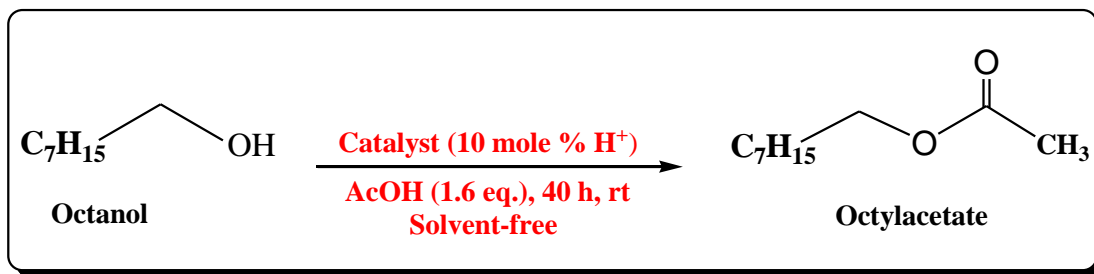


Scheme 1.51: Synthesis of 2-(2-nitro-1-phenyl)cyclohexanone using choline based IL

Esterification reactions:

Mesoporous sulfonic acid SBA-15-Pr-SO₃H was impregnated with an acetone solution of 1-methyl-3-octylimidazolium hydrogen sulfate [MOIm]HSO₄ (0.8 mL of IL in 5 mL absolute acetone). After 3 h stirring at room temperature, the solvent was evaporated under vacuum then we obtained IL@SBA-15-Pr-SO₃H. This catalyst was used for esterification of 1-octanol with acetic acid at room temperature(Scheme 1.52)[133].

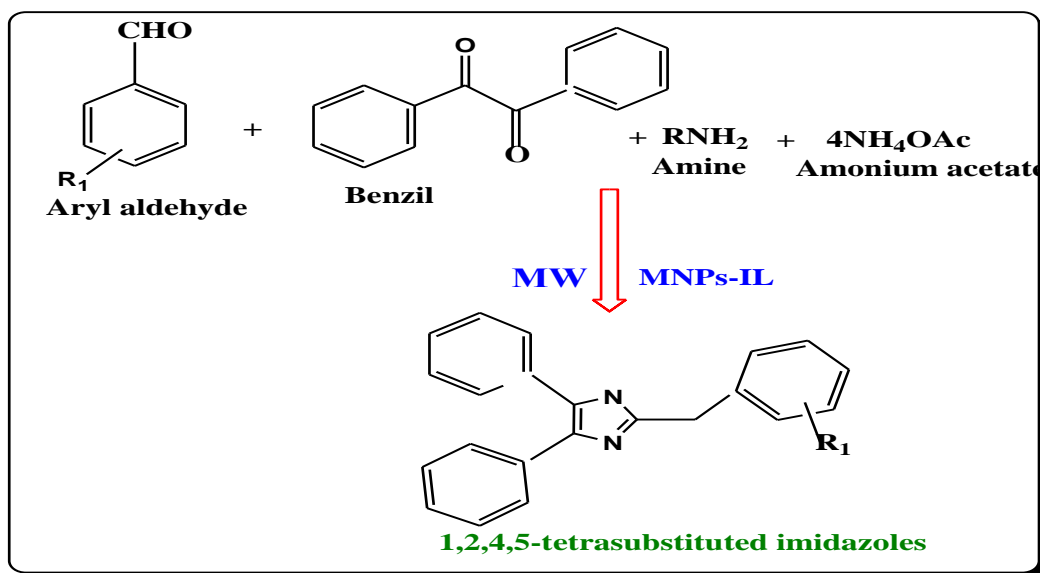
1-(propyl-3-sulfonate) imidazolium hydrosulfate ([(CH₂)₃SO₃H-HIM]HSO₄) Brønsted acidic ionic liquid was immobilized on chloromethyl polystyrene grafted silica gel. This prepared catalyst showed high catalytic activity for a series of esterifications [134].



Scheme 1.52: IL@SBA-15-Pr-SO₃H catalyzed esterification of 1-octanol with acetic acid

Synthesis of heterocyclic compounds:

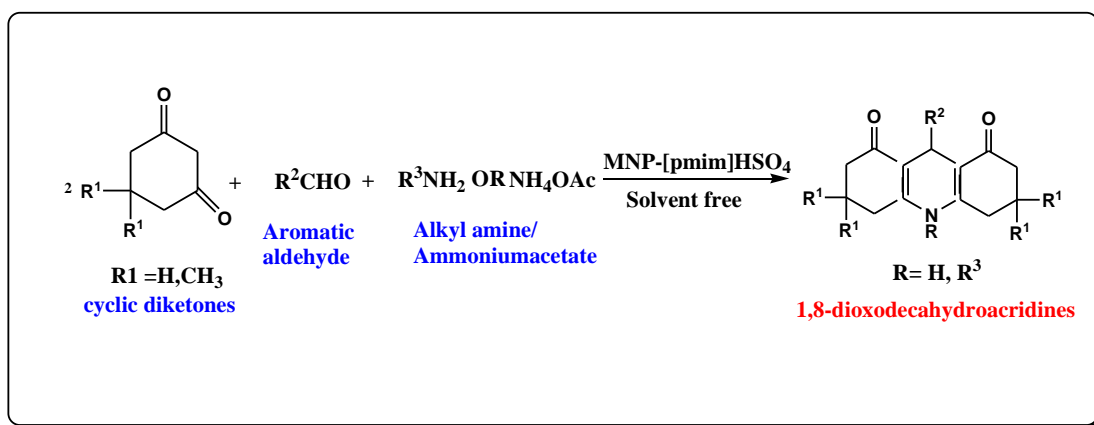
The ionic liquid 1-methyl-3-(3-trimethoxysilylpropyl) imidazolium chloride was immobilized on superparamagnetic Fe₃O₄ nanoparticles (IL-MNPs) and used as an efficient heterogeneous catalyst for the one-pot synthesis of 1,2,4,5-tetrasubstituted imidazoles under solvent-free conditions using microwave irradiation as given in Scheme 1.53[134].



Scheme 1.53: synthesis of tetrasubstituted imidazoles using IL-MNPs catalyst

- **Synthesis of Decahydroacridines**

1-methyl-3-(triethoxysilyl)propyl imidazolium chloride ([pmim]Cl) ionic liquid was anchored onto silica-coated magnetic Fe₃O₄ particles, and Cl⁻ anion exchange by treatment with H₂SO₄ afforded the corresponding immobilized ionic liquid MNP-[pmim]HSO₄. The catalytic activity of synthesized catalyst was examined in synthesis of 1,8-dioxodecahydroacridines by condensation reaction of cyclic diketones with aromatic aldehydes and ammonium acetate or primary amines under solvent-free conditions as shown in Scheme 1.54[135].



Scheme 1.54: Synthesis of Decahydroacridines over MNP-[pmim]HSO₄ catalyst

1.4 Conventional and microwave heating

Microwave-assisted organic synthesis (MAOS) known as “non-conventional” synthetic method has shown wide applications as a very efficient way to producing high yields and higher selectivity, lower quantities of side products and enhances the product purity and improves the reproducibility. MAOS is a branch of green chemistry, principally since many organic reactions can be carry out in solvent-free conditions [136]. Conventional organic synthesis is carried out by superficial heating process and the energy is transferred from the surface to the bulk by convection and conduction which is shown in Figure 4[137]. This is less efficient and time consuming process for transferring energy into system, since it depends on the thermal conductivity of the various materials that must be penetrated, and results in the temperature of the reaction vessel being higher than that of the reaction mixture. In contrast, Microwave irradiation produces efficient internal heating by direct coupling of microwave energy with the molecules (solvents, reagents, catalysts) that are present in the reaction mixture. The magnitude of the energy transfer depends on the dielectric properties of the molecules. Microwave heating diminishes potential energy barrier and favours the easier and earlier formation of thermodynamic product depending upon the dipole moment of reactants and their interaction with microwave irradiation. Three different mechanisms, namely, dipolar polarization, conduction and interfacial polarization are responsible for microwave heating[138] The differences between microwave and conventional heating are described in table 1.

Recently MAOS use ILs as solvent or catalyst, since they are “ecofriend solvents” [139] and since their ionic nature, allows a very effective coupling with microwave energy [140]. MAOS has also been widely employed to synthesized different ILs[141]. The application of microwave on ILs synthesis improved dramatically the time required to obtain these compounds. Coupling of microwave with the use of ionic liquid supported catalysts under solvent free conditions, provides clean chemical processes with the

advantages of enhanced reaction rates, higher yields and selectivity. Avoiding organic solvents during reactions in organic synthesis, use of microwave irradiation, less production of wastes during the whole procedure leads to a clean, atom efficient, and economical technology as per the principles of green chemistry.

Table 1.1 Comparison between conventional and microwave heating

Conventional heating	Microwave heating
1. Reaction mixture heating proceeds from a surface usually inside of reaction vessel	Reaction mixture heating proceeds direct inside mixture
2. The vessel should be in physical contact with surface that is at a higher temperature source.	No need of physical contact of reaction with the higher temperature source. While vessel is kept in microwave cavities.
3. By thermal or electric source heating take place	By electromagnetic wave heating take place
4. Heating mechanism involve-conduction	Heating mechanism involve-dielectric polarization and conduction.
5. Transfers of energy occur from the wall, surface of vessel, to the mixture and eventually to reacting species.	The core mixture is heated directly while surface is source of loss of heat.
6. All the compound in mixture are heated equally	In microwave, specific component can be heated specifically.
7. Heating rate is less	Heating rate is several fold high
8. In conventional, the highest temperature that can be achieved is limited by boiling point of particular mixture.	In microwave, the temperature of mixture can be raised more than its boiling point.

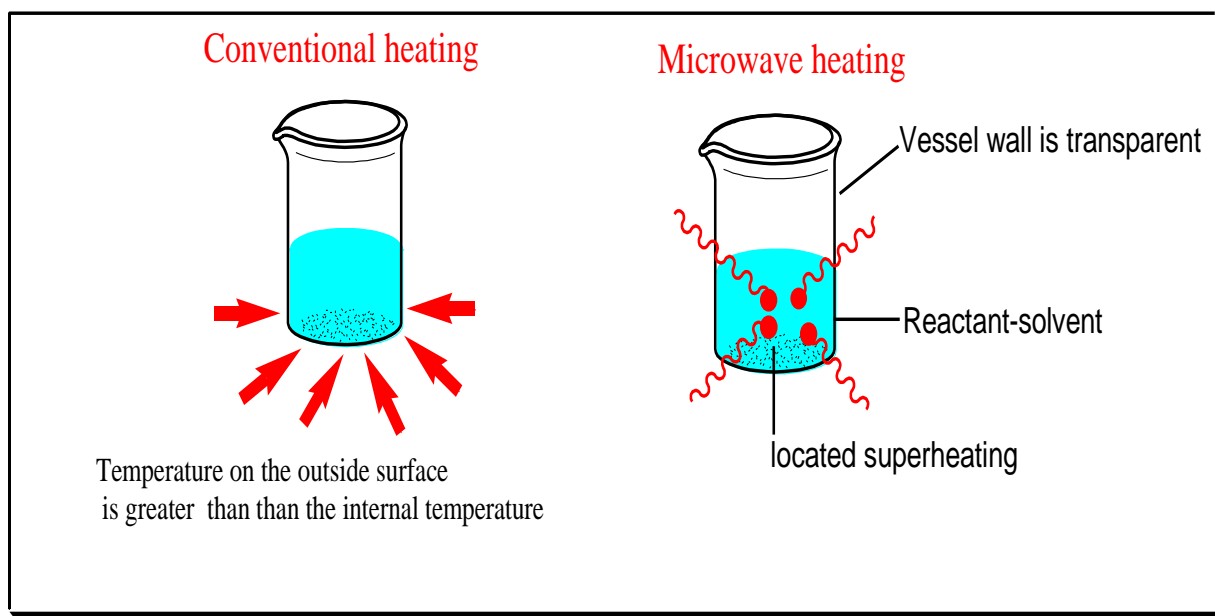


Figure 1.3 Difference between conventional and microwave heating

1.5 Scope of the work

The present research work proposed the surfacial modification of FA through suitable activation techniques in order to convert them into innovative support material having similar activity as other commercial support material. The fly ash supported ionic liquid catalyst reported in this work are synthesized by immobilization of ionic liquids using various methodologies viz. simple impregnation, grafting, sol-gel method, encapsulation, or pore trapping. The mechanical activation induces chemical phase transformation and enhanced reactivity of FA. Due to mechanical activation the solid particles of fly ash undergo a large number of inter/intra collisions which modify their surface properties by creating micro defects, increasing their silica percentage, amorphous or crystalline nature, specific surface area, surface roughness and catalytic activity etc. During the present work the chemical activation is performed to increase silica content and surface area due to leaching of metal ions from silico-aluminate skeleton and thus increasing surface free silanol groups. The fly ash supported ionic liquid catalysts are prepared in reflux assembly by refluxing ionic liquid with activated fly ash under N₂ atmosphere. The functionalization of ionic liquid is carried out either by creating covalent bonds between the IL and surface free silanol groups of activated FA, by physical adsorption onto FA. The synthesized catalysts are characterized by different analytical techniques like XRD, FTIR, SEM-EDX, TGA, BET surface area, UV-Visible, H¹NMR to evaluate their physico-chemical properties. The prepared catalysts are applied as potential heterogeneous catalysts for industrial important reactions such as esterification, Friedel-Crafts acylation, benzoylation etc. using conventional and microwave assisted methods. The foremost advantages of using microwave irradiations in this work are the very short time periods involved in the synthesis process, higher yield of products, enhanced reaction kinetics and simplifications of many reactions. The catalysts are investigated for recyclability and reuse to ensure the presence of sufficient stable active sites for number of cycles of organic synthesis. The reactions are performed in solvent free conditions, the catalysts are separated by simple filtration,

vacuum drying, regenerated and reused several times in eco-friendly and economic way. The present work elaborates microwave mediated synthesis of different ionic liquids which is further immobilized on activated FA to prepare a heterogeneous organocatalyst, active towards solvent free various organic transformations under dielectric heating. To the best of our knowledge, this report is novel as firstly presenting activated fly ash based supported ionic liquid catalyst. The present work provides a innovative pathway to utilize abundantly available solid waste fly ash, as support material for synthesis of highly selective supported ionic liquid catalysts.

1.6 References

1. S. Sobhani, M. Honarmand *Appl. Catal. A: Gen.* 467 (2013) 456–462.
2. T.S.Phan, C.W.Jones, *J.Mol.Catal.A:Chem.* 253 (2006)123–131.
3. Y.P. Sun, K. Fu , Y. Lin , W. Huang , *Acc. Chem. Res.* 35 (2002) 1096–1104.
4. H. Kuzmany, A. Kukovecz, F. Simon, M. Holzweber, Ch. Kramberger, T. Pichler, *Synthetic Met.* 141 (2004) 113–122.
5. P. Intarapong, S. Iangthanarat, A. Luengnaruemitchai, S. Jai-In , *Chiang Mai J. Sci.* 41 (2014) 128-137.
6. S. Chena, Z. Qina, X.Xub, J. Wang, *Appl. Catal A: Gen.* 302 (2006) 185–192.
7. S.P. Varkey, R. F. Lobo, K. H. Theopold, *Catal. Lett.* Vol. 88 (2003) 227–229.
8. M. Dams, L. Drijkoningen, B. Pauwels, G. Van Tendeloo, D. E. De Vos, P. A. Jacobs, *J. of Catal.* 209 (2002) 225–236.
9. J. P Patel, J. R. Avalani, D. K. Raval, *J. Chem. Sci.* 125, (2013) 531–536.
10. E. Błaż, J. Pielichowski, *Molecules* 11(2006) 115-120.
11. F. Adam, K. Kandasamy, S. Balakrishnan, *J. of Colloid Interface Sci.* 304 (2006) 137–143.
12. C. Khatri, D. Jain, A. Rani, *Fuel* 89 (2010) 3853–3859.

13. A. Rani, C. Khatri, R. Hada, *Fuel Process. Technol.* 116 (2013) 366- 373.
14. M. Tamura and H. Fujihara, *J. Am. Chem. Soc.* 125 (2003) 15742.
15. D. Girija, H. S. Bhojya Naik, B. V. Kumar, C. N. Sudhamani, *Amer. Chem. Sci. J.* 1(3) (2011) 97-108.
16. K. Marubayashi, S. Takizawa, T. Kawakusu, T. Arai, H. Sasai, *Org. Lett.* 5 (2003) 4409.
17. J. P. Patel, J. R. Avalani, D. K. Raval, *J. Chem. Sci.* 125 (2013) 531–536.
18. L. Tao An, J. P. Zou, L. L. Zhang, *Catal. Commun.* 9 (2008) 349–354.
19. V. M. Fuchs, L. R. Pizzio, M. N. Blanco, *Stud. in Surf. Sci. and Cataly.* 162 (2006) 793–800.
20. H.J. Yoon, S.M. Leea, J.H. Kim, H.J. Choa, J. W. Choi, S.H. Leeb, Y.S. Lee, *Tetrahedron Lett.* 49 (19) (2008), 3165–3171.
21. J.M. Zhu, F. Xin, Y.C. Sun, X. C. Dong, *Theor. Found. Chem. Eng.* 48 (2014) 787–792.
22. Y. Kawanami, H. Yuasa, F. Toriyama, S. Yoshida, T. Baba, *Catal. Commun.* 4 (2003) 455–459.
23. Y. Ono, T. Baba, *Catal. Today* 38 (1997) 321-337.
24. H. R. Shaterian, K. Azizi, N. Fahimi, *Arab. J. of Chem.* 10 (2012) S42–S55.
25. V. S. Marakatti, D. Mumbaraddi, G. V. Shanbhag, A. B. Halgeri, S. P. Maradur, *RSC Adv.* 5 (2015) 93452–93462.
26. A. Djaidja, A. Barama, M.M. Bettahar, *Catal. Today* 61 (2000) 303–307.
27. H.V. Lee, J. C. Juan, N. F. Binti Abdullah, R. Nizah MF, Y. H. Taufiq-Yap, *Chem. Cent. J.* 8 (2014) 30.
28. D. P. Sawant, B.M. Devassy, S.B. Halligudi, *J. of Mol. Catal. A: Chem.* 217 (2004) 211–217.
29. M. H. Sarvari, E. Sodagar, M. M. Doroodmand, *J. Org. Chem.* 76 (8) (2011) 2853–2859.
30. A. P. Maciel, M. H. A. Tavares, R. S. Melo, F. C. Silva, L. E. B. Soledade, C. J. Dalmaschio, E. R. Leite, E. Longo, *Cerâmica* 60 (2014) 154-159.
31. Y. Tang, J. Xu, X. Gu, *J. Chem. Sci.* 125 (2) (2013) 313–320.

32. A. P. Vyas a, N. Subrahmanyam, P. A. Patel, *Fuel* 88 (2009) 625–628.
33. P. Intarapong, S. Iangthanarat, A. Luengnaruemitchai, S. Jai-In, Chiang Mai J. Sci. 41(1) (2014) 128-137.
34. I. Kharbargar, R. Rohman, H. Mecadon, B. Myrboh, *Int. J. of Org. Chem.* 2 (2012) 282-286.
35. Y.Wu, X. Chen, W. Dong, C. Zhao, Z. Zhang, D. Liu, C. Liang, *Energy Fuels* 27 (8) (2013) 4804–4809.
36. R. Bal, S. Sivasanker, *Appl. Catal. A: Gen.* 246 (2003) 373–382.
37. L. Q. Wu, Y. F. Wu, C. G. Yang, L. M. Yang, L. J. Yang, *J. Braz. Chem. Soc.* 21 (5) (2010) 941-945.
38. C. R. Deltcheff, A. Aouissi, S. Launay, M. Fournier, *J. of mol. Catal. A: Chem.* 114(1-3) (1996) 331-342.
39. P. C. Giancarlo, G. M. Emanuele P. V. Santacroce, R. Maggi. *ARKIVOC* 7 (2015) 1-9.
40. M. A. Zolfigol, A. Khazaei, A. Zare, M. Mokhlesi, T. Hekmat-Zadeh, A. Hasaninejad, F. Derakhshan-Panah, A. R. Moosavi-Zare, H. Keypour, A. Ali Deghani-Firouzabadi, M. Merajoddin, *J. of Chem. Sci.* 124(2) (2012) 501-508.
41. K. P. Boroujeni, *Turk J Chem.* 34 (2010) 621 – 630.
42. J. Zhu, A. Holmen, D. Chen, *Chem.Cat. Chem.* 5 (2013) 378–401.
43. Q. Zhang, J.Q. Huang, M.Q. Zhao, W.Z. Qian, F. Wei, *Chem.Sus.Chem.* 4 (2011)864–889.
44. D.S. Su, *Chem. Sus. Chem.* 4 (2011) 811–813.
45. N. Muthuswamy, J.L.G. de la Fuente, P. Ochal, R. Giri, S. Raaen, S. Sunde, M.Rønning, D. Chen, *Phys. Chem. Chem. Phys.* 15 (2013) 3803–3813.
46. C. Li, Z.F. Shao, M. Pang, C.T. Williams, C. Liang, *Catal. Today* 186 (2012) 69–75.
47. J.L. Figueiredo, M.F.R. Pereira, *Catal. Today* 150 (2010) 2–7.
48. J. Zhang, X. Liu, R. Blume, A. Zhang, R. Schlogl, D.S. Su, *Sci.* 322 (2008) 73-77.

49. D. Lee, *Molecules* 18 (2013) 8168-8180.
50. A. Davoodnia, A. Tavakoli-Nishaburi, N. Tavakoli-Hoseini, *Bull. of the Korean Chem. Soc.* 32 (2) (2011) 635-638.
51. X.Y. Liu, M. Huang, H. L. Ma, Z. Q. Zhang, J. M. Gao, Y. L. Zhu, X. J. Han, X. Y. Guo, *Molecules* 15 (2010) 7188-7196.
52. M. Sarangi, S. Bhattacharyya, R. C. Behera, *Phase transition* 82 (5) (2009) 377 — 386.
53. V. Panwar, A. Bansal, S. S. Ray, S. L. Jain, *RSC Adv.* 6 (75) (2016) 71550-71556.
54. F. Shirini, S. A. Dadamahaleh, A. M. Khah, *Chin. J. of Catal.* 34 (2013) 2200–2208.
55. F. Adam, J. Andas, *J. of Colloid and Inter. Sci.* 311 (2007) 135–143.
56. F. Adam, K. M. Hello, T. H. Ali, *Appl. Catal. A: Gen.* 399 (2011) 42–49.
57. T. J. Al-Hasani , H. H. Mihsen , K. M. Hello, F. Adam, *Arab. J. of Chem.* 10 (2017) S1492–S1500.
58. S. Wang, H. Wu, *J. Hazard. Mater.* 136 (2006) 482–501.
59. ASTM standard specification for coal fly ash and raw or calcined natural pozzolan for use in concrete (C618-05). In: Annual book of ASTM standards, concrete and aggregates, vol. 04.02. American Society for Testing Materials 2005.
60. J. Pizarroa, X. Castillob, S. Jarab, C. Ortizc, P. Navarrob, H. Cidc, H. Riosecoa, D. Barrosc, N. Belzile, *Fuel* 156 (2015) 96–102.
61. C. Khatri, M.K. Mishra, A. Rani, *Fuel Proces. Technol.* 91 (2010) 1288–1295.
62. P. Pradhan, R. Chakraborty, *Asia-Pac. J. Chem. Eng.* 11 (2016) 4–13.
63. D. Jain, A. Rani, *Am. Chem. Sci. J.* (2011) 37–49.
64. A.Rani, C. Khatri, R. Hada, *Fuel Process Technol.* 116 (2013) 366-373.
65. C. Khatri, D. Jain, A. Rani, *Fuel* 89 (2010) 3853–3859.
66. K. Srivastava, V. Devra, A. Rani, *Fuel Process Technol.* 121 (2014) 1-8.
67. D. Jain, M.K. Mishra, A. Rani, *Fuel Process. Technol.* 95 (2012) 119–126.

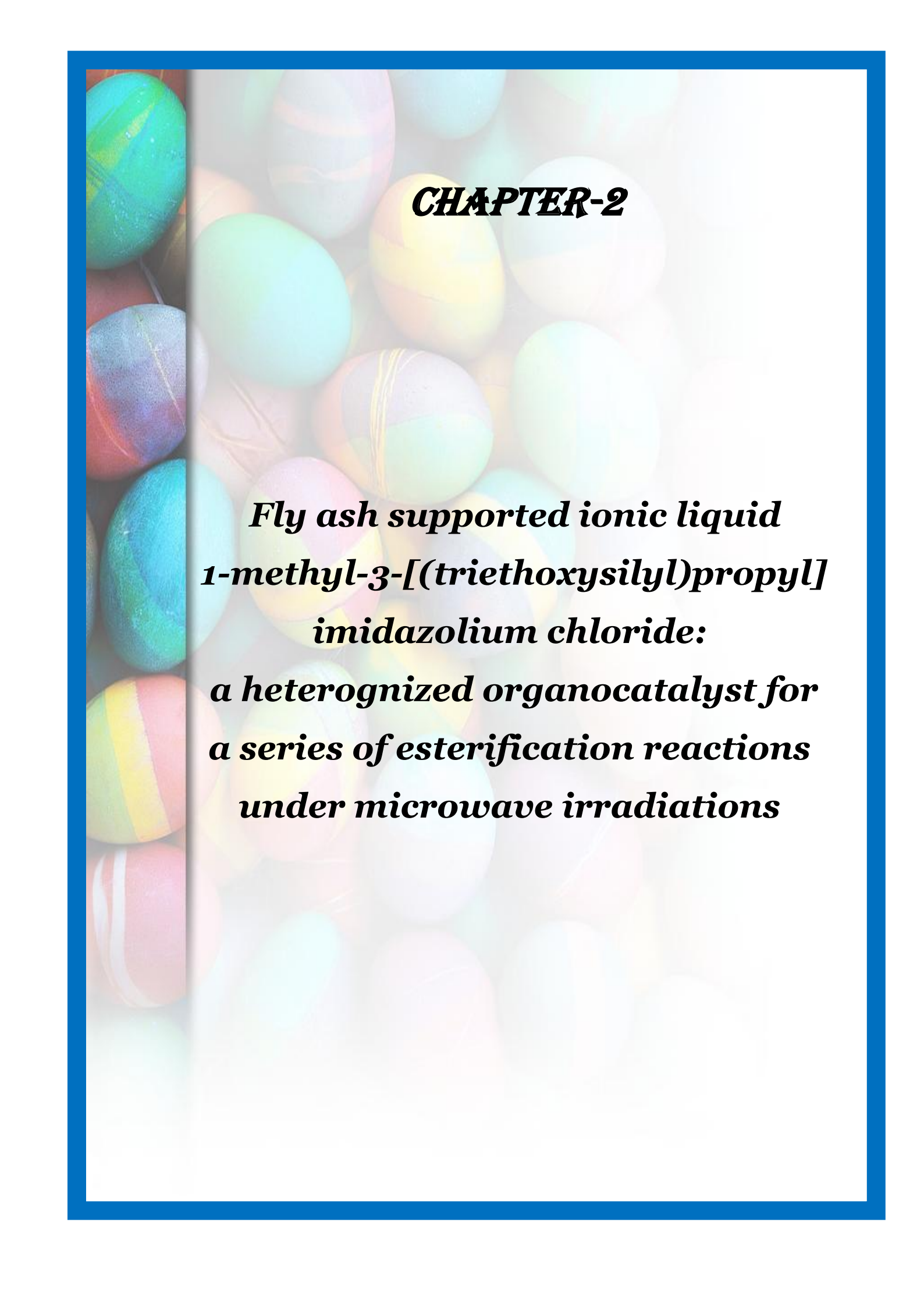
68. V. Radonjića, J. Krstića, D. Lončarevića, D. Jovanovića, N. Vukelićb, M. Stankovića, D. Nikolovac, M. Gabrovska, *Russ. J. of Phys. Chem. A* 89 (13)(2015) 2359–2366.
69. A. Ramazani, M. Rouhani, E. Mirhadi, M. Sheikhi, K. Šlepokura, T. Lis, *Nano. Chem. Res.* 1(1) (2016) 87-107.
70. E. Kolvari, N. Koukabi, M. M. Hosseini, *J. of Mol. Catal. A: Chem.* 397 (2015) 68–75.
71. M. Esmailpour, B. Akhlaghinia, R. Jahanshahi, *J. Chem. Sci.* 129 (3) (2017) 313–328.
72. J. Mondal, M. Nandi, A. Modak, A. Bhaumik, *J. of Mol. Catal. A: Chem.* 363–364, (2012) 254–264.
73. X. B. Tang, L.S. Qiang, J. Ma, Y. L. Yang, *Sci. of Adv. Mater.* 3 (6) (2011) 1019-1024.
74. S. Himmler, S. Horma, R. van Hal, P.S. Schulz, P. Wasserscheid, *Green Chem.* 8 (2006).
75. D.C. Donata, F. Marida, H. Migen, University of Torino, <http://lem.ch.unito.it/didattica/infocimica/Liquidi%20Ionici/Composition.html> (accessed 20 June, 2006).
76. T. Welton, *Chem. Rev.* 99 (1999) 2071–2084.
77. J.F. Brennecke, E.J. Maginn, *AIChE J.* 47 (2001) 2384–2388.
78. A. Shariati, K. Gutkowski, C.J. Peters, *AIChE J.* 51 (2005) 1532–1540.
79. L. Crowhurst, P. Mawdsley, J.M. Perez-Arlandis, P.A. Salter, T. Welton, *Phys. Chem.* 5 (2003) 2790.
80. S. Caddick, *Tetrahedron* 51 (1995) 10403.
81. N. E. Leadbeater and H. M. Torenius, *J. Org. Chem.* 67(9) (2000) 3145.
82. A. Aupoix, B. Pe'got, G. Vo-Thanh, *Tetrahedron* 66 (2010) 1352–1356.
83. B. Xin, J. Hao, *Chem. Soc. Rev.* 43 (2014) 7171–7187.
84. D.W. Kim, D. Y. Chi, *Angew. Chem. Int. Ed.* 43 (2004) 483.
85. B. Xin, J. Hao, *Chem. Soc. Rev.* 43 (2014) 7171–7187.
86. H. Li, P.S. Bhadury, B. Song, S. Yang, *RSC Adv.* 2 (2012) 12525–12551.

87. S. Breitenlechner, M. Fleck, T.S. Müller, A. Suppan, *J. Mol. Catal. A* 214 (2004) 175.
88. D.W. Kim, D.Y. Chi, *Angew. Chem. Int. Ed.* 43 (2004) 483.
89. P. Virtanen, J. P. Mikkola, T. Salmi, *Ind. Eng. Chem. Res.* 46 (2007) 9022-9031.
90. C. V. Doorslaer, J. Wahlen, P. Mertens, K. Binnemans, D. De Vos, *Dalton Trans.* 39 (2010) 8377–8390.
91. A. Riisager, R. Fehrmann, S. Flicker, R. van Hal, M. Haumann, P. Wasserscheid, *Angewandte Chemie-International Edition* 44 (2005) 815.
92. A. Wolfson, I. F. J. Vankelecom and P. A. Jacobs, *Tetrahedron Lett.* 44 (2003) 1195.
93. H. Hagiwara, Y. Sugawara, K. Isobe, T. Hoshi and T. Suzuki, *Org. Lett.* 6 (2004) 2325.
94. C. Sievers, O. Jimenez, R. Knapp, X. Lin, T. E. Muller, A. Turler, B. Wierczinski and J. A. Lercher, *J. Mol. Catal. A: Chem.* 279 (2008) 187.
95. C. deCastro, E. Sauvage, M. H. Valkenberg and W. F. Holderich, *J. Catal.* 196 (2000) 86–94.
96. C. P. Mehnert, E. J. Mozeleski and R. A. Cook, *Chem. Commun.* (2002) 3010–3011.
97. H. Hagiwara, Y. Sugawara, K. Isobe, T. Hoshi and T. Suzuki, *Org. Lett.* 6 (2004) 2325–2328.
98. S. Breitenlechner, M. Fleck, T. E. Muller and A. Suppan, *J. Mol. Catal. A: Chem.* 214 (2004) 175–179.
99. H. Hagiwara, Y. Sugawara, K. Isobe, T. Hoshi, T. Suzuki, *Org. Lett.* 6 (2004) 2325–2328.
100. L.F. Xiao, F.W. Li, J.J. Peng, C.G. Xia, *J. Mol. Catal. A Chem.* 253 (2006) 265–269.
101. M. Gruttadauria, S. Riela, P.L. Meo, F. D’Anna, R. Noto, *Tetrahedron Lett.* 45 (2004) 6113–6116.

102. L.L. Lou, K. Yu, F. Ding, W. Zhou, X. Peng, S. Liu, *Tetrahedron Lett.* 47 (2006) 6513–6516.
103. C. P. Mehnert, *Chem.–Eur. J.* 11 (2005) 50–56.
104. J. Miao, H. Wan, Y. Shao, G. Guan, B. Xu, *J. of Mol. Catal. A: Chem.* 348 (2011) 77–82.
105. Y. Lin, F. Wang, Z. Zhang, J. Yang, Y. Wei, *Fuel* 116 (2014) 273–280.
106. P. H. Li, B. L. Li, H. C. Hu, X. N. Zhao, Z. H. Zhang, *Catal. Commun.* 46 (2014) 118–122.
107. K. B. Sidhpuria, A. L. D. D. Silva, T. Trindade, J. A. P. Coutinho, *Green Chem.* 13 (2) (2011) 340–349.
108. J. Sun, W. Cheng, W. Fan, Y. Wang, Z. Meng, S. Zhang, *Catal. Today* 148 (2009) 361–367.
109. M. j. Jin, A. Taher, H. j. Kang, M. Choi, R. Ryoo, *Green Chem.* 11 (3) (2009): 309–313.
110. C. P. Mehnert, E. J. Mozeleski, R. A. Cook, *Chem. Commun.* 24 (2002) 3010–3011.
111. T. Sasaki, M. Tada, C. Zhong, T. Kume, Y. Iwasawa, *J. of Mol. Catal. A: Chem.* 279 (2008) 200–209.
112. J. Isaad, *RSC Adv.* 4 (2014) 49333.
113. M. Seddighi, F. Shirini, M. Mamaghani, *C. R. Chimie* xxx (2015) xxx–xxx.
114. H. Qiu, S. M. Sarkar, D. H. Lee, M. j. Jin, *Green Chem.* 10 (2008) 37–40.
115. L. Han, S. W. Park, D. W. Park, *Energy Environ. Sci.* 2 (2009) 1286–1292.
116. H. Hagiwara, Y. Sugawara, K. Isobe, T. Hoshi and T. Suzuki, *Org. Lett.* 6 (2004) 2325.
117. Y. Yang, C. Deng, Y. Yuan, *J. of Catal.* 232 (2005) 108–116.
118. H. Hagiwara, T. Nakamura, T. Hoshi, T. Suzuki, *Green Chem.* 13 (2011) 1133–1137.
119. R. Knapp, A. Jentys, J. A. Lercher, *Green Chem.* 11 (2009) 656–661.
120. S. Doherty, P. Goodrich, C. Hardacre, V. P[^]arvulescu, C. Paun, *Adv. Synth. Catal.* 350 (2008) 295.

121. B. M. L. Dooos, P. A. Jacobs, *J. Catal.* 243 (2006) 217.
122. Q. Zhang, J. Luo, Y. We, *Green Chem.* 12 (12) (2010): 2246-2254.
123. X. Zhang, D. Wang, N. Zhao, A. S.N. Al-Arifi, T. Aouak, Z. A. Al-Othman, W. Wei a, Y. Sun, *Catal. Commun.* 11 (2009) 43–46.
124. J. Sun, W. Cheng, W. Fan, Y. Wanga, Z. Meng, S. Zhang, *Catal. Today* 148 (2009) 361–367.
125. Li Q. Kang, Y. Q. Cai, Lin Cheng, *Monatsh Chem.* 144(2) (2013): 247-249.
126. B. Karimi, A. Maleki, D. Elhamifar, J. H. Clark, A. J. Hunt, *Chem. Commun.* 46 (2010) 6947–6949.
127. L.Q. Kang, Y.Q. Cai, Y.Q. Peng, X. L. Ying, G. H. Song, *Mol Divers* 15 (2011) 109–113.
128. J. Zhu, P.C. Wang, M. Lu, *RSC Adv.* 2 (2012) 8265–8268.
129. S. Ivanova, L. F. Bobadilla, A. Penkova, F. R. Sarria, M. A. Centeno, J. A. Odriozola, *Catalysts* 1 (2011) 52-68.
130. M. I. Burguete, H. Erythropel, E. G. Verdugo, S. V. Luis, V. Sans, *Green Chem.* 10 (2008) 401–407.
131. R. Sugimura, K. Qiao, D. Tomida, C. Yokoyama, *Catal. Commun.* 8 (2007) 770–772.
132. E. J. G. Suárez, C. M. Vázquez, A. B. García, *J. of Mol. Liq.* 169 (2012) 37–42.
133. B. Karimi, M Vafaezadeh, *Chem. Commun.* 48 (27) (2012) 3327-3329.
134. J. Safari, Z. Zarnegar, *C. R. Chimie* xxx (2013) xxx–xxx.
135. H. Alinezhad, M. Tajbakhsh, N. Ghobad, *Res Chem Intermed.* 41 (2015) 9979–9992.
136. A. Loupy, A. Petit, J. Hamelin, F. T. Boulet, P. Jacquault, D. Mathé, *Synthesis* 9 (1998) 1213-1234.
137. A. S. Grewal, K. Kumar, S. Redhu, S. Bhardwaj, *Int. Res J Pharm. App Sci.* 3 (5) (2013) 278-285.
138. N. E. Leadbeater, H. M. Torenus, *J. Org. Chem.* 67(9) (2002) 3145.
139. H. Zhao, V. Malhotra, *Aldrichimica Acta* 35 (2002) 75-83.

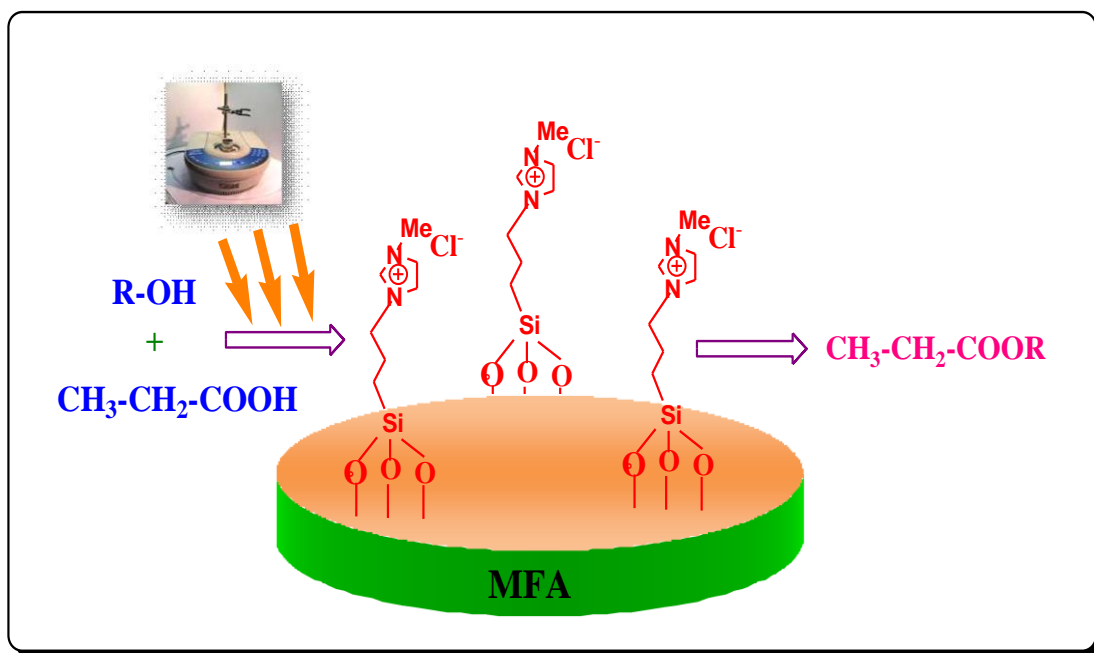
140. J. Karkkainen, J. Asikkala, R.S. Laitinen, M.K.Z. Lajunen, *Naturforsch. B* 59 (2004) 763-770.
141. R.M. Palou, *J. Mex. Chem. Soc.* 51(4) (2007) 252-264.

The background of the slide is a collection of colorful Easter eggs in various colors including green, blue, yellow, pink, and purple. Some eggs have stripes or patterns. The eggs are arranged in a way that they appear to be in a basket or scattered together. The overall image is slightly faded and serves as a decorative backdrop for the text.

CHAPTER-2

***Fly ash supported ionic liquid
1-methyl-3-[(triethoxysilyl)propyl]
imidazolium chloride:
a heterognized organocatalyst for
a series of esterification reactions
under microwave irradiations***

Abstract



Esterification reaction over fly ash supported 1-methyl-3-[triethoxysilyl propyl]imidazolium chloride

2.1. Introduction

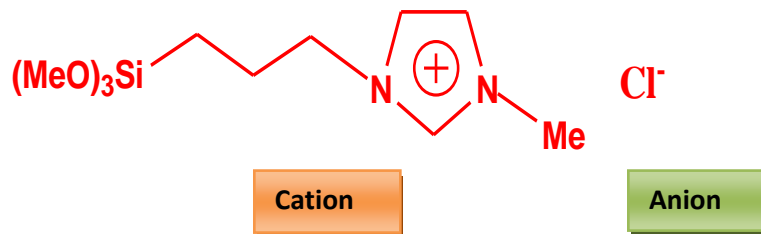
Organic esters are widely used in a variety of industries such as flavoring, perfumery, pharmaceuticals, plastics, solvents, and intermediates [1]. Flavor esters have great importance due to their application mainly in food additive, perfume ery and fragrance, but also as environment benign- solvents and intermediates in chemical and pharmaceutical processes. Particular butyl propionate is mainly used for painting, appliance coatings or for automobile repainting. Commonly liquid inorganic acid catalysis and solid acid catalysis are widely used for synthesis of esters. However, homogeneous acids [2,3] cause corrosion in reaction vessel and need to be neutralized with large amounts of base after the reaction which is not environmentally friendly. Solid acid catalysts[4,5,6] also have their disadvantages such as easy deactivation and adsorption of products which make their application limited[7]. Thus there is an urgent need to replace such unsafe catalysts by eco-friendly, green, noncorrosive, sustainable catalysts.

Among the recent advancements in green catalysis, the use of ionic liquids especially those based on imidazolium derivative cations have become an interesting area of research. Imidazolium ionic liquids (ILs) possess pre-organized structures mainly through hydrogen bonds which induce structural directionality[8]. These IL structures can adapt or be adaptable to many species, as they provide hydrophobic or hydrophilic regions, and a high directional polarizability [9,10] The high thermal stability, high conductivity, low vapour pressure and structure tuneability make ILs a versatile material for designing innovative catalytic system for numerous synthetic applications[11, 12] 1-alkyl-3-methylimidazolium ionic liquids (ILs) had high efficiency for catalyzing the formylation of amines using CO₂ and phenylsilane at room temperature, producing the corresponding formylated products in excellent yields under the metal free condition[13]. A task-specific Imidazolium-Based Phosphinite Ionic Liquid was found to efficiently catalyze the Knoevenagel condensation of arylaldehydes with malononitrile, dimethyl(diethyl)malonate, and ethyl cyanoacetate[14]. Based on economic criteria, it is desirable to reduce amount of ionic liquid utilized in

potential process. Recently, immobilization processes involving ionic liquids on various solid supports have been introduced in which minimum amount of IL is required to catalyze organic reactions. Supported ionic liquid catalysts are prepared by fixing thin film of IL on active solid supports via different methods such as simple impregnation, grafting, polymerization, sol-gel method, encapsulation, or pore trapping[15-21], have achieved high catalytic performance in the field of organic synthesis through green catalytic pathways.

Immobilized ionic liquids have been used as novel heterogeneous catalysts for catalyzing various reactions such as esterification, nitration reactions[22], acetal formation[23], Baeyer-Villiger reaction[24], synthesis of α -aminonitriles[25] and bis-pyrazolones[26]. Knoevenagel condensation reactions[27], cycloaddition reaction[28] Henry reaction[29], acetalization reaction[30], hydrogenation of alkynes[31], Suzuki coupling reactions[32], CO₂ cycloaddition reactions[33]. Several catalyst have been synthesized by immobilization of number of imidazolium based ILs on various mesoporous materials such as on silica gel[34], SBA-15[35], magnetic nanoparticles[36] giving highly selective product.

In the present research an innovative support material Fly ash is selected which is a solid waste generated in power plants and being rich in silica is recently used in synthesizing several heterogeneous catalysts[37-42] having wide applications in production of many drug intermediates and fine chemicals under thermal and microwave heating both. Mechanical milling of fly ash has significantly increased surface roughness and silanol groups to make it an efficient, cost effective catalytic support material for synthesizing green heterogeneous catalysts. In the present work we have described efficient solventless one-pot procedure for the synthesis of liquid **1-methyl-3-[(triethoxysilyl) propyl] imidazolium chloride (TMICl)** under microwave irradiation in which 1-methylimidazole was modified by organosilane (3-chloropropyl triethoxysilane). The molecular structure of TMICl is give in Scheme 2.1.



Scheme 2.1: The structure of 1-methyl-3-[(triethoxysilyl)propyl] imidazolium chloride

The prepared ionic liquid is immobilized on mechanically activated fly ash (MFA) by co-condensation method to develop an active organocatalyst (TMICl/MFA). The properties of samples were characterized by different techniques viz, XRD, FTIR, SEM-EDX, TGA, BET surface area, UV-Visible, H^1 NMR are used. The prepared TMICl/MFA catalyst is tested for microwave assisted esterification of aliphatic alcohols and propionic acid.

2.2 Experimental

2.2.1 Materials

Fly ash [Class F type ($SiO_2 + Al_2O_3$) > 70%], collected from Kota Thermal Power Plant (Rajasthan, India) was used as support for the preparation of the supported ionic liquid catalyst. Acids and alcohols were obtained from S.D. Fine Chem. Ltd., India. Ionic liquid precursors 1-methylimidazole (99%), 3-chloropropyltriethoxysilane (95%) were purchased from Sigma Aldrich.

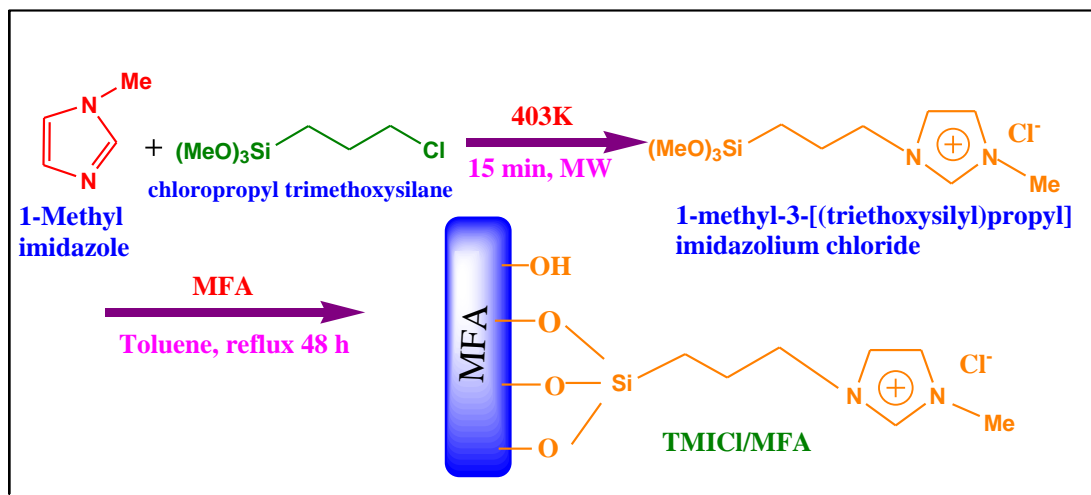
2.2.2 Catalyst preparation

- *Activation of Fly ash*

As received Fly ash (FA) was washed with distilled water followed by drying at 100°C for 3h, thereafter mechanical activation was performed using high energy planetary ball mill (Retsch PM-100, Germany) in an agate grinding jar using agate balls of 5 mm ball sizes for 5, 10, 15 and 40 h with 250 rpm to get mechanically activated fly ash (MFA 5-40). The ball mill was loaded with ball to powder weight ratio (BPR) of 10:1. All mechanically activated samples were thermally activated by calcination at 800°C for 3h to remove carbon, sulphur and other adsorbed moieties. MFA-40 having higher specific surface area (36 m²/g) was selected for immobilizing ionic liquid.

Synthesis of imidazolium based ionic liquid

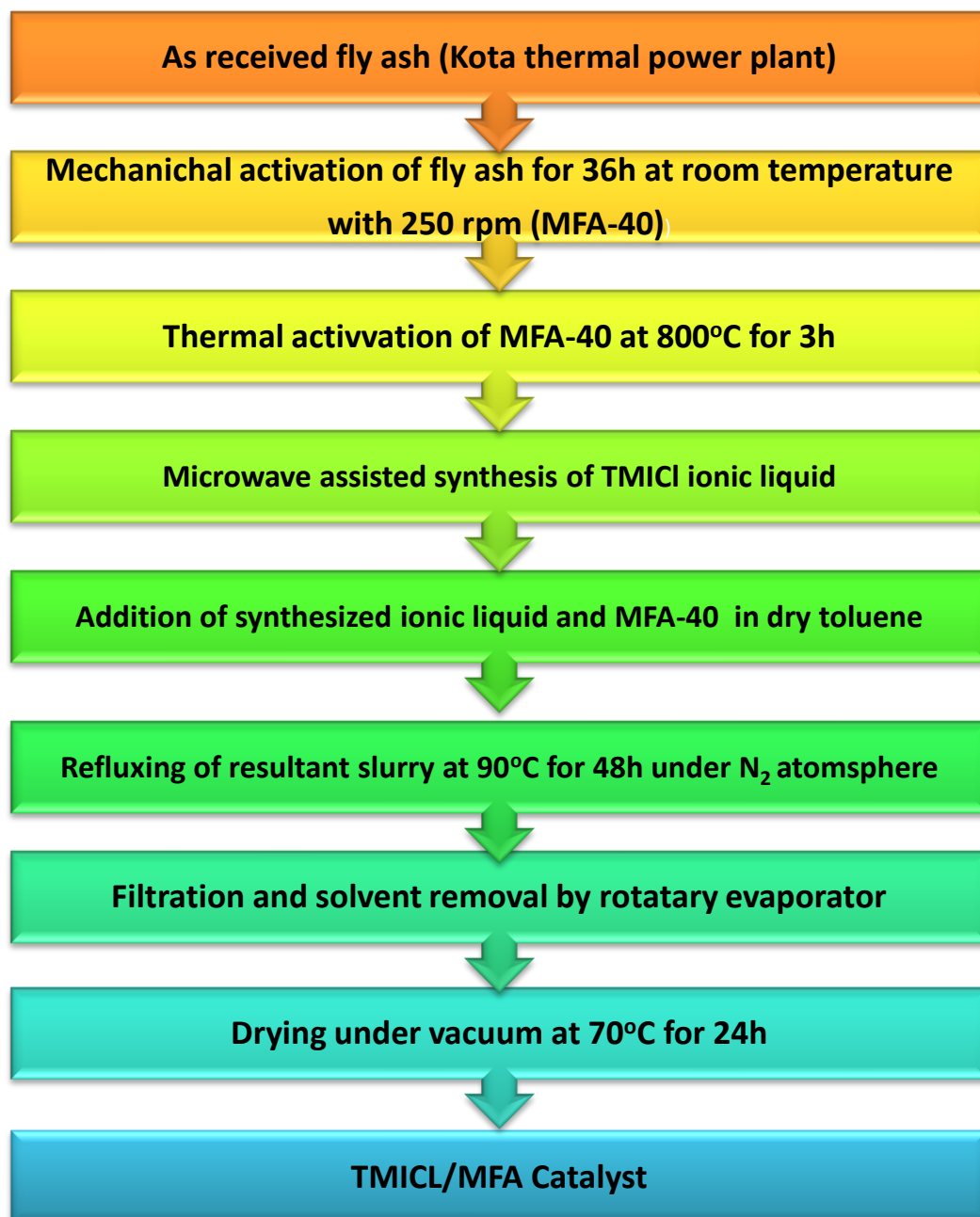
For synthesis of 1-methyl-3-[(triethoxysilyl)propyl] imidazolium chloride (TMICl, Scheme 2.2) mixture of 1-methylimidazole (0.82gm, 10mmol) and chloropropyl trimethoxysilane (1.98gm, 10mmol) was sealed in stirred closed tube of microwave batch synthesis system under N₂ atmosphere at 120° C for 15 min at 50 psi pressure. The obtained yellowish viscous liquid was brought to room temperature and thoroughly washed three times with diethyl ether (3×20ml). The diethyl ether was removed by rotatory evaporator. The viscous product was dissolved in methylene chloride and subsequently filtered over silica gel and dried overnight in a vacuum at 70 °C. The TMICl was characterized by ¹H NMR (CDCl₃): 10.80(s,1H), 7.39(s,1H), 7.30(s,1H), 4.37(t,2H), 4.12(s,3H), 3.80(q,6H), 2.02(q,2H), 1.21(t,9H), 0.60(t,2H). IR (CDCl₃, cm⁻¹): 667.53, 756.27, 1135.8, 1061, 1464.98, 1571.65, 1588.69, 1637.37, 2860.08, 2936.74, 2962.73, 3416.57.



Scheme 2.2. The synthesis route of TMICl functionalized FA.

Synthesis of TMICl/MFA

Prior to immobilization, MFA-40 was activated at 550°C for 1 h and TMICl was dried at 70°C under vacuum for 1 h. The pretreated MFA-40 (5gm) and 2gm of TMICl were co-dispersed in 50 ml dry toluene in a refluxing assembly under vacuum. The mixture was refluxed under N₂ atmosphere at 90°C for 48 h. The toluene solvent was removed by filtration and solid material was transferred to a rotary evaporator. The excess of physisorbed ionic liquid was removed using rotatory evaporator under reduced pressure. Finally the solid was dried under vacuum at 70°C for 24 h to give brown powder of TMICl/MFA to be used as a catalyst (Scheme-2.2) for esterification reactions. The steps of synthesis TMICl/MFA catalyst are summarized in Scheme 2.3.



Scheme 2.3 : Steps for Synthesis of TMICL/MFA Catalyst

2.2.3 Equipment

Microwave synthesizer

The reactions are performed on single mode, PC operated synergy.exe software based microwave equipment (CEM Focussed MicrowaveTM Synthesis System, Model Discover) shown in Figure 2.1, comprising of closed and open vessel system, with a working frequency of 2.45GHz, temperatures ranging from 25-250°C, pressure range from 0-300 Psi. an infrared detector controls the temperature during the reaction and teflon spill cup protects the detector from exposure. An air compressor connected with the equipment is utilized for cooling of reactions. The reactions are preferred in Power_{MAX} mode, using simultaneous heating and cooling method, under controlled conditions as maximum number of microwave radiations is utilized in this work.

The Discover system used in this study consists of following steps:

- **Infrared temperature control system-** the standard temperature control system consists of non-contact infrared sensor which monitors and controls the temperature conditions of the reaction vessel located in the instrument cavity. The temperature sensor is centrally located beneath the cavity floor and looks up at the bottom of the vessel, shown in Figure 2.2(a). a lens is positioned between sensor and cavity floor to protect the sensor. The temperature sensor data is set up in a feedback control loop with the magnetron to regulate the power output to maintain the temperature setpoint through the onboard processor.
- **IntelliventTM pressure control system-** this pressure control system as shown in Figure 2.2(b) consists of load cell to enable pressure measurement and control of the reaction environment that senses changes in the external deflection of the septa on top of the sealed pressure vial. The sensor housing incorporates a capture and release mechanism that secures the reaction vessel in the cavity with operator selectable power out from 0-300 watts(+/-) programmable in 1-watt increments.

- A self adjusting, single mode microwave cavity that is manually accessed via multiple attenuator ports (both ports are included)
- A 4-line x 20-character vacuum fluorescent display with alphanumeric keypad and on-board computer for programming and operational control of the system.
- 3 safety interlocks and an interlock monitoring system to prevent microwave emission when the attenuator port is not properly installed.
- **Stirring option-** the stirring option consists of a rotating magnetic plate located below the floor of the microwave. Stirring occurs when the rotating the magnetic field couples with stir bar in the vessel.
- **Cooling option-** The cooling option consists of necessary valves and ports to direct a cooling gas (either nitrogen or clean air) onto the vessel in the system cavity. This option will decrease the temperature of a 2ml solution in a 10ml pyrex reaction vessel from 150 °C to 40 °C in less than 120 seconds. The gas is user supplied at a minimum pressure level of 20 psi (1.5 bar) and flow rate of 25 liters/min.

Rotary evaporator

A Rotary evaporator (Heidolph G3, Germany) is used for the efficient and gentle removal of solvents from samples by evaporation as shown in Figure 2.3. Rotary evaporation is a technique most commonly used in organic chemistry to remove a solvent from a higher-boiling point compound of interest. A typical rotary evaporator has a water bath that can be heated in either a metal container or crystallization dish.. This keeps the solvent from freezing during the evaporation process. The solvent is removed under vacuum, is trapped by a condenser and is collected for easy reuse or disposal.

High energy planetary ball mill

RETSCH Planetary Ball Mills as shown in Figure 2.4 pulverize and mix soft, medium-hard to extremely hard, brittle and fibrous materials. They are suitable for both dry and wet grinding. These versatile mills are used successfully in virtually all industry and research sectors, where the quality control process places the highest demands on purity, speed, fineness and reproducibility.

2.2.4 Catalyst characterization

Physicochemical properties of all prepared samples are evaluated using XRD, FTIR, SEM-EDX, TGA, BET surface area, UV-Visible, $^1\text{H-NMR}$ techniques as described in **Annexure-I**. Crystallite size of the crystalline phase was determined from the peak of maximum intensity ($2\theta = 26.57$) by using Scherrer formula (Cullity et al., 2001) as Eq. (2.1) with a shape factor (K) of 0.9.

$$\text{Crystallite size} = K \cdot \lambda / W \cdot \cos\theta \quad (2.1)$$

where, $W = W_b - W_s$; W_b is the broadened profile width of experimental sample and W_s is the standard profile width of reference sample.

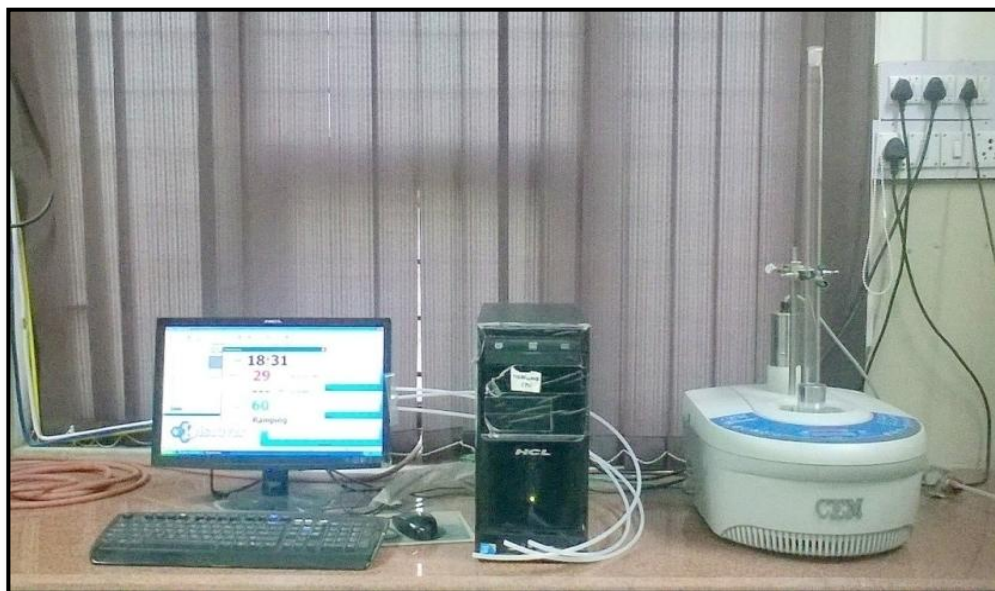


Figure 2.1: CEM Focused MicrowaveTM Synthesis System (Discover Model)

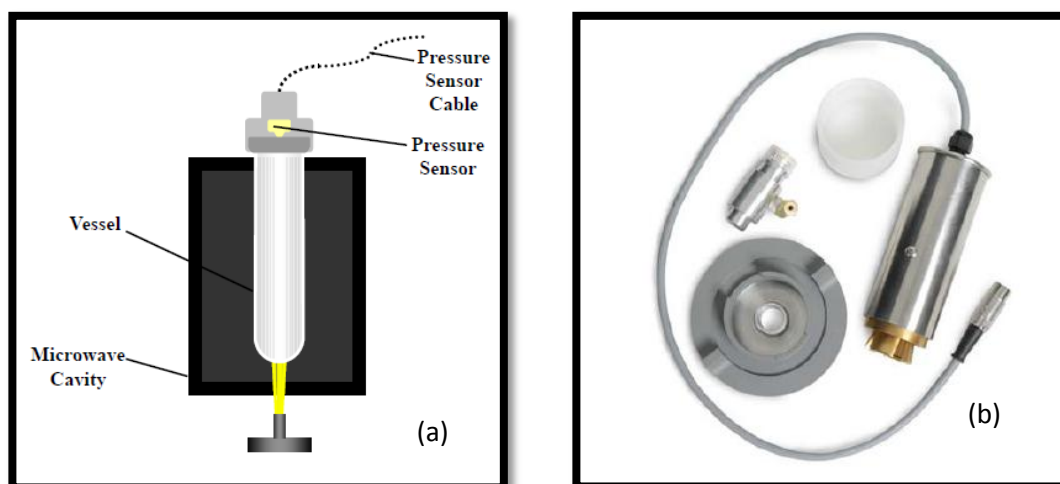


Figure 2.2: (a) Infrared temperature sensor and (b) Intelligent pressure sensor assembly



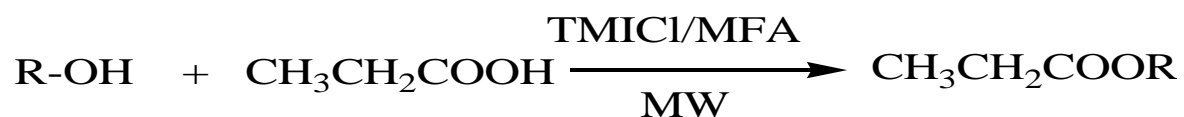
Figure 2.3 : Rotary evaporator (Heidolph G3, Germany)



Figure 2.4: RETSCH Planetary Ball Mill

2.2.5 Catalytic activity of TMICl/MFA

In order to evaluate the catalytic behaviors of TMICl/MFA catalyst the microwave assisted solvent free esterification of different alcohols with propanoic acid was tested. (Scheme 2.4).



Scheme 2.4: Microwave-assisted solvent-free synthesis of ester over TMICl/MFA catalyst

The typical procedure was performed as follows, 20 mmol of aliphatic alcohol, 10 mmol of propanoic acid were filled in reactor tube. The reaction mixture was fed with preheated (80 °C, 1h) catalyst in acid/catalyst weight ratio of 5:1. The reaction is

carried out in closed vessel system at 300 Psi pressure, by placing the vial on microwave cavity under constant stirring at different time periods, temperatures and power outputs. Then, the system is shut by an attenuator which prevents the passage of harmful microwaves into surroundings. After input of temperature, hold time, power and pressure parameters, the reaction is started by clicking on 'Play' button under $\text{Power}_{\text{max}}$. On conditions Initially, a beep sound appears and reaction runs on 'Ramp time' mode. Therein, the equipment attains all the desired parameters and then mode changes to 'Hold time', where the reaction runs for the specified time period under simultaneous heating and cooling conditions. Usually, equipment takes 10-15 minutes to achieve all the set points i.e., ramp time. After completion of holding time, the instrument is turned off and the reaction is cooled through air compressor. Then, the catalyst is separated the product is purified and conversion analyzed by Gas Chromatograph. Figure 1.3 shows an example heating profile of a typical microwave experiment, in which the parameters are accurately measured and recorded throughout the whole experiment process. The filtered catalyst is washed with dichloromethane to remove organic impurities. The ester was isolated by transferring into a separatory funnel together with 250 mL brine and basifying the mixture using NaHCO_3 . The resultant organic layer was dried over anhydrous sodium sulphate and solvent removed under reduced pressure. The desired product was characterized by FTIR. The reaction conditions were varied to obtain maximum yield and conversion into ester. The reactions were analyzed using a GC with oven temperature range 70-240°C and N_2 (25 ml/min) as a carrier gas. The yield of ester was calculated by selectivity and conversion from GC analysis using following equation (2.2).

$$\text{selectivity}(\%) = \frac{\text{yield}}{\text{conversion}} \times 100 \quad (2.2)$$

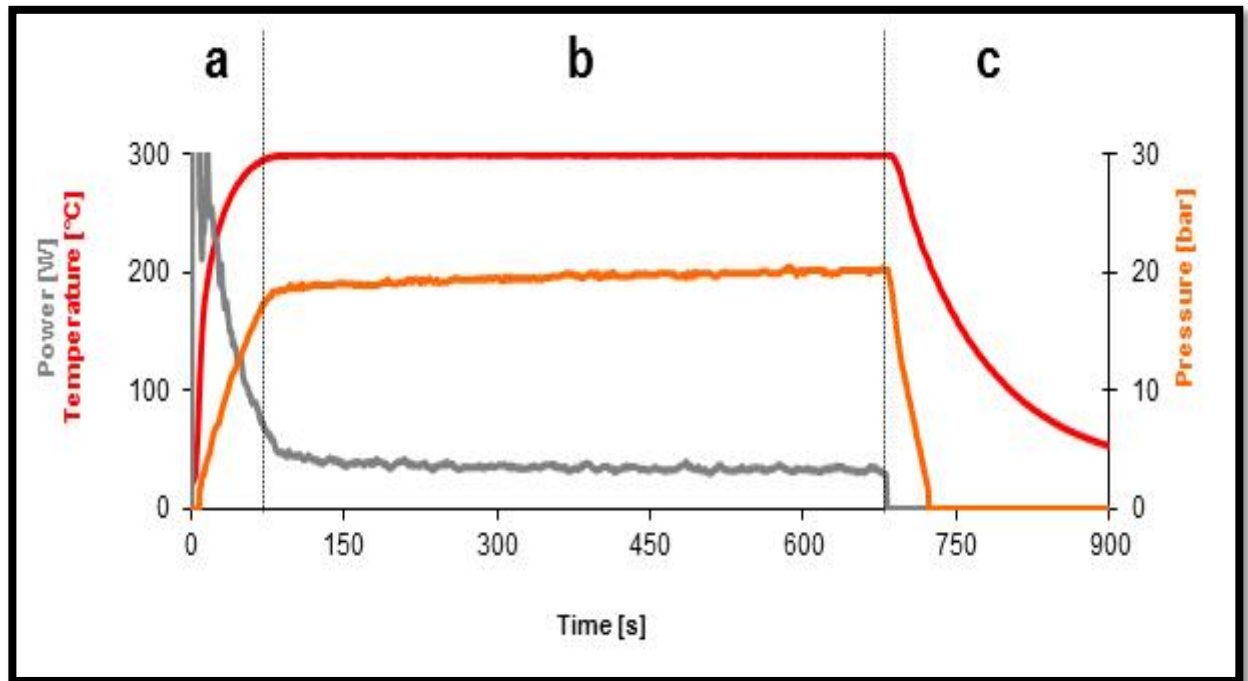


Figure 2.5 : Temperature and power profile of microwave experiment

2.3 Results and Discussion

2.3.1 BET analysis

BET specific surface area of fly ash samples as given in Table 2.1. Indicates that with enhancing milling time from 5 to 40h, specific surface area of fly ash also increases from 9 to 36m²/g . On immobilization of ionic liquid, the specific surface area of TMICl/MFA catalyst decreases due to agglomeration of small particles of fly ash.

Table 2.1: BET surface area data of samples

Sample	Specific surface area, m ² /g
FA	9
MFA-5	11
MFA-10	15
MFA-15	17
MFA-40	36
TMICI/MFA	19

Figure 2.6 shows the distribution of pores in MFA-40 on the basis of their size. It can be clearly seen that majority of pores are mesoporous in nature and lie in the range of 10-100nm. Average pore diameter of MFA-40 is calculated to be 4.76nm depicting its mesoporous nature. Adsorption isotherm for MFA-40 as shown in Figure 2.6, shows resemblance with Type II and III adsorption isotherms, characteristic of a material, which is not porous, or possibly macroporous [43]

Although it also shows some deviation from Type II isotherm, conferring the transition from macroporous to mesoporous behavior as a consequence of mechanical activation. For fly ash as shown. It is not possible to get any of the ideal types of isotherm due to availability of heterogeneous particles with large variations in size, shape and porosity arrangements. The BET plot are observed with linear range for saturation pressure range (0.05 to 0.28) i.e. pressure observed over (P/P^0) for the BET equation which resembles to most of inorganic silica material[43]. High adsorption energy of FA ash is responsible for active immobilization of ionic liquid on it and making suitable catalyst support.

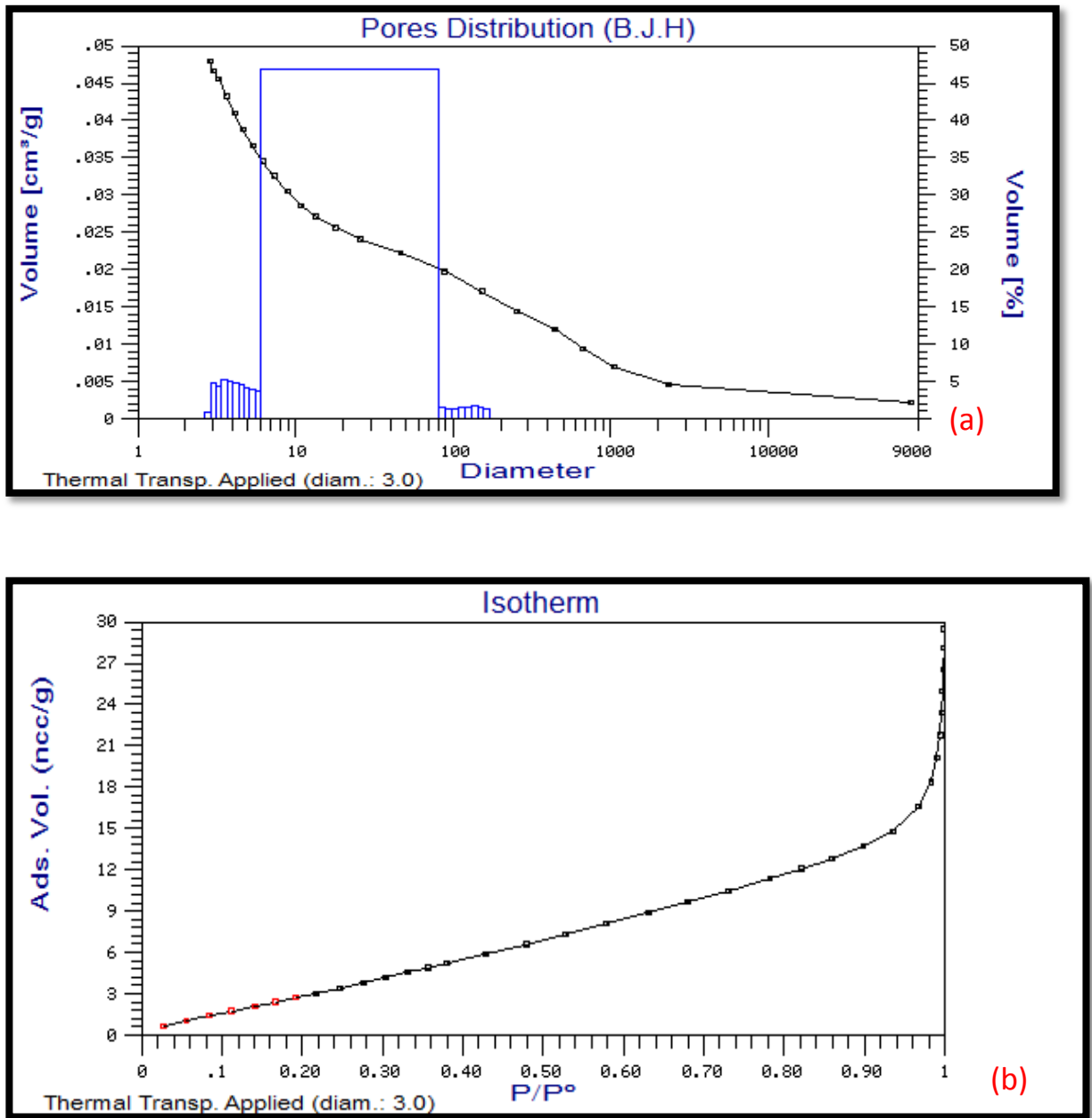


Figure 2.6: (a) Pore distribution curve of MFA-40, (b) B.E.T. adsorption isotherm of MFA-40

2.3.2 X-ray diffraction analysis

The X-Ray diffraction patterns of the as received FA as well as MFA are given in the Figure 2.7 (a,b) show decrement in the crystallinity of fly ash and increase in

the amorphous nature as inferred with decrease in the crystalline size of fly ash from 33nm to 16nm on milling. The peaks at 16.4° and 26.2° show mullite (aluminosilicate) phase while quartz (silica) exhibits strong peaks at 20.7° , 26.6° , 40.6° and 49.9° of 2θ values. As a result of ball milling mostly quartz and mullite crystalline phases are reduced.

In XRD pattern of TMICl/MFA catalyst the peak intensities remained almost unchanged as compared to the MFA pattern, which indicates an ordered mesoporosity of the support material, even after modification(Figure 2.7(c))

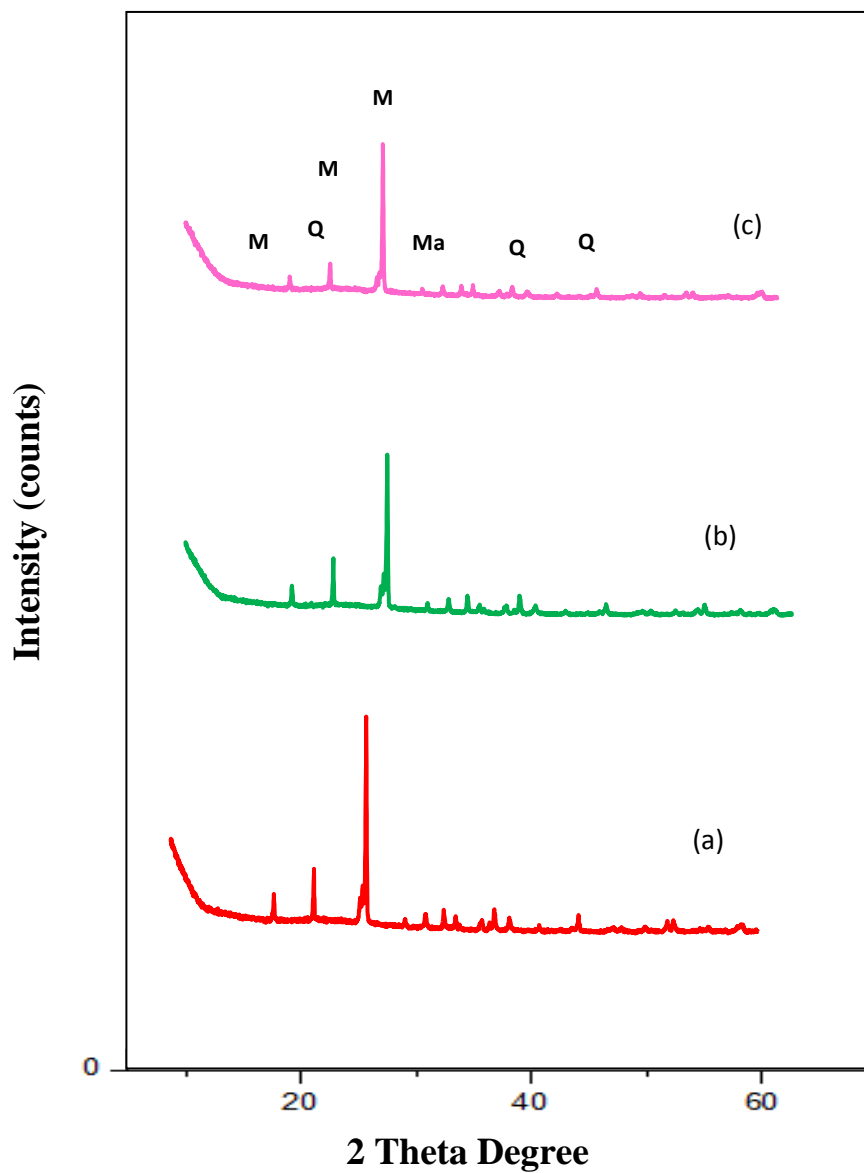


Figure 2.7 : X-ray diffraction patterns of (a) Pure FA, (b) MFA-40 (c) TMICI/MFA

2.3.3 Fourier transform infrared analysis

The FT-IR spectra of FA and MFA-40 in Figure 2.8 show broad band between 3400-3000 cm^{-1} , which is attributed to surface -OH groups of Si-OH and adsorbed water molecules on the surface.

The increment in broadness after ball milling for 36h is an evidence for the breaking down of the quartz structure and formation of Si-OH groups [44]. A peak at 1650 cm^{-1} in the spectra of FA is attributed to bending mode (δ O-H) of water molecule. However, FT-IR study clearly shows changes in the broadening of IR peaks corresponding to Si-O-Si asymmetric stretching vibrations (1101, 1090 cm^{-1}) indicating structural rearrangement during mechanical milling[45].

The FT-IR spectra of TMICl/MFA given in Figure 2.9(ii) shows characteristic bands at 1642 cm^{-1} , 1567 cm^{-1} , 3139 cm^{-1} , 1153 cm^{-1} and 1046 cm^{-1} which are ascribed to C=C, C=N, and C-H stretching vibrations of the imidazole ring[46] The adsorption band around 2962 cm^{-1} assigned to C-H stretching vibration which confirms the presence of propyl groups of ionic liquid[47].

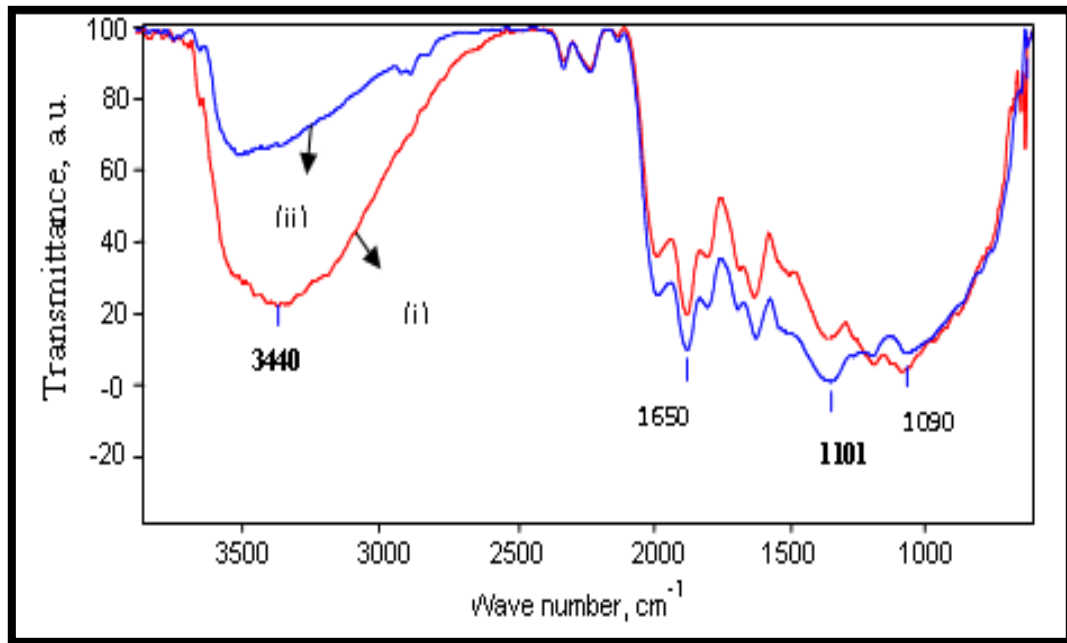


Figure 2.8: FTIR spectra of (i) FA (ii) MFA-40

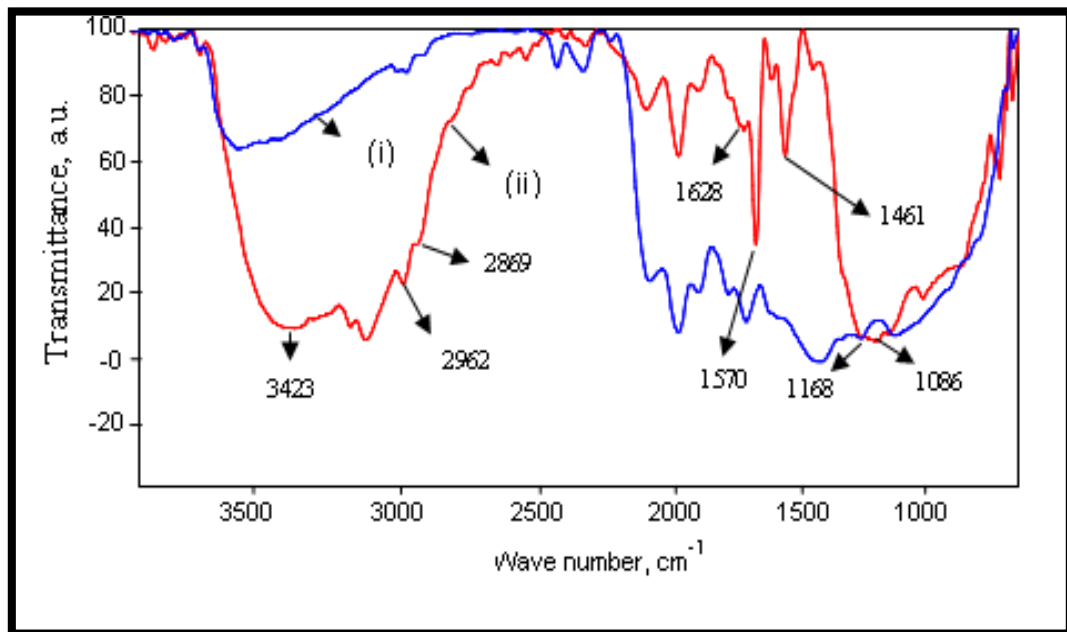


Figure 2.9: FTIR spectra of (i) MFA-40(ii) TMICl/MFA

2.3.4 SEM and SEM-EDX analysis

The energy dispersive spectrum (EDX) shows the presence of C, Fe, Si, O, and Al and other metals in FA and MFA samples shown in Figure 2.10(a,b). However, the presence of high carbon and chloride in TMICl/MFA catalyst confirms immobilization of TMICl on activated surface of fly ash. On the basis of wt% of C and Cl it is resulted that TMICl grafting is in higher percentage on the surface of MFA than on FA (Table 2.2).

The SEM photograph of pure fly ash (Fig. 2.11A) is observed with hollow cenospheres, irregularly shaped unburned carbon particles, mineral aggregates and agglomerated particles. As a result of mechanical activation the structural break down of larger particles and increased surface roughness are observed (Fig. 2.11B).

Typical SEM images of TMICl/MFA show that the resulting particles are represented by irregular structures composed of large blocks with many small particles stacked together to form the bigger particles. All particles are wrapped by IL forming a thin layer over the surface of MFA clearly seen in Figure 2.11(D) and (E).

Table 2.2. EDX analysis of FA, MFA, TMICl/FA and TMICl/MFA Catalyst

Sample	Amount of O, wt %	Amount of Si, wt %	Amount of Al, wt %	Amount of Ca, wt%	Amount of Fe, wt %	Amount of C, wt %	Amount of Cl, wt %
FA	55.45	25.88	16.11	0.68	0.79	-	-
MFA	55.20	27.01	4.47	0.56	2.81	-	-
TMICl/FA	60.05	35.11	6.41	1.02	2.50	2.15	0.9
TMICl/MFA	95.9	41.88	7.60	1.05	2.72	4.96	2.75

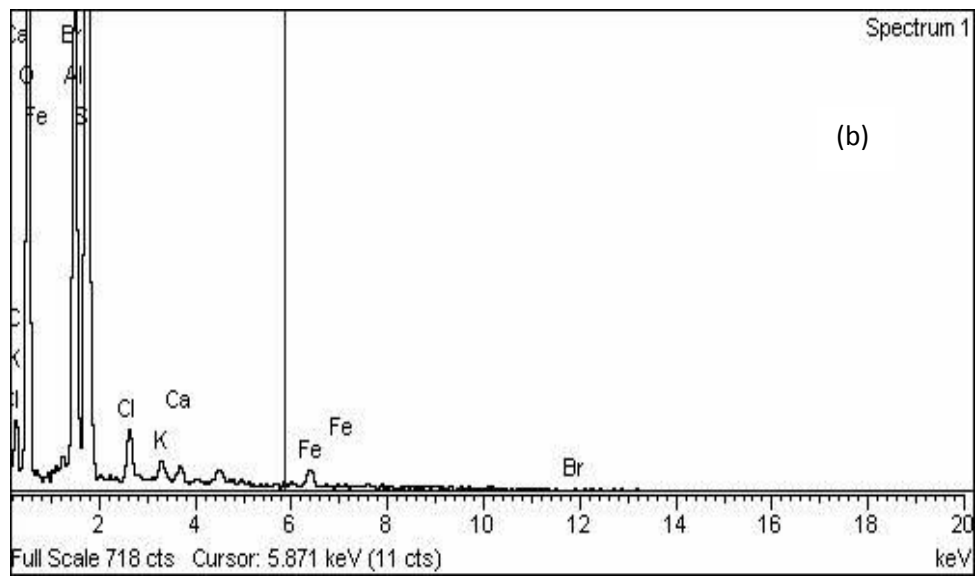
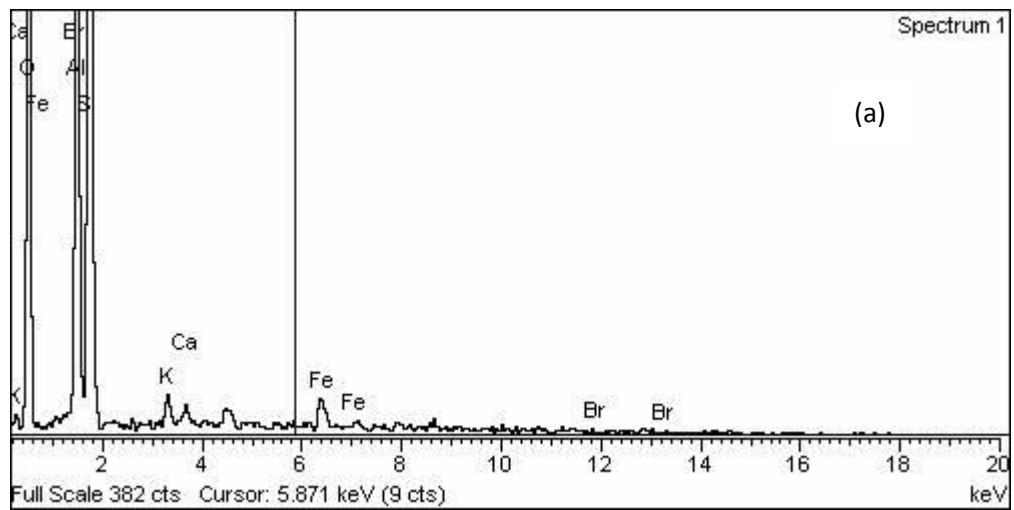


Figure 2.10: EDX spectrum of (a) MFA-40 (b) TMICl/MFA

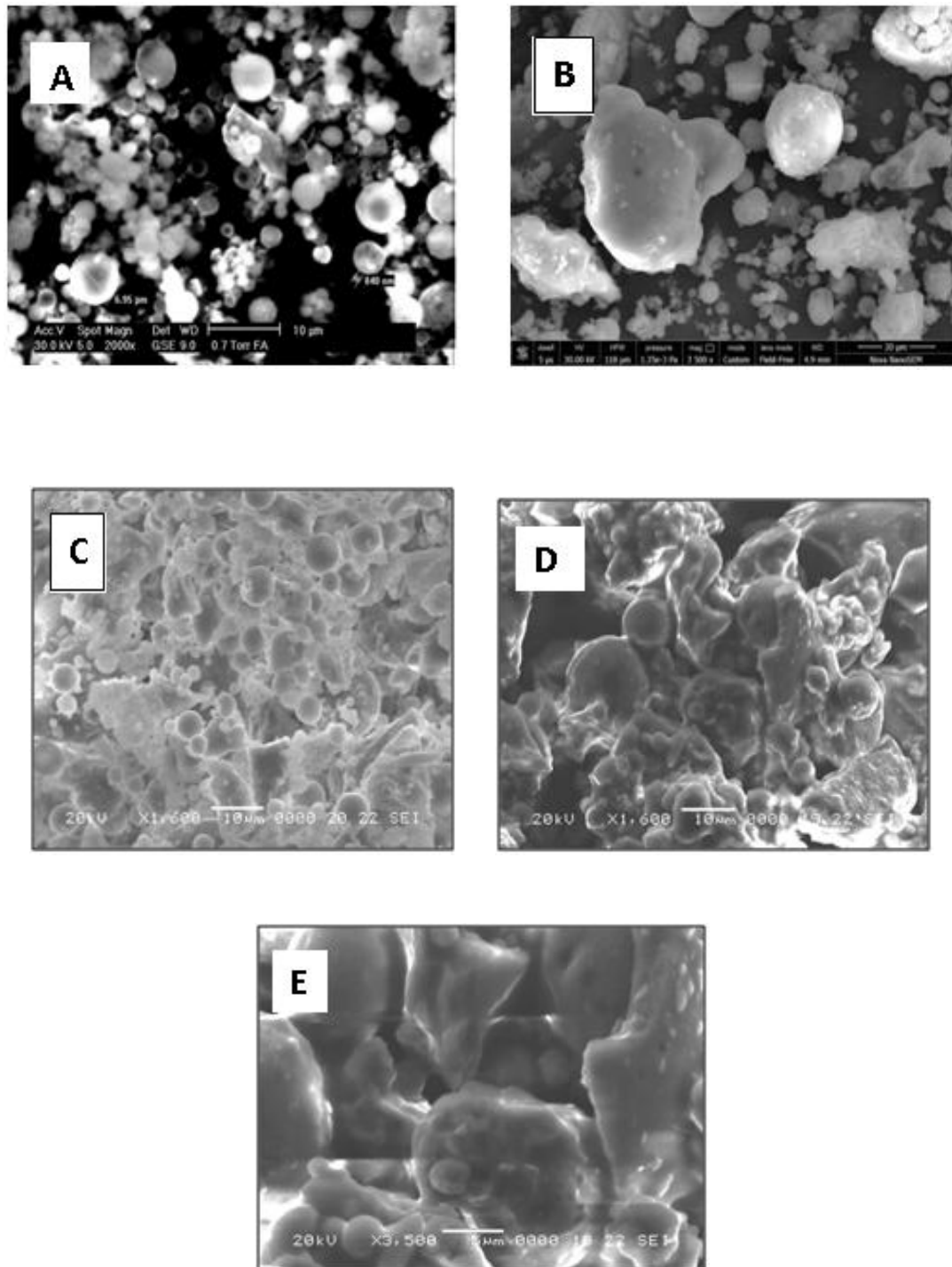


Figure 2.9 : SEM micrographs (A) pure FA (B) TMICL/FA (C) MFA-40 (D, E) TMICI/MFA and magnified image of TMICI/MFA

2.3.5 Ultra violet Visible spectroscopy

The UV-Vis spectra of the pure ionic liquid (1-methyl-3-triethoxysilylpropyl imidazolium chloride) in the scanning range 200-800 nm as shown in Figure 2.12. No absorption peak below 290 nm has been observed which clearly confirmed the absence of any colored impurities.

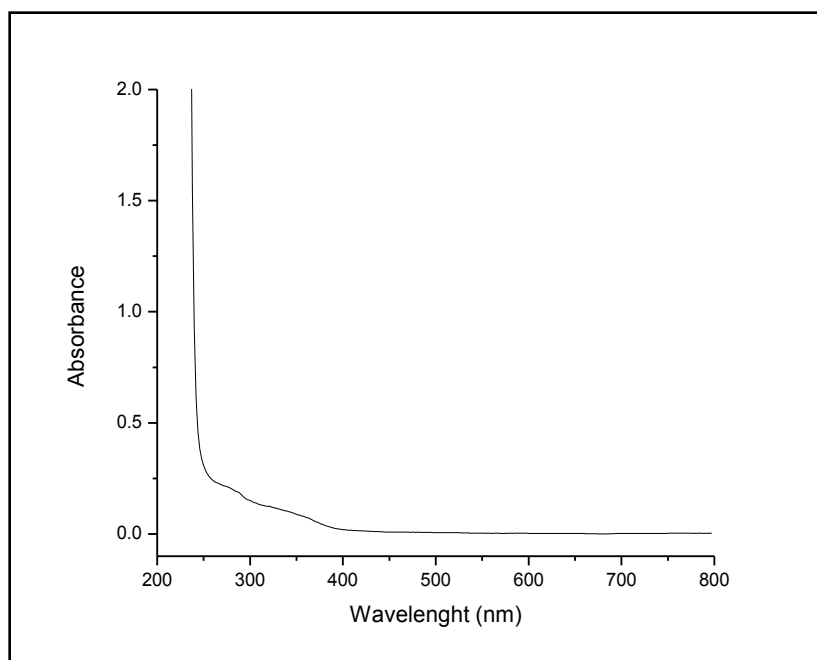


Figure 2.12: UV-VIS spectrum of purity of (1-methyl-3triethoxysilyl propyl imidazolium chloride)

2.3.6 Thermogravimetric analysis

The thermal stability of TMICl/MFA was determined by thermo gravimetric analysis (Figure 2.13). The TGA curve indicated initial weight loss within 200° C mainly attributed to the desorption of physisorbed water and residual solvent. When the temperature further increased to 250° C, the weight of TMICl/MFA decreased rapidly due to removal of IL. Finally, it was observed that the TMICl/MFA catalyst

exhibited good thermal stability up to about 250° C and the residual weight loss of TMICI/MFA was about 10% at around 800° C.

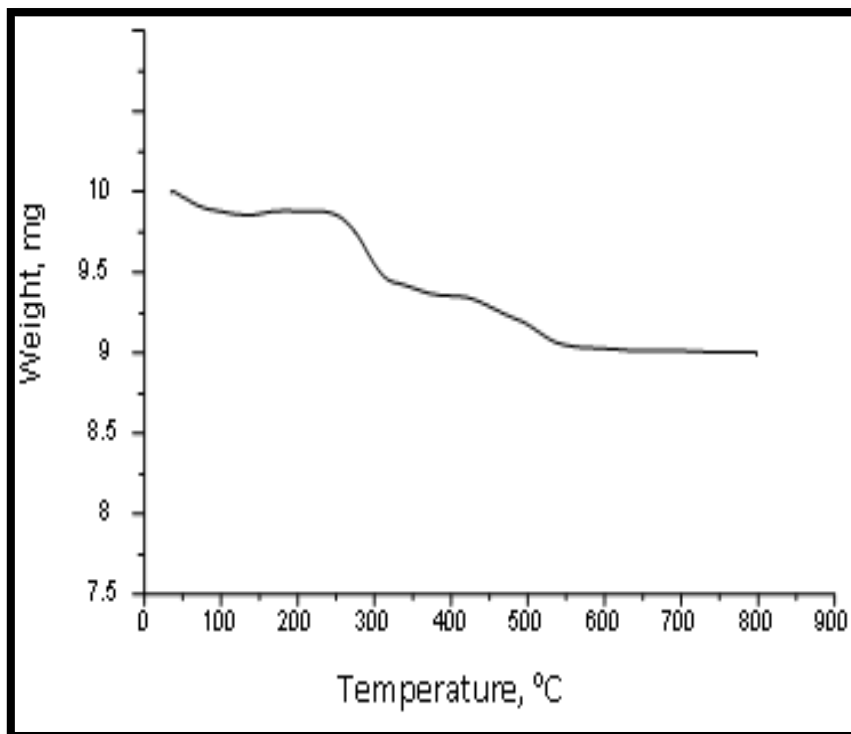


Figure 2.13 : TGA patterns of TMICI/MFA

2.4 Catalytic activity

In order to evaluate the catalytic activity of synthesized catalysts, the esterification was carried out with and without catalyst. The yield of the product in each case is given in Table 2.3. For uncatalyzed reaction the yield of the product just could reach 15.0%. When reaction was carried out in homogeneous medium, TMICL showed good catalytic activity but separation of pure product was difficult with no possibility of catalyst reuse. However, TMICl supported on FA and MFA, could be easily separated by vacuum filtration and reused. In order to establish the MFA a better support for ionic liquid grafting the TMICI/FA and TMICI/MFA both were

reused in second cycle. Interestingly regenerated TMICl/FA gave only 25% yield due to leaching of ionic liquid during first cycle of reaction as well as during washing whereas TMICl/MFA showed no significant loss in the yield of ester during second cycle confirming the high stability of catalytic sites. FA and MFA without grafting Ionic Liquid have not shown significant catalytic activity for studied reaction.

Table 2.3 : Esterification reaction between propanoic acid and octanol

Propanoic acid(10mmol), octanol (20 mmol), propanoic acid/catalyst weight ratio (5:1)

Sample	Catalysts	Temperature, °C	Time, min	Yield, %
1	Blank	110	15	15.04
2	MFA-36	110	15	20.03
3	TMICl	110	15	80
4	TMICl/FA	110	15	50
5	TMIClMFA	110	15	91
6	TMICl/FA (cycle 2)	110	15	25
7	TMICl/MFA (cycle 2)	110	15	90

Microwave assisted solvent-free synthesis of esters using different aliphatic alcohol and propanoic acid was performed in the presence of TMICl/MFA catalysts and results are summarized in Table 2.4.

Table 2.4 : Microwave assisted esterification reactions catalyzed by TMICl/MFA at T=110°C, Time=15, molar ratio (acid: alcohol) =1:2, P=100W, Pmax. =ON

Entry	Acid	Alcohol	Product	Yield, %
1	Propionic acid	Propanol	Propylpropionate	92
2	Propionic acid	Isopropanol	Isopropyl propionate	94
3	Propionic acid	Butanol	Butylpropionate	90
4	Propionic acid	Heptanol	Heptylpropionate	92
5	Propionic acid	Octanol	Octylpropionate	91
6	Propionic acid	Isobutyl alcohol	Isobutylpropionate	89
7	Propionic acid	Isoamyl alcohol	Isoamylpropionate	88

Microwave assisted solvent-free synthesis of octylpropionate using octanol and propanoic acid was performed at different temperature ranging 90 °C to 130 °C for 3 to 20 min. to optimize the reaction temperature, time and catalyst and reactants molar ratio . The results of optimization of operating conditions for various studied reactions are given in Table 2.5.

.On the basis of above results (Table 2.5) the optimal conditions were; molar ratio, 1:2 ; reactant to catalyst ratio, 5:1 ; reaction temperature, 110°C ; reaction time, 15min.

Table 2.5 : Optimization of reaction conditions for octylpropionate ester using TMICI/MFA catalyst

S.NO	Molar ratio	Reactant to catalyst weight ratio	Time, min	Temp, °C	Conversion, %	Yield, %
1	1:1	5:1	15	110	35	41
2	1:1.5	5:1	15	110	64	73
3	1:2	5:1	15	110	89	91
4	1:3	5:1	15	110	78	81
5	1:2	10:1	15	110	74	76
6	1:2	2:1	15	110	85	89
7	1:2	5:1	15	70	45	50
8	1:2	5:1	15	90	60	74
9	1:2	5:1	15	130	89	91
10	1:2	5:1	3	110	20	25
11	1:2	5:1	5	110	35	41
12	1:2	5:1	10	110	70	75
13	1:2	5:1	20	110	89	91

2.4.1 Effect of reaction temperature

On increasing reaction temperature, conversion % of propanoic acid showed a linear increase up to 110 °C with maximum 89 % conversion and after which remained almost constant up to 140 °C (Figure 2.14).

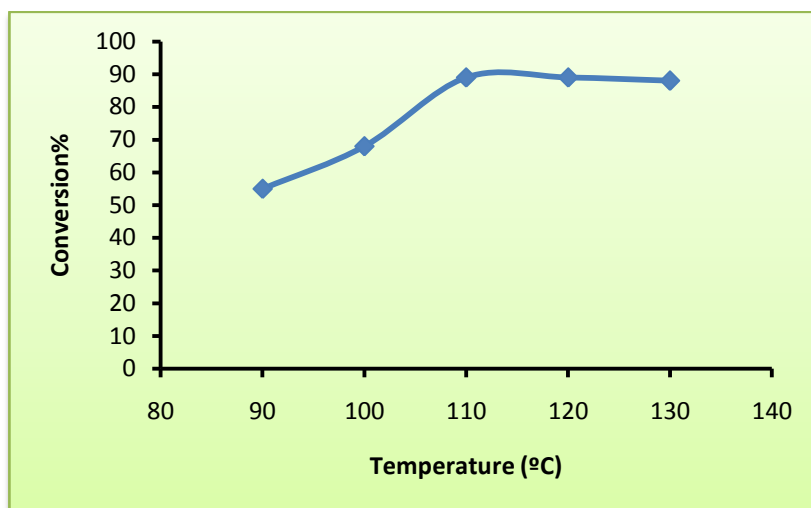


Figure 2.14: Variation of conversion (%) of propanoic acid over TMICl/MFA catalyst with temperature.

2.4.2 Effect of reaction period

Optimization of reaction time period was carried to achieve maximum conversion of propanoic acid to ester ranging from 5 to 20 min as shown in **Figure 2.15** maintaining rest of the reaction parameters same. In the first 10 min, the conversion of propanoic acid increased linearly up to 89 % which remained constant up to 20 min.

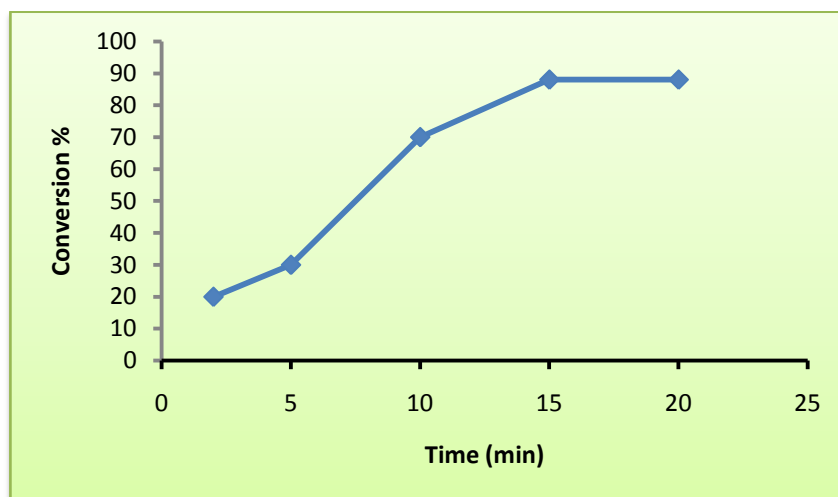


Figure 2.15: Variation of conversion (%) of propanoic acid over TMICl/MFA catalyst with reaction time

2.4.3 Effect of reactant molar ratio

The influence of molar ratio of propanoic acid and different aliphatic alcohol on conversion % of propanoic acid was monitored at different molar ratios from 1:1 to 1:3 by increasing the amount of alcohol only. However, due to solubility restrictions higher concentration studies with propanoic acid could not be conducted. As shown in Table 2.6, on increasing molar ratio of propanoic acid to alcohol from 1:1 to 1:2, maximum conversion (89 %) and 91 % yield of ester was obtained. The above results show that the yield of product increased with increasing the molar ratio of propanoic acid to alcohol. This is mainly due to the reversible nature of the esterification reaction, with the increase in molar ratio propanoic acid to alcohol leads to a shift of the equilibrium to the direction of ester production. However, further increasing molar ratio to 1:3, decrease in yield % of the ester.

Table 2.6: Effect of molar ratio of propanoic acid/alcohol on conversion (%) of propanoic acid to Ester over TMICI/MFA catalyst

S.No.	Molar ratio (propanoic acid: alcohol)	Conversion (%)	Yield (%)
1	1:1	35	41
2	1:1.5	64	73
3	1:2	89	91
4	1:3	78	81

Reaction conditions under microwave irradiation: Temperature = 110 °C; Time = 15 min; Power = 100W; Pmax = ON

2.4.4. Effect of propanoic acid to catalyst weight ratio

The propanoic acid to catalyst weight ratio on conversion of propanoic acid was monitored by varying the amount of catalyst under optimized reaction conditions as shown in Table 2.7. Weight ratio of 5:1 gave maximum conversion of 89 % of propanoic acid attributed to availability of sufficient amount of catalytic active sites. On further increase in the amount of catalyst no further change in conversion % was observed.

Table 2.7: Effect of Propanoic acid to TMICl/MFA catalyst weight ratio on conversion (%) of propanoic acid to Ester

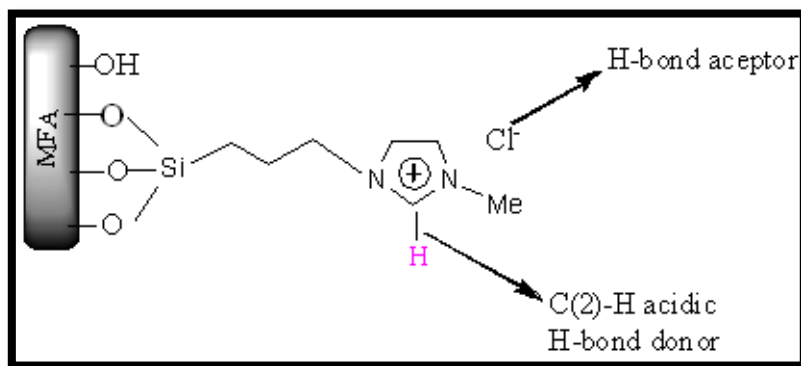
S.No.	Propanoic acid to SILC weight ratio	Conversion (%)	Yield (%)
1	10:1	74	76
2	5:1	89	91
3	2:1	89	91

Reaction conditions under microwave irradiation: Temperature = 110 °C; Time = 15 min; molar ratio (Propanoic acid: octanol) = 1:2; Power = 100W; Pmax = ON

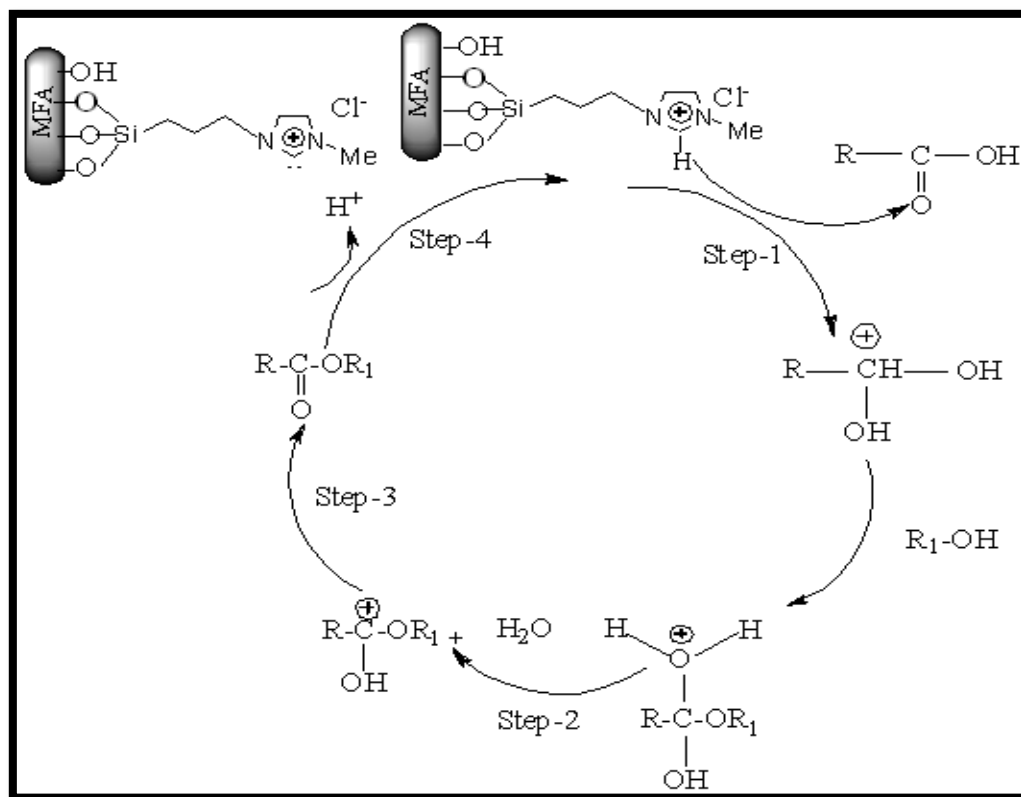
2.5 Proposed mechanism of ester formation over an acidic site

A model structure of the synthesized catalyst is represented in Scheme 2.5. The plausible mechanism for TMICl/MFA catalyzed esterification is schematically presented in Scheme 2.6. The C2 of the IL is positively charged due to the electron deficit in the C= N bond whereas the other carbons are practically neutral[48]. This resulting acidity of the C2 hydrogen atom of TMICl/MFA initiates esterification reaction by donating a proton[49-50] to the carboxylic acid in step 1. Then carboxylic acid becomes susceptible for a nucleophilic attack by the hydroxyl group(step 2).

When alcohol (polar species) interacts with microwave it starts oscillating. During oscillation, the polar species collide with neighboring charged particles i.e. carbonium ion, resulting an intermolecular friction. This molecular friction generate intense internal heat liable for the formation of intermediate species which further leads to formation of ester with subsequent removal of water as a byproduct. In the last step (step 4), the imidazolium cation is regenerated. A similar mechanism is reported by Yifeng et al in the esterification of α -tocophenol with succinic acid catalyzed by imidazolium based ILs[49]. The acidic nature of C2 proton of imidazolium cation is also evidenced by Olofson etal[50]



Scheme 2.5: Proposed model of TMICl/MFA catalyst



Scheme 2.6: Proposed mechanistic pathway of microwave-assisted esterification of propanoic acid with aliphatic alcohol over TMICl/MFA catalyst

2.6 Catalyst Regeneration and Reusability

For catalytic reusability test the used catalyst was recovered by filtration from the initial run, washed thoroughly with dichloromethane and dried in vacuum oven at 80 °C for 24 h followed by activation at 70 °C for 1 h in vacuum oven. The regenerated catalyst was used in next reaction cycles under the same reaction conditions following the procedure described as above. The catalyst could be used up to four reaction cycles without any significant loss in product yield (Table 2.8) which indicates that the acidic sites are not deactivated during regeneration. The conversion% is decreased after fifth reaction cycle, due to the deposition of carbonaceous materials on the surface of catalyst which could block the surface active sites of catalyst. The stability, heterogeneous nature of TMICl/MFA catalyst

and possibility of leaching of ionic liquid in reaction medium is further analyzed by shledon's hot filtration test which involves filtration of catalyst from reaction mixture in between the reaction and further continuance of reaction in absence of catalyst. The results show that the reaction stops on filtering off the catalyst in mid of the reaction, hence it is confirmed that ionic liquid responsible for catalytic activity do not get leached off during course of reaction.

Table 2.8: The reusability test of TMICl/MFA

Reaction conditions under microwave irradiation: Temperature = 110 °C; propanoic acid/catalyst weight ratio=5:1; Power = 100W; Pmax = ON

Entry	Catalysts	Test	Time, min	Conversion, %	Yield, %
1	TMICl /MFA	fresh	15	89	91
2	TMICl /MFA	1 reuse	15	86	89
3	TMICl /MFA	2 reuse	15	85	88
4	TMICl /MFA	3 reuse	15	84	86

2.7 Conclusion

The present research work provides an energy efficient microwave methodology over traditional thermal refluxing for synthesis of ionic liquids. Surface roughness and stable free silanol groups of fly ash increased by mechanical activation. Synthesized TMICl was successfully grafted over mechanically activated fly ash, the resulting heterogeneous catalyst TMICl/MFA exhibited excellent catalytic activity for microwave assisted esterification of propionic acid with various alcohols at optimized reaction conditions. moreover, the catalyst is found to be extremely stable

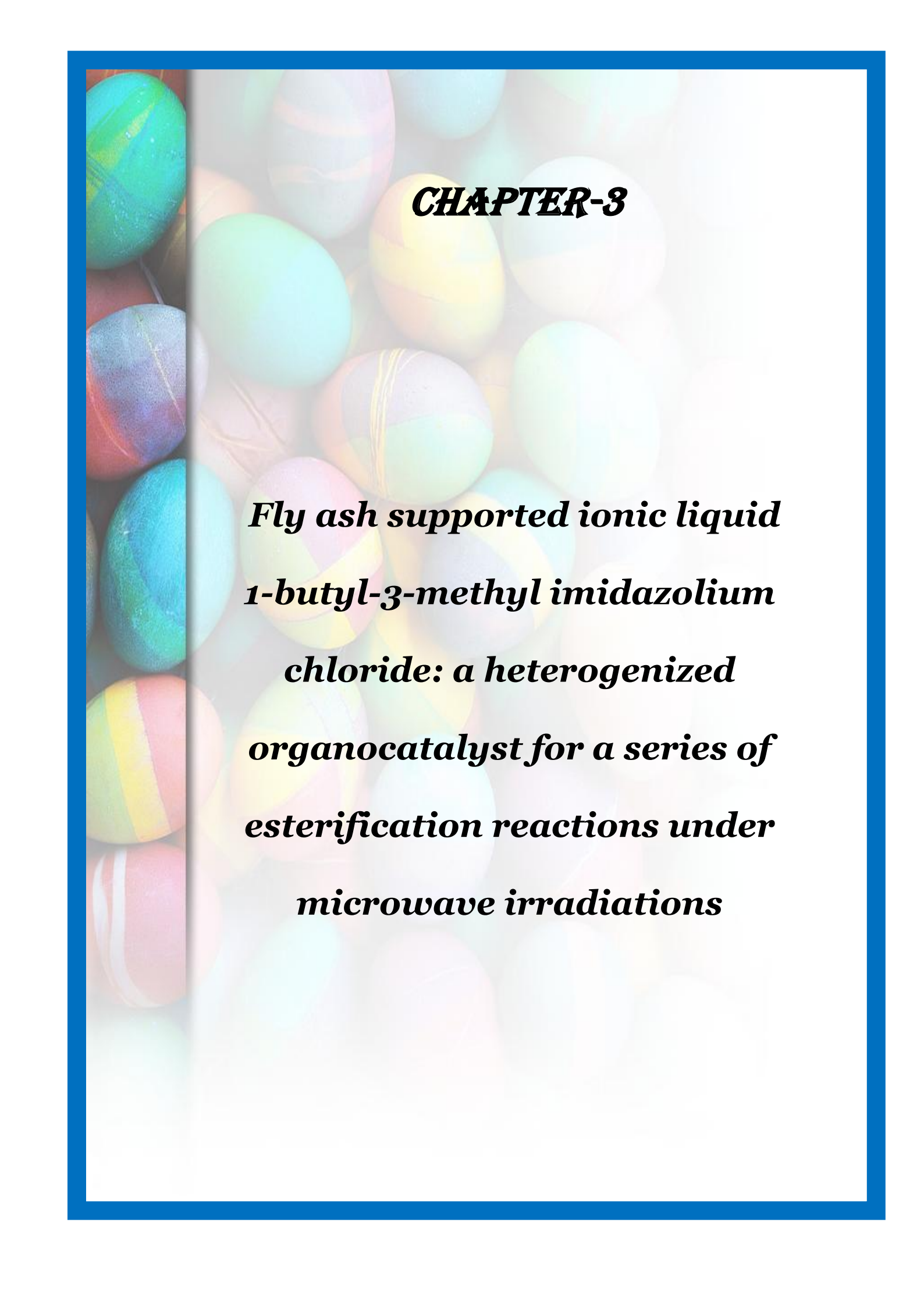
under microwave irradiations, suggesting a new greener area of time-saving catalysis for fly ash supported catalyst. The catalyst could be reused after thermal activation up to four cycles without significant loss in its catalytic activity. In addition the textural property of fly ash has a great influence on stability of grafted ionic liquid during reaction. The mechanical activated FA can replace other costly support materials for synthesis of IL based heterogeneous catalysts for their effective use in atom efficient green chemical processes.

2.8 References

1. R.E. Kirk, D.F. Othmer, Encyclopedia of Chemical Technology, CD-ROM, 4th ed., John Wiley and Sons, New York, 2001, pp. 1–37.
2. M. Mäki-Arfela, T. Salmi, M. Sundell, K. Ekman, R. Peltonen, J. Lehtonen, *Appl. Catal. A: Gen.* 184 (1999) 25.
3. P.W. Greene, P.G.M. Wuts, Protective Groups in Organic Chemistry, Wiley, New York, 1999 (Chapter 5).
4. A. Heidekum, M.A. Harmer, W.F. Hoelderich, *J. Catal.* 181 (1999) 217.
5. I.J. Dijs, H.L.F. van Ochten, C.A. van Walree, J.W. Geus, L.W. Jenneskens, *J. Mol. Catal. A: Chem.* 188 (2002) 209.
6. R.A. Crane, S.H. Brown, L. De Caul, USP 5973193 (1999).
7. Y. Zhao, J. Long, F. Deng, X. Liu, Z. Li, C. Xia, J. Peng, *Catal. Commun.* 10 (2009) 732–736.
8. J. Dupont and P. A. Z. Suarez, *Phys. Chem.* 8 (2006) 2441–2452.
9. C. S. Consorti, P. A. Z. Suarez, R. F. de Souza, R. A. Burrow, D. H. Farrar, A. J. Lough, W. Loh, L. H. M. da Silva and J. Dupont, *J. Phys. Chem. B* 109 (2005) 4341–4349.
10. J. Dupont, *J. Braz. Chem. Soc.* 15 (2004) 341–350.
11. M. Picquet, D. Poinso, S. Stutzmann, I. Tkatchenko, I. Tommasi, P. Wasserscheid, J. Zimmermann, *Top. Catal.* 29 (2004) 139–143.

12. B.Y. Liu, J. Han, J.F. Dong, F.X. Wei, Y.H. Cheng, *Chin. J. Org. Chem.* 27 (2007) 1236–1243.
13. L. Hao, Y. Zhao, B. Yu, Z. Yang, H. Zhang, B. Han, X. Gao, Z. Liu, *ACS Catal.* 5 (2015) 4989–4993.
14. H. Valizadeh, H. Gholipour, *Synth. Commun.* 1 (2010) 1477–1485.
15. H. Li, P.S. Bhadury, B. Song, S. Yang, *RSC Adv.* 2 (2012) 12525–12551.
16. S. Breitenlechner, M. Fleck, T.S. Müller, A. Suppan, *J. Mol. Catal. A* 214 (2004) 175.
17. D.W. Kim, D.Y. Chi, *Angew. Chem. Int. Ed.* 43 (2004) 483.
18. A. Riisager, R. Fehrmann, S. Flicker, R. Van Hal, M. Haumann, P. Wasserscheid, *Angew. Chem. Int. Ed.* 44 (2005) 815.
19. C.P. Mehnert, *Chem. Eur. J.* 11 (2005) 50.
20. F. Shi, Q. Zhang, D. Li, Y. Deng, *Chem. Eur. J.* 11 (2005) 5279.
21. F. Wang, W. Zhang, J. Yang, L. Wang, Y. Lin, Y. Wei, *Fuel.* 107 (2013) 394–399.
22. K. Qiao, H. Hagiwarab, G. Yokoyamaa, *J. of Mol. Catal. A: Chem.* 246 (2000) 65–69.
23. R. S. Földes, *Mol.* 19 (2014) 8840–8884.
24. A. Chrobok, S. Baj, W. Pudlo, A. Jarzebski, *Appl. Catal. A: Gen.* 366 (2009) 22–28.
25. M. N. Sefat, D. Saberi, K. Niknam, *Catal. Lett.* 141 (2011) 1713–1720.
26. M. Baghernejad, K. Niknam, *Int. J. of Chem.* 4 (2012) 52–60.
27. M. N. Parvina, H. Jina, M. B. Ansaria, S.M. Ohb, S.E. Park, *Appl. Catal. A: Gen.* 413–414 (2012) 205–212.
28. J. Sun, W. Cheng, W. Fa, Y. Wang, Z. Meng, S. Zhang, *Catal. Today* 148 (2009) 361–367.
29. M. I. Burguete, H. Erythropel, E. G. Verdugo, S. V. Luis, V. Sans, *Green Chem.* 10 (2008) 401–407.
30. R. Sugimura, K. Qiao, D. Tomida, C. Yokoyama, *Catal. Commun.* 8 (2007) 770–772.

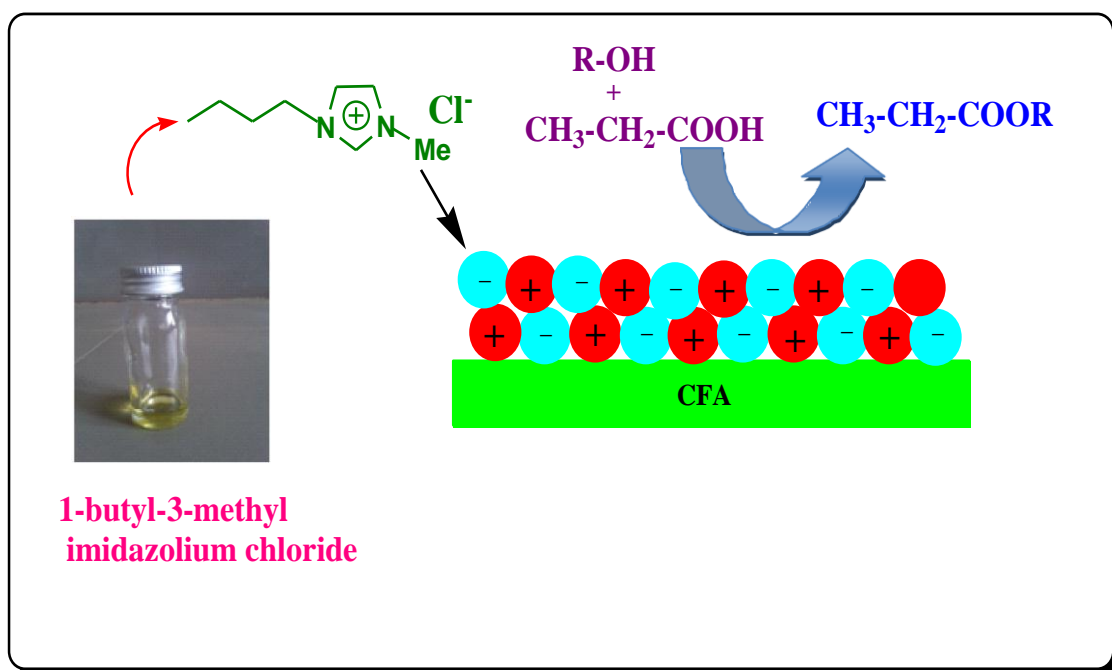
31. R. A. Reziq, D. Wang, M. Post, H. Alper, *Adv. Synth. Catal.* 349 (2007) 2145 – 2150.
32. B. Karimi, F. Mansouri, H. Val, *Green Chem.* 16 (2014) 2587-2596.
33. J. Sun, W. Cheng, W. Fa, Y. Wang, Z. Meng, S. Zhang, *Catal. Today* 148 (2009) 361–367.
34. J. Miao, H. Wan, Y. Shao, G. Guan, B. Xu, *J. of Mol. Catal. A: Chem.* 348 (2011) 77– 82.
35. Y. Lin, F. Wang, Z. Zhang, J. Yang, Y. Wei, *Fuel* 116 (2014) 273–280.
36. P. H. Li, B. L. Li, H. C. Hu, X. N. Zhao, Z. H. Zhang, *Catal. Commun.* 46 (2014) 118–122.
37. D. Jain, C. Khatri, A. Rani, *Fuel Process. Technol.* 91 (2010) 1015–1021.
38. D. Jain, C. Khatri, A. Rani, *Fuel* 90 (2011) 2083–2088.
39. C. Khatri, D. Jain, A. Rani, *Fuel* 89 (2010) 3853–3859.
40. C. Khatri, A. Rani, *Fuel* 87 (2008) 2886–2892.
41. N. Shringi, K. Srivastava, A. Rani, *Chem. Sci. Rev. Lett.* 4 (2015) 561-570.
42. K. Srivastava, V. Devra, A. Rani, *Fuel Process Technol.* 121 (2014) 1-8.
43. J.B. Condon, surface area and porosity determination by physisorption, 2006.
44. G.A. Patil, S. Anandhan, *J. Energy Eng.* 2 (2012) 57-62.
45. A. Sharma, K. Srivastava, V. Devra, A. Rani, *Ameri. Chem. Sci. J.* 2 (2012) 177-187.
46. S. Sahoo, P. Kumar, F. Lefebvre, S.B. Halligudi, *Appl. Catal. A: Gen.* 354 (2009) 17–25.
47. C. Yuan, Z. Huang, J. Chen, *Catal. Commun.* 24 (2012) 56–60.
48. Y. Tao, R. Dong, I. V. Pavlidis, B. Chen, T. Tan, *Green Chem.* 18 (2016) 12401248.
49. S. Sowmiah, V. Srinivasadesikan, M. C. Tseng, Y.H. Chu, *Mol.* 14 (2009) 3780-3813.
50. H. Olivier-Bourbigou, L. Magna, D. Morvan, *Appl. Catal. A: Gen.* 373 (2010) 1–56

The background of the slide is a collection of colorful Easter eggs in various patterns and colors, including solid colors like blue, green, and pink, as well as multi-colored stripes and marbled patterns. The eggs are arranged in a dense, overlapping manner, creating a vibrant and festive atmosphere. The entire scene is framed by a thick blue border.

CHAPTER-3

***Fly ash supported ionic liquid
1-butyl-3-methyl imidazolium
chloride: a heterogenized
organocatalyst for a series of
esterification reactions under
microwave irradiations***

Abstract



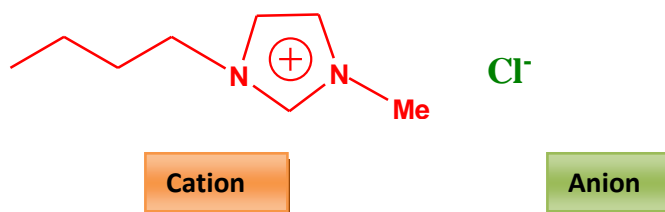
**Esterification reaction over fly supported 1-butyl-3-methyl-imidazolium
chloride catalyst**

3.1. Introduction

Fly ash, a waste product has been used as innovative support material. Acid activation of FA is widely used for developing acidic sites for catalytic applications as solid acid[1]. Activation of FA with mineral acids induces remarkable changes in the crystal structure of aluminosilicate minerals due to dissolution of structural ions and/or rearrangement of the structure[2]. Acid activation involves leaching of several metal oxides and aluminium ions from the silico-aluminate layers of the FA thus increases high amorphous silica content and specific surface area of FA which is responsible for different catalytic reactions and provides hydroxylated surface for loading of different catalytic species. Fly ash with increased silica content can be used as heterogeneous solid acid catalysts for different acid catalyzed organic transformations and esterification reactions. Esterification is the most widely used reaction in the organic chemical synthesizing industries because a lot of applications ranging from natural product synthesis for lab scale to industrial scale applications. Many metal oxides[3-4], metal triflates[5-6], acids[7-10] etc. supported over chemically activated fly ash have been reported in the literature but fly ash immobilized ionic liquids are yet unreported in the literature.

Ionic liquids (IL) are a synthetic group of chemicals widely used as green solvents and catalysts in synthetic chemistry [11]. Their remarkable properties including melting points below 100°C, negligible vapor pressures, high thermal stabilities, high viscosities, and possibilities of great number of anions and cations make them a powerful alternative to the molecular organic solvents and catalysts[12-13]. The

Synthesis of imidazolium based ionic liquid usually involves a highly exothermic and fast alkylation reaction. A large amount of solvent has to be used to ensure low operational temperature to avoid thermal degradation of the product which reduces reaction rate in batch synthesis. In the present work we have synthesized solvent free **1-butyl-3-methyl imidazolium ionic liquid** under microwave exposure. The molecular structure of ionic liquid is given in Scheme 3.1.



Scheme 3.1: The molecular structure of 1-butyl-3-methyl imidazolium chloride ionic liquid

Microwave flash heating has successfully been used for synthesis of imidazolium based ILs involve a consecutive quaternisation-anion metathesis procedure. The monoalkyl substituted cations [H-MIM] of imidazolium IL show unusual physical properties due to the additional proton donor on the nitrogen atom of the imidazolium ring [14] suitable for catalysis. ILs have been successfully applied to different field of chemistry such as organic and inorganic synthesis, biphasic catalysis, separation processes, electrochemistry etc. [15-17]. However, industrial applications of ionic liquids are still limited due to several drawbacks such as unendurable viscosity, high cost, separation of the product etc in the homogeneous systems [18]. Recently supported ionic liquid (SIL) has been reported widely in which a thin layer of IL is immobilized on an inert solid support material and effectively used for organic

transformations. Mesoporous materials viz. silica[19], polymers[20], and magnetic materials[21] are extensively used as support for immobilizing ionic liquids using impregnation, grafting, polymerization, sol-gel, encapsulation, or pore trapping [22-28] methods. Supported ionic liquids are reported to catalyze various organic reactions such as esterification, nitration [29] Baeyer-Villiger reaction [30] heterocyclic synthesis [31] Knoevenagel condensation [32]. hydroformylation [33-35] hydrogenation [36-37] chlorination [38] carbonylation [39] Friedel–Crafts acylation [40-41] and Heck reaction [42] etc. During the present work fly ash is chemically treated with sulphuric acid to enhance surface silanol groups [43] for stabilizing alkyl substituted Imidazolium based ILs in fly ash mesopores through strong hydrogen bonding to synthesize a highly stable, versatile and efficient catalytic system for no. of esterification reactions. The present work elaborates microwave mediated synthesis of [bmim]Cl which is further immobilized on CFA to prepare a heterogeneous organocatalyst [bmim]Cl/CFA active towards dielectric synthesis of industrially important esters under solvent free conditions.

3.2. Experimental

3.2.1 Material

Fly ash [Class F type ($\text{SiO}_2 + \text{Al}_2\text{O}_3$) > 70%], collected from Kota Thermal Power Plant (Rajasthan, India) was used as support for the preparation of the supported ionic liquid catalyst. Acids and alcohols were obtained from S.D. Fine Chem. Ltd., India. Ionic liquid precursors 1-methylimidazole (99%), chlorobutane were purchased from Sigma aldrich.

3.2.2 Catalyst preparation

Activation of Fly Ash

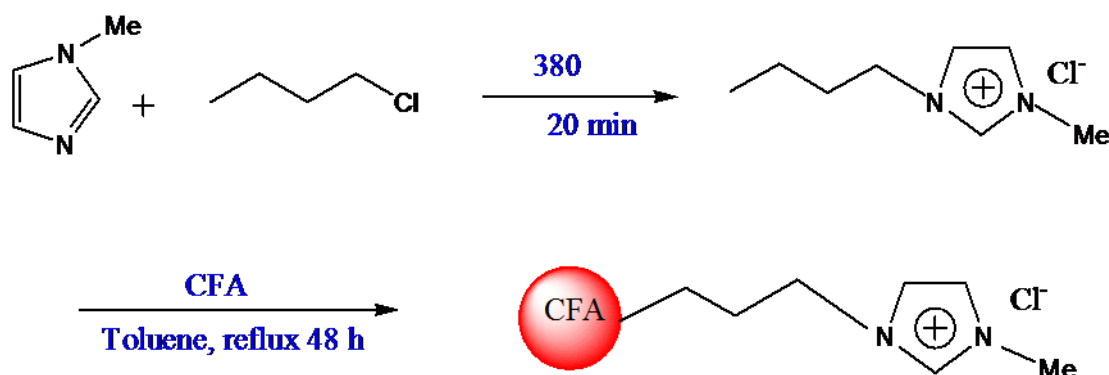
As received fly ash (FA) was washed with distilled water followed by drying at 100 °C for 24h. Dried FA was heated at 900 °C for 4 h at the rate 18 °C/min to remove C, S and other impurities. The chemical activation of FA was carried out in a stirred reactor by stirring 5M aqueous solution of H₂SO₄ in the ratio of 1:2 (FA: H₂SO₄) for 24h at 110 °C temperature followed by washing till pH 7.0 with complete removal of soluble ionic species (Cl⁻, NO₃⁻, SO₄²⁻, ClO₄⁻ etc.) and drying at 110 °C for 24h. The obtained solid product was calcined at 500 °C for 4h under static conditions.

Synthesis of ionic liquid [bmim]Cl

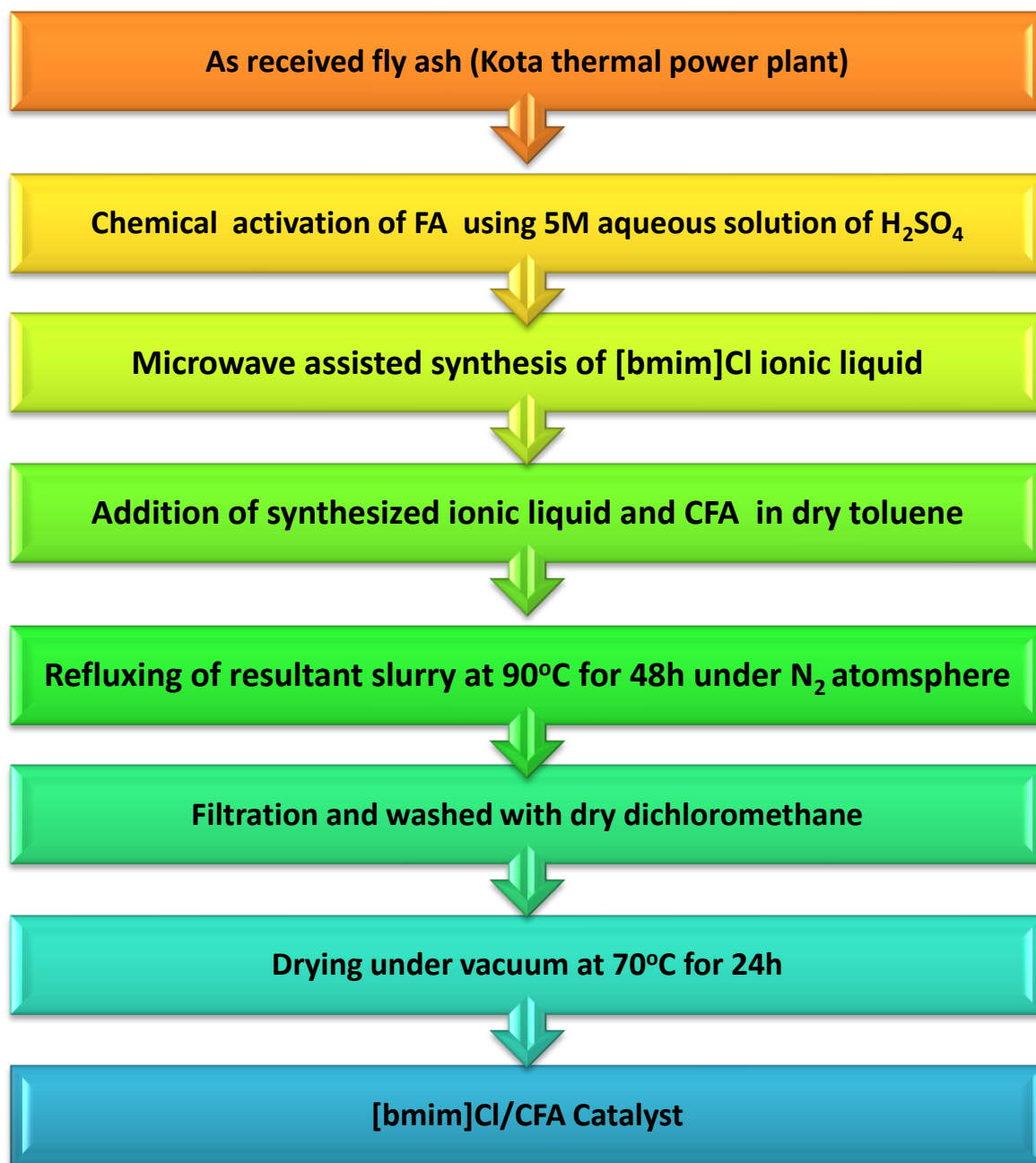
The synthetic procedure of IL [bmim]Cl was given in Scheme 3.2. A mixture of 1-methylimidazole (1.23g, 15mmol) and chlorobutane (1.38 g, 15mmol) was sealed in microwave reactor tube and irradiated at 110 °C for 20 min at 50 psi pressure. After cooling to room temperature, the obtained yellow viscous liquid was thoroughly washed five times with diethyl ether and the solvent was removed by rotatory evaporator. The viscous product was dissolved in methylene chloride and subsequently filtered over silica gel and dried overnight in a vacuum oven at 70 °C. The pure product was characterized by ¹H NMR (CDCl₃); 0.93(t), 1.36(sextet), 1.84(q), 4.11(s), 4.31(t), 7.50(s), 7.65(s), 10.38(s). IR (CDCl₃, cm⁻¹): 667.53, 756.27, 1135.89, 1061, 1464.98, 1572.65, 1637.37, 2860.08, 2936.74, 2962.73, 3416.57.

Synthesis of [bmim]Cl/CFA

Prior to the grafting, CFA was activated at 550 °C for 1 h and [bmim]Cl was dried at 70°C under vacuum for 1 h. The pretreated CFA (5g) was dispersed in 50 mL anhydrous toluene, followed by taking 1gm of [bmim]Cl in a refluxing assembly under vacuum. The mixture was refluxed under N₂ atmosphere at 90 °C for 48 h. After cooling to room temperature the product was filtrated, washed with dry dichloromethane to remove the excess of ionic liquid and dried under vacuum at 70 °C for 24 h to give brown catalyst powder [Scheme 3.2]. The steps of synthesis of catalyst are summarized in Scheme 3.3.



Scheme 3.2. The synthesis route of [bmim]Cl functionalized FA.



Scheme 3.3: Steps for synthesis of [bmim]Cl/CFA catalyst

3.2.3 Instrumentation

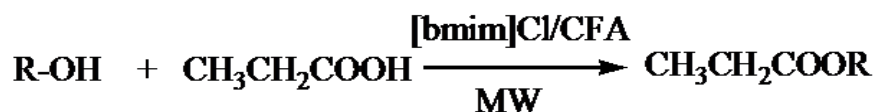
Thermal activation was performed in high temperature muffle furnace and microwave furnace (CEM make). The mechanical activation of fly ash (FA) was carried out in high energy planetary ball mill. The synthesis of ionic liquid and esterification reaction was carried out in microwave synthesis system. The removal of solvents was performed in rotary evaporator (Heidolph G3, Germany).

3.2.4 Characterization Techniques

Physicochemical properties of all prepared samples are evaluated using XRD, FTIR, SEM-EDX, TGA, BET surface area, UV-Visible, $^1\text{H-NMR}$ techniques, as described in [Annexure-I](#).

3.2.5. Catalytic activity of [bmim]Cl /CFA

The catalytic behaviors of [bmim]Cl /CFA was evaluated by microwave assisted solvent free esterification of different alcohols with butyric acid (Scheme 3.4) to give ester as a test reaction in microwave reactor.



Scheme 3.4: Microwave-assisted solvent-free synthesis of ester over [bmim]Cl/CFA

In a typical procedure 20 mmol of aliphatic alcohol, 10 mmol of butyric acid were taken in 10 ml reactor tube covered by intelligent septa cap. The catalyst (acid to catalyst weight ratio = 5), activated at 80 °C for 1 h prior to the reaction in vacuum,

was added in the reaction mixture. The reaction is carried out in closed vessel System at 50 Psi pressure, by placing the vial in microwave cavity under constant stirring at different time periods, molar ratio, temperatures and power outputs. After input of temperature, hold time, power and pressure parameters, the reaction is started by clicking on play botton under Power_{max}- On conditions. The pressurized glass vial with continuous stirring checked the vapor loss during the reaction proceeding at desired temperature and time. After completion of the reaction, the mixture was cooled at room temperature through air pump before releasing the pressure of the reactor tube.

The filtered catalyst is washed with dichloromethane to remove organic impurities. The product is separated by ether. The reaction conditions were varied to obtain maximum yield and conversion into ester. The reactions were analyzed using a GC with oven temperature range 70-240 °C and N₂ (25 ml/min) as a carrier gas. The conversion of butyric acid and yield of ester was calculated by using weight percent method.

The conversion % of alcohol is calculated by using following method.

$$\text{Conversion (\%)} = 100 \times \frac{\text{Intial wt \%} - \text{Final wt \%}}{\text{Intial wt \%}}$$

3.3 Results and Discussion

3.3.1 Characterization of catalyst

The chemical composition and physico-chemical properties of FA and CFA are summarized in Table 3.1. After chemical activation the silica content in CFA is

greatly increased (55% to 81%) [7]. The increase in silica content after activation shows the loss of other components during the chemical activation with higher concentration of H₂SO₄.

Table 3.1 Chemical composition of FA samples and CFA

Sample	SiO ₂ (wt%)	Al ₂ O ₃ (wt%)	Fe ₂ O ₃ (wt%)	CaO (wt%)	MgO (wt%)	Na ₂ O (wt%)	K ₂ O (wt%)	TiO ₂ (wt%)	Other element
FA	55	30.7	3.65	0.86	0.56	0.44	0.79	2.33	5.67
CFA	81	12.7	2.60	0.22	0.18	0.06	0.39	1.87	0.98

3.3.2 BET analysis

BET specific surface area of samples as given in Table 3.2 indicates that on chemical activation, specific area of fly ash increases from 9.18 to 28.16 m²/g due to increase in amorphous silica content as a result of acid treatment. Silica transformation become quite easier on using concentrated acids. After immobilization of [bmim]Cl on CFA surface, surface area decreases due to agglomeration of small particles of FA..

Table : 3.2 BET specific surface area data of samples

Samples	BET specific surface area
Fly ash	9.18
CFA	28.16
[bmim]Cl/CFA	18.10

3.3.3 X-ray diffraction analysis

The XRD patterns of pure fly ash (FA, Figure 3.1a), chemically activated fly ash (CFA, Figure 3.1b), and fly ash supported ionic liquid ([bmim]Cl/CFA, Figure 3.1c) show the presence of crystalline and amorphous phases. The amorphous phases of fly ash were increased by chemical activation, which resulted in decreased crystallite size from 33 nm to 12 nm [7]. The chemical activation removes some of the crystalline components present in the fly ash, lowering the crystallinity and increases the amorphous content [9].

In [bmim]Cl/CFA catalyst (Figure 3.1c) the peak intensities remained almost unchanged as compared to the CFA pattern, which indicates an ordered mesoporosity of the support material, even after immobilization of ionic liquid on the surface of CFA.

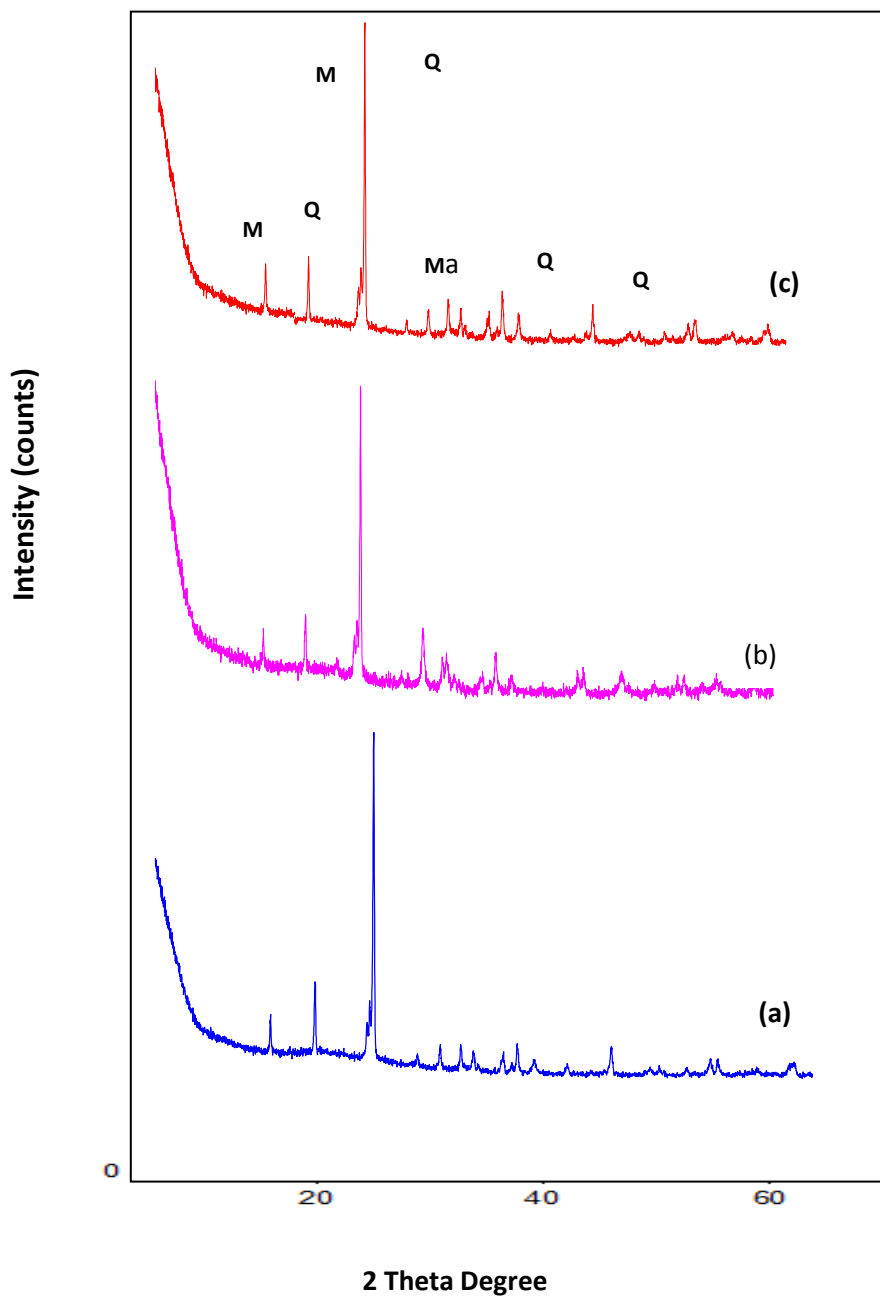


Figure 3.1 : X-ray diffraction patterns of (a) Pure FA, (b) CFA (c) [bmim]Cl/CFA

3.3.4 FT-IR Fourier transform infra-red analysis

The FT-IR spectra of FA (Figure 3.2(i)) shows broad band at 3500-3000 cm^{-1} attributed to surface –OH groups of Si-OH and adsorbed water molecule adsorbed on the surface. The FT-IR spectra of CFA (Figure 3.2(ii)), shows a significant increment in broadness at 3500-3000 cm^{-1} compared to

FA due to increased silanol groups and adsorbed water molecules on the surface[9, 43]. The increased amorphous silica in the activated fly ash is characterized by an intense band in the range 1000 1300 cm^{-1} , corresponding to the valence vibrations of the silicate oxygen skeleton. The main absorption band of the valence oscillations of the groups Si-O-Si in quartz appears with a main absorption maximum at 1100 cm^{-1} [10]. Increase in silica content, significantly increasing surface free silanol groups, which stabilized thin layer of IL on the surface of CFA via strong hydrogen bonding between anions of IL and surface free silanols groups.

The FT-IR spectrum of [bmim]Cl/CFA in Figure 3.3(ii) shows the typical strong peak corresponding to OH stretching frequency centered at about 3410 cm^{-1} , and characteristic bands observed at 1094 cm^{-1} , 1571.7 cm^{-1} , and 1636 cm^{-1} associated with stretching frequencies of the imidazolium ring [44]. The adsorption band around 2970 cm^{-1} assigned to C–H stretching vibration which confirms the presence of alkyl groups of ionic liquid.

3.3.5 Ultra violet Visible spectroscopy

The UV-Vis spectra of the pure ionic liquid (1-butyl-3-methylimidazolium chloride) in the scanning range 200-800 nm are shown in Figure 3.4. Due to some colour impurities there is a absorption peak at 260 nm in the scanning range 200-800 nm.

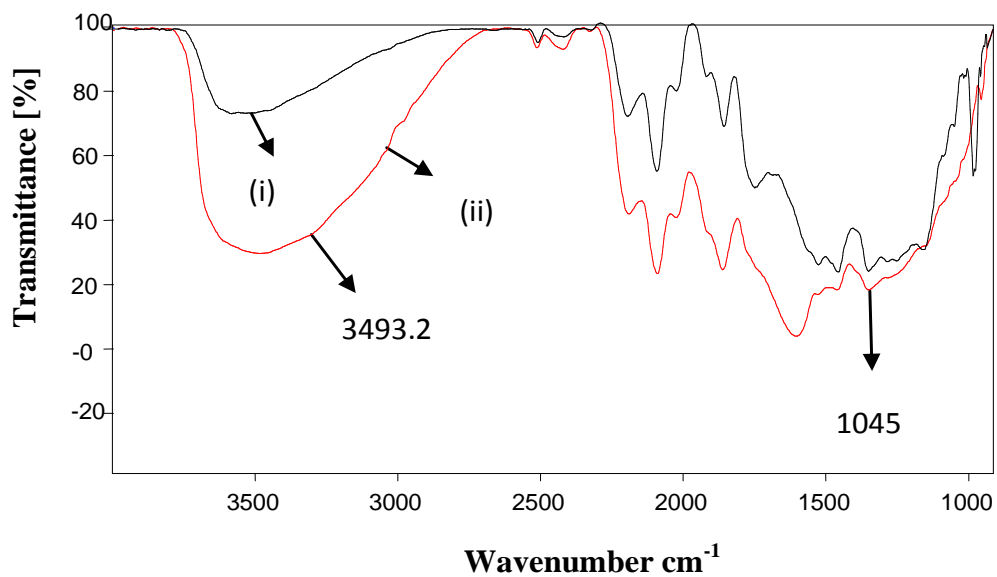


Figure 3.2. FTIR spectra of (i) FA (ii) CFA

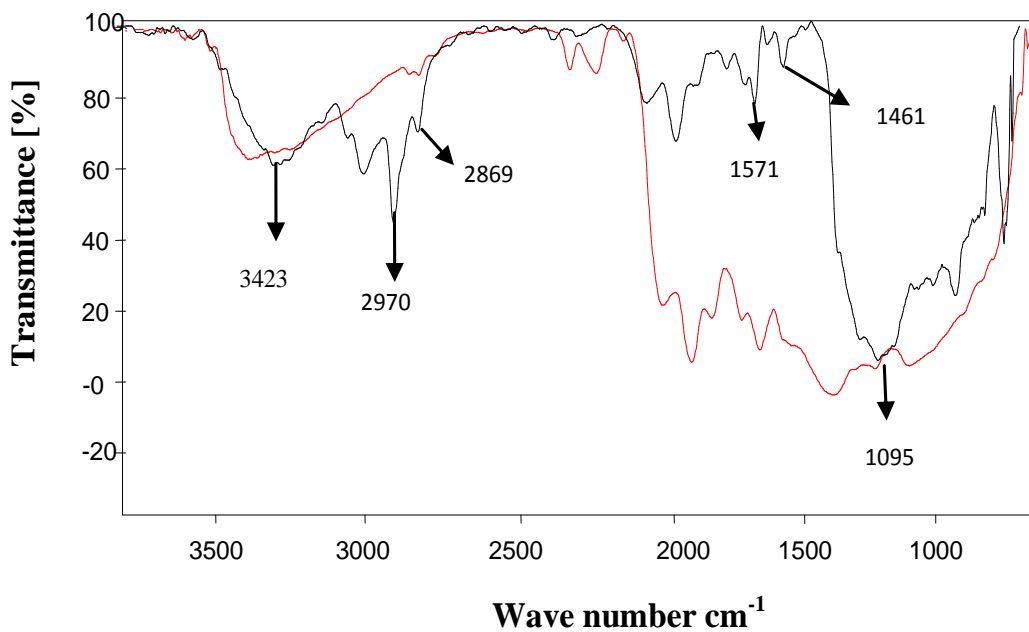


Figure 3.3. FTIR spectra of (i)CFA and (ii) [bmim]Cl/CFA

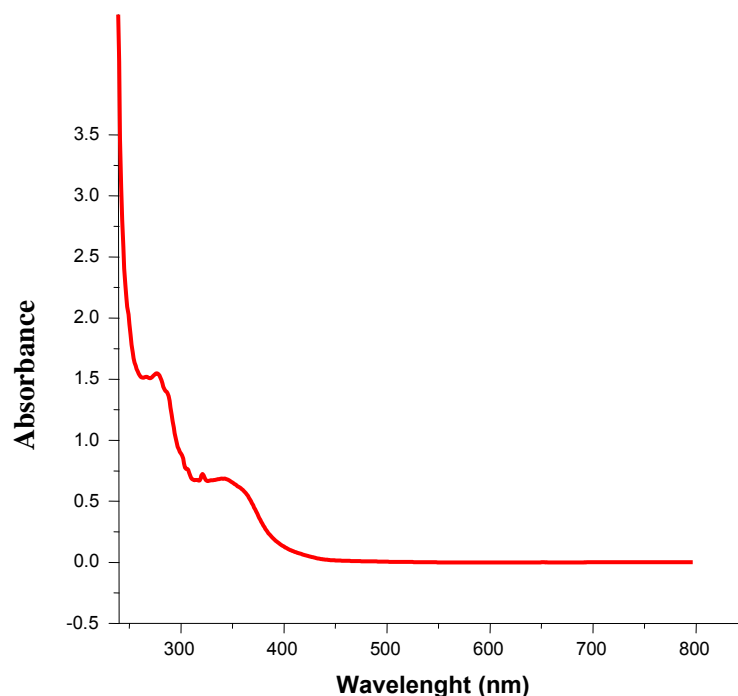
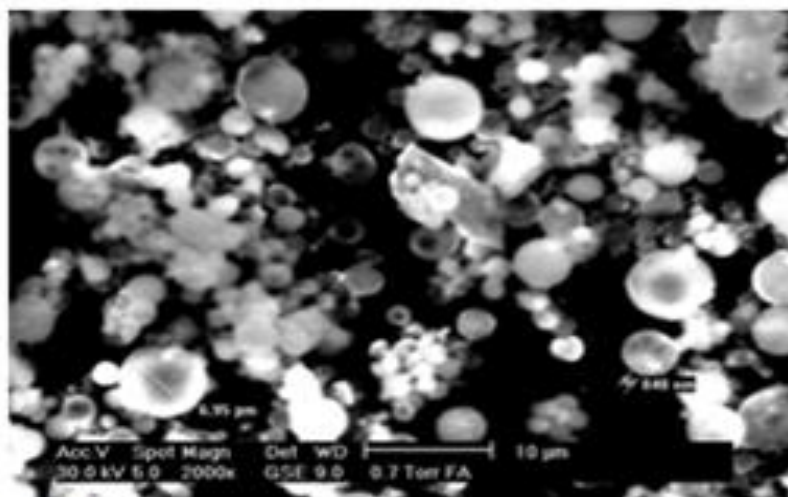


Figure 3.4: Uv-Visible spectra of [bmim]Cl/CFA

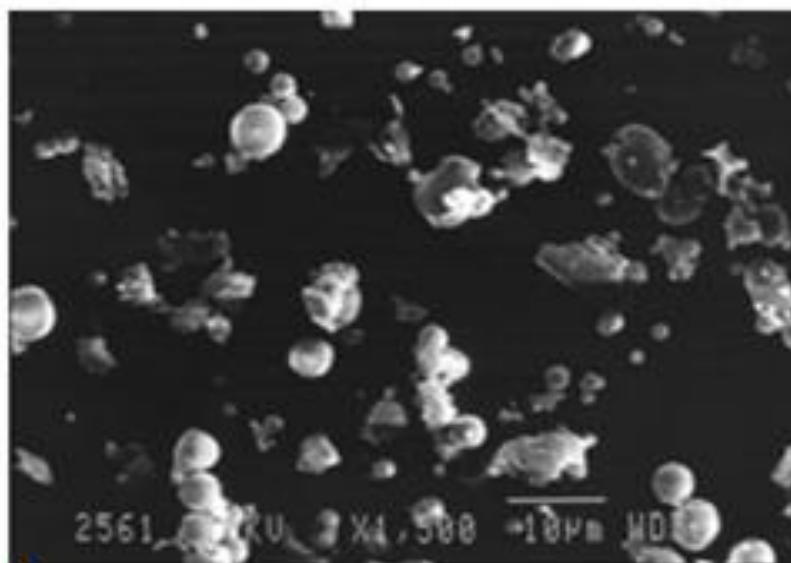
3.3.6 SEM and SEM-EDX analysis

SEM micrographs of raw FA in Figure 3.5a revealed different shaped, relatively smooth surface hollow cenospheres. In CFA shown in Figure 3.5b the crystalline and spherical particles break down into smaller size particles dissolving some of the crystalline phases. The SEM images of [bmim]Cl/CFA showed the irregular structures composed of large blocks with many small particles stacked together to form the bigger particles. All particles are wrapped by IL forming a thin layer over the surface of CFA clearly seen in Figure 3.5(d).

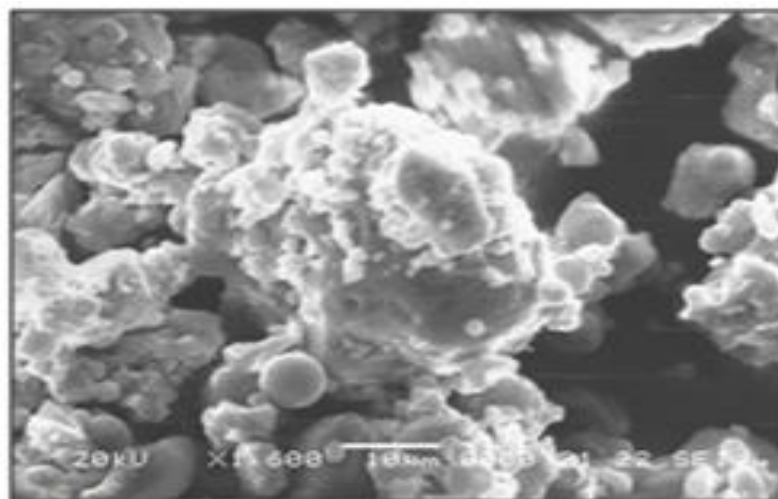
The energy dispersive spectrum (EDX) shows the presence of C, Fe, Si, O, and Al and other metals in FA and CFA samples. However the presence of high carbon (4.96%) and chloride (2.75%) in [bmim]Cl/CFA catalyst confirms immobilization of [bmim]Cl on activated surface of fly ash (Figure 3.6) .



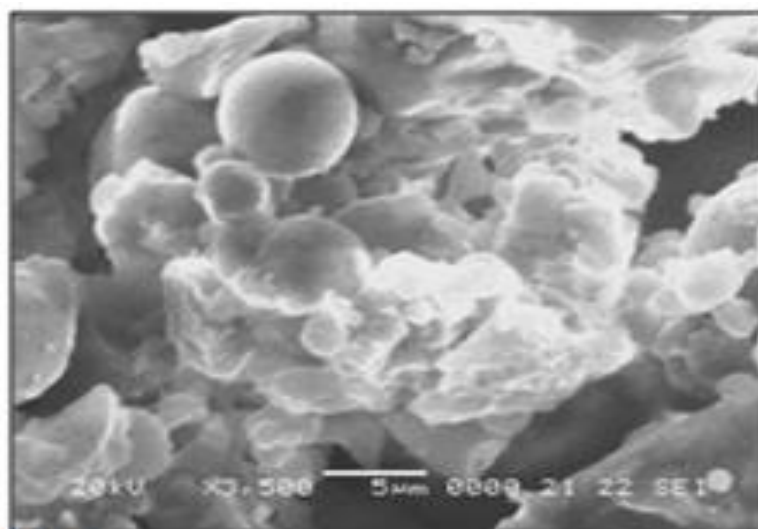
a



b



c



d

Figure 3.5. SEM micrographs (A) pure FA (B) CFA (C, D) [bmim]Cl /CFA and magnified image of [bmim]Cl/CFA

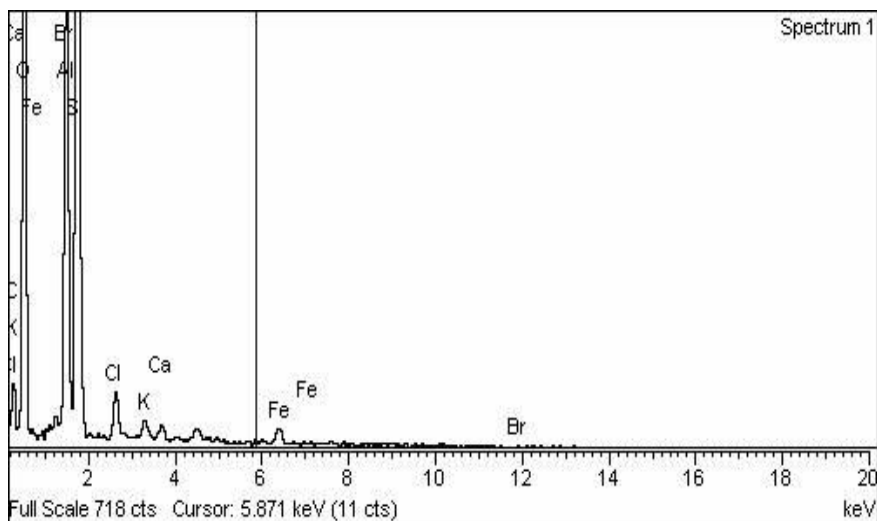


Figure 3.6: EDX spectrum of [bmim]Cl/CFA

3.3.7 Thermogravimetric analysis

The thermal stability of [bmim]Cl/CFA was determined by thermogravimetric analysis (Figure 3.7). The TGA curve indicated initial weight loss within 150°C mainly attributed to the desorption of physisorbed water and residual solvent. When the temperature further increased to 250 °C, the weight of [bmim]Cl/CFA decreased rapidly due to removal of IL. Finally, it was observed that the [bmim]Cl/CFA catalyst exhibited good thermal stability under 250 °C and the residual weight loss of [bmim]Cl/CFA was about 6% at around 800 °C.

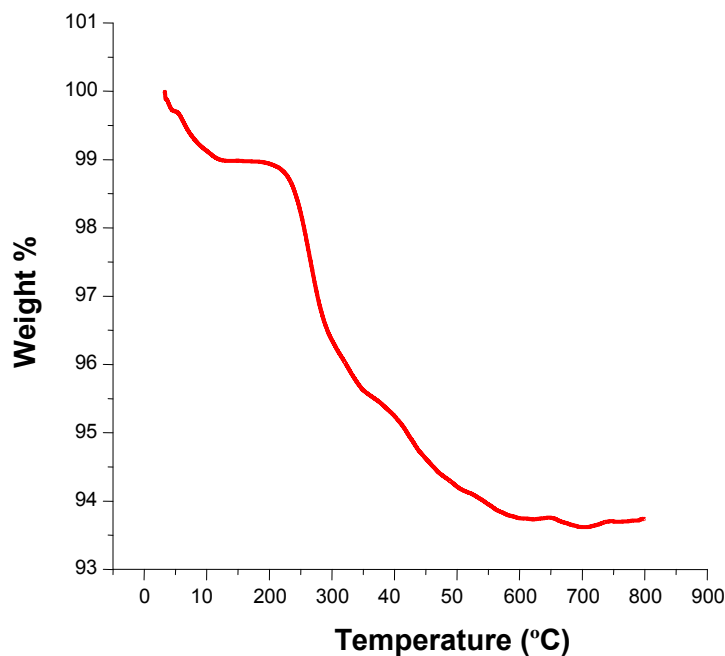


Figure 3.7. TGA pattern of [bmim]Cl/CFA

3.4 Catalytic activity

To evaluate the catalytic activity of synthesized catalysts, the esterification of butyric acid with octanol was carried out with and without catalyst. The yield of the product in each case is given in Table 3.3. For uncatalyzed reaction the yield of the product could reach only 15.0%. When reaction was carried out in homogeneous medium, [bmim]Cl showed good catalytic activity but separation of pure product was difficult with no possibility of catalyst reuse. [bmim]Cl/CFA showed no significant

loss in the yield of ester during second cycle confirming the high stability of catalytic sites. CFA without grafting Ionic Liquid have not shown significant catalytic activity for studied reaction.

Table 3.3. Esterification reaction between octanol alcohol and butyric acid

Sample	Catalysts	Temperature (°C)	Time (min.)	Yield (%)
1	Blank	110	15	15.04
	H ₂ SO ₄	110	20	40
2	CFA	110	15	45.03
3	[bmim]Cl	110	15	60
4	[bmim]Cl /CFA	110	15	91
5	[bmim]Cl /CFA (cycle 2)	110	15	90

Butyric acid (10mmol), octanol (20 mmol), acid/catalyst weight ratio (5:1)

Microwave assisted solvent-free synthesis of ester using different aliphatic alcohol and butyric acid was performed at different temperature ranging 90 °C to 120 °C for 5 to 20 min. to optimize the reaction temperature, time and catalyst and reactants molar ratio . The results of optimization of operating conditions for various studied reactions are given in Table 3.4.

Table 3.4. Optimization of reaction conditions for different esters using

[bmim]Cl/CFA catalyst

S.No.	Substrate	Molar Ratio	Catalyst amount	Product	Time (min.)	Temp (°C)	Conversion (%)
1	Butyric acid + propanol	1:1	0.4	Propy butanoate	10	80	56
		1:1	0.4		15	110	76
		1:2	0.4		15	110	95
		1:2	0.4		15	120	84
2	Butyric acid + butanol	1:1	0.4	Butyl butanoate	5	100	50
		1:1	0.4		10	110	65
		1:2	0.4		15	110	94
		1:2	0.4		15	120	86

3	Butyric acid + pentanol	1:1	0.4	Pentyl pentanoate	5	100	55
		1:1	0.4		15	110	75
		1:2	0.4		15	110	96
		1;2	0.4		20	120	84
4	Butyric acid + hexanol	1:1	0.4	Hexyl butanoate	10	100	58
		1:1	0.4		15	110	76
		1:2	0.4		15	100	78
		1:2	0.4		20	110	95
5	Butyric acid + octanol	1:1	0.4	Octyl butanoate	10	100	60
		1:1	0.4		15	110	76

		1:2	0.4		15	100	79
		1:2	0.4		15	110	96

3.4.1 Effect of reaction temperature

To optimize the reaction temperature for giving maximum conversion %, the reaction are studied at different temperature ranging from 80°C to 120°C for 15 minutes. The result showed that the conversion% of alcohols gradually increases with increase in temperature from 80°C to 110° as shown in Figure 3.7, which confirms endothermic nature of the reaction. The maximum conversion % is obtained at 110°C within 15 minutes which get decreased on increasing temperature up to 120°C. Given that boiling temperature of most of the reactants is very low, so above that temperature they become volatile, thus the contact time between the reactants reduces resulting in decrease in conversion%.

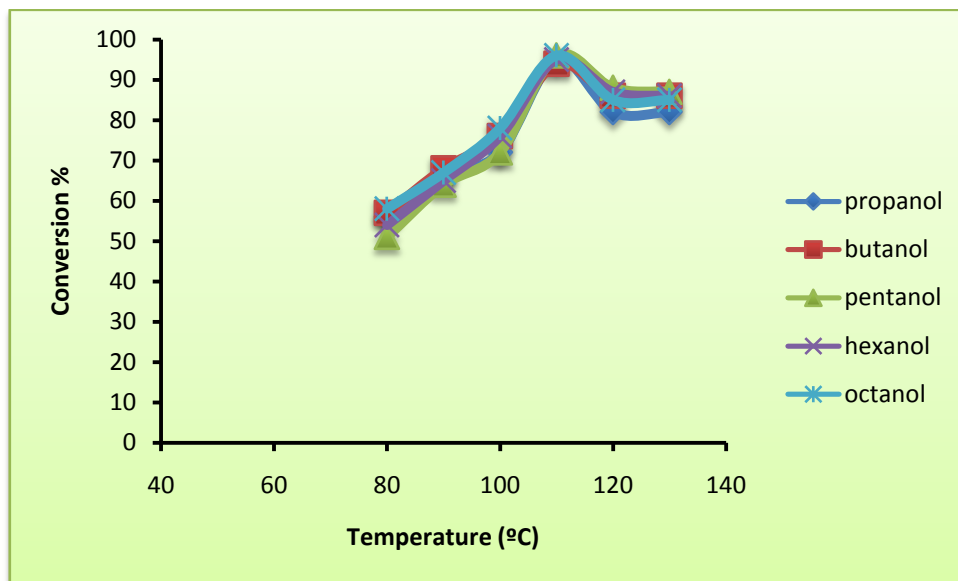


Figure 3.7: Variation of conversion% of alcohol over catalyst with temperature.

Reaction conditions under microwave irradiation: Power = 100W; Pmax = ON; time = 15 min, molar ratio(aliphatic alcohol/butyric acid)=1:2, substrate/catalystratio=5:1

3.4.2 Effect of reaction time

The effect of reaction time on conversion% is evaluated by performing reaction at 110°C to achieve maximum conversion% of product in the range of 5 to 20 min. as shown in Figure 3.8. In the first 10 min, the conversion % increased linearly which remained constant up to 20 min.

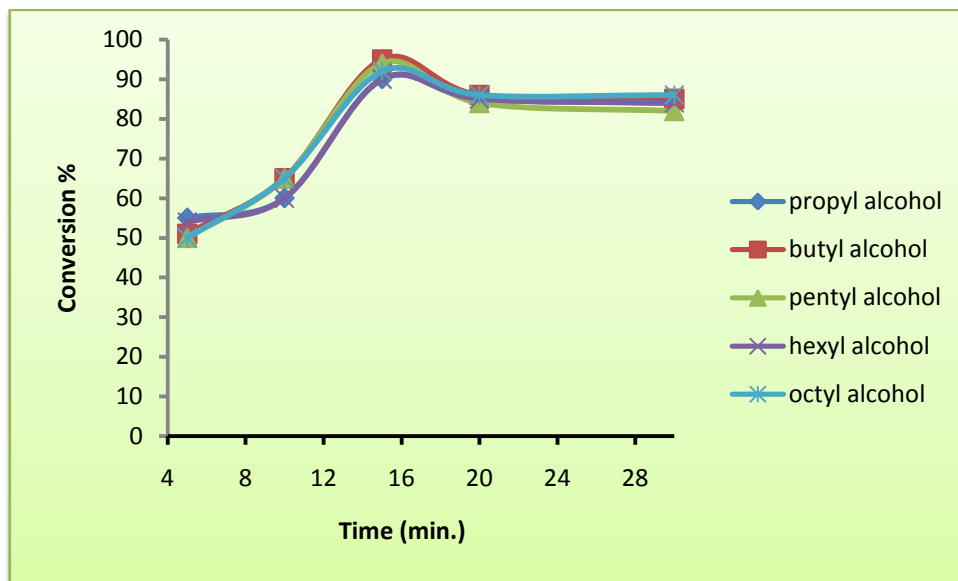


Figure 3.8: Variation of conversion% of alcohols over catalyst with time.

Reaction conditions under microwave irradiation: Temperature = 110 °C; Power = 100W; Pmax = ON; molar ratio(aliphatic alcohol/butyric acid)=1:2, substrate/catalystratio=5:1

3.4.3 Effect of molar ratio

The effect of molar ratio of alcohols and butyric acid on conversion% is studied by employing different molar ratio varying from 1:1 to 2:1 as shown in Figure 3.9. The conversion% of alcohols is found maximum at 1:2 molar ratio. Conversion% is drastically very less when alcohol is either in excess or equimolar quantity as large amount of alcohol may prevent access of acid to the catalytic active sites, formation of carbocation decreases and thus ester production was reduced.

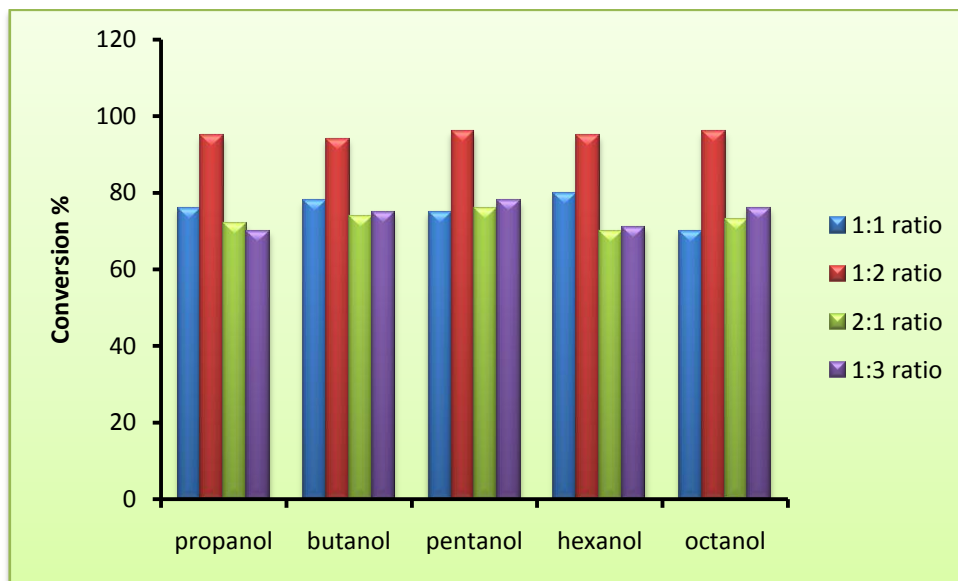


Figure 3.9: Variation of conversion (%) of alcohols over catalyst with molar ratio of reactants

Reaction conditions under microwave irradiation: Temperature = 110 °C; Power = 100W; Pmax = ON; time = 15 min, substrate/catalystratio=5:1

3.4.4 Effect of power output

The influence of power output of microwave instrument on conversion% is monitored at different power outputs ranging from 40 to 60W as shown in Figure 3.10. The optimized power output is found to be 50W where the conversion% of alcohols is maximum. On further increasing power output, no significant change in conversion% is seen.



Figure 3.10: Variation of conversion (%) of alcohols over catalyst with power output.

3.4.4 Effect of substrate to catalyst weight ratio

The effect of substrate to catalyst weight ratio on conversion % is studied by varying the amount of catalyst under optimized conditions as inferred from figure 3.11. On increasing catalytic species from 10 to 5 weight%, conversion% increases. It can be attributed due to availability of sufficient number of catalytic active sites for the adsorption of the reactants. On further increase in the amount of catalyst no significant change is observed.

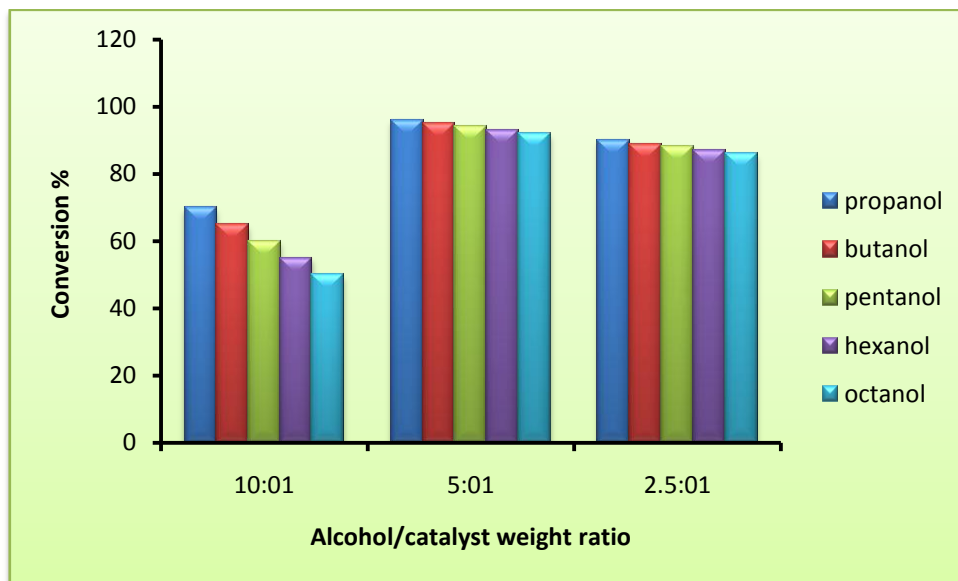


Figure 3.11: Variation of conversion(%) of alcohols over catalyst with substrate to catalyst weight ratio.

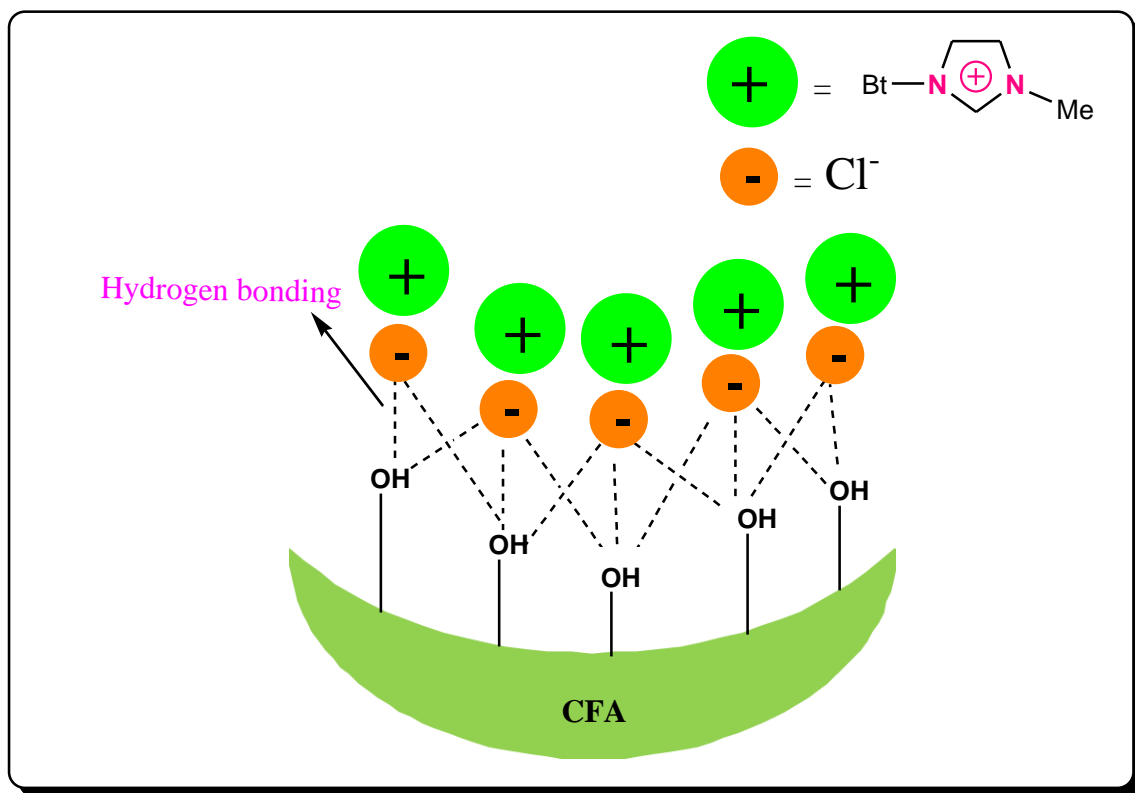
Reaction conditions under microwave irradiation: Temperature = 110 °C; Power = 100W; Pmax = ON; time = 15 min, molar ratio(aliphatic alcohol/butyric acid)=1:2

The maximum conversion% of products in a series of fisher esterification reaction(Table 3.5) is found when reaction is carried out at 110°C for 15min, taking alcohols and acid in 1:2 molar ratio, power output of 50W and substrate to catalyst ratio of 5:1 over [bmim]Cl/CFA.

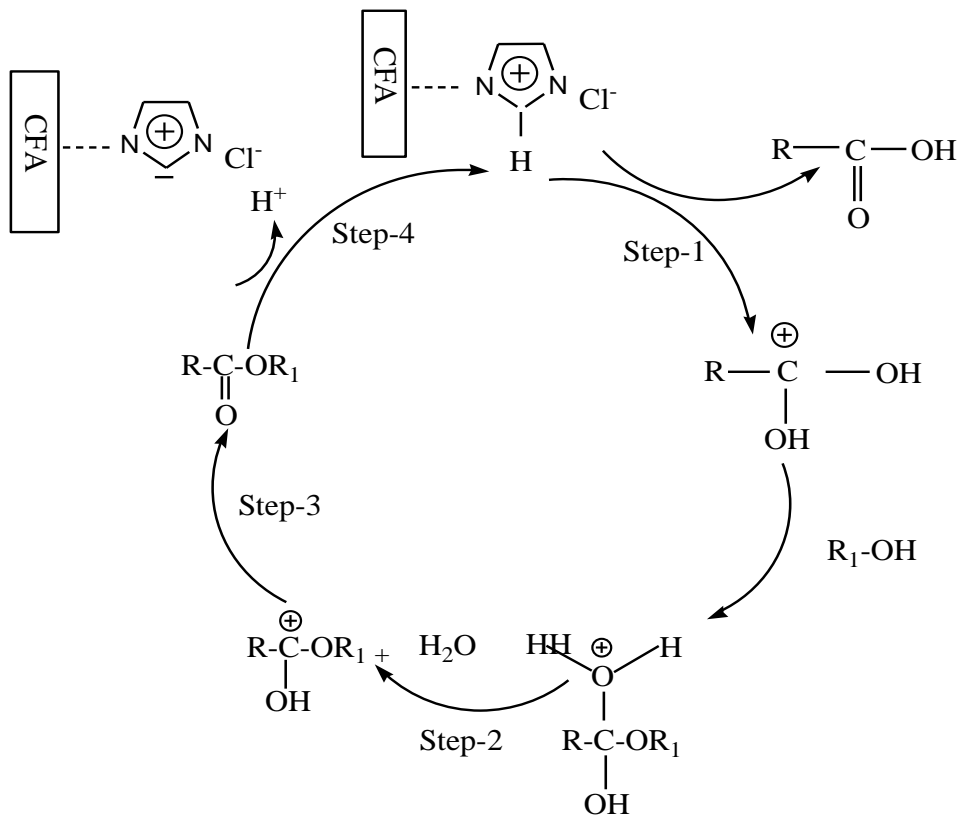
3.5 Proposed mechanism of ester formation

A proposed structure of the synthesized catalyst is shown in Scheme 3.5. The plausible mechanism for [bmim]Cl/CFA catalyzed esterification is schematically presented in Scheme 3.6. The C2 of the IL is positively charged due to the electron deficit in the C= N bond whereas the other carbons are practically neutral[45].This

resulting acidity of the C2 hydrogen atom of [bmim]Cl/CFA initiates esterification reaction by donating a proton[46-48] to the carboxylic acid in step 1. Then carboxylic acid becomes susceptible for a nucleophilic attack by the hydroxyl group (step 2). When alcohol (polar species) interacts with microwave it starts oscillating. During oscillation, the polar species collide with neighboring charged particles i.e. carbonium ion, resulting an intermolecular friction. This molecular friction generate intense internal heat liable for the formation of intermediate species which further leads to formation of ester with subsequent removal of water as a byproduct. In the last step (step 4), the imidazolium cation is regenerated.



Scheme 3.5: The proposed structure of [bmim]Cl/CFA catalyst



Scheme 3.6: Proposed mechanistic pathway of microwave-assisted esterification of propanoic acid with aliphatic alcohol over [bmim]Cl/CFA catalyst

3.6 Regeneration and reusability of catalyst

The regenerated catalyst could be used up to four reaction cycles giving conversion% of octanol in the range of 96-85%, as shown in (Table 3.5) which indicates that the acidic sites are not leixivated during regeneration. The conversion% was slightly decreased with increasing reuse run, which may due to the deposition of significant

amount of carbonaceous material on the surface of used catalyst that may block the active sites present on the catalyst.

Table 3.5: The reusability test of [bmim]Cl/CFA for test esterification of octanol and butyric acid

S.No.	Run	Conversion (%)
1	Fresh catalyst	96
2	First cycle	92
3	Second cycle	89
4	Third cycle	85

Reaction conditions under microwave irradiation: Temperature = 110 °C; Power = 100W; Pmax = ON; time = 15 min, molar ratio(octanol/butyric acid)=1:2, substrate/catalystratio=5:1

3.7 Conclusion

The present work here in reveals the promising use of fly ash as an innovative solid support material for synthesis heterogeneous catalyst through thermal followed by chemical activation with sulphuric acid. The chemical activation of fly ash consequence in increased amorphous silica content and surface free hydroxyl groups, which ultimately results in enhanced hydrogen bonding between ionic liquid anions and silanol groups. Dielectric heating was applied for synthesis of ionic liquid and esters. Synthesized [bmim]Cl was successfully grafted over CFA, the resulting

heterogeneous catalyst [bmim]Cl/CFA exhibited excellent catalytic activity for microwave assisted esterification of butyric acid with various alcohols at optimized reaction conditions. The catalyst is easily filtered, regenerated and used for four reaction cycles with analogous efficiency, suggesting that the active sites of catalyst remain stable during reaction process. The use of FA based catalysts may lead to an cost effective synthetic technology for industrially important ester synthesis.

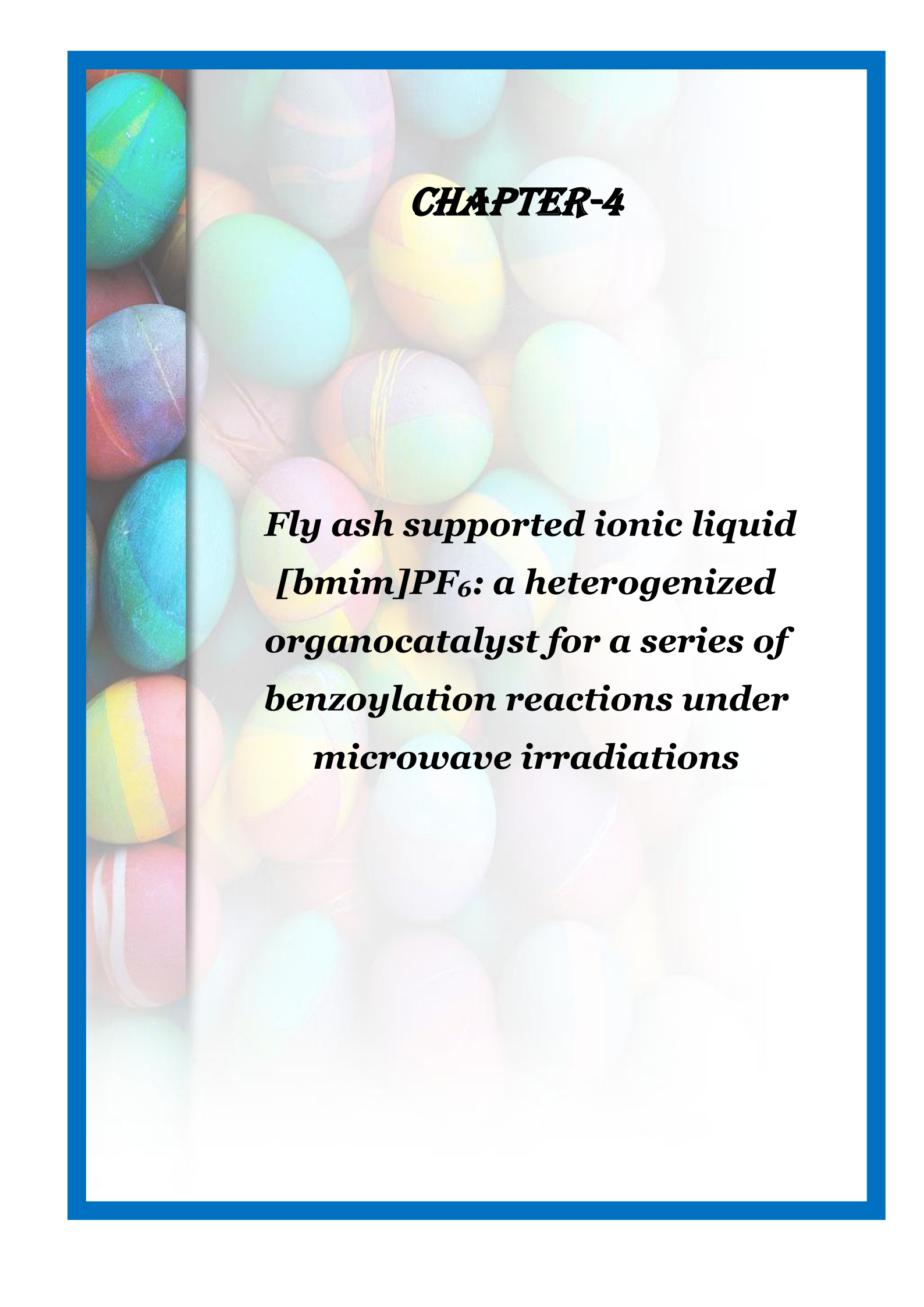
3.8 Reference

1. G. Koehl, N. Keller, F. Garin, V. Keller, *Appl. Cat. A: Gen.* 289 (2005) 37-43.
2. G. Koehl, N. Keller, F. Garin, V. Keller, *Clays Clay Miner.* 50 (2002) 771-783.
3. D. Jain, C. Khatri, A. Rani, *Fuel Process. Technol.* 91 (2010) 1015–1021.
4. D. Jain, A. Rani, *Amer. Chem. Sci. J.* 1 (2011) 37- 49.
5. C. Khatri, D. Jain, D. Rani, *Fuel* 89 (2010) 3853–3859.
6. A. Rani, C. Khatri, R. Hada, *Fuel Process. Technol.* 116 (2013) 366-373.
7. C. Khatri, A. Rani, *Fuel* 87 (2008) 2886–2892.
8. N. Shringi, K. Srivastava, A. Rani, *Chem. Sci. Rev. Lett.* 4 (2015) 561-570.
9. C. Khatri, A. Rani, Green catalytic process for aspirin synthesis using fly ash as hetero-geneous solid acid catalyst, Indian Patent No. - 1980/DEL/2007.
10. C. Khatri, M.K. Mishra, A. Rani, *Fuel Process. Technol.* 91 (2010) 1288–95.
11. T. Welton, *Chem Rev.* 99 (1999) 2071.
12. M. Picquet, D. Poinot, S. Stutzmann, I. Tkatchenko, I. Tommasi, P. Wasserscheid, J. Zimmermann, *Top. Catal.* 29 (2004) 139–143.
13. B.Y. Liu, J. Han, J.F. Dong, F.X. Wei, Y.H. Cheng, *Chin. J. Org. Chem.* 27 (2007) 1236–1243.

14. S. Sahoo, P. Kumar, F. Lefebvre, S.B. Halligudi, *Catal. A: Gen.* 354 (2009) 17–25.
15. D. Zhao, M. Wu, Y. Kou, E. Min, *Catal. Today* 74 (2002) 157.
16. J. Dupont, R.F. Souza, P.A.Z. Suarez, *Chem.Rev.* 102 (2002) 3667.
17. R. Sugimura, K. Qiao, D. Tomida, C. Yokoyama, *Catal. Commun.* 8 (2007) 770.
18. H. Vallette, S. Pican, C. Boudou, J. Levillainb, J.C. Plaqueventa, A.C. Gaumont, *Tetrahedron Lett.* 47 (2006) 5191–5193.
19. J. Miao, H. Wan, Y. Shao, G. Guan, B. Xu, *J. of Mol. Catal. A: Chem.* 348 (2011) 77–82.
20. Y. Lin, F. Wang, Z. Zhang, J. Yang, Y. Wei, *Fuel* 116 (2014) 273–280.
21. P.H. Li, B. L. Li, H. C. Hu, X. N. Zhao, Z. H. Zhang, *Catal. Commun.* 46 (2014) 118-122.
22. H. Li, P.S. Bhadury, B. Song, S. Yang, *RSC Adv.* 2 (2012) 12525–12551.
23. S. Breitenlechner, M. Fleck, T.S. Müller, A. Suppan, *J. Mol. Catal. A* 214 (2004) 175.
24. D.W. Kim, D.Y. Chi, *Angew. Chem. Int. Ed.* 43 (2004) 483.
25. A. Riisager, R. Fehrmann, S. Flicker, R. Van Hal, M. Haumann, P. Wasserscheid, *Angew. Chem.Int. Ed.* 44 (2005) 815.
26. C.P. Mehnert, *Chem. Eur. J.* 11 (2005) 50.
27. F. Shi, Q. Zhang, D. Li, Y. Deng, *Chem. Eur. J.* 11 (2005) 5279.
28. F. Wang, W. Zhang, J. Yang, L. Wang, Y. Lin, Y. Wei, *Fuel* 107 (2013) 394-399.
29. K. Qiao, H. Hagiwarab, G. Yokoyamaa, *J. of Mol. Catal. A: Chem.* 246 (2000) 65- 69.
30. A. Chrobok, S. Baj, W. Pudlo, A. Jarzebski, *Appl. Catal. A: Gen.* 366 (2009) 22-28.
31. M.N. Sefat, D. Saberi, K. Niknam, *Catal. Lett.* 141 (2011) 1713-1720.
32. M.N. Parvina, H. Jina, M.B. Ansaria, S.M. Oh, S.E. Park, *Appl. Catal. A: Gen.* 413– 414 (2012) 205– 212.

33. C.P. Mehnert, R.A. Cook, N.C. Dispenziere, M. Aferwork, *J. Amer. Chem. Soc.* 124 (2002) 12932–12933.
34. A. Riisager, R. Fehrmann, M. Haumann, P. Wasserscheid, *Eur. J. Inorg. Chem.* 4 (2006) 695–701.
35. A. Riisager, P. Wasserscheid, P. Van Hal, R. Fehrmann, *J. Catal.* 219 (2003) 452–455.
36. C.P. Mehnert, E.J. Mozeleski, R.A. Cook, *Chem. Commun.* 24 (2002) 3010–3011.
37. P.M. Arvela, J.P. Mikkola, P. Virtanen, H. Karhu, T. Salmi, D.Y. Mursin, in: E.M. J. Gaineaux, et al. (Eds.), *Scientific Bases for the Preparation of Heterogeneous Catalysts*, Elsevier B.V. (2006) 87–94.
38. J. Zhao, S. Gu, X. Xu, T. Zhang, Y. Yu, X. Di, NI, Z. Pan, Z. Li, *Catal. Sci. Technol.* 6 (2016) 3263–3270.
39. A. Riisager, B. Jorgensen, P. Wasserscheid, R. Fehrmann, *Chem. Commun.* 9 (2006) 994–996.
40. J. Joni, M. Haumann, P. Wasserscheid, *Adv. Synth. Catal.* 351 (2009) 423–43.
41. A. Riisager, R. Fehrmann, M. Haumann, P. Wasserscheid, *Top. Catal.* 40 (2006) 91–102.
42. H. Hagiwara, Y. Sugawara, K. Isobe, T. Hoshi, T. Suzuki, *Org. Lett.* 6 (2004) 2325–2328.
43. A. Sharma, K. Srivastava, V. Devra, A. Rani, *Amer. Chem. Sci. J.* 2(4) (2012) 177–187.
44. S. Sahoo, P. Kumar, F. Lefebvre, S.B. Halligudi, *Appl. Catal. A: Gen.* 354 (2009) 17–25.
45. Y. Tao, R. Dong, I. V. Pavlidis, B. Chen, T. Tan, *Green Chem.* 18 (2016) 1240–1248.

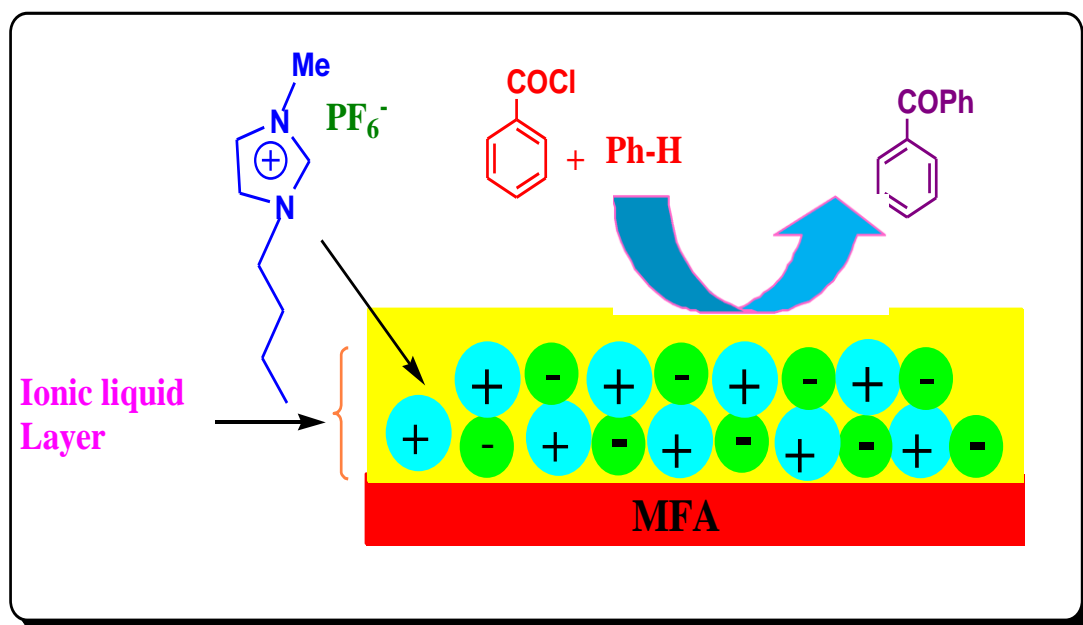
46. S. Sowmiah, V. Srinivasadesikan, M. C. Tseng, Y.H. Chu, *Molecules* 14 (2009) 3780-3813.
47. H. Olivier-Bourbigou, L. Magna, D. Morvan, *Appl. Catal. A: Gen.* 373 (2010) 1–56
48. R. S. Földes, *Molecules*, 19 (2014) 8840-88.

The background of the slide is a collection of colorful Easter eggs in various patterns and colors, including solid colors like blue, green, yellow, and pink, as well as multi-colored stripes and marbled patterns. The eggs are arranged in a dense, overlapping manner, creating a vibrant and festive atmosphere. The entire slide is framed by a thick blue border.

CHAPTER-4

***Fly ash supported ionic liquid
[bmim]PF₆: a heterogenized
organocatalyst for a series of
benzoylation reactions under
microwave irradiations***

Abstract



Benzoylation reaction over fly ash supported 1-butyl-3-methyl-imidazolium hexafluorophosphate catalyst

4.1 Introducton

Friedel-Crafts benzoylation reactions of aromatic substrates is key reaction of synthetic chemistry as it produces diaryl ketones like ibrupofen, S-naproxen, musk fragrance useful in synthesis of various valuable pharmaceutical compounds, dyes, fragrances and agrochemicals etc[1]. Benzoylation is aromatic electrophilic substitution reaction in which the carbocation intermediate is produced by complexation between benzoyl halide and catalyst. Over past few decades benzoylation resction has been performed extensively using organic solvents with homogeneous catalysts such as AlCl_3 , FeCl_3 , BF_3 , ZnCl_2 , TiCl_4 , ZrCl_4 , bronsted acids like H_2SO_4 , Polyphosphoric acid [2]. Taking into consideration growing environmental concerns, high amount of toxic effluents generated in neutralization process is unbearable and thus, replacement of homogeneous lewis acids is essential . Solid acids used in this protocol are zeolites [3], clays [4] modified metal oxides [5], ion-exchange resins [6], silica supported heteropoly acid [7], heteropoly acids, microencapsulated scandium triflate etc. numerous benzoylating agents are employed for performing benzoylation reactions, such as benzoyl chloride, benzoyl tetrazole, 2-benzoxy-1-methyl pyridinium chloride, benzoic anhydride. [8-11] benzoyl chloride is widely used benzoylating agent due to its availability and low cost. Conventional solid acid catalysts have disadvantages such high mass transfer resistance, easy to deactivation and use of solvent system which are inconvenient for industrial applications.

Aiming to reduce the amount of hazardous, volatile solvents and corrosive catalysts require an increasing emphasis on the use of green, ecofriendly and less toxic materials. Recently green chemistry have introduced ionic liquid as very interesting substituent for volatile solvents. Ionic liquids are low-melting organic salts typically contain a large asymmetric cation and a weakly coordinating anion (e.g. BF_4^- , PF_6^- or Tf_2N^-) which reduce the lattice energy of the crystalline structure of the salt and hence to lower their melting point so that they generally remain liquid at or near room

temperature[12]. Their physicochemical properties can be finely tuned by a criterious choice of the cation and/or the anion. In this chapter we have synthesized **1-butyl-3-methylimidazolium hexafluorophosphate [Bmim]PF₆** from 1-butylchloride, 1-methylimidazole, sodium hexafluorophosphate using microwave heating by one-pot under solvent-free conditions . This method requires only a few minutes of reaction time, in contrast to the several hours needed using conventional methods by two pots that requires a lot of organic solvent. The reaction yield of ionic liquids with intermittent microwave heating is much higher than that of ionic liquids with conventional microwave heating. 1-Butyl-3-methylimidazolium hexafluorophosphate ([bmim][PF₆]) is a colorless liquid with many favorable qualities. This is stable in both air and water [13]. It is also very viscous. At 298 K the ionic liquid's viscosity is 312mPa-s. [BMI][PF₆], has a melting point of -64°C and exhibits crystalline diffraction patterns at -20°C consistent with a long range molecular ordering. [Bmim][PF₆] is hydrophobic and is immiscible in water which make it ideal substance for liquid-liquid extractions and product separation[14] . The 3D structure of prepared ionic liquid is given in Figure 4.1. Due to its green characteristic

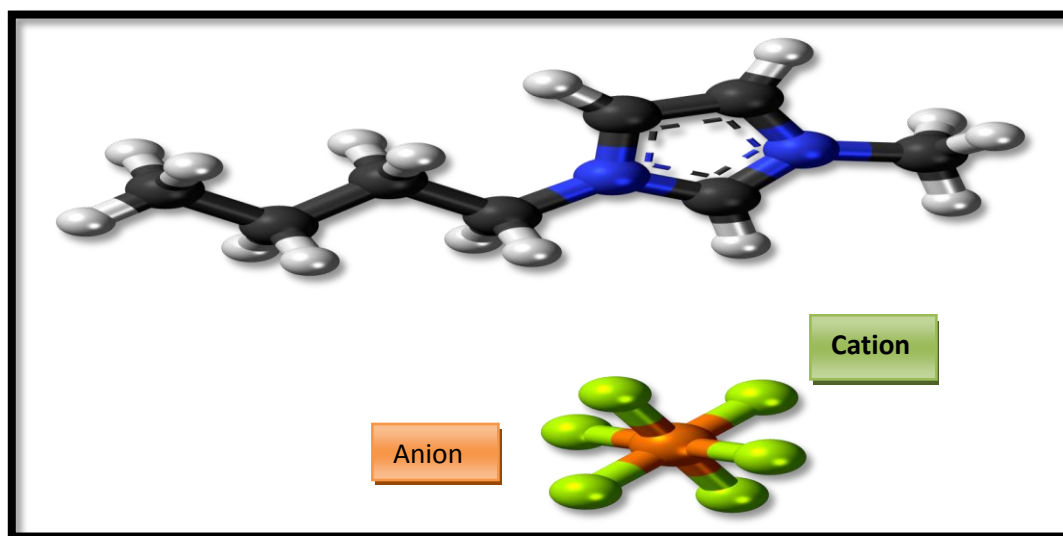


Figure 4.1 3D structure of 1-Butyl-3-methylimidazolium hexafluorophosphate ionic liquid

Although this IL are commercially available but large consumption of IL as solvent or catalyst and unendurable viscosities restricted their industrial applications. Due to its green characteristics studies of immobilization of [BMI][PF₆] on various support materials have been reported. Palladium acetate -[BMI][PF₆] matrix immobilized MFI-zeolite has been efficiently used as catalyst for Suzuki-coupling reaction[15]. Palladium nanoparticles, immobilized on [bmim][PF₆] films supported on laponite clay, have been investigated for Mizoroki–Heck cross-couplings of aryl halides[16].

In present research work an fairly economic, recyclable, potentially active and microwave stable heterogeneous solid catalyst has been synthesized by immobilization of ionic liquid [bmim]PF₆ on mechanically activated fly ash(MFA) through simple impregnation method. The ionic liquid was synthesized using consecutive quaternisation-anion metathesis method under microwave irradiation. As synthesized catalyst are characterized by N₂ adsorption-desorption, X-ray diffraction, fourier transform infrared, scanning electron microscopy, thermo-gravimetric analysis, ultra-visible spectroscopy, ¹HNMR techniques. The catalytic activity is evaluated by a series of microwave assisted benzylation of arenes and benzoyl chloride of Giving highly selective products up to four reaction cycles under solvent free reaction conditions. The effect of various reaction parameters like time, temperature, power output etc. on conversion% is also studied in this chapter. Surface free silanol groups, surface roughness, silica percentage and thus the potential of fly ash as innovative support material is increased by mechanical activation. This work provides ecofriendly pathway for development of cost effective, modified fly supported ionic liquid catalyst and its novel application in industrially important microwave assisted benzylation reactions.

4.2 Experimental

4.2.1 Material

Fly ash [Class F type ($\text{SiO}_2 + \text{Al}_2\text{O}_3$) > 70%], collected from Kota Thermal Power Plant (Rajasthan, India) was used as support for the preparation of the supported ionic liquid catalyst. Aromatic compounds, benzoyl chloride, dichloromethane and diethylether were obtained from S.D. Fine Chem. Ltd., India. Ionic liquid precursors 1-methylimidazole (99%), chlorobutane, Sodium hexafluorophosphate were purchased from Sigma aldrich.

4.2.2 Catalyst preparation

Activation of fly ash

As received Fly ash (FA) was washed with distilled water followed by drying at 100°C for 3h thereafter mechanical activation was performed using high energy planetary ball mill. The activation procedure of FA to synthesize MFA-40 is described in chapter-2. MFA-40 was selected for immobilizing [bmim][PF₆] on surface of MFA.

Synthesis of [bmim]PF₆

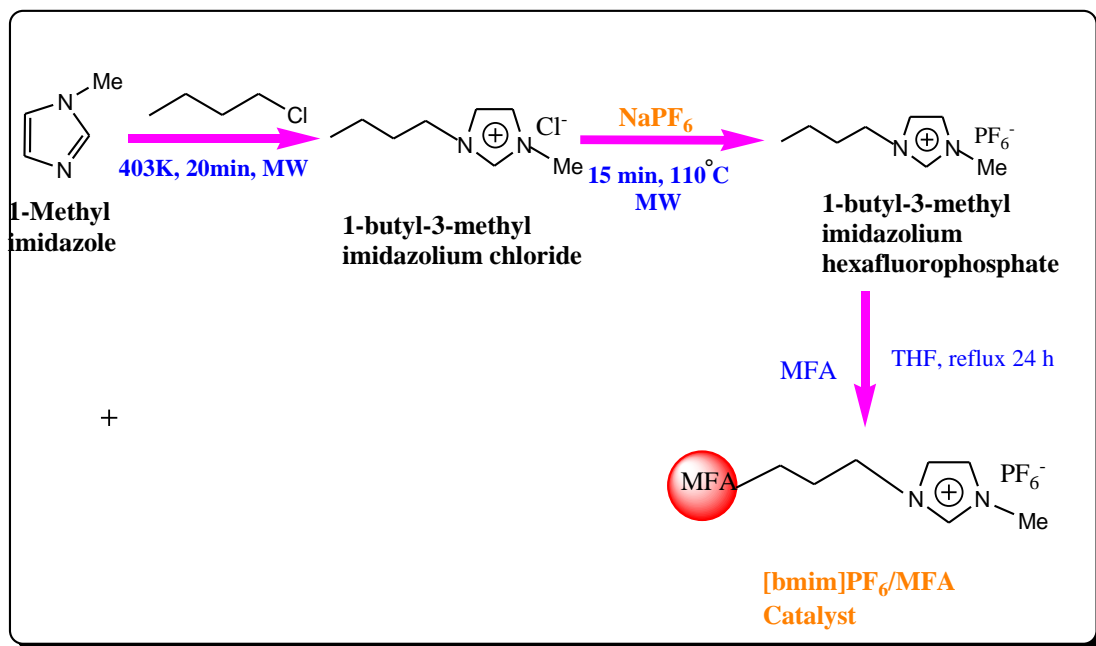
A mixture of 1-methylimidazole 1 (1.23 g, 15 mmol) and 1-chlorobutane (1.38 g, 15 mmol) was placed in reactor tube and irradiated under microwave at 110 °C for 20 min. Sodium hexafluorophosphate (20 mmol) was added and the resulting mixture was then placed under MW irradiation for 15 min at 110 °C. The reaction mixture was brought to room temperature and CH₂Cl₂ (5 mL) was added. NaCl was separated through filtration and crude product was washed with Et₂O (25 mL) and dried under reduced pressure to afford yellow colored liquid, which did not need further purification. The synthesized IL [bmim]PF₆ was characterized by ¹H-NMR(CdCl₂, 400MHz): δ(ppm) = 8.29 (s, 1H, NCHN), 7.258 (d, 1H, CH₃NCHCHN), 7.22 (d, 1H,

CH₃NCHCHN), 4.05 (m, 2H, NCH₂(CH₂)₂CH₃), 3.78 (s, 3H, NCH₃), 1.71 (m, 2H, NCH₂CH₂CH₂CH₃), 1.25 (m, 2H, N(CH₂)₂CH₂CH₃), 0.816 (t, 3H, N(CH₂)₃CH₃).

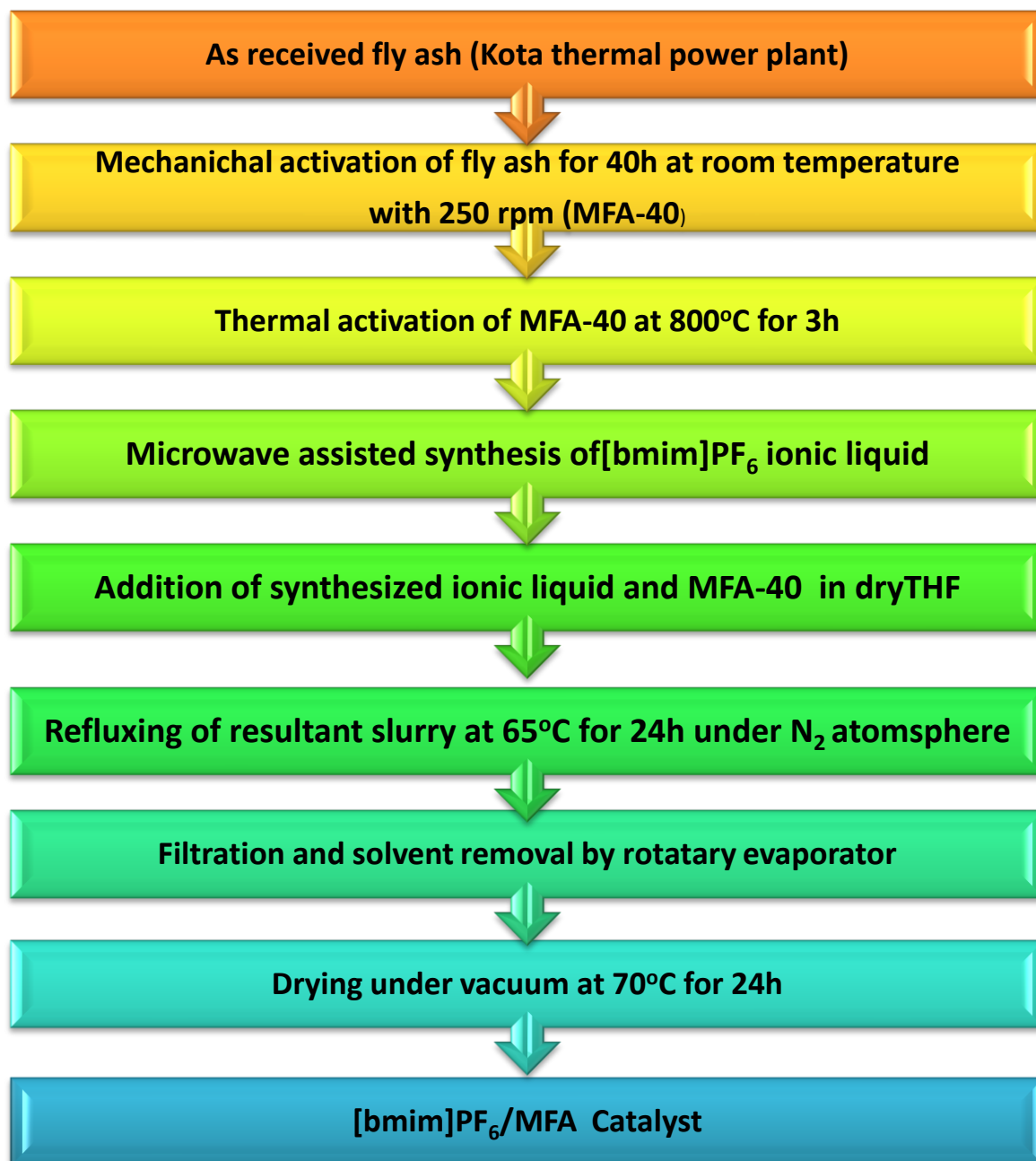
IR (CDCl₃, cm⁻¹): 623.27, 755.04, 1030.54, 1053.53, 1572.27, 1636.71, 2875.27, 2933.93, 2961.27, 3155.33, 3422.71.

Synthesis of [bmim]PF₆/MFA

During immobilization process, firstly MFA was activated at 550 °C for 1 h and [bmim]PF₆ was dried at 70°C under vacuum for 1 h. 1gm of [bmim]PF₆ was dissolved in 50 ml THF, followed by taking 5gm of pretreated MFA in a refluxing assembly under vacuum. The mixture was refluxed under N₂ atmosphere at 65 °C for 24 h. After cooling to room temperature the product was filtrated, washed with dry dichloromethane to remove the excess of ionic liquid and dried under vacuum at 70 °C for 24 h to give brown catalyst powder. The steps of synthesis [bmim]PF₆/MFA catalyst are summarized in Scheme 4.2.



Scheme 4.1: The synthesis route of [bmim]PF₆ functionalized FA.



Scheme 4.2: Steps for synthesis of [bmim]PF₆/MFA catalyst

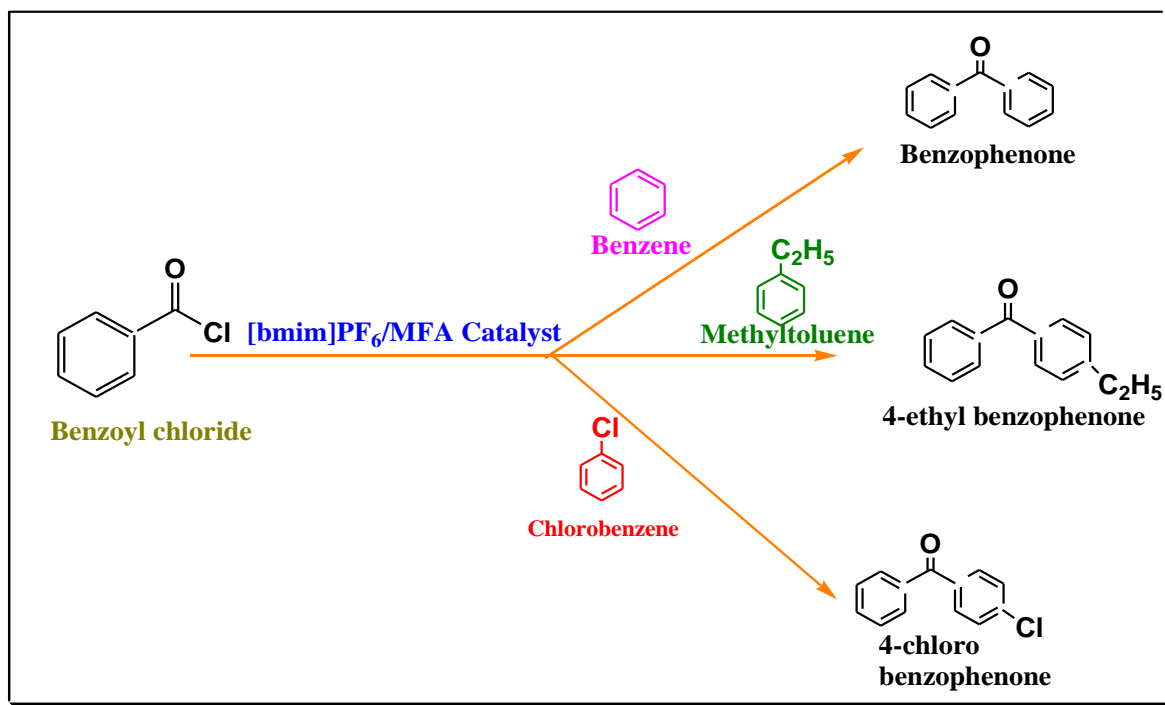
4.3.6 Characterization techniques

Physicochemical properties of all prepared samples are evaluated using XRD, FTIR, SEM-EDX, TGA, BET surface area, UV-Visible, ^1H NMR techniques as described in

Annexure-I

4.2.7 Catalytic activity of $[\text{bmim}]\text{PF}_6/\text{MFA}$

The performance of $[\text{bmim}]\text{PF}_6/\text{MFA}$ catalyst as a heterogeneous catalyst was tested using microwave assisted solvent free Friedel-Crafts benzylation of aromatic compounds with benzoyl chloride (Scheme 4.3) as a test reaction in microwave reactor.



Scheme 4.3: Simplified reaction pathway of benzylation of aromatic substrates by benzoyl chloride over $[\text{bmim}]\text{PF}_6/\text{MFA}$ catalyst to give corresponding benzophenone and its substituents.

A mixture of aromatic compounds and benzoyl chloride (different molar ratio) were placed in the reactor tube. Prior to the reaction catalyst, activated for 1h at 80 °C under vacuum, was added in the reaction mixture. The reaction was carried out at different molar ratio of reactants at different temperatures ranging from 50-140°C for time in the range of 5-30min. During the reaction proceeding checked the vapor loss and continuous stirring of the pressurized glass vial. After completion of the reaction, the mixture was cooled at room temperature through air pump before releasing the pressure of the reactor tube. The filtered catalyst was washed with dichloromethane to remove organic impurities. The filtrate was diluted with ethyl acetate (50 mL), washed with H₂O (3 × 20 mL), aqueous NaHCO₃ (2 × 20 mL), and brine (20 mL), and dried over Na₂SO₄. The solvent was removed on a rotary evaporator. was separated by ether. The reaction conditions were varied to obtain maximum yield and conversion to ester. The reactions were analyzed using a GC with oven temperature range 70-240 °C and N₂ (25 ml/min) as a carrier gas. The conversion of aromatic compound and yield% of product was calculated by using weight percent method given below.

$$\text{Conversion (\%)} = 100 \times \frac{\text{Intial wt \%} - \text{Final wt \%}}{\text{Intial wt \%}}$$

4.3 Results and Discussion

4.3.1 BET analysis

Bet specific surface area of fly ash samples as given in Table 4.1. indicates that with enhancing milling time from 5 to 40h, specific surface area of fly ash also increases from 9 to 36m²/g . On immobilization of ionic liquid, the specific surface area of [bmim]PF₆ /MFA catalyst decreases due to agglomeration of small particles of fly ash.

Table 4.1 : Characterization of fly ash before and after mechanical activation

Sample	Specific surface area, m ² /g
FA	9
MFA-5	11
MFA-10	15
MFA-15	17
MFA-40	36
[bmim]PF ₆ /MFA	20

4.3.2 X-ray diffraction analysis

The X-Ray diffraction patterns of the as received FA as well as MFA as described in chapter 2 show decrement in the crystallinity of fly ash and increase in the amorphous nature as inferred with decrease in the crystalline size of fly ash from 33nm to 16nm on milling. The peaks at 16.4° and 26.2° show mullite (alumino-silicate) phase while quartz (silica) exhibits strong peaks at 20.7°, 26.6°, 40.6° and 49.9° of 2θ values. As a result of ball milling mostly quartz and mullite crystalline phases are reduced.

4.3.3 Fourier transform infrared analysis

The FT-IR spectra of FA and MFA-36 in Figure 4.2 show broad band between 3400-3000 cm⁻¹, which is attributed to surface -OH groups of Si-OH and adsorbed water molecules on the surface.

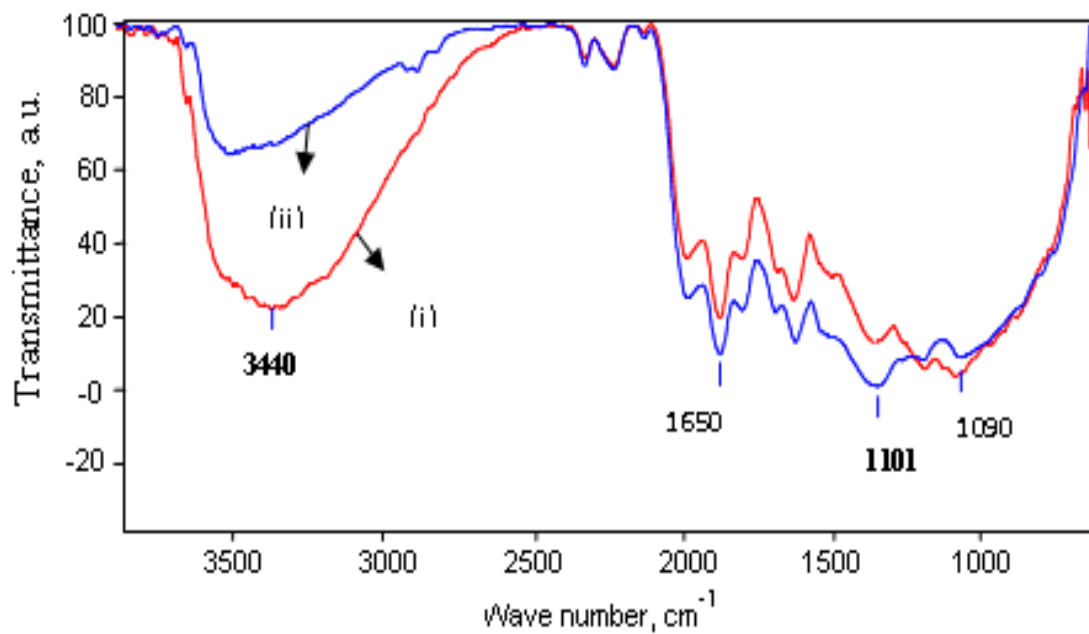


Figure 4.2 FTIR spectra of (i) FA (ii) MFA-40

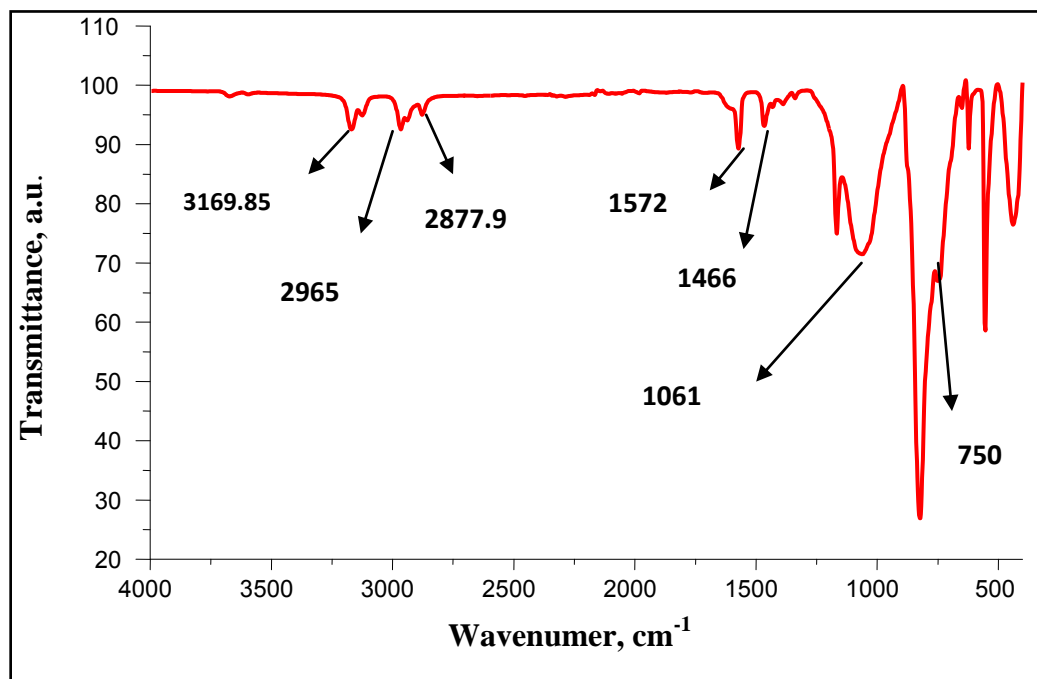


Figure 4.3: FTIR spectra of [bmim]PF₆/MFA

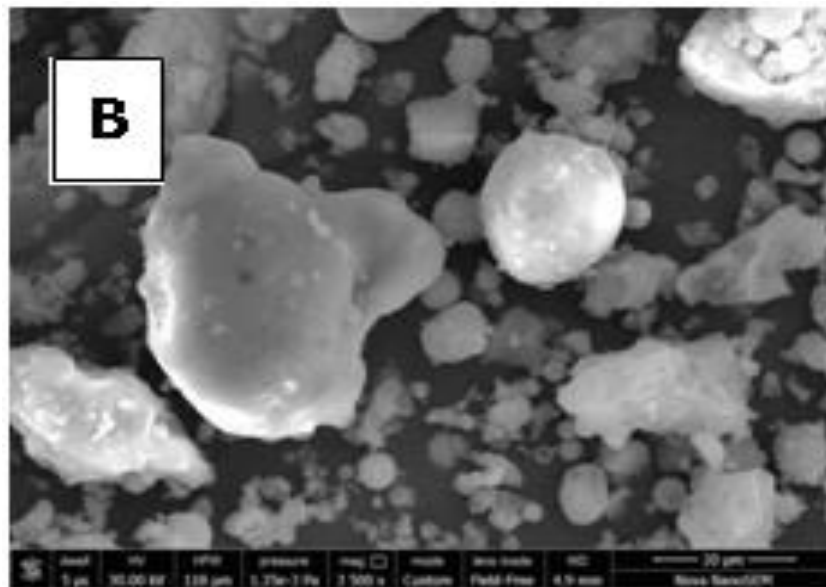
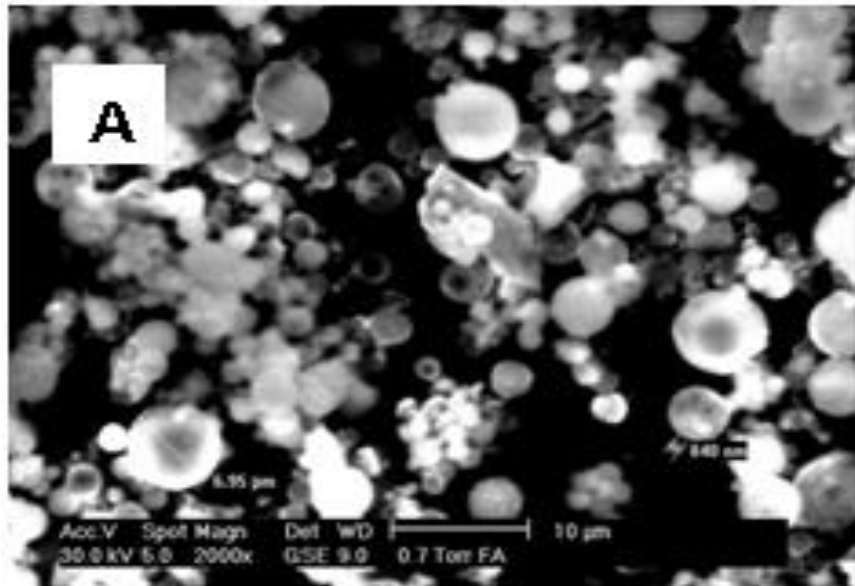
The increment in broadness after ball milling for 40h is an evidence for the breaking down of the quartz structure and formation of Si-OH groups[17]. A peak at 1650 cm^{-1} in the spectra of FA is attributed to bending mode ($\delta\text{O-H}$) of water molecule. However, FT-IR study clearly shows changes in the broadening of IR peaks corresponding to Si-O-Si asymmetric stretching vibrations ($1101, 1090\text{ cm}^{-1}$) indicating structural rearrangement during mechanical milling[18].

The FT-IR spectra of $[\text{bmim}]\text{PF}_6$ /MFA given in Figure 4.3 shows characteristic bands at 1572 cm^{-1} , 1466 cm^{-1} which are ascribed to C=N, stretching vibrations of imidazole rings and C-H deformation vibrations of alkyl groups[19]. The adsorption band at 2962 cm^{-1} , 2877 cm^{-1} assigned to aliphatic asymmetric and symmetric (C-H) stretching vibrations of methyl groups[20]. In the spectrum the IR bands at 3159 and 3112 cm^{-1} were assigned to C-H stretching vibrations of aromatic imidazole rings. Peak at wave number 748.38 and 623.01 cm^{-1} is due to C-N stretching vibration.

4.3.4 SEM and SEM-EDX analysis

The SEM photograph of pure fly ash (Figure 4.4A) is observed with hollow cenospheres, irregularly shaped unburned carbon particles, mineral aggregates and agglomerated particles. As a result of mechanical activation the structural break down of larger particles and increased surface roughness are observed (Figure 4.4B).

Typical SEM images of $[\text{bmim}]\text{PF}_6$ /MFA is clearly different from that of MFA which depict the resulting particles are wrapped by IL forming a thin layer over the surface of MFA clearly seen in Figure 4.4 (D).



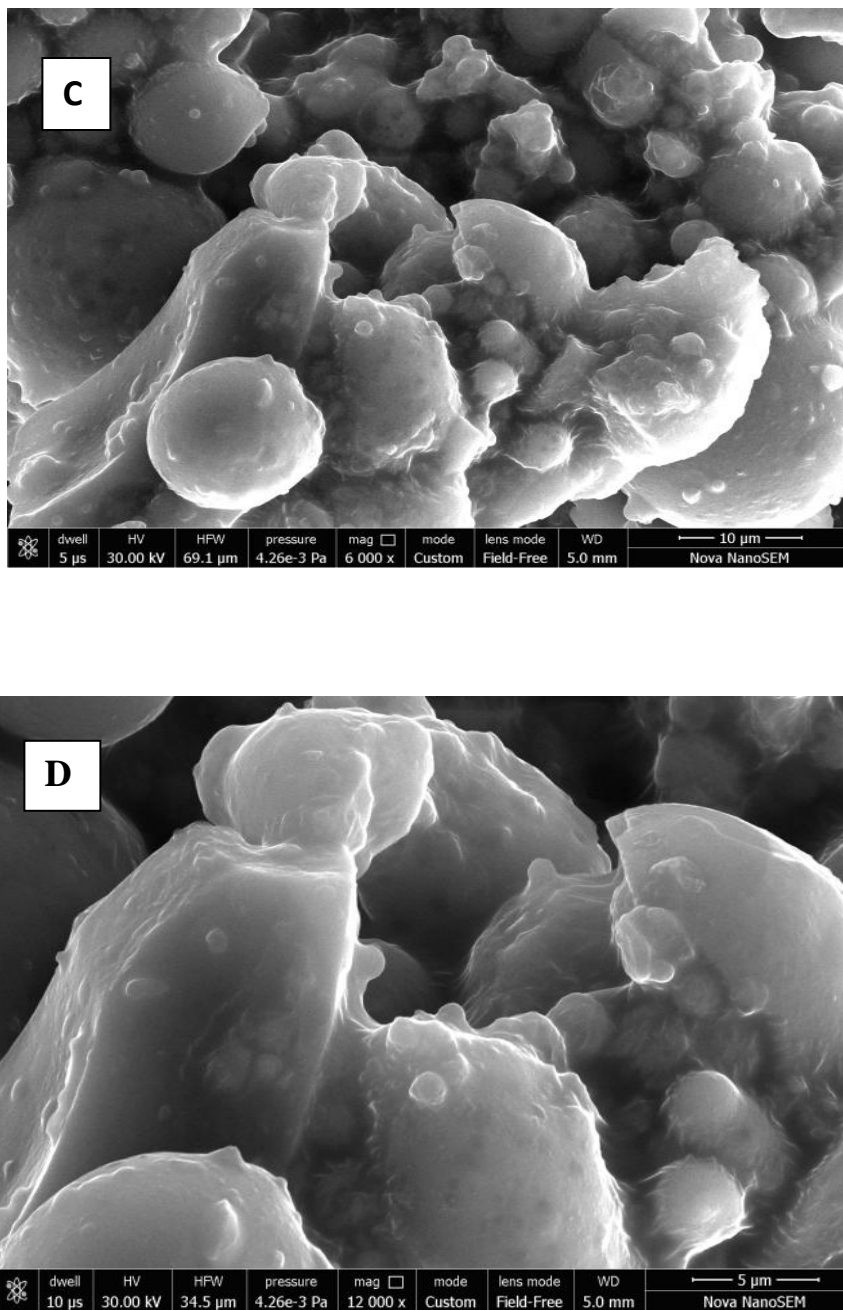


Figure 4.4 : SEM micrographs (A) pure FA (B) MFA-40 (C,D) [bmim]PF₆ /MFA and magnified image of [bmim]PF₆ /MFA

4.3.5 Thermogravimetric analysis (TGA)

The thermal stability of [bmim]PF₆ /MFA was determined by thermo gravimetric analysis (Figure 4.5). The TGA curve indicated initial weight loss within 150° C mainly attributed to the desorption of physisorbed water and residual solvent. The major weight loss is attributed to the decomposition of immobilized ionic liquid which is chemically bonded onto the surface of MFA. The amount of organic compounds bound on the surface of the MFA is estimated from the percentage of weight loss from the TGA curve. The immobilized ionic liquid [bmim]PF₆ started to decompose at about 250° C and was completely burned out at about 600° C Finally, it was observed that the [bmim]PF₆ /MFA catalyst exhibited good thermal stability under 250° C.

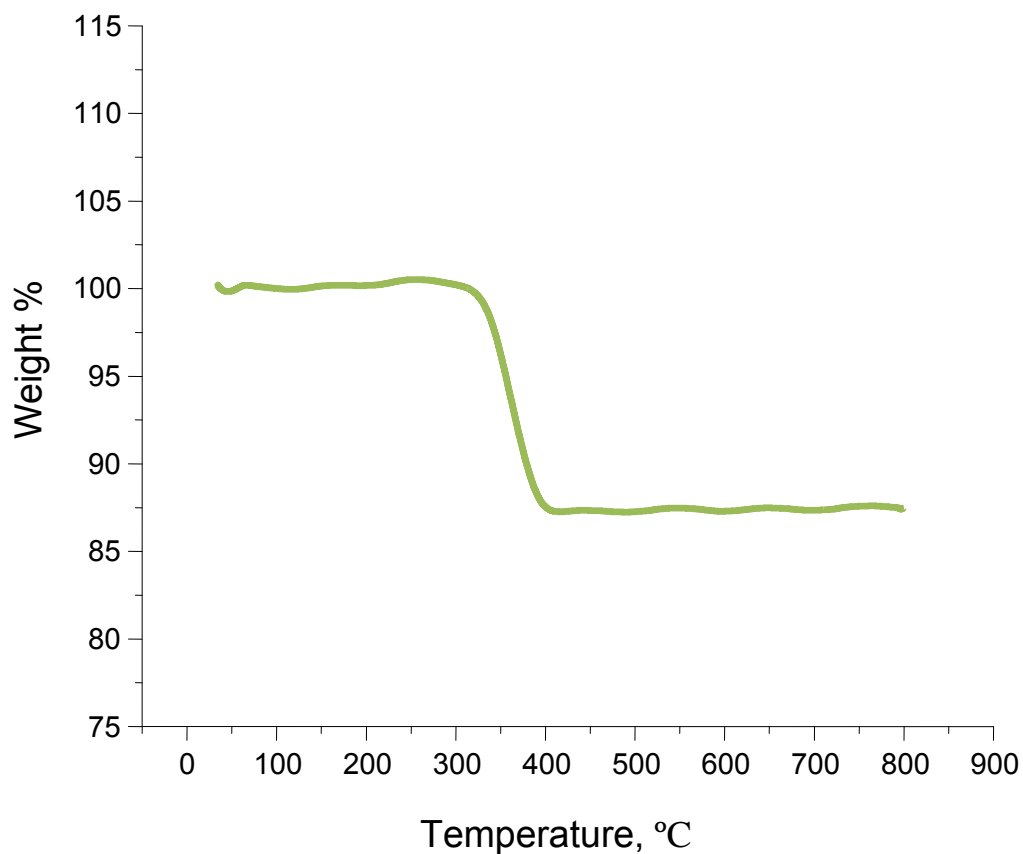


Figure 4.5 : TGA patterns of [bmim]PF₆/MFA

4.3.6 Ultra violet Visible spectroscopy

Figure 4.5 shows the UV-Vis spectra of 1-butyl-3-methylimidazolium hexafluorophosphate ionic liquid. No absorption peak below 290 nm has been observed which clearly confirmed the absence of any colored impurities.

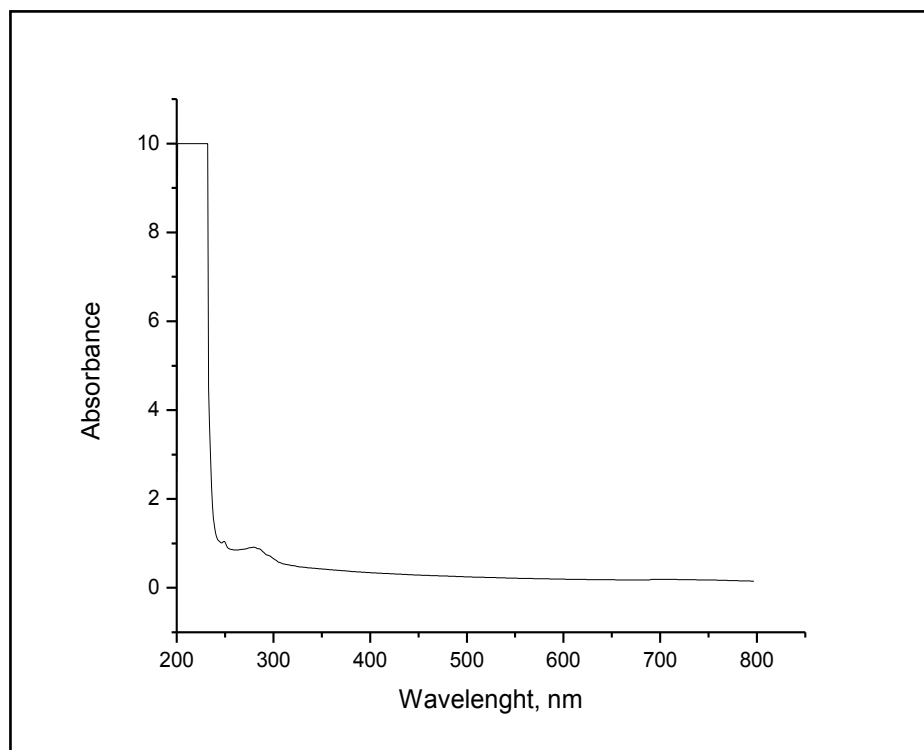


Figure 4.6 : UV-VIS spectrum for purity of [bmim]PF₆

4.4 Catalyst selection

The catalytic activity of prepared catalyst is evaluated by benzoylation reaction of benzene with benzoyl chloride to give benzophenone under dielectric heating. Reaction is carried out at 70°C for 10min, taking benzene/benzoyl chloride molar ratio

1:2 and benzene to catalyst ratio of 5:1 .result depicted in Table 4.2 show that no reaction occurs in absence of catalyst, as well as FA and MFA do not possess any catalytic activity towards this reaction. [bmim]PF₆ show less catalytic activity toward this reaction. [bmim]PF₆/MFA show maximum conversion % owing to presence of sufficient catalytic active sites.

Table 4.2: Catalytic activity of different catalysts for benzylation reaction benzene by benzoyl chloride.

Catalysts	Conversion %
Without catalyst	Nil
FA	Nil
MFA	Nil
[bmim]PF ₆	35
[bmim]PF ₆ /MFA	88

In light of above inferences, effect of various reaction parameters like reaction time and temperature, molar ratio of reactants, substrate/catalyst ratio, microwave power output for series of benzylation reaction of different arenes by benzoyl chloride are studied in detail using [bmim]PF₆/MFA catalyst. Consequently, optimized reaction conditions are determined to achieve maximum conversion% of desired products.

4.5 Catalytic activity

4.5.1 Effect of reaction temperature

The effect of reaction temperature on conversion and selectivity % is studied to optimize the reaction temperature. The benzylation of benzene, methyltoluene, chlorobenzene is performed at different temperature ranging from 50-130°C for 5-30 min. Figure 4.7 indicates that conversion % of benzene increases linearly up to 70°C with 100% selectivity of benzophenone. However, on further increasing temperature up to 90°C, the conversion remain constant with decrease in selectivity from 100% to

78%. Similarly, on increasing temperature optimized temperature in case of methyltoluene, chlorobenzene i.e. 100 and 110°C respectively, the conversion remains constant while product selectivity % decrease abruptly as shown in Figures 4.8 and 4.9 for methyltoluene, chlorobenzene respectively. At higher temperature, possibility of consecutive benzylation reactions between thus aromatic compounds and benzoyl chloride increases forming di or tri benzyolated products and consequently selectivity % of desired product. Moreover, benzylation is C-C bond forming reaction, but at higher temperature, O-benzylation can also occur producing ester as minor products thus decreasing the overall desired product selectivity% of the reaction.

In case of methyltoluene, at higher temperature, selectivity towards thermodynamically stable product, 3-ethyl benzophenone also increases and thus selectivity of desired product 4-ethyl benzophenone decreases.

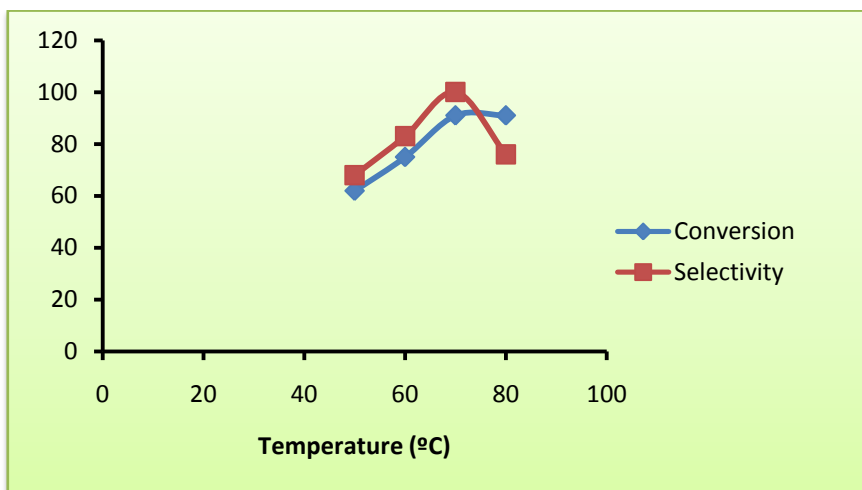


Figure 4.7: Variation of conversion and selectivity (%) of benzene over [bmim]PF₆/MFA with temperature.

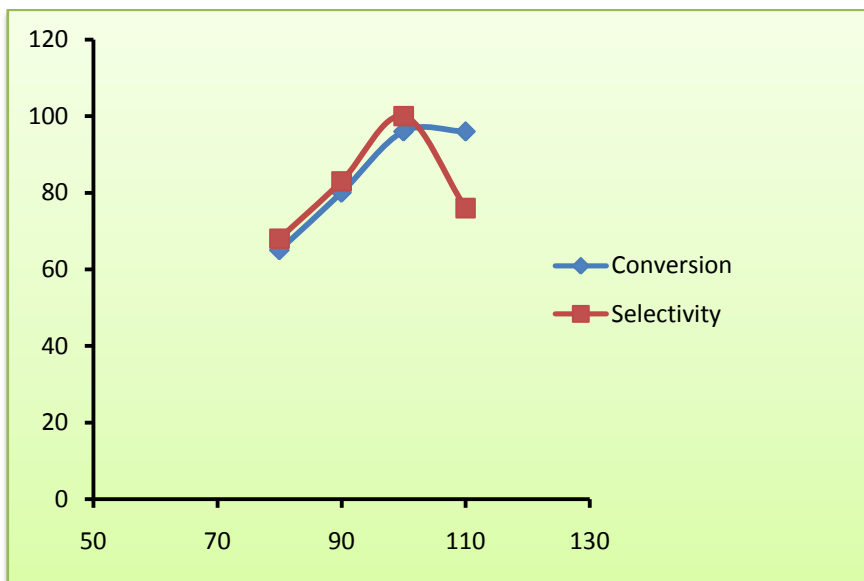


Figure 4.8: Variation of conversion and selectivity (%) of methyltoluene over [bmim]PF₆/MFA with temperature.

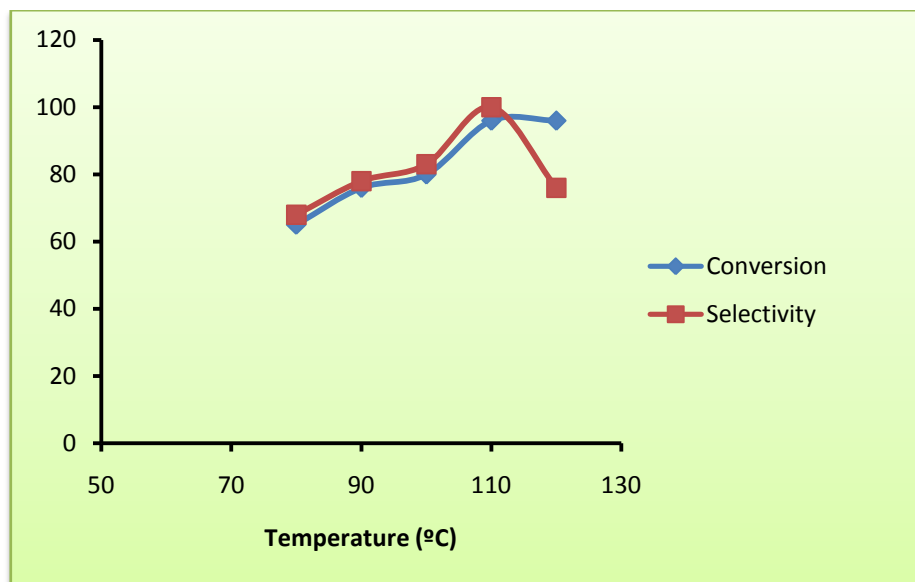


Figure 4.9: Variation of conversion and selectivity (%) of chloro benzene over [bmim]PF₆/MFA with temperature.

4.5.2 Effect of reaction time

To investigate the effect of reaction time on conversion and selectivity%, benzylation of benzene, methyltoluene, chlorobenzene are performed for different time intervals ranging from 5-30min at 70°C, 100°C and 110°C respectively. The conversion% of benzene increases up to 10 min. Then remains constant till 20 min as shown in Figure 4.10. The conversion% of methyltoluene and chlorobenzene also increases up to 15 and 20 min. respectively and remains constant at higher time periods as inferred from figure 4.11 and figure 4.12. While on increasing time period, selectivity% decreases in all reactions, because on giving more contact time to reactants, probability of continuous benzylation reaction increases and thus, di or tri benzyolated products are formed more decreasing the total selectivity% of desired product.

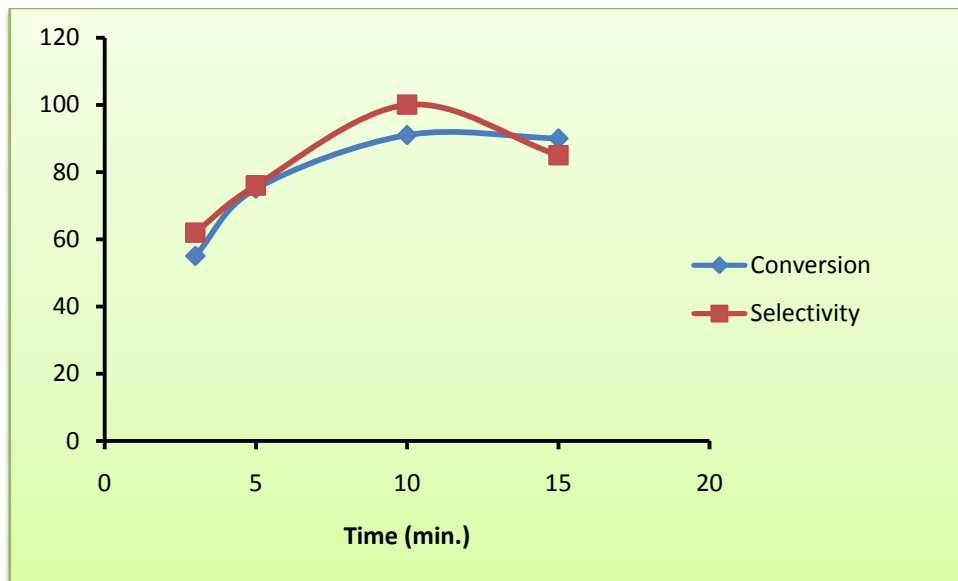


Figure 4.10: Variation of conversion and selectivity (%) of benzene over [bmim]PF₆/MFA with time.

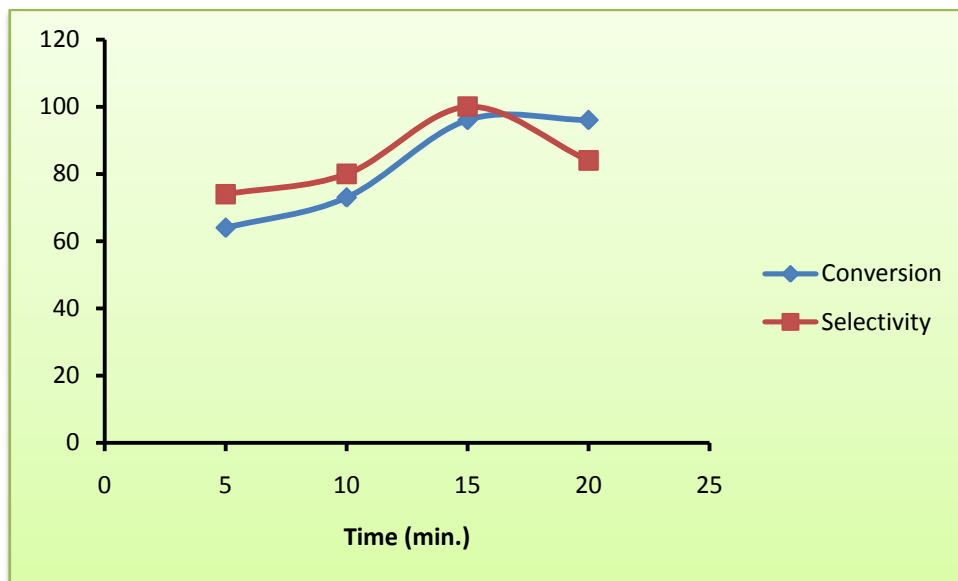


Figure 4.11: Variation of conversion and selectivity (%) of methyltoluene over [bmim]PF₆/MFA with time.

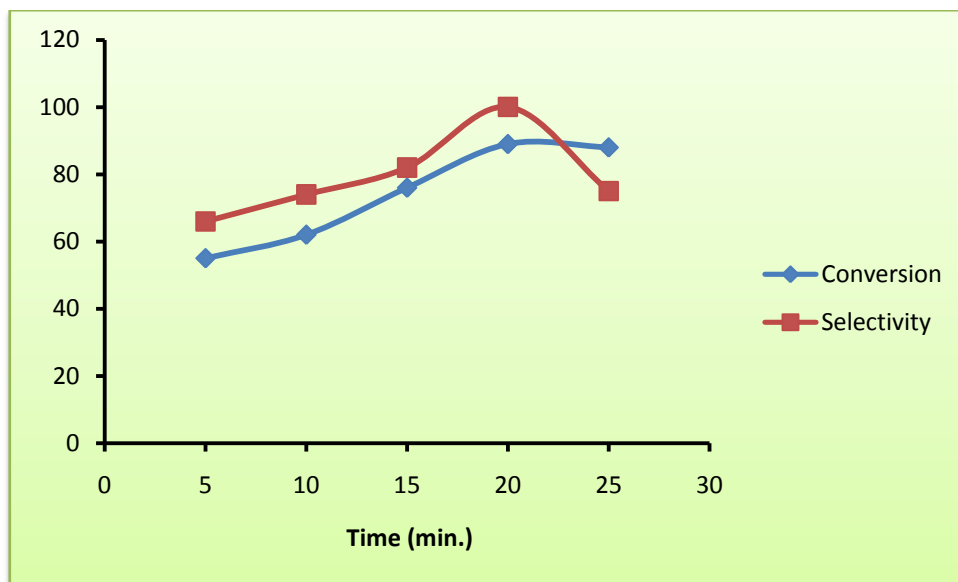


Figure 4.12: Variation of conversion and selectivity (%) of chloro benzene over [bmim]PF₆/MFA with time.

4.5.3 Effect of molar ratio of reactants

The effect of molar ratio of benzene, methyltoluene and chlorobenzene to benzoyl chloride on conversion and selectivity % of product is also studied over catalyst under optimized reaction conditions. On the basis of data given in Table 4.3, it is found that at molar ratio 1:2, maximum conversion % of benzene, methyltoluene and chlorobenzene with highest selectivity of their respectively products. At 2:1 molar ratio, less conversion% is observed due to inadequate quantity of benzoyl chloride and thus most of arenes remain unreacted in reaction medium. When methyltoluene is taken in higher amount, possibility of formation of 3-ethyl benzophenone increases thus whole selectivity % of reaction decreases. In case of higher amount of benzoyl chloride the selectivity % decreases due to formation of di or tri benzoylated products by repeatative benzoylation reactions between excessive benzoyl chloride and as formed benzoylated products.

Table 4.3: Effect of molar ratio of arenes/benzoyl chloride on conversion and selectivity % over [bmim]PF₆/MFA catalyst

Molar ratio	Conversion % of benzene	Selectivity % of benzene	Conversion % of methyltoluene	Conversion % of methyltoluene	Conversion % of chloro benzene	Conversion % of chloro benzene
2:1	62	68	58	71	55	60
1:1	77	82	83	80	76	82
1:2	91	100	96	100	89	100
1:5	85	78	82	76	72	70

4.5.4 Effect of substrate to catalyst weight ratio

The effect of substrate to catalyst weight ratio on conversion% of desired products is examined by varying amount of catalyst under optimized reaction conditions. As shown in Figure 4.13 on increasing catalytic amount, conversion increases in all reactions. It can be ascribed to availability of enhanced number of catalytic active sites. On further increase in the amount of catalyst no significant change is observed.

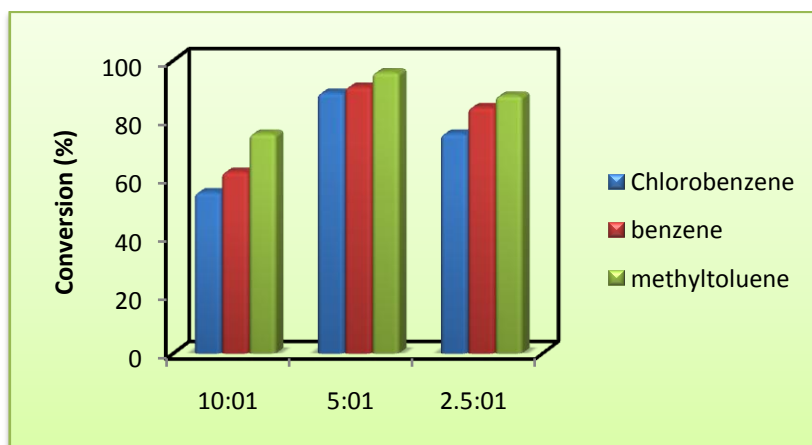


Figure 4.13: Variation of conversion% of benzene, methyltoluene, chloro benzene over [bmim]PF₆/MFA with substrate to catalyst weight ratio.

4.5.5 Effect of power out

The effect of power output of microwave instrument on conversion% is studied at different power outputs ranging from 40 to 80 W as shown in Figure 4.14. The conversion% of aromatic compounds is found maximum at 60 W suggesting that much power of microwave irradiations are adequate for occurrence of benzylation of aromatic compounds with highest conversion%. On increasing power output from 60 to 80W no sustainable change is seen in terms of conversion%.

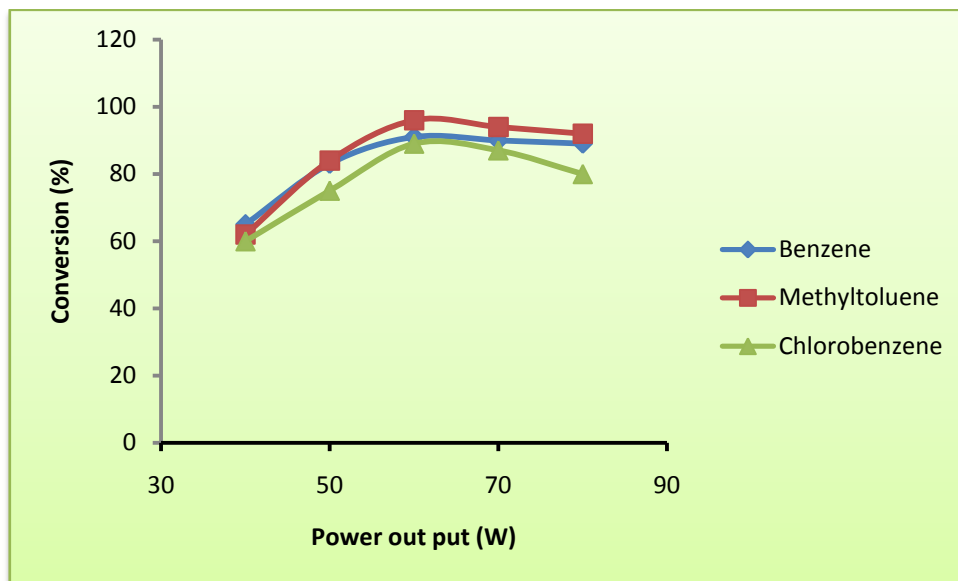


Figure 4.14: Variation of conversion % of benzene, methyltoluene, chlorobenzene over [bmim]PF₆/MFA with power output.

4.5.6 Effect of aromatic substrate

The reactivity of aromatic compounds are in order- chlorobenzene < Benzene < methyltoluene. This can be demonstrated on the basis of ortho-para-directing effect of alkyl substituent present on the ring. The electron rich methyl toluene favor electrophilic substitution at aromatic nucleus while electron deficient chlorobenzene show less reactivity towards electrophilic substitution. Hence in methyltoluene, electrophilic attack of benzoyl carbocation on substituted aromatic ring is favoured, leading to formation of benzoylated product at higher rate than that expected in absence of electron donating group.

The optimized reaction parameters for series of benzoylation reactions over catalyst in order to achieve maximum conversion and selectivity are listed in Table 4.4.

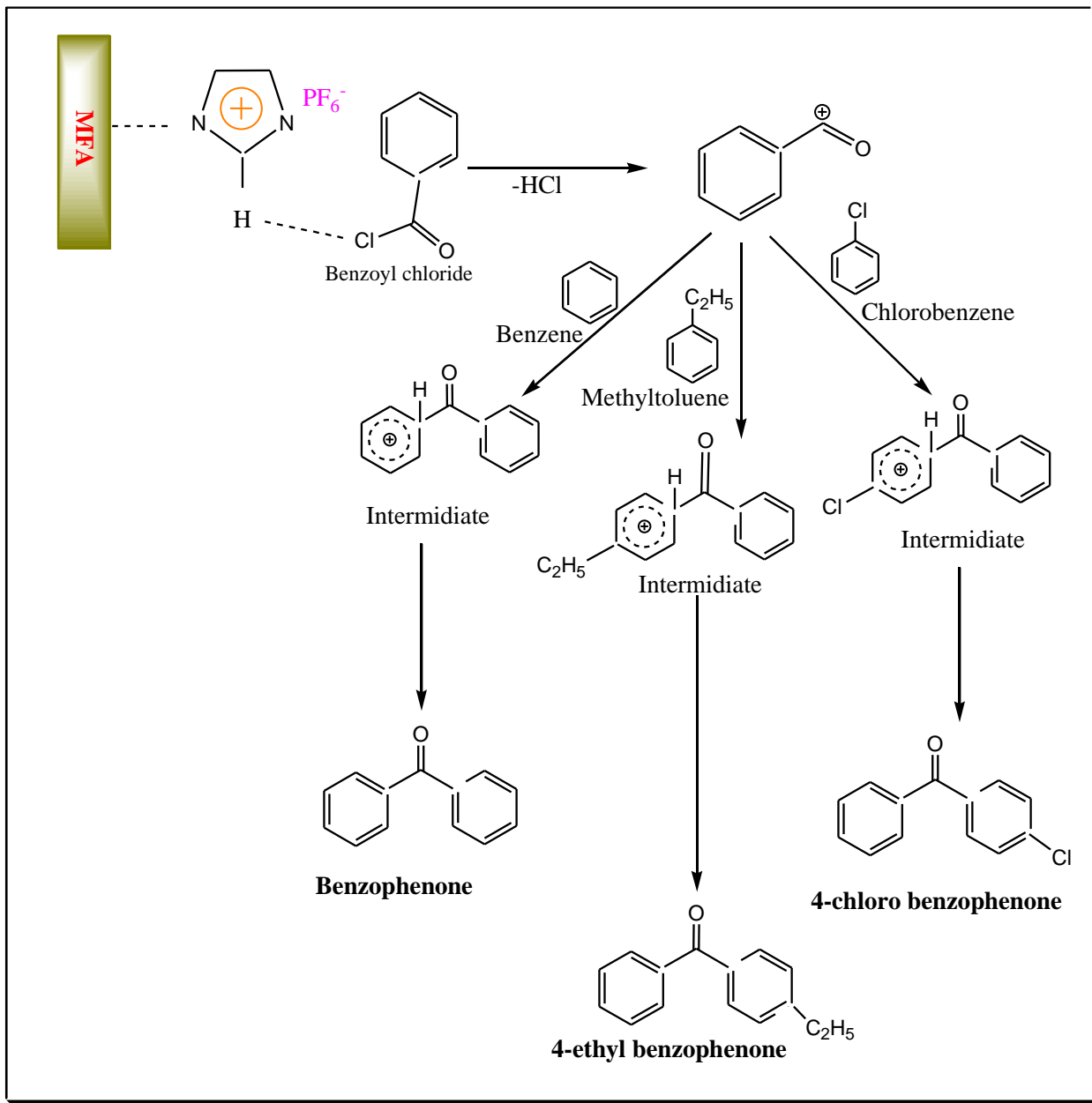
Table 4.4: Optimized reaction parameters for series of benzoylation reaction of aromatic compounds by benzoyl chloride over catalyst with maximum conversion and selectivity % of major products.

S. no.	Aromatic substrate	Reaction temperature (°C)	Reaction time (min.)	Conversion %	Major product with selectivity %
1	Benzene	70	10	91	Benzophenone(100%)
2	Methyltoluene	100	15	96	4-ethyl benzophenone(98%)
3	Chlorobenzene	110	20	89	4-chloro benzophenone(99%)

Due to bulky nature of benzoyl chloride group, para- substitution predominates. Owing to deactivating character of $-ArCO$ group of benzoyl chloride, chances of formation dibenzoylated of products is less under optimized conditions.

4.6 Proposed mechanism

A proposed structure of the synthesized [bmim]PF₆/MFA catalyst is shown in Scheme 4.4. The plausible mechanism for [bmim]PF₆/MFA catalyzed benzoylation is schematically presented in Scheme 4. The C2 of the IL is positively charged due to the electron deficit in the C=N bond whereas the other carbons are practically neutral[40]. This resulting acidity of the C2 hydrogen atom of [bmim]PF₆/MFA initiates benzoylation reaction by donating a proton[41-43] and helps in formation of carbocation which acts as surface electrophile, then attacks on aromatic substrate present in liquid phase and form benzoylated product by electrophilic substitution reaction. Thus, in reaction mechanism formation of carbocation is an important step. Electron rich ethyl group increase electron density on aromatic ring make it more vulnerable towards electrophilic attack benzene and chlorobenzene for benzoylation.



Scheme 4.4 : Proposed mechanism of benzoylation of aromatic substrates using benzoyl chloride over [bmim]PF₆/MFA

4.7 Regeneration and reusability of catalyst

The catalyst are recovered from reaction mixture using filtration method and washed thoroughly with dichloromethane and dried in vacuum oven at 80 °C for 24 h followed by activation at 70 °C for 1 h in vacuum oven. The regenerated catalyst was used in next reaction cycles under the same reaction conditions following the procedure described as above. The catalyst could be used up to four reaction cycles without any significant loss in product yield (Table 4.5) which indicates that the acidic sites are not deactivated during regeneration. The conversion% is decreased after fifth reaction cycle, due to the deposition of carbonaceous materials on the surface of catalyst which could block the surface active sites of catalyst. The stability, heterogeneous nature of [bmim]PF₆/MFA catalyst and possibility of leaching of ionic liquid in reaction medium is further analyzed by Sheldon's hot filtration test which involves filtration of catalyst from reaction mixture in between the reaction and further continuance of reaction in absence of catalyst. The results show that the reaction stops on filtering off the catalyst in mid of the reaction, hence it is confirmed that ionic liquid responsible for catalytic activity do not get leached off during course of reaction.

Table 4.5: Benzoylation of benzene, methyltoluene, chlorobenzene using benzoyl chloride over fresh and regenerated [bmim]PF₆/MFA catalyst

Reaction cycle	Conversion(%) of benzene	Conversion(%) of methyltoluene	Conversion(%) of chlorobenzene
I	91	96	89
II	91	95	88
III	89	92	85
IV	87	90	83

4.8 Identification of products

The product confirmation done by ^1H NMR and ^{13}C NMR techniques by comparison with standard products.

Benzophenone

^1H NMR (500 MHz, CDCl_3): $\delta = 7.81 - 7.59$ (m, 4H), 7.55 (m, 2H), 7.45 (m, 4H).

^{13}C NMR (125 MHz, CDCl_3): $\delta = 196.7, 137.6, 132.4, 130.1, 128.3$.

4-Ethyl benzophenone

^1H NMR (500 MHz, CDCl_3): $\delta = 7.78$ (dd, $J = 8.3, 1.3$ Hz, 2H), 7.76 – 7.72 (m, 2H), 7.56 (s, 1H), 7.46 (t, $J = 7.6$ Hz, 2H), 7.30 (d, $J = 8.4$ Hz, 2H), 2.73 (q, $J = 7.6$ Hz, 2H), 1.28 (t, $J = 7.6$ Hz, 3H).

^{13}C NMR (125 MHz, CDCl_3): $\delta = 196.5, 149.4, 138.0, 135.2, 132.1, 130.3, 130.1, 130.0, 129.9, 128.4, 128.2, 127.8, 28.9, 15.2$.

4-chloro benzophenone

^1H NMR (500 MHz, CDCl_3): $\delta = 7.76$ (m, 4H), 7.59 (t, $J = 7.4$ Hz, 1H), 7.53 – 7.43 (m, 4H) ^{13}C NMR (125 MHz, CDCl_3): $\delta = 195.5, 138.9, 137.3, 135.9, 132.6, 131.5, 129.9, 128.6, 128.4$.

4.9 Conclusion

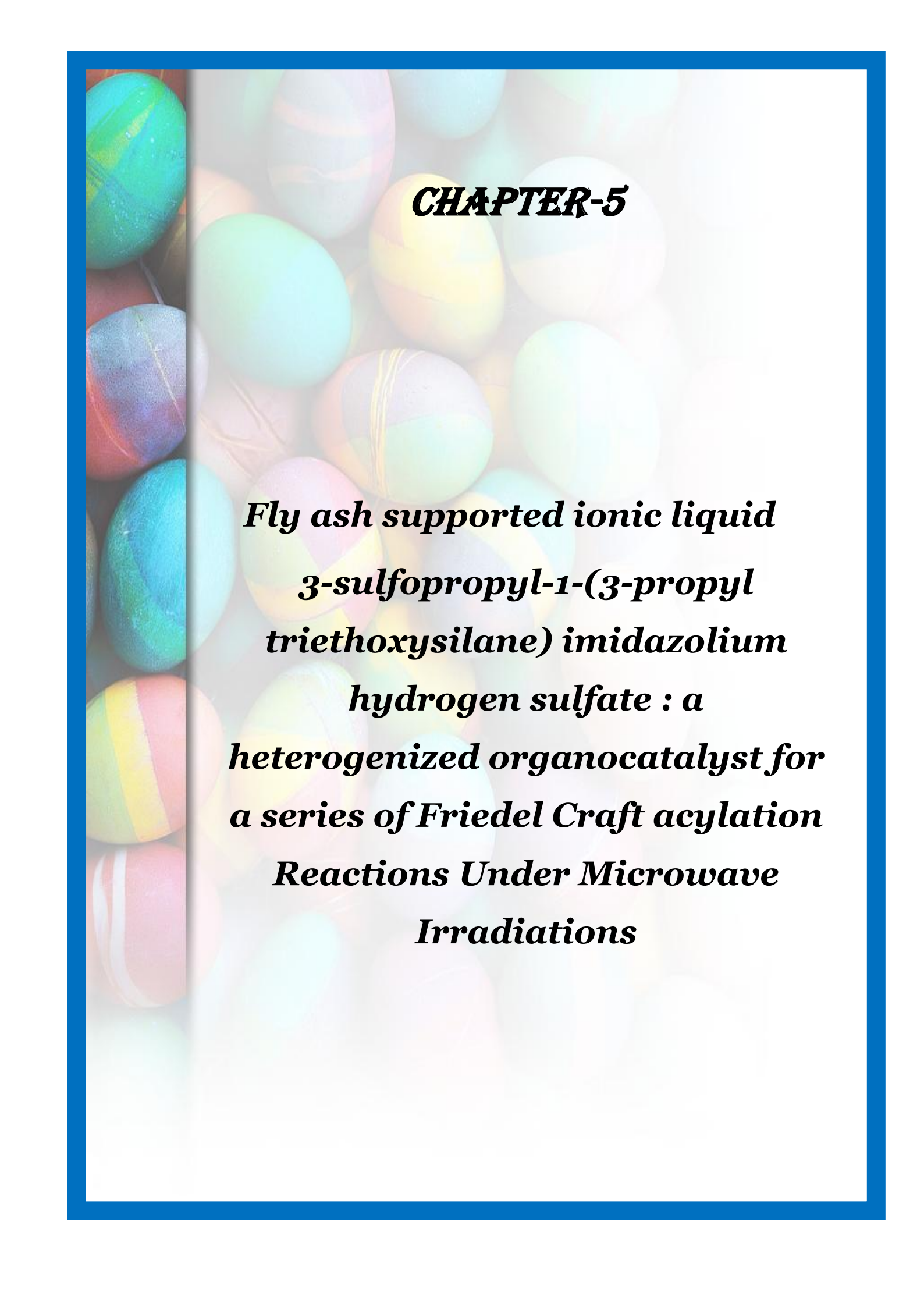
In the present work an efficient organo-heterogeneous catalyst synthesized by functionalization of mechanical activated fly ash with $[\text{bmim}]\text{PF}_6$. The mechanical activation provides hydroxylated surface which are responsible strong hydrogen bonding between anion of IL and surface free silanol group. thus a thin film of ionic liquid stabilized on MFA surface. Rapid and solvent free methodology for synthesis of ionic liquid through microwave heating was used and this synthesized IL was immobilized on the surface of FA. The prepared catalyst efficiently catalyze a series

of liquid phase benzylation reaction of arenes utilizing benzoyl chloride as benzylation agent. The efficiency of catalyst is further proved by conversion% obtained in all reactions. In addition, catalyst can also be reutilized up to four cycle Sheldon hot filtration confirmed that ionic liquid is stabilized on surface of fly ash and do not get leached out during reaction conserving the heterogeneous nature of catalyst during whole procedure. The effect of various reaction parameters are studied during reaction which helps in determining optimized reaction conditions to obtain maximum conversion and selectivity%. Hence, coal generated fly ash, an abundant waste material can be successfully utilized as an active support material for synthesis of a stable, high efficient and recyclable heterogeneous catalyst which has a promising future as an alternative for other commercial solid catalysts area of microwave assisted benzylation reactions useful in pharmaceutical, fine chemicals applications etc. The synthesized benzophenone can be used as a photo initiator in UV-curing applications such as inks, imaging, and clear coatings in the printing industry. Benzophenone and its derivative are used in the manufacture of insecticides, agricultural chemicals, hypotonic drugs, antihistamines and other pharmaceutical chemicals.

4.10 References

1. G.A. Olah, Friedel-Crafts and Related Reactions, vols. 1–4, Wiley, New York, 1963–1964.
2. M. Spagnol, L. Gilbert, D. Alby, in: J.R. Desmurs, S. Rattoy (Eds.), The Roots of Organic Development, Elsevier, Amsterdam, (1996) 29.
3. B. Yuan, Z. Li, Y. Liu, S. Zhang, *J Mol Catal A: Chem.* 280 (2008)210–8.
4. H. Schuster, W.F. Hölderich, *Appl Catal A: Gen.* 350 (2008)1–5.
5. J. Deutsch, V. Quaschnig, E. Kemnitz, A. Auroux, H. Ehwald, H. Lieske, *Top Catal* 13 (2000)281–5.
6. M.A. Harmer, Q. Appl Catal A: Gen 2001;221:45–62.
7. L.M.A. Cardoso, W. J. Alves, A.R.E. Gonzaga, L.M.G. Aguiar, H.M.C. Andrade, *J Mol Catal A: Chem* 209 (2004)189–97.

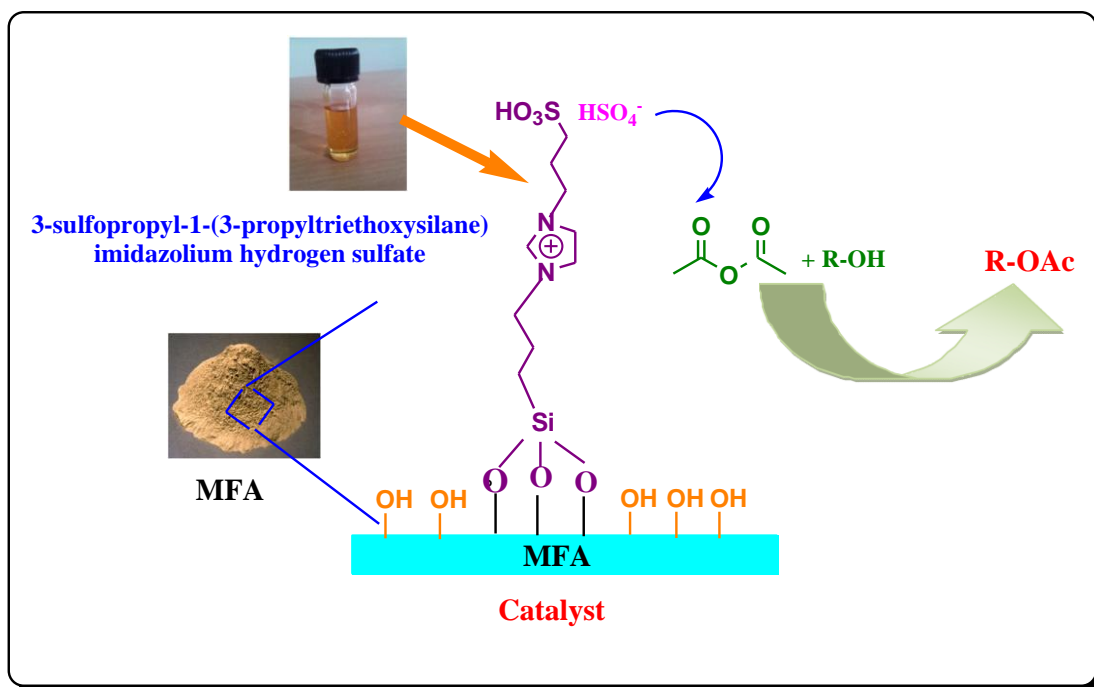
8. Pearson, A.L.; Roush, W.J. Handbook of Reagents for Organic Synthesis: Activating Agents and Protecting Groups; John Wiley and Sons Ltd.: London, (1999) 42-44.
9. H.T. Clarke, E.J.Rahrs, Org. Synth. Coll. Vol. I, 2nd Ed., 1941, 91.
10. J. Stawinski, T. Hozumi, S.A. Narang, *J. Chem. Soc. Chem. Commun.* 1976 243.
11. M. Yamada, Watabe, T. Sakakibara, R. Sudoh, *J. Chem. Soc. Chem. Commun.*(1979) 179.
12. M. G. Freire, L.M.N.B.F. Santos, A. M. Fernandes, J. A.P. Coutinho, I. M. Marrucho, *Fluid Phase Equilibria* 261 (2007) 449–454.
13. J.G. Huddleston, H.D. Willauer, R.P. Swatloski., A.E. Visser, R.D. Rogers, *Chem Commun* 16 (1998), 1765-1766.
14. L. Rodr'iguez-P'erez, Y. Coppel, I. Favier, E. Teuma, P. Serp, M. G'omez, *Dalton Trans.* 39 (2010) 7565–7568.
15. M. J. Jin, A. Taher, H. J. Kang, M. Choi, R. Ryoo, *Green Chem.* 11 (2009) 309–313.
16. V. Alejandro, A.J. Mart'inez, G.I.J Mayoral, *Appl. Catal A: Gen.* 472 (2014) 21-28.
17. A. Sharma, K. Srivastava, V. Devra, A. Rani, *Amer. Chem. Sci. J.* 2(4) (2012) 177-187.
18. G.A. Patil, S. Anandhan, *J. Energy Eng.* 2 (2012) 57-62.
19. H. Alinezhad, M. Tajbakhsh, N. Ghobadi, *Res Chem Intermed* 41 (2015) 9979–9992.
20. M.N. Parvina, H. Jina, M.B. Ansaria, S.M. Oh, S.E. Park, *Appl. Catal. A: Gen.* 413– 414 (2012) 205– 212.

The background of the slide features a collection of colorful Easter eggs in various patterns and colors, including solid colors like blue, green, and pink, as well as multi-colored stripes and marbled designs. The eggs are arranged in a dense, overlapping manner, creating a vibrant and festive atmosphere. The entire scene is framed by a thick blue border.

CHAPTER-5

***Fly ash supported ionic liquid
3-sulfopropyl-1-(3-propyl
triethoxysilane) imidazolium
hydrogen sulfate : a
heterogenized organocatalyst for
a series of Friedel Craft acylation
Reactions Under Microwave
Irradiations***

Abstract



Friedel craft acylation reaction of aromatic alcohols with acetic anhydride over FA supported 3-sulfopropyl-1-(3-Propyl triethoxysilane) imidazolium hydrogen sulfate catalyst

5.1 Introduction

Microwave (MW) irradiation has been proved to be highly efficient pathway for the rapid synthesis of a variety of compounds, some include Friedel–Crafts acylations[1-2]. Microwave assisted reactions are green, energy saving, reproducilble, having fast reaction rates, suppress side products and waste production and hence enhances selectivity of desired products. Conventional heating is relatively inefficient and time consuming as it induces heating on walls of vessel, while microwave produce in-core volumetric heating of reactants thus making the whole process efficient and fast up to 1000 folds. Chemical reactions are accelerated essentially because of selective absorption of microwave energy by polar molecules being inert to the microwave dielectric loss[3].

The acylation of functional groups, especially hydroxyl is the most frequently used organic transformations which provides a useful and efficient protection protocol in a multistep synthetic process.[4] Acylation is usually carried out by treatment of a alcohol with acetyl chloride or acetic anhydride in the presence of an acid or base catalyst in a suitable organic solvent. The most efficient base catalysts are 4-(dimethylamino)pyridine (DMAP) and phosphines and the powerful acid catalysts employed include CoCl_2 , TaCl_5 , $\text{Cu}(\text{OTf})_2$, Me_3SiOTf , $\text{Sc}(\text{OTf})_2$ and yttria-zirconica based Lewis acids[5-10]. Thus, apart from some practical disadvantages like moisture-sensitivity and high cost of many of these catalysts these reaction procedures using toxic metal derivatives and chlorinated hydrocarbons as solvents also do not fulfill the requirements of sustainable processes[11].The development of sustainable synthesis proceses are strongly required, owing to the continuously rising environmental concerns of conventional chemical approaches.

Recently the use of ionic liquids (ILs) as catalysts is widely deemed to be a sustainable alternative way to achieve the concept of green chemistry[12]. For the case of acetate synthesis *via* direct acylation of alcohols, several green approaches are available such as microwave methodology and using functionalized ionic liquids as

dual solvent catalyst possess many advantages compared to acid/base catalysis, such as the mild reaction conditions, high selectivity, creation of less waste, possibility of solvent free system and reusability[13]. Brønsted acidic ionic liquids consist of the useful green characteristics of solid acids and mineral liquid acids and are designed to replace traditional mineral liquid acids[14-16] in synthesis processes. On the basis of functionality Bronsted acidic ILs can be divide into two types, one type having no functionality on cation with HSO_4^- anion while in others functionality such as SO_3H or COOH or H functional group have been incorporated into cation with an anion [17]. The alkylated SO_3H was tethered covalently to the cation of the IL which renders it a strong Bronsted acid and thereby received more interest in various applications [18-19]. the ILs with SO_3H functionalized group have revealed great potential as they are immiscible with various organic solvents, flexible, noncorrosive, and non-volatile [18].The SO_3H functionalized ionic liquids have been employed in numerous catalytic reactions including, esterification [20-21], alkylation [22], nitration of aromatic compounds [23], Beckmann rearrangement [24], and alkene polymerizations [25]. The ionic nature of ILs allows a very effective coupling with microwave energy [18]. The combination of microwave chemistry and ionic liquids offers a number of opportunities in organic synthesis[26]

Although the catalytic ability of acidic ionic liquid has been demonstrated successfully in many catalytic reactions. However, the immobilization of a thin film of ionic liquids on inert solid support material is highly desirable approach because of the ease of separation and recovery of catalyst. Several literature about silica based immobilized acidic ionic liquids catalysts for various organic transformations has been reported[27-31]. In continuation we have synthesized acidic ionic liquid **3-sulfobutyl-1-(3-propyl triethoxysilane) imidazolium hydrogen sulfate (CIPTES-[(CH_2)₃ SO_3H -HIM]HSO₄)** having structure as shown in Scheme5.1. It contain 3-sulfobutyl-1-(3-propyl triethoxysilane) imidazolium cation and hydrogen sulphate anion. The synthesized IL was immobilized on surface of MFA using covalent bonding between cation of IL and surface free silanol.



Scheme 5.1: Molecular structure of 3-sulfopropyl-1-(3-propyl triethoxysilane) imidazolium hydrogen sulfate (CIPTES-[(CH₂)₃SO₃H-HIM]HSO₄)

Previously silica immobilized 3-sulfobutyl-1-(3-propyltriethoxysilane) imidazolium hydrogen sulfate was exhibited high catalytic activity for multicomponent condensation of aldehydes with 2-naphthol and amides. The immobilized ionic liquid catalyst could be recovered easily and reused for 10 times for the synthesis of amidoalkyl naphthols without significant loss of catalytic activity[32]. Many immobilized acidic ionic liquids are efficiently used as heterogeneous catalyst in various transformations like hydrolysis of cellulose[33], esterification[34], acetalization, biodiesel synthesis[35] and condensation[36]

In this present study we have introduced fly ash supported 3-sulfopropyl-1-(3-propyl triethoxysilane imidazolium hydrogen sulfate as a highly powerful supported acidic ionic liquid for microwave assisted acylation reactions of aromatic alcohol and acetic anhydride to give the products in excellent yields in very short reaction times for four successive cycles. The immobilized acidic ionic liquid was characterized with a variety of techniques, including infrared spectroscopy (FT-IR), X-ray diffraction (XRD), thermo- gravimetric analysis (TGA), scanning electron microscopy (SEM) and pH analysis. The acidity plays important role in the catalytic activity of prepared catalyst for acylation reaction. The catalyst shows high thermal stability and was recovered and reused without any noticeable loss of activity.

5.2 Experimental

5.2.1 Materials

Imidazole (99%), sodium ethoxide, 1,3-propane-sultone (99%), 3-chloropropyl triethoxysilane (CIPTES,98.8%) were purchased from Sigma aldrich. Aromatic alcohol, acetic anhydride, ethanol and ether were bought from S.D.Fine Chem. Ltd., India. All chemical were used as received. Fly ash [Class F type ($\text{SiO}_2 + \text{Al}_2\text{O}_3$) > 70%], collected from Kota Thermal Power Plant (Rajasthan, India) was used as support material for the preparation of the supported ionic liquid catalyst.

5.2.2 Catalyst preparation

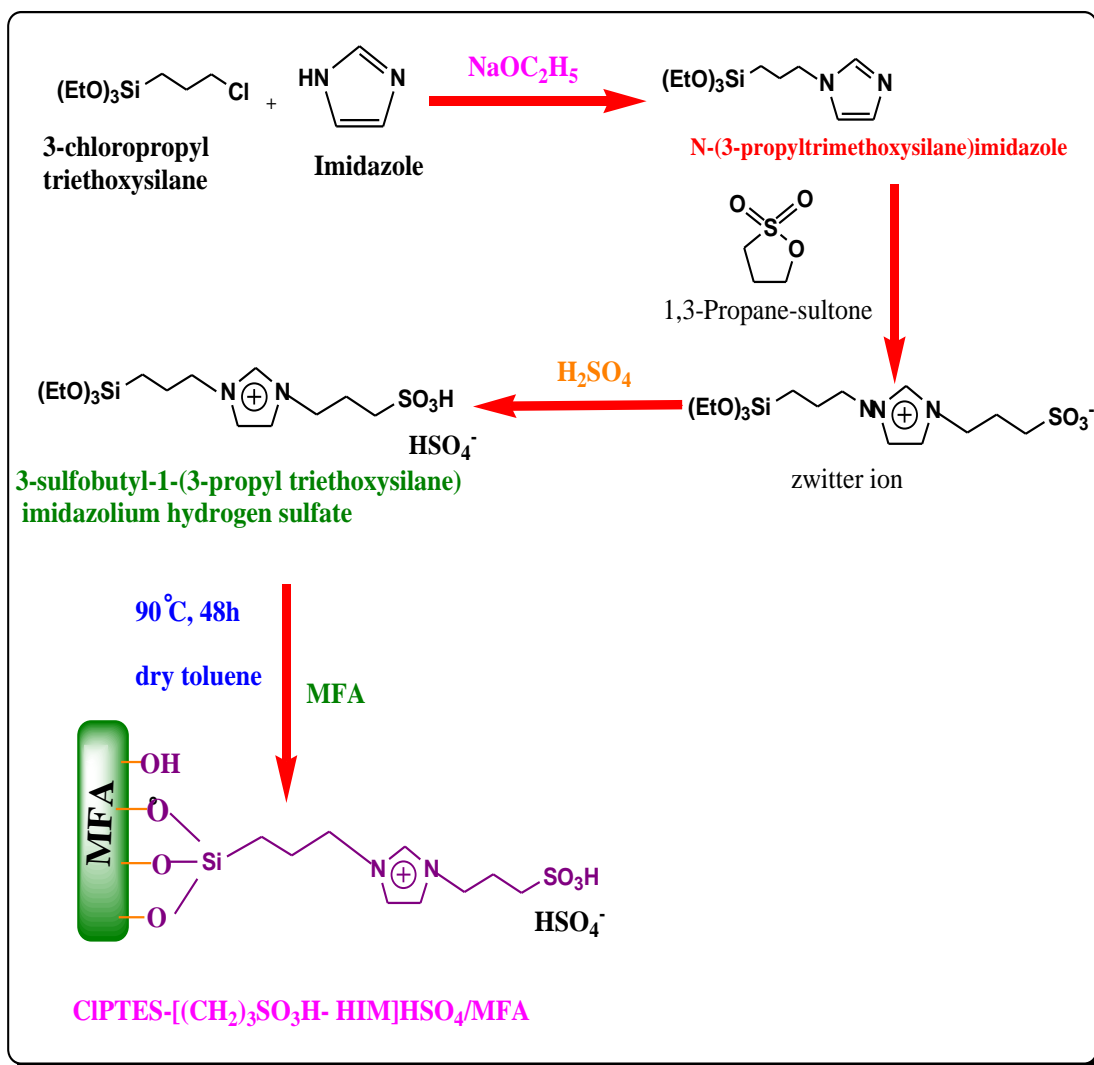
Synthesis of CIPTES-[(CH₂)₃SO₃H-HIM]HSO₄

Imidazole (6.8 g) and sodium ethoxide (6.8 g) were placed in a round bottom flask equipped with a magnetic stirrer and dissolved in ethanol (100 mL). The mixture was stirred at 70 °C for 8 h to give sodium imidazole [26]. Subsequently, CIPTES (24.05 g) was added drop-wise and the reaction mixture was refluxed further for 12 h under N₂ atmosphere. After cooling to room temperature, the obtained orange suspension was filtered to remove NaCl precipitate from the solution [27]. The solvent was removed by rotatory evaporator under reduced pressure and an yellowish oil containing N-(3-propyltrimethoxysilane)imidazole was obtained. To stirred equal-molar mixture of N-(3-propyltrimethoxysilane)imidazole in ethanol (100 mL) was added 1,3-Propane-sultone (12.2 g) dropwise. The mixture was stirred at 50 °C for 8 h and ethanol was removed by rotatory evaporation under reduced pressure. Then equimolar H₂SO₄ was added drop-wise and solution was stirred at 60 °C for another 12 h. Finally, the obtained product CIPTES-[(CH₂)₃SO₃HHIM] HSO₄ was washed with diether for 4 times and dried under vacuum at 50 °C for 5 h (Scheme 5.1).

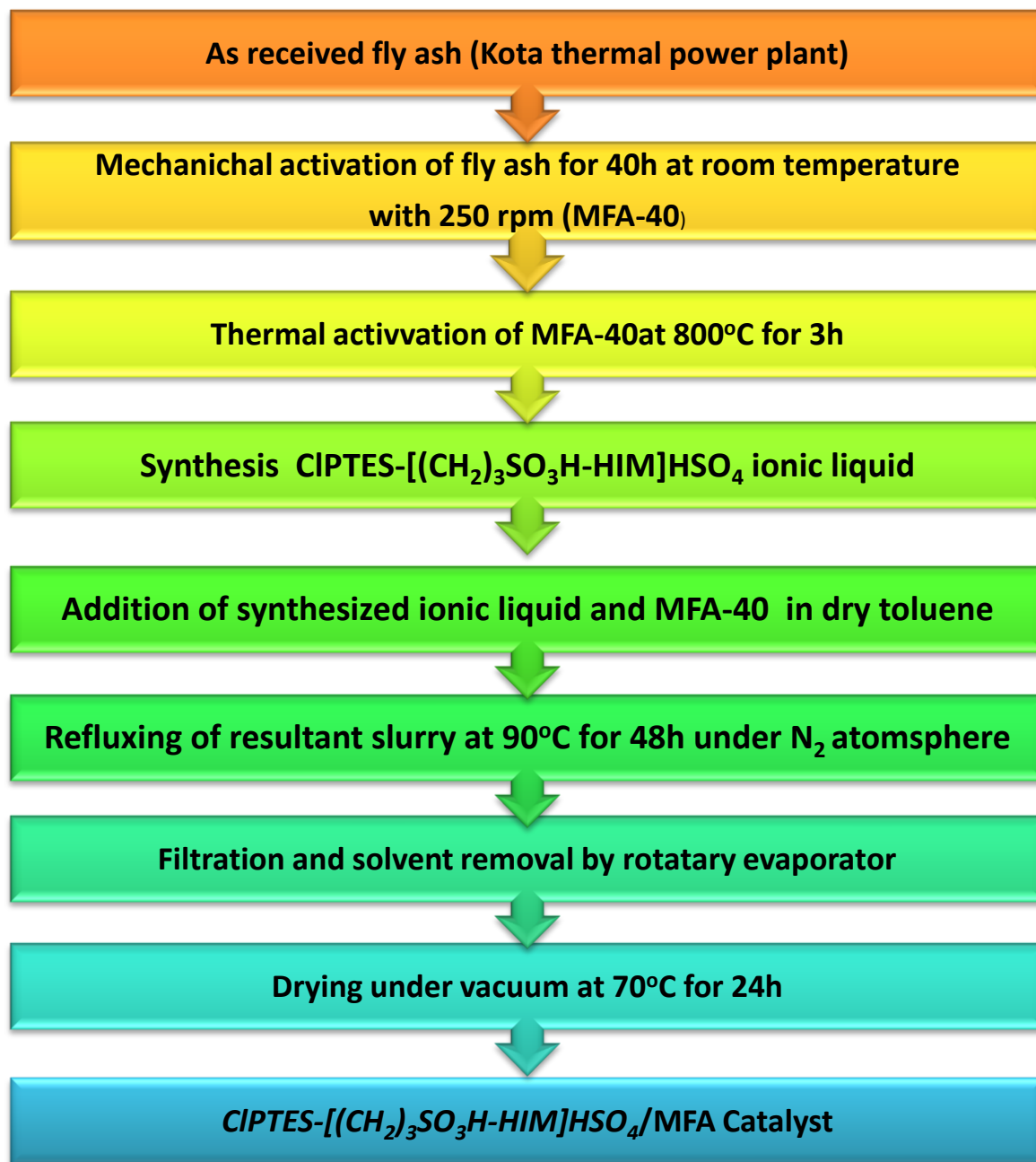
This IL was characterized by FT-IR: (CDCl_3 , cm^{-1}): 581, 755.04, 1163.54, 1036.53, 1566.27, 1642, 2875.27, 2933.93, 2962, 3155.33, 3435.

Preparation of immobilized ionic liquid catalyst CIPTES-[(CH₂)₃SO₃H-HIM]HSO₄/MFA

CIPTES-[(CH₂)₃SO₃HHIM] HSO₄ functionalized FA was synthesized as follow : the mechanical activation was performed using high energy planetary ball mill in an agate grinding jar using agate balls of 5 mm ball sizes for 5, 10, 15 and 40 h with 250 rpm to get MFA(5-40). The ball mill was loaded with ball to powder weight ratio (BPR) of 10:1. All mechanically activated samples were thermally activated by calcination at 800°C for 3h to remove carbon, sulphur and other adsorbed moieties. Prior to immobilization, MFA-40 was activated at 550°C for 1 h and CIPTES-[(CH₂)₃SO₃HHIM] HSO₄ was dried at 70°C under vacuum for 1 h. The pretreated MFA-40 (5gm) and 2gm of CIPTES-[(CH₂)₃SO₃HHIM] HSO₄ were co-dispersed in 50 ml dry toluene in a refluxing assembly under vacuum. The mixture was refluxed under N₂ atmosphere at 90°C for 48 h. The toluene solvent was removed by filtration and solid material was transferred to a rotary evaporator. The excess of physisorbed ionic liquid was removed using rotatory evaporator under reduced pressure. Finally the solid was dried under vacuum at 70°C for 24 h to give brown powder of CIPTES-[(CH₂)₃SO₃HHIM] HSO₄ /MFA to be used as a catalyst (Scheme-5.1) for acylation reaction. The steps of synthetic procedure are summarized in Scheme 5.2



Scheme 5.1: The synthesis route of CIPTES-[(CH₂)₃SO₃HHIM] HSO₄ functionalized FA.



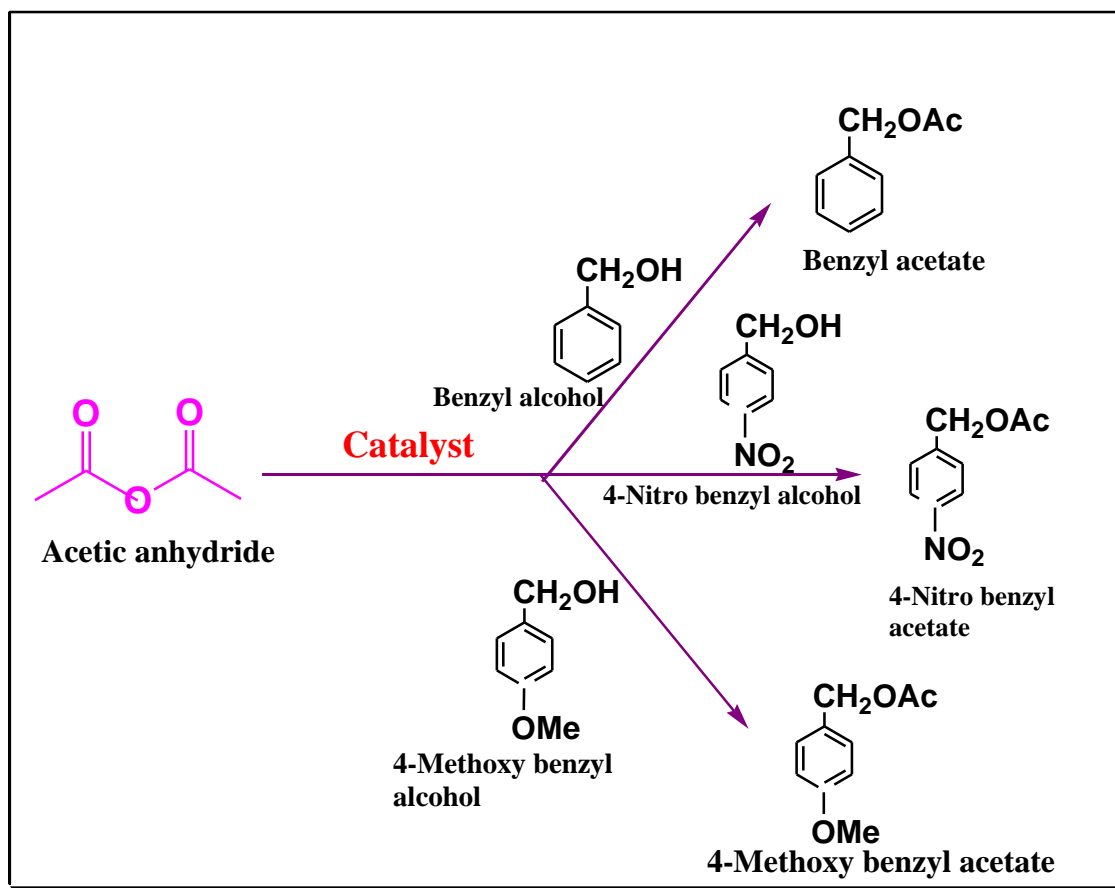
Scheme 5.2 : Steps for Synthesis of CIPTES-[(CH₂)₃SO₃H-HIM]HSO₄/MFA

5.2.3 Characterization techniques

Physicochemical properties of all prepared samples are evaluated using XRD, FTIR, SEM-EDX, TGA, BET surface area, UV-Visible, ^1H NMR techniques, as described in [Annexure-I](#)

5.2.4 Catalytic activity of CIPTES- $[(\text{CH}_2)_3\text{SO}_3\text{HHIM}] \text{HSO}_4/\text{MFA}$

To check the catalytic activity of catalyst, acylation of aromatic alcohols with acetic anhydride was carried out under solvent free conditions in microwave reactor. [Scheme 5.3]



Scheme 5.3: Simplified reaction pathway of acylation of aromatic alcohol by acetic anhydride over CIPTES- $[(\text{CH}_2)_3\text{SO}_3\text{HHIM}] \text{HSO}_4/\text{MFA}$.

In a typical procedure aromatic alcohol(1mmol), freshly distilled acetic anhydride (1.5mmol) were charged into reactor tube with magnetic stirrer. The catalyst (acid to catalyst weight ratio = 5), activated at 80 °C for 1 h prior to the reaction in vacuum, was added in the reaction mixture. The pressurized glass vial with continuous stirring checked the vapor loss during the reaction proceeding at desired temperature and time. After completion of the reaction, the mixture was cooled at room temperature through air pump before releasing the pressure of the reactor tube.

The filtered catalyst is thoroughly washed with dichloromethane to remove organic impurities. The crude desired product was washed with 10% NaHCO₃ solution and distill water and then dried over anhydrous Na₂SO₄. The reaction conditions were varied to obtain maximum yield and conversion of various aromatic alcohols to the corresponding acetates. The desired product was characterized by FTIR and ¹HNMR and analyzed using a Gas Chromatograph with oven temperature range 70-240 °C and N₂ (25 ml/min) as a carrier gas.

The conversion of aromatic alcohol is calculated by using following method-

$$\text{Conversion(\%)} = \frac{[\text{Initial wt\%} - \text{Final wt\%}]}{\text{Initial wt\%}} \times 10$$

5.3 Results and Discussion

5.3.1 Characterization of catalyst

The effect of mechanical activation on properties of FA as given in chapter 2. The silica percentage is increased marginally after milling for 5 to 40h but the specific surface area is increased from 9 to 36 m²/g. As compared with FA, the crystallite size is reduced from 33 to 17 nm as milling time was increase up to 40h. After immobilization of ionic liquid , the specific surface area of CIPTES-[(CH₂)₃SO₃HHIM] HSO₄/MFA catalyst decreases from 36m²/g to 19 m²/g due to agglomeration of small particles of fly ash.

5.3.2 Fourier transform infrared analysis

The FT-IR spectra of MFA-40 given in chapter 2 shows increment in broadness between 3600-3300 cm^{-1} evidence for the breaking down of the quartz structure and formation of Si-OH groups[37]. A peak at 1650 cm^{-1} in the spectra of FA is attributed to bending mode (δ O-H) of water molecule. However, FT-IR study clearly shows changes in the broadening of IR peaks corresponding to Si-O-Si asymmetric stretching vibrations (1101, 1090 cm^{-1}) indicating structural rearrangement during mechanical milling. After activation of FA, increase in surface roughness, mesopores and concentration of free silanols groups on the surface make it suitable for stabilized ionic liquid layer on MFA-36 via strong covalent bonding.

To confirm the immobilization of ionic liquid CIPTES- $[(\text{CH}_2)_3\text{SO}_3\text{HHIM}] \text{HSO}_4$ on MFA, FT- IR spectroscopic studies were carried out. The FT-IR spectra of CIPTES- $[(\text{CH}_2)_3\text{SO}_3\text{HHIM}] \text{HSO}_4/\text{MFA}$ given in Figure 5.1 shows characteristic bands at 581 cm^{-1} , 1642 cm^{-1} , 1566 cm^{-1} , 3139 cm^{-1} , 1163 cm^{-1} and 1036 cm^{-1} which are ascribed to C-H, C=C, C=N, stretching vibrations of the imidazole ring[30] and S=O symmetric stretching vibrations of the $-\text{SO}_3\text{H}$ group, respectively [38,39,40]. The band at 3435 cm^{-1} was assigned to the O-H of physical adsorbed water. The adsorption band around 2962 cm^{-1} assigned to C-H stretching vibration which confirms the presence of propyl groups of ionic liquid[41].

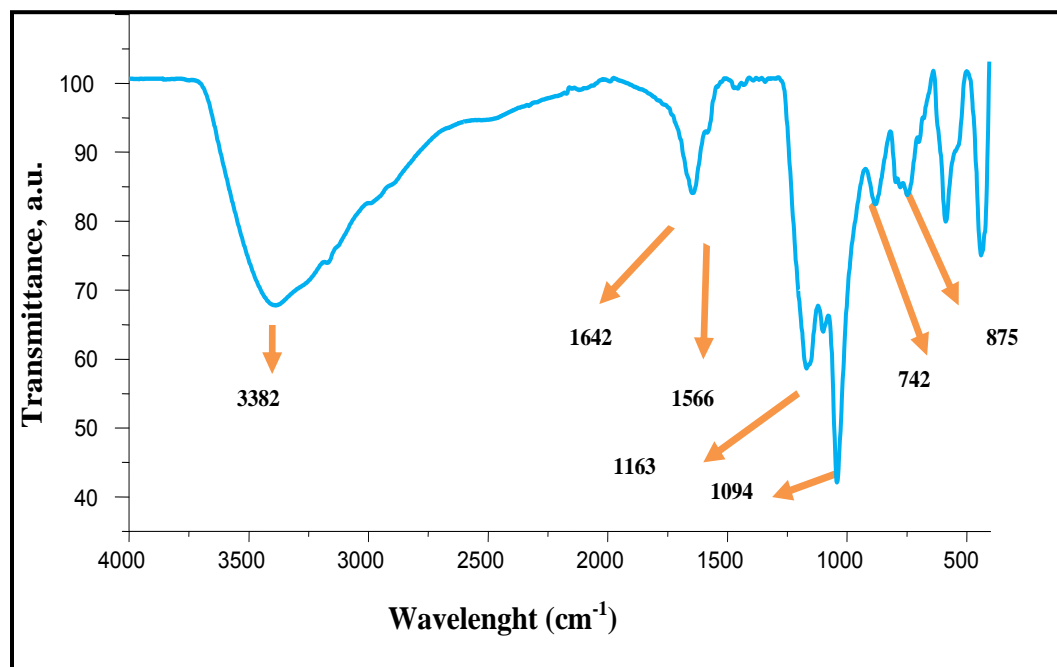


Figure 5.1: FT-IR spectra of CIPTES-[(CH₂)₃SO₃HHIM] HSO₄/MFA catalyst.

5.3.3 X-ray diffraction analysis

The X-Ray diffraction patterns of the as received FA as well as MFA are already described in chapter 2. The peaks at 16.4° and 26.2° show mullite (alumino-silicate) phase while quartz (silica) exhibits strong peaks at 20.7°, 26.6°, 40.6° and 49.9° of 2θ values. As a result of ball milling mostly quartz and mullite crystalline phases are reduced[37].

5.3.4 Ultra violet Visible spectroscopy

The UV-Vis spectra of the pure ionic liquid CIPTES-[(CH₂)₃SO₃HHIM] HSO₄ in the scanning range 200-800 nm as shown in Figure 5.2. No absorption peak below 290 nm has been observed which clearly confirmed the absence of any colored impurities.

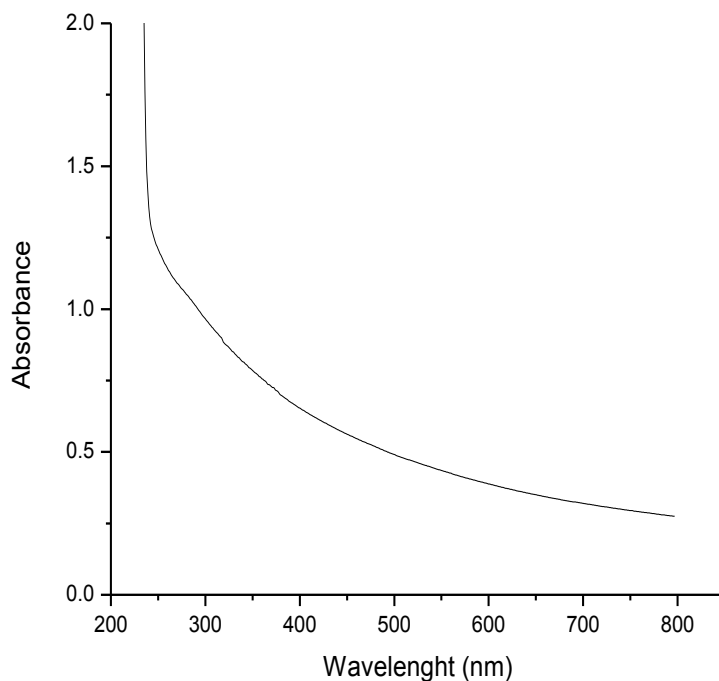


Figure 5.2 : UV-VIS spectrum of purity of ionic liquid

5.4.5 SEM and SEM-EDX analysis

The SEM photograph of pure fly ash (Figure 5.3A) is observed with hollow cenospheres, irregularly shaped unburned carbon particles, mineral aggregates and agglomerated particles. As a result of mechanical activation the structural break down of larger particles and increased surface roughness are observed (Figure 5.3B).

Typical SEM images of Typical SEM images of CIPTES-[(CH₂)₃SO₃HHIM] HSO₄/MFA show that the resulting particles are stacked together to form the bigger particles. All particles are wrapped by IL forming a thin layer over the surface of MFA clearly seen in Figure 5.3 (D).

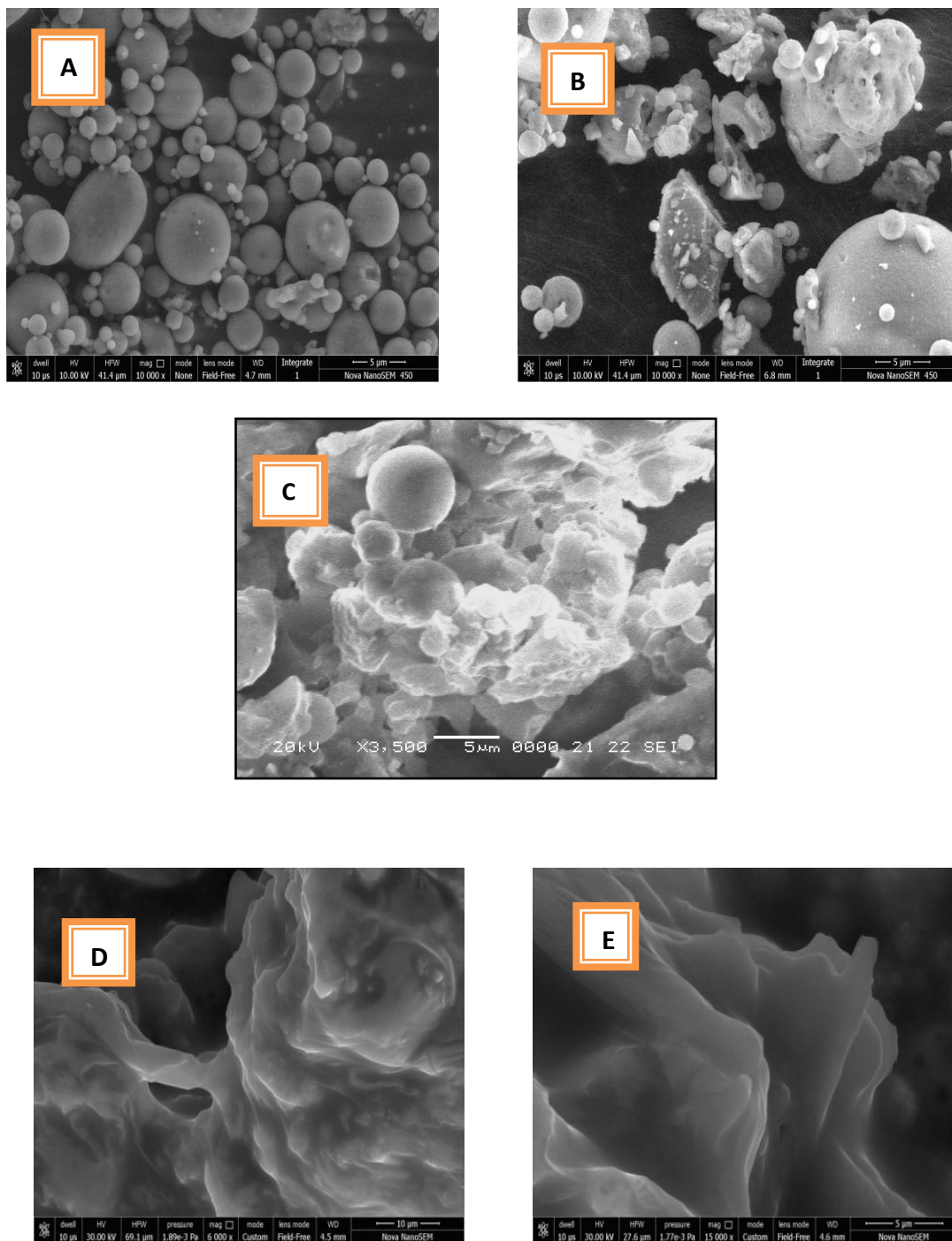


Figure 5.3: SEM micrographs (A) pure FA (B) MFA-40 (C) CIPTES-[(CH₂)₃SO₃HHIM]HSO₄/FA (D, E) CIPTES-[(CH₂)₃SO₃HHIM]HSO₄/MFA and magnified image of CIPTES-[(CH₂)₃SO₃HHIM]HSO₄/MFA

5.3.6 Thermogravimetric analysis (TGA)

The thermal stability of CIPTES-[(CH₂)₃SO₃HHIM] HSO₄/MFA was determined by thermo gravimetric analysis (Figure 5.4). The TGA curve indicated initial weight loss within 200° C mainly attributed to the desorption of physisorbed water and residual solvent. When the temperature further increased to 150° C, the weight of CIPTES-[(CH₂)₃SO₃HHIM] HSO₄/MFA decreased rapidly due to the organic components of ionic liquid and the propyl of CIPTES separated from the surface of MFA. Finally, it was observed that the CIPTES-[(CH₂)₃SO₃HHIM] HSO₄/MFA catalyst exhibited good thermal stability under 250°C and the residual weight loss of CIPTES-[(CH₂)₃SO₃HHIM] HSO₄/MFA was about 10% at around 800° C.

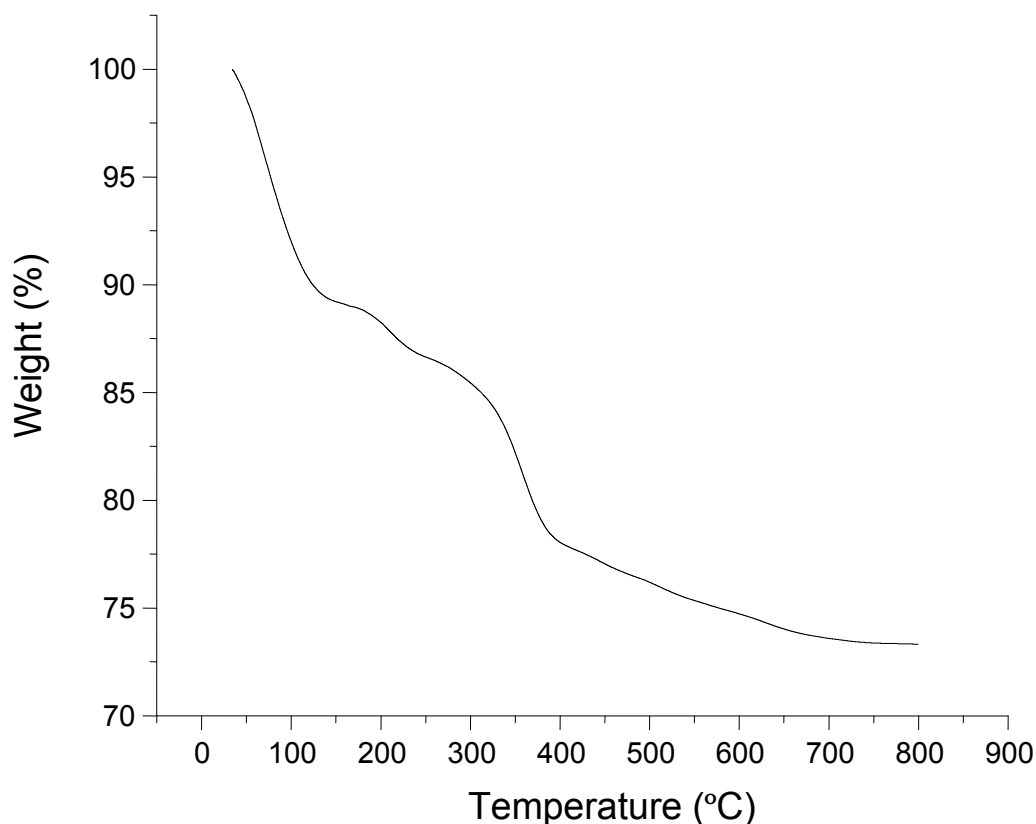


Figure 5.4: TGA patterns of CIPTES-[(CH₂)₃SO₃HHIM] HSO₄/MFA

5.3.7 pH analysis of the catalyst

For pH analysis of the catalyst, to 25 mL of an aqueous solution of NaCl (1 M) with a primary pH 5.8, CIPTES-[(CH₂)₃SO₃HHIM] HSO₄/MFA (0.5 g) was added and the resulting mixture was stirred for 2 h at room temperature, after which the pH of the solution decreased to 1.76. This is equal to a loading of 0.86 mmol H⁺/g [38].

5.4 Catalytic activity

In order to evaluate the catalytic activity of synthesized catalysts, the acylation reaction of benzyl alcohol with acetic anhydride was carried out with and without catalyst. The yield of the product in each case is given in Table 5.1. For uncatalyzed reaction the yield of the product just could reach 16.0%. When reaction was carried out in homogeneous medium, CIPTES-[(CH₂)₃SO₃HHIM] HSO₄ showed good catalytic activity but separation of pure product was difficult with no possibility of catalyst reuse. However, CIPTES-[(CH₂)₃SO₃HHIM] HSO₄ supported on FA and MFA, could be easily separated by vacuum filtration and reused. In order to establish the MFA a better support for ionic liquid grafting the CIPTES-[(CH₂)₃SO₃HHIM] HSO₄/FA and CIPTES-[(CH₂)₃SO₃HHIM] HSO₄/MFA both were reused in second cycle. Interestingly regenerated CIPTES-[(CH₂)₃SO₃HHIM] HSO₄/FA gave only 26% yield due to leaching of ionic liquid during first cycle of reaction as well as during washing whereas CIPTES-[(CH₂)₃SO₃HHIM] HSO₄/MFA showed no significant loss in the yield of acetate during second cycle confirming the high stability of catalytic sites. FA and MFA without grafting Ionic Liquid have not shown any catalytic activity for studied reaction.

**Table 5.1: Catalytic activity of different catalysts for Friedel-Crafts acylation
Reaction of benzyl alcohol with acetic anhydride**

Sample	Catalysts	Temperature, °C	Time, min	Yield, %
1	Blank	90	10	15.04
2	MFA-40	90	10	20.03
3	CIPTES[(CH ₂) ₃ SO ₃ HHIM] HSO ₄	90	10	80
4	CIPTES[(CH ₂) ₃ SO ₃ HHIM] HSO ₄ /FA	90	10	50
5	CIPTES[(CH ₂) ₃ SO ₃ HHIM] HSO ₄ /MFA	90	10	91
6	CIPTES[(CH ₂) ₃ SO ₃ HHIM] HSO ₄ /FA (cycle 2)	90	10	25
7	CIPTES[(CH ₂) ₃ SO ₃ HHIM] HSO ₄ /MFA (cycle 2)	90	10	90

Optimized of reaction parameters such as effect of reaction time and temperature, molar ratio of reactants, power output are also studied in order to attain maximum conversion%.

5.4.1 Effect of reaction temperature

To study the influence of reacton temperature on conversion%, acylation of aromatic aicohols is conducted at different temperature ranging from 70 to 120°C for 5 to 20 minutes. The results illustrated that the conversion of aromatic alcohols gradually increases with increase in temperature as shown in Figure 5.5. The

maximum conversion is obtained at 90°C for benzyl alcohol while , for 4-methoxy benzyl alcohol and 4-nitro benzyl alcohol maximum conversion% is obtained at 100°C and 110°C respectively which get decreased on increasing temperature.

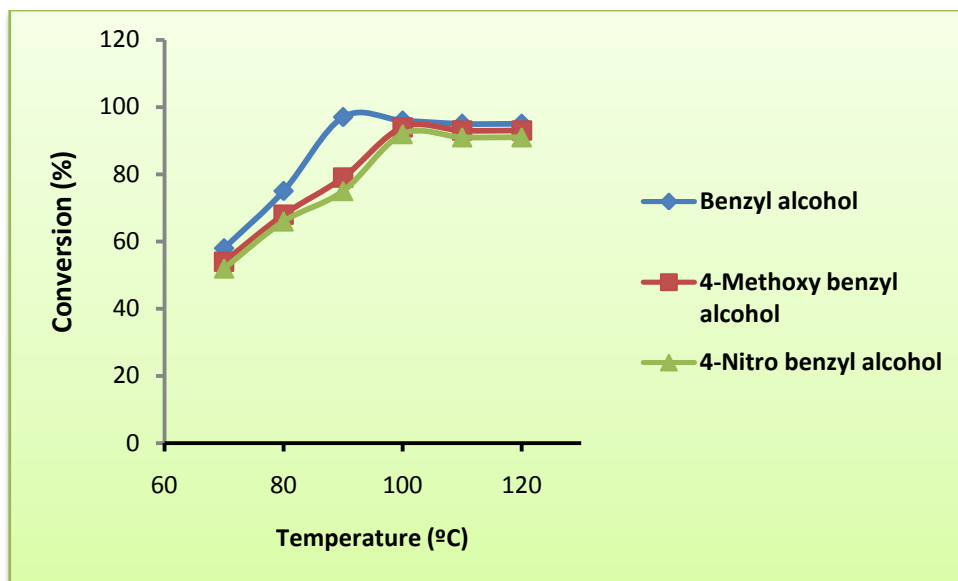


Figure 5.5: Variation of conversion% of aromatic alcohols over CIPTES[(CH₂)₃SO₃HHIM] HSO₄/MFA with temperature.

5.4.2 Effect of reaction time

The effect of reaction time on conversion% is carried out in the range of 4 to 20 min at 90, 100 and 110°C for benzyl alcohol, 4-methoxy benzyl alcohol and 4-nitro benzyl alcohol respectively as shown in Figure 5.6. It is found that in first 15 minutes, the conversion% increases linearly giving highest conversion% at 6, 10, 12 minutes which remain almost constant further. In this reaction, chances of formation of di or tri-acylated products is very less, so even if contact time between two reactions is increased, no significant effect is seen on conversion%.

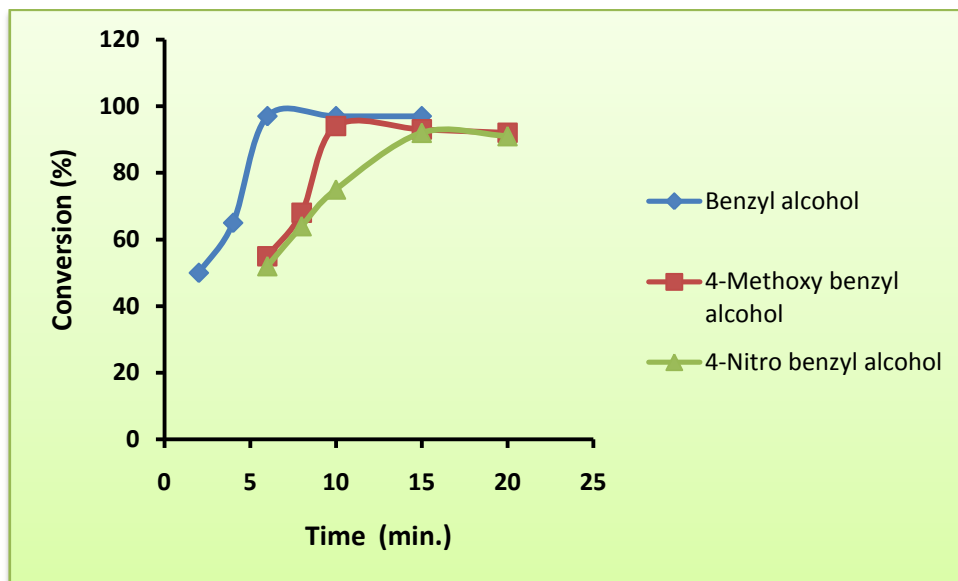


Figure 5.6: Variation of conversion% of aromatic alcohols over CIPTES[(CH₂)₃SO₃HHIM] HSO₄/MFA with time.

5.4.3 Effect of molar ratio of reactants

The effect of molar ratio of aromatic alcohols and acetyl chloride on conversion% is studied at different molar ratio varying from 1:1 to 1:2 as shown in Figure 5.7. At 1:1 ratio the conversion% is obtained very less due to insufficient amount of both reactants to react each other. If excess of acetyl chloride is taken, then chances of C-acylation increases which decreases selectivity of reaction towards acetate formation. The conversion of alcohols is found maximum at 1:1.5 molar ratio.

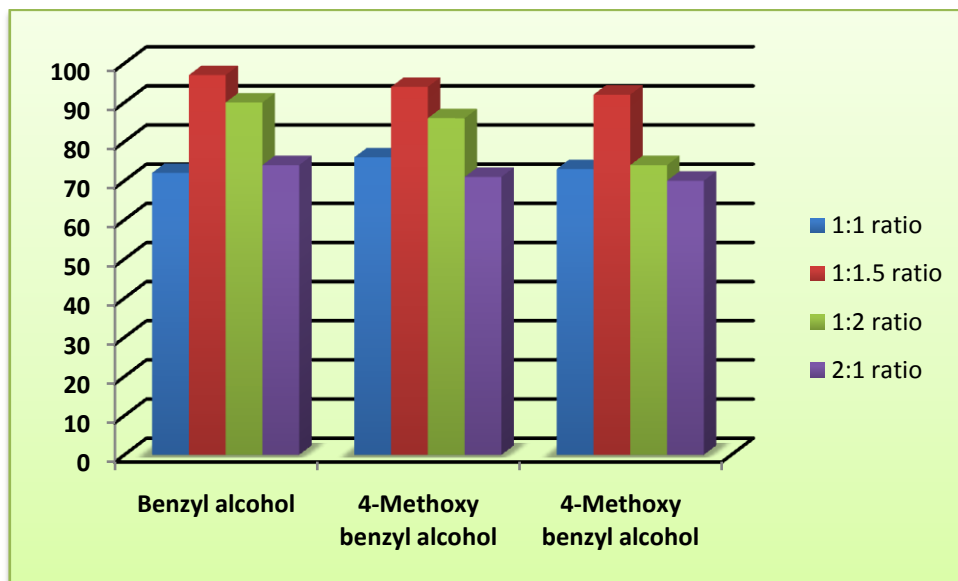


Figure 5.7: Variation of conversion% of aromatic alcohols over

CIPTES[(CH₂)₃SO₃HHIM] HSO₄/MFA with molar ratio of reactants.

5.4.4 Effect of power output

The effect of power output of microwave instrument on conversion% is studied at different power output ranging from 40 to 80W as shown in Figure 5.8. The conversion% of aromatic alcohols is found at 70W suggesting that this much power of microwave irradiation are adequate for occurrence of acylation of aromatic alcohols with highest conversion%. On increasing power output from 70 to 80W no sustainable change is seen in terms of conversion%.

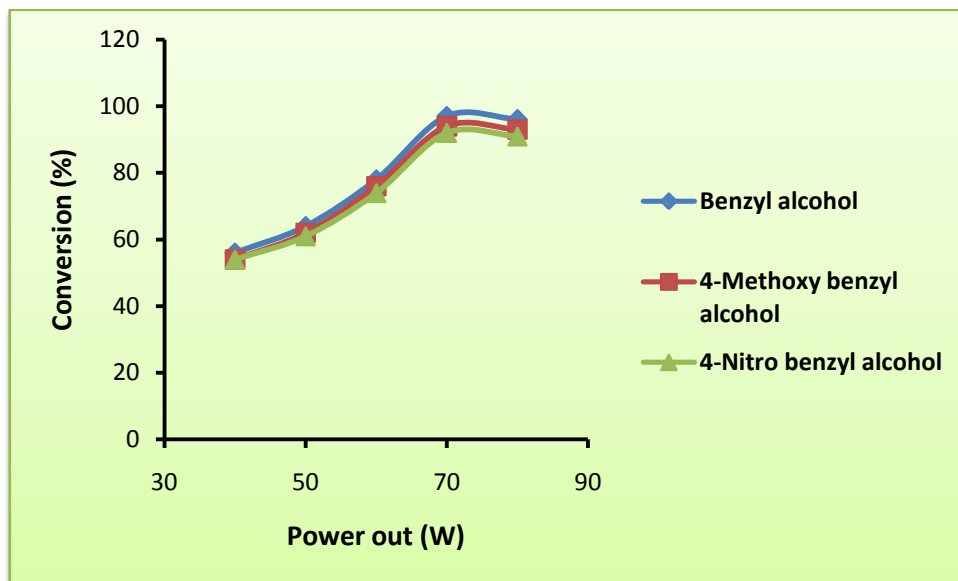


Figure 5.8: Variation of conversion% of aromatic alcohols over CIPTES[(CH₂)₃SO₃HHIM] HSO₄/MFA with power output

5.4.5 Effect of substrate to catalyst weight ratio

The effect of substrate to catalyst weight ratio on conversion% of aromatic alcohol and yield% of product is studied by varying the amount of catalyst under optimized reaction conditions. As inferred from Table 5.2, it can be said that at on increasing catalytic amount, conversion and yield% increases. It can be attributed due to availability of enhanced number of catalytic active sites. On further increase in the amount of catalyst no significant change is observed.

Table 5.2: Effect of substrate to catalyst weight ratio on conversion%

CIPTES[(CH₂)₃SO₃HHIM] HSO₄/MFA

Substrate to catalyst weight ratio	Conversion% of Benzyl alcohol	Conversion% of 4-methoxy benzyl alcohol	Conversion% of 4-nitro benzyl alcohol
10:1	57	58	52
5:1	97	94	92
2.5:1	92	89	87

Reaction conditions: Molar ratio (aromatic alcohol/acetic anhydride= 1:1.5); Temperature = 90-120°C; Time = 5 to 20 min.

The optimized reaction parameters for a series of acylation reactions over CIPTES-[(CH₂)₃SO₃HHIM] HSO₄/MFA in order to achieve maximum conversion and selectivity% are listed below in Table5.3.

Table 5.3: Optimized reaction parameters for a series of acylation reaction of aromatic alcohol by acetic anhydride over CIPTES-[(CH₂)₃SO₃HHIM] HSO₄/MFA with maximum conversion and selectivity% of major products.

S. No.	Aromatic alcohol	Reaction temperature (°C)	Reaction time (min.)	Conversion %	Major products Yield %
1	Benzyl alcohol	90	6	97	99
2	4-methoxy benzyl alcohol	100	10	94	96
3	4-nitro benzyl alcohol	110	12	92	94

Reaction conditions : Molar ratio (aromatic alcohol/acetyl chloride= 1:1.5);
Substrate/catalyst weight ratio=5:1.

5.4.6 Comparison with other reported catalyst

As depicted in Table 5.4, it can be said that CIPTES-[(CH₂)₃SO₃HHIM] HSO₄/MFA higher yield of desired products for a series of acylation reactions than some previously documented commercial catalysts.

Table 5.4: A comparison of acylation reaction of aromatic alcohols by acetic anhydride using different catalysts

Catalysts	Benzyl alcohol Yield %	4-methoxy benzyl alcohol yield %	4-nitro benzyl alcohol Yield %	References
ZnAl ₂ O ₄ @SiO ₂ nanocomposite*	92	88		42
[Hmim]HSO ₄ **	87	98	90	43
CIPTES- [(CH ₂) ₃ SO ₃ HHIM] HSO ₄ /MFA ***	96	99	94	This study

Reaction conditions:

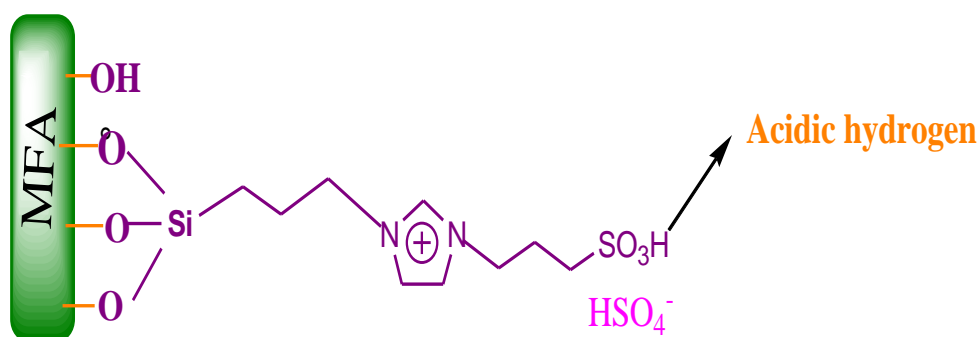
*Time = 20 min.; Temperature = 75°C; molar ratio(benzyl alcohol/acetic anhydride) = 1:1; catalyst weight = 0.1 gm

**Time = 20 min. ; Temperature = 50°C; molar ratio(benzyl alcohol/acetic anhydride) = 1:2; catalyst weight = 0.036 gm

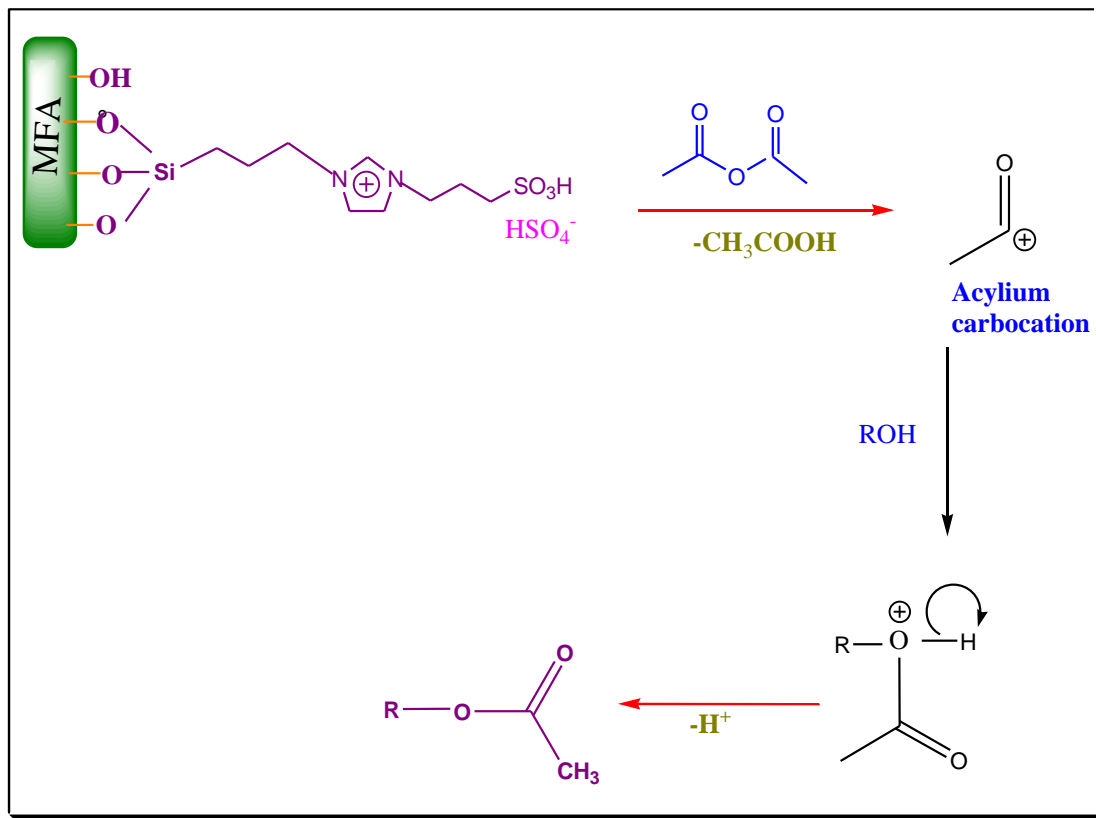
***Time = 6 min. ; Temperature = 90°C; molar ratio(benzyl alcohol/acetic anhydride) = 1:1.5; catalyst weight = 0.2 gm

5.5 Mechanistic aspects

The proposed model structure for active sites of CIPTES-[(CH₂)₃SO₃HHIM] HSO₄/MFA is given in Scheme 5.4. The possible pathway for acylation of aromatic alcohols using acetic anhydride by CIPTES-[(CH₂)₃SO₃HHIM] HSO₄/MFA catalyst is shown in Scheme 5.5. In the first step acidic hydrogen of SO₃H group of CIPTES-[(CH₂)₃SO₃HHIM] HSO₄ helps to generate acylium ion from acetic anhydride[38]. This intermediate in turn reacts with aromatic alcohols to form desired products (acetates).



Scheme 5.4: Model structure of CIPTES-[(CH₂)₃SO₃HHIM] HSO₄/MFA



Scheme 5.5: Proposed mechanism of acylation of aromatic alcohol by acetyl chloride over CIPTES-[(CH₂)₃SO₃HHIM] HSO₄/MFA catalyst

5.6 Regeneration and reusability of catalyst

For catalytic reusability test the used catalyst was recovered by filtration from the initial run, washed thoroughly with dichloromethane and dried in vacuum oven at 80 °C for 24 h followed by activation at 70 °C for 1 h in vacuum oven. The regenerated catalyst was used in next reaction cycles under the same reaction conditions following the procedure described as above. This catalyst show efficient catalytic activity up to four reaction cycles giving similar conversion% of alcohols as shown in Table 5.5 which indicates the the acidic sites are not deactivated during regeneration process. The conversion% is decreased after four cycle, due to the deposition of carbonaceous materials on the surface of catalyst which could block the

surface active sites of catalyst. The stability, heterogeneous nature of prepared catalyst and possibility of leaching of soluble ionic liquid CIPTES-[(CH₂)₃SO₃HHIM] HSO₄ in reaction medium is analyzed using Sheldon's hot filtration test which involves filtration of catalyst from reaction mixture in between the reaction and continuance of reaction in absence of catalyst. The results reveal that the reaction stops on filtering off the catalyst in mid of the reaction, hence proved that acidic ionic liquid CIPTES-[(CH₂)₃SO₃HHIM] HSO₄ responsible for catalytic activity do not get leached off during course of reaction (Table 5.5).

Table 5.5: Friedel-craft acylation of aromatic alcohols by acetic anhydride over fresh and regenerated CIPTES-[(CH₂)₃SO₃HHIM] HSO₄/MFA

Reaction run	Conversion(%)
I	95
II	93
III	93
IV	90

Reaction conditions: temperature =70 -120°C, time=4-20 min, power output=70W, molar ratio(aromatic alcohol/ acetic anhydride)=1:1.5), substrate/catalyst ratio=5:1

5.7 Identification of products

Benzyl acetate- ¹H NMR (300 MHz, CDCl₃) 7.38 (s, 5H, ArH), 5.15 (s, 2H, CH₂), 2.12 (s, 3H, CH₃). IR (KBr) 3034, 2930, 1742, 1497, 1455, 1380, 1362, 1228, 1026, 966, 750, 698 cm⁻¹.

4-Methoxy benzyl acetate- ¹H NMR (300 MHz, CDCl₃) 7.28 (d, J = 8.5 Hz, 2H, ArH), 6.88 (d, J = 8.5 Hz, 2H, ArH), 5.02 (s, 2H, CH₂), 3.78 (s, 3H, OCH₃), 2.05 (s, 3H, CH₃). IR (KBr) 3015, 2957, 2838, 1737, 1613, 1518, 1464, 1379, 1240, 1176, 1125, 1031, 961, 823 cm⁻¹.

4-Nitro benzyl acetate- ^1H NMR (300 MHz, CDCl_3) 8.25 (d, $J = 9.3$ Hz, 2H, ArH), 7.53 (d, $J = 9.3$ Hz, 2H, ArH), 5.22 (s, 2H, CH_2), 2.15 (s, 3H, CH_3). IR (KBr) 3074, 2939, 1737, 1601, 1518, 1449, 1343, 1235, 1108, 1048, 921, 860, 741 cm^{-1} .

5.8 Conclusion

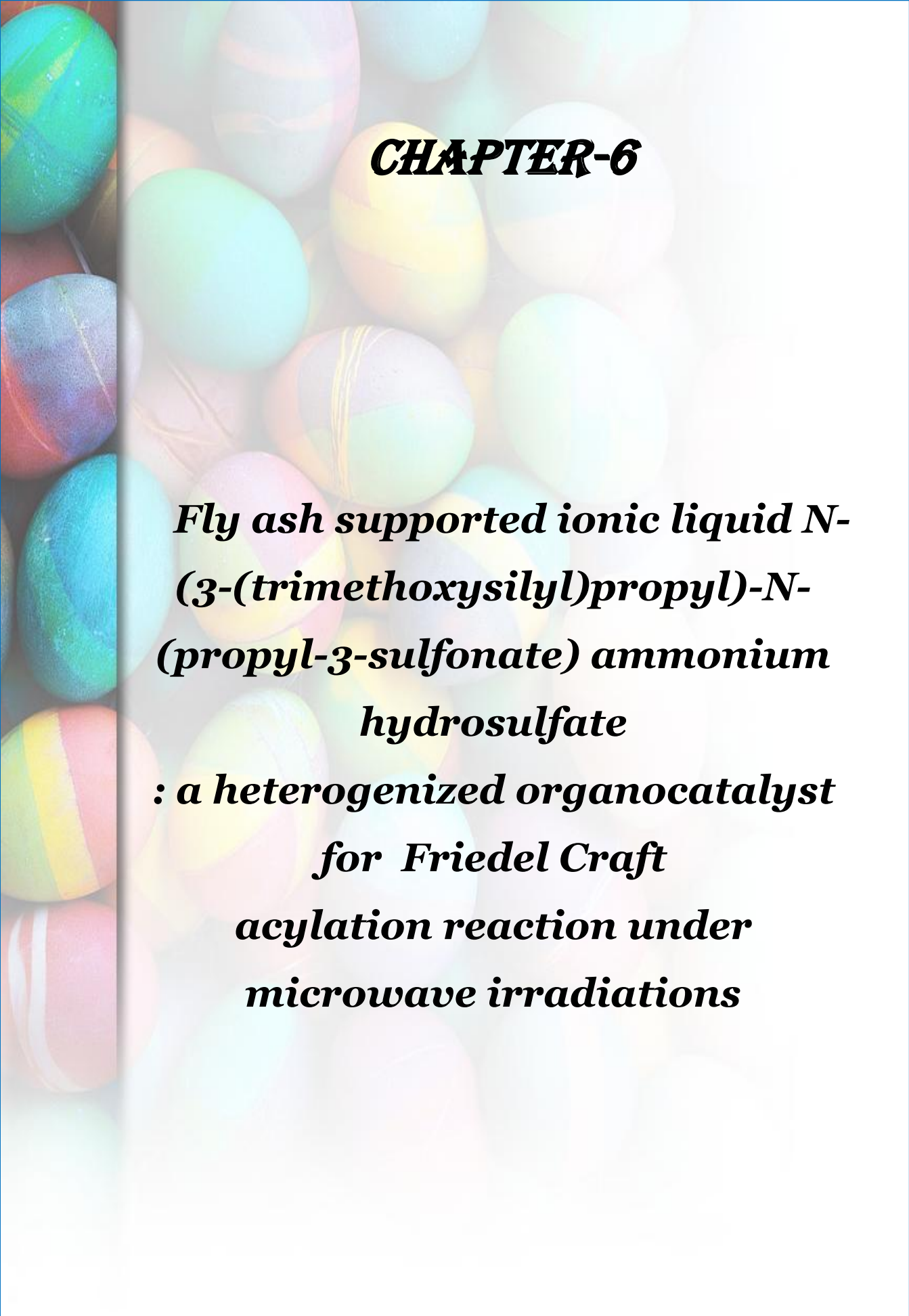
The present investigation elaborates the synthesis of sulphonic group functionalized acidic ionic which is successfully immobilized on the surface modified fly ash by covalent bonding. Thus formed ionic liquid functionalized fly ash behave as highly efficient, ecofriendly, recyclable catalyst for microwave assisted Friedel Craft acylation reaction of aromatic alcohols and acety chloride, offering practical convenience in product separation over pure ionic liquid system. More importantly, the immobilized acidic ionic liquid, especially, that using material of fly ash as innovative support posses much better reusability as comparision with pure ionic liquid. The synthesized catalyst having sufficient acidity successfully catalyze a series of friedel craft acylation reactions, giving excellent conversion%. Moreover, the catalyst could be reused after thermal activation up to four cycles without significant loss of its catalytic activity. This work gives a new idea to utilize coal generated fly ash an industrial soild waste,for synthesis of a novel heterogeneous catalyst, CIPTES- $[(\text{CH}_2)_3\text{SO}_3\text{HHIM}] \text{HSO}_4/\text{MFA}$ which have potential to replace other commercial solid acid catalysts in area of microwave assisted Friedel Craft acylation reactions useful in pharmaceutical, fine chemical and industrial applications. The synthesized benzyl acetate and its derivatives used as a composition of perfumery (floral, fruity; reminiscent of jasmine) ,flavouring (Reminiscent of apple and pear) and as a solvent in plastics and resin, celluloseacetate , nitrate, oils, lacquers, polishes and inks.

5.9 References

1. J.P. Tierney, P. Lidström (Eds.), *Microwave Assisted Organic Synthesis*, Blackwell, Oxford, 2005.
2. K. Hiroki, M. Hatori, H. Yamashita, J. Sugiyama, *Chem. Lett.* 37 (2008) 320.
3. A. S. Grewal, K. Kumar, S. Redhu, S. Bhardwaj, *Int. Res J Pharm. App Sci.* 3 (2013) 278-285.
4. S.S. Rana, J.J. Barlow, K.L. Matta, *Tetrahedron Lett.* 22(50), (1981) 5007-5010.
5. E. Vedejs, S.T. Diver, *J. Am. Chem. Soc.* 115 (1993) 3358.
6. A.C. Cope, E.C. Herrick, *Org. Synth.* 4 (1963) 304.
7. R.H. Baker, F.G. Bordwell, *Org. Synth.* 3 (1995) 141.
8. J. Iqbal, R.R. Srivastava *J. Org. Chem.* 57 (1992) 2001.
9. K. Ishihara, M. Kubota, H. Kurihara, H. Yamamoto, *J. Org. Chem.* 61 (1996) 4560
10. A. Orita, C. Tanashi, A. Kakuda, Otera *J. Angew. Chem., Int. Ed.* 39 (2000) 2877
11. R.C. Brindaban, S.D. Suwendu, H. Alakananda, *Green Chem.* 5 (2003) 44-46.
12. S. Wenda, S. Illner, A. Mell and U. Kragl, *Green Chem.* 13 (2011) 3007-3047
13. Y. Tao, R. Dong, I. V. Pavlidis, B. Chen, T. Tan, *Green Chem.* 18 (2016) 1240-1248
14. B. Gadenne, P. Hesemann, J.J. Moreau, *Chem Commun* 15 (2004) 1768-1769
15. F. Shi, Q.H. Zhang, D.M. Li, Y.Q. Deng, *Chem Eur J.* 11 (2005) 5279-5288
16. M. Gruttadauria, S. Riela, P.L. Meo, F. D'Anna, R. Noto *Tetrahedron Lett.* 45 (2004) 6113-6116
17. C. Yue, D. Fang, L. Liu, T.-F. Yi, *J. Mol. Liq.* 163 (2011) 99-121.

18. Y. Gu, F. Shi, Y. Deng, *J. Mol. Catal. A Chem.* 212 (2004) 71–75.
19. X. Jiang, W. Ye, X. Song, W. Ma, X. Lao, R. Shen, *Int. J. Mol. Sci.* 12 (2011) 7438–7444.
20. D. Jiang, Y.Y. Wang, L.Y. Dai, *React. Kinet. Catal. Lett.* 93 (2008) 257–263.
21. Y. Zhao, J. Long, F. Deng, X. Liu, Z. Li, C. Xia, J. Peng, *Catal. Commun.* 10 (2009) 732–736.
22. K. Qiao, C. Yokoyama, *Chem. Lett.* 33 (2004) 472–473.
23. K. Qiao, C. Yokoyama, *Chem. Lett.* 33 (2004) 808–809.
24. K. Qiao, Y. Deng, C. Yokoyama, H. Sato, M. Yamashina, *Chem. Lett.* 33 (2004) 1350–1351.
25. Y. Gu, F. Shi, Y. Deng, *Catal. Commun.* 4 (2003) 597–601.
26. R. M. Palou, *J. Mex. Chem. Soc.* 51(4) (2007) 252–264
27. J. Fischer, W. Hölderich, *Appl. Catal. A: Gen.* 180 (1999) 435.
28. M.E. González-Núñez, R. Mello, A. Olmos, G. Asensio, *J. Org. Chem.* 70 (26) (2005) 108–79.
29. M.E. González-Núñez, R. Mello, A. Olmos, G. Asensio, *J. Org. Chem.* 71 (17) (2006) 6432–6436
30. K. Qiao, H. Hagiwara, C. Yokoyama, *J. Mol. Catal. A: Chem.* 246 (2006) 65.
31. R. Sugimura, K. Qiao, D. Tomida, C. Yokoyama. *Catal. Commun.* 8 (2007) 770.
32. Q. Zhang, J. Luo, Y. Wei, *Green Chem.* 12(12) (2010) 2246–2254.
33. A.S. Amarasekara, O. S. Owereh, *Catal. Commun.* 11 (2010) 1072–1075.
34. Y. Shao, H. Wan, J. Miao, G. Guan, *Reac Kinet Mech Cat.* 109 (2013) 149–158
35. W. Ma, W. Wang, Z. Liang, S. Hub, R. Shen, C. Wu, *Kinetics and Catal.* 55 (2014) 665–670.
36. M. Seddighi, F. Shirini, M. Mamaghani, *C. R. Chimie* xxx (2015) xxx–xxx.
37. A. Sharma, K. Srivastava, V. Devra, A. Rani, *Amer. Chem. Sci. J.* 2(4) (2012) 177–187.

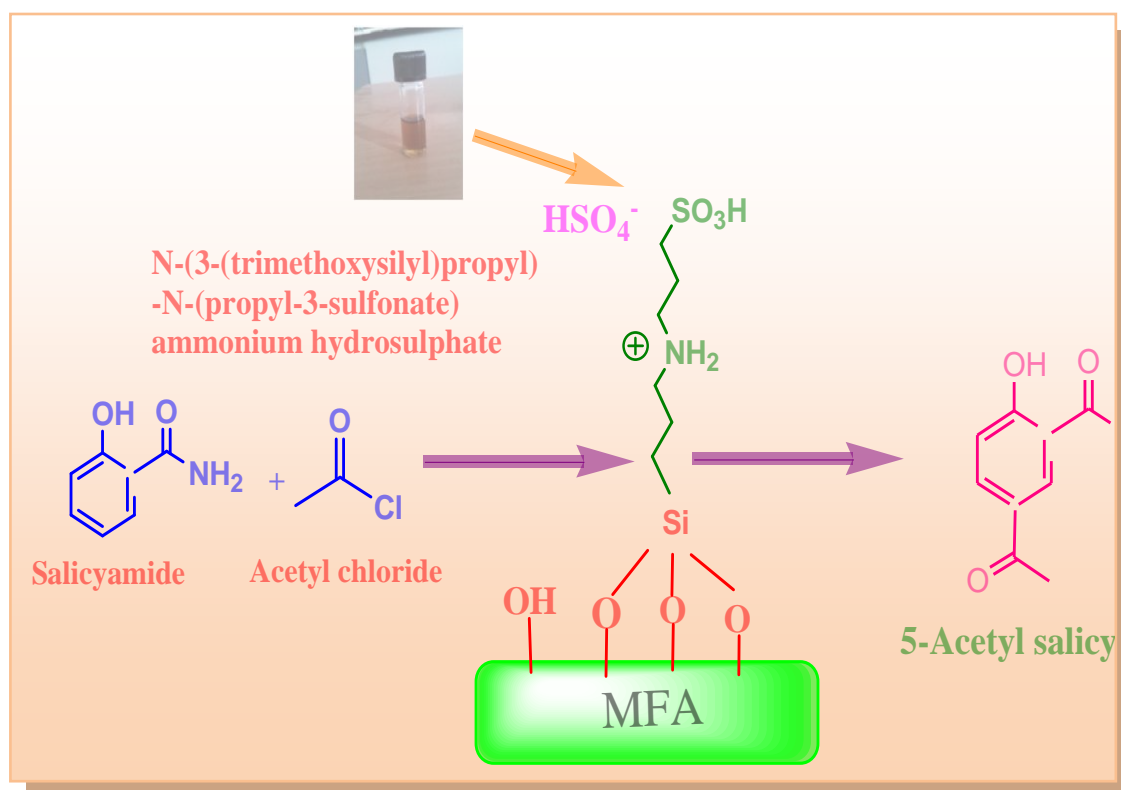
38. Z.J. Xu, H. Wan, J.M. Miao, M.J. Han, C. Yao, G.F. Guan, *J. Mol. Catal. A: Chem.* 332 (2010) 152–157.
39. J.M. Miao, H. Wan, G.F. Guan, *Catal. Commun.* 12 (2011) 353–356.
40. Y.H. Shan, J.H. Deng, F.R. Lin, M.H. Lu, S.S. Li, *Chin. J. Appl. Chem.* 26 (2009) 1428–1434.
41. M.N. Sefat, D. Saberi, K. Niknam, *Catal. Lett.* 141 (2011) 1713–1720.
42. S. Farhadi, K. Jahanara, *Chin. J. of Catal.* 35 (2014) 368–375.
43. A.R. Hajipour, L. Khazdoozb, A. E. Ruoho, *J. of the Chin. Chem. Soc.* (2009) 56, 398-403.



CHAPTER-6

***Fly ash supported ionic liquid N-(3-(trimethoxysilyl)propyl)-N-(propyl-3-sulfonate) ammonium hydrosulfate
: a heterogenized organocatalyst
for Friedel Craft
acylation reaction under
microwave irradiations***

Abstract



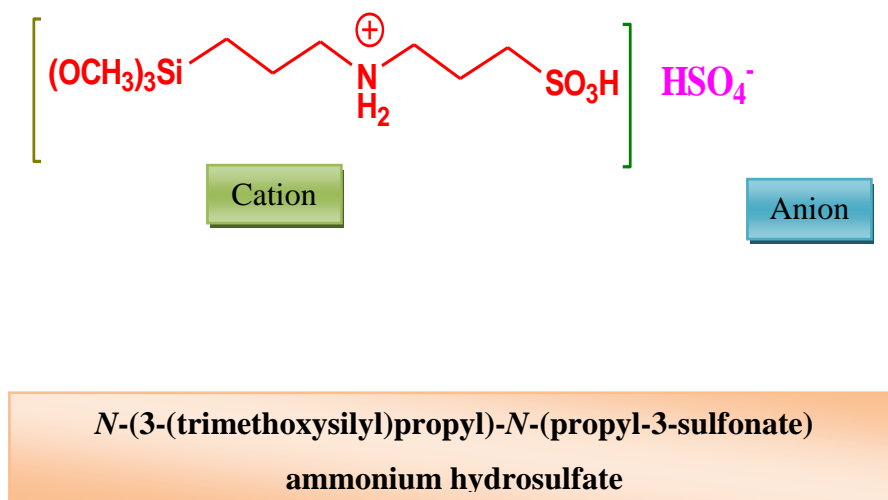
Friedel Craft Acylation reaction of Salicylamide over *N*-(3-(trimethoxysilyl)propyl)-*N*-(propyl-3-sulfonate) ammonium hydrosulphate/MFA

6.1 Introduction

Friedel Crafts acylation of aromatic compounds is used largely as intermediates in the fine chemical and pharmaceutical industries[1-2]. Conventional catalysts such as Lewis acids and some Bronsted acids, polyphosphoric and sulfuric acids, are widely used for Friedel–Crafts reactions, including acylation and alkylation[3]. The industrial production of 5- acetylsalicylamide by acylation of salicylamide with acetyl chloride in nitrobenzene caused serious environmental pollution due to carcinogenic nature of nitrobenzene[4]. However these catalysts suffer from inherent shortcomings such as serious corrosion of equipments, complicated separation procedures, environmental problems, and no recyclability of catalysts[5-7].

Recently Functionalized acidic ionic liquids have been introduced as ecofriendly approach in the ionic liquid arena developed for various special applications like catalyst, fossil fuel desulfurization reagents, lubricants and as monomers for the synthesis of ionic polymers [8-11]. The sulfonic acid group functionalized acidic ionic liquids are an important subgroup in the ionic liquid based catalysts class because they possess simultaneously the proton acidity and the characteristic properties of ionic liquids. Ionic liquids can be paired up by an enormous number of cations such as trialkylphosphonium, trialkylammonium, imidazolium, pyridinium and anions viz. halides, phosphates, sulphates, borates, acetates etc. [12-14]. Their green characteristics, such as chemical and thermal stability, negligible vapor pressure, excellent dissolution capability, non-flammability, tunable composition [15-16] make IL s environmentally benign catalysts and solvents in variety of catalytic reactions [17-21]. Wu et al. have introduced different ILs like triethylammonium ILs, imidazolium ILs, and pyridinium ILs functionalized by SO₃H group for the transesterification of cottonseed oil [22].The imidazole- and pyridine-based ILs have some disadvantages such as high cost, difficult preparation, and high toxicity [23-24] which restrict their industrial applications. Compare to imidazole and pyridinium

based ILs ammonium cation based ILs are cheaper Less toxic and easily available [25]. Tricaprylmethylammonium chloride could be produced in ton-scale and widely used as metal extraction agent, phase transfer catalyst, surfactant, or antistatic agent. In the present research we have synthesized SO₃H functionalized IL based on ammonium cation using 3-Aminopropyl)trimethoxysilane with 1,3-propane sultone to form sulfonate zwitterions Then, a stoichiometric amount of the acid H₂SO₄ was added to the zwitterion to obtain the ionic liquid ***N*-3-(trimethoxysilyl)propyl)-*N*-(propyl-3-sulfonate) ammonium hydrosulfate** in quantitative yield . This IL is made by sulphonic group containing cation and hydrogen sulphate anion as shown in Scheme 6.1.



Scheme 6.1: Structure of *N*-3-(trimethoxysilyl)propyl)-*N*-(propyl-3-sulfonate) ammonium hydrosulfate

The presence of both SO₃H functional groups and hydrogen sulfate counter anions can obviously enhance their acidities [12]. 3-Aminopropyl)trimethoxysilane is used as a linker, which could enter the silica framework easily through the covalent bonding. Silica immobilized *N*-3-(trimethoxysilyl)propyl)-*N*-(propyl-3-sulfonate) ammonium hydrosulfate has been investigated for synthesis of biodiesel from

rapeseed oil and methanol and acetalization of benzaldehyde and 1,2 ethanediol[26]. The Immobilization of the functionalized ionic liquids have the benefits of combining the ionic liquid characteristics with the common advantages of immobilizations, such as ease of recycling and improved selectivity in applications involving catalytic activity. The other acidic ionic liquids immobilized on silica gel by covalent bonds showed high activities for acetalization[27-28].

N-(3-(trimethoxy silyl) propyl)-*N*-(propyl-3-sulfonate) ammonium hydrosulphate is described under conventional thermal reactor. Mechanically activated F-type flyash is used as solid support to immobilize synthesized ionic liquid after proper purification strategy. The ionic liquid introduced the acid sites on the surface of fly ash catalyzing the acylation of salicylamide with acetyl chloride to give 5-acetylsalicylamide under microwave exposure which is an important intermediate exploited to synthesize medicaments for curing heart and irritability diseases. Fly ash-supported *N*-(3-(trimethoxysilyl)propyl)-*N*-(propyl-3-sulfonate) ammonium hydrosulfate is a novel and efficient catalyst and is a promising way of bulk utilization of waste fly ash by developing cost effective catalyst system for industrially important Friedel–Crafts acylation reactions.

6.2 Experimental

6.2.1 Materials

Fly ash [Class F type ($\text{SiO}_2 + \text{Al}_2\text{O}_3 > 70\%$)], collected from Kota Thermal Power Plant (Rajasthan, India) was used as support material for the preparation of the heterogeneous catalyst. Aromatic compounds and acetyl chloride were obtained from S.D. Fine Chem. Ltd., India. Ionic liquid precursors 1-methylimidazole (99%), 3-Aminopropyl)trimethoxysilane (95%), 1,3-propane sulfonate were purchased from Sigma Aldrich.Chemicals.

6.2.2 Catalyst preparation

Activation of fly ash

As received Fly ash (FA) was washed with distilled water followed by drying at 100°C for 3h thereafter mechanical activation was performed using high energy planetary ball mill as already described in chapter-2. MFA-40 was selected for immobilizing on *N*-(3-(trimethoxysilyl)propyl)-*N*-(propyl-3-sulfonate) ammonium hydrosulfate surface of MFA.

Synthesis of acidic ionic liquid

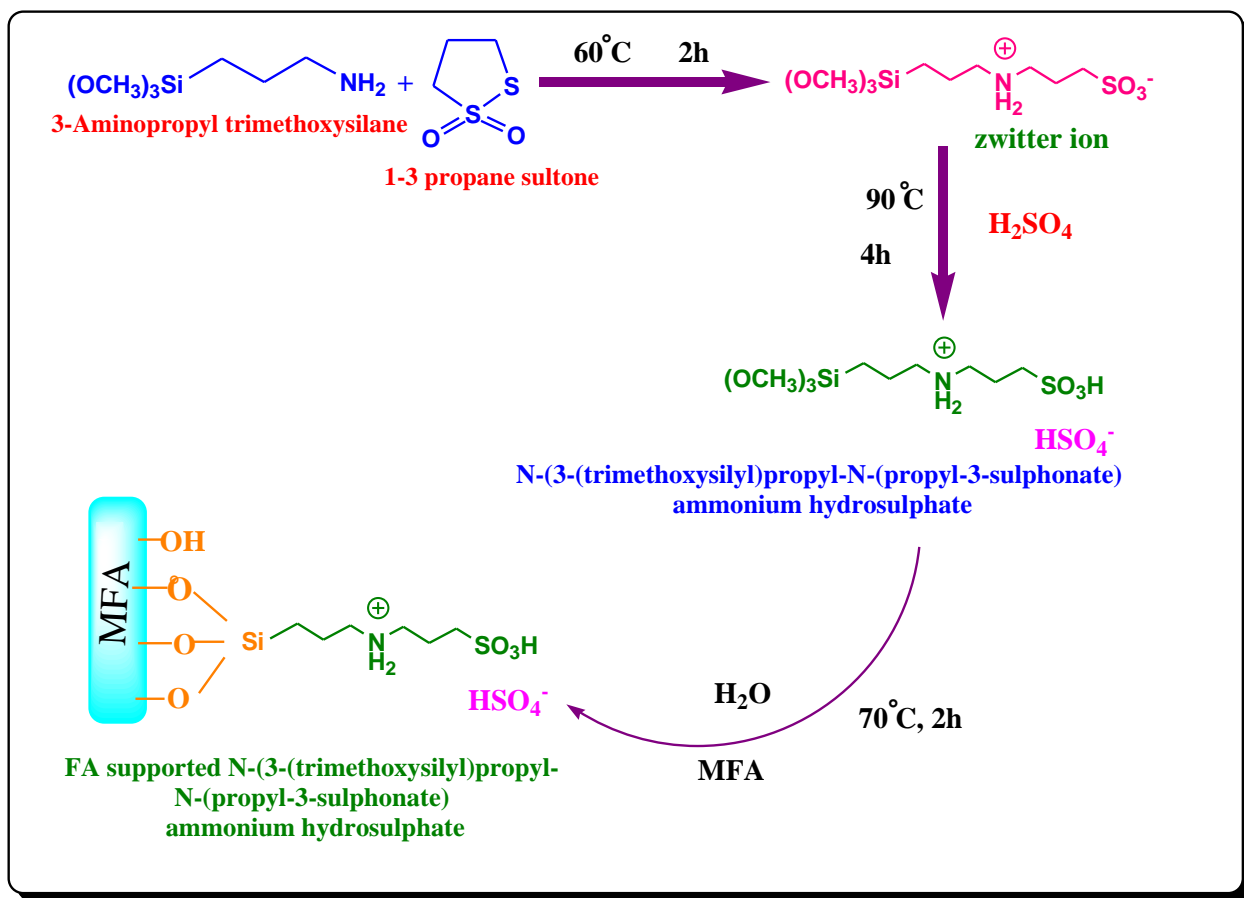
(3-Aminopropyl)trimethoxysilane (1.79 g, 0.01 mol) and 1,3-propane sulfonate (1.22 g, 0.01 mol) were added to a round-bottom flask containing 20 ml tetrahydrofuran and the mixture was stirred at 60°C for 2 h producing a white solid zwitter ion. The white solid zwitterion was filtered off and washed repeatedly with ether and dried in vacuum at 110°C for 12h. Formed solid(3.99 g, 10 mmol) and equimolar sulfuric acid were mixed and stirred at 90°C under vacuum. After 4h, product defined as *N*-(3-(trimethoxysilyl)propyl)-*N*-(propyl-3-sulfonate) ammonium hydrosulfate was obtained(Scheme 6.2). This IL was characterized by FT-IR (CDCl₃, cm⁻¹): 570.27, 1060.54, 1053.53, 1540.27, 1636.71, 2875.27, 2933.93, 2961.27, 3155.33, 3422.71.

¹H NMR for the zwitterions (400 MHz, DMSO, TMS): δ 0.8 (t, *J* = 7.2 Hz, 2H), 1.9 (m, 2H), 2.2(t, *J*H–H = 7.4 Hz, 2H), 2.7 (m, 2H), 3.1 (m, 2H), 3.2(m, 2H), 3.4 (t, *J* = 7.6 Hz, 2H), 3.5 (s, 9H).

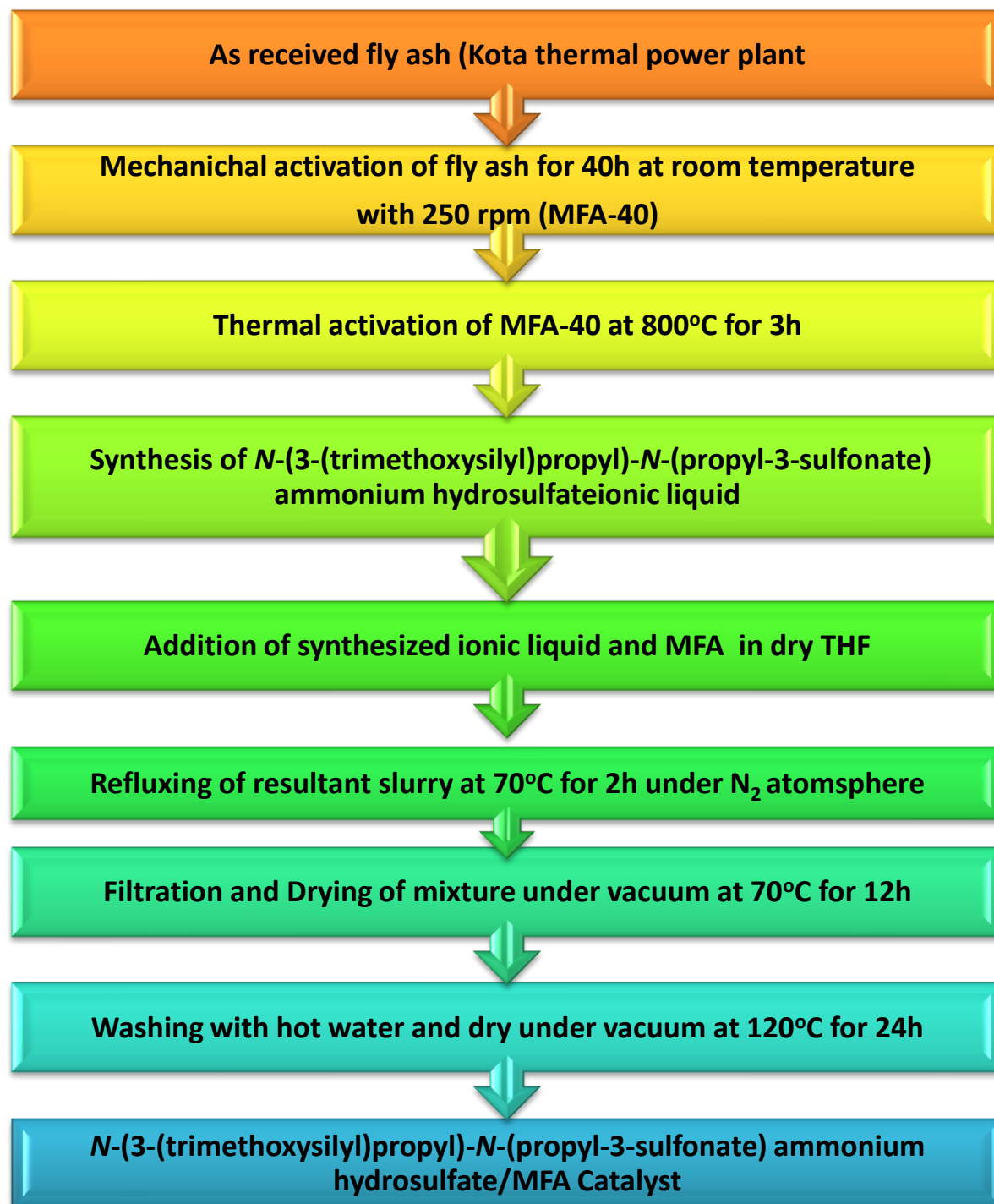
Synthesis of N-(3-(trimethoxy silyl) propyl)-N-(propyl-3-sulfonate) ammonium hydrosulphate

During immobilization process, firstly MFA was themally activated at 550 °C for 1 h and IL was dried at 80°C under vacuum for 1 h .The synthesized IL (1 gm) dissolved in 10 ml water are added to 10gm modified MFA and the mixture was stirred at 70°C

for 2 h. Then, the mixture was dried under vacuum at 60°C for 12h. The solid powdered was obtained and washed with hot water until no acidity could be detected in the filtrate. The prepared ionic liquid immobilized on MFA was obtained after drying at 120°C overnight in vacuum oven (Scheme 6.2). The steps of synthetic procedure is given in Scheme 6.3.



Scheme 6.2: The synthesis route of N-(3-(trimethoxy silyl) propyl)-N-(propyl-3-sulfonate) ammonium hydrosulphate functionalized FA.

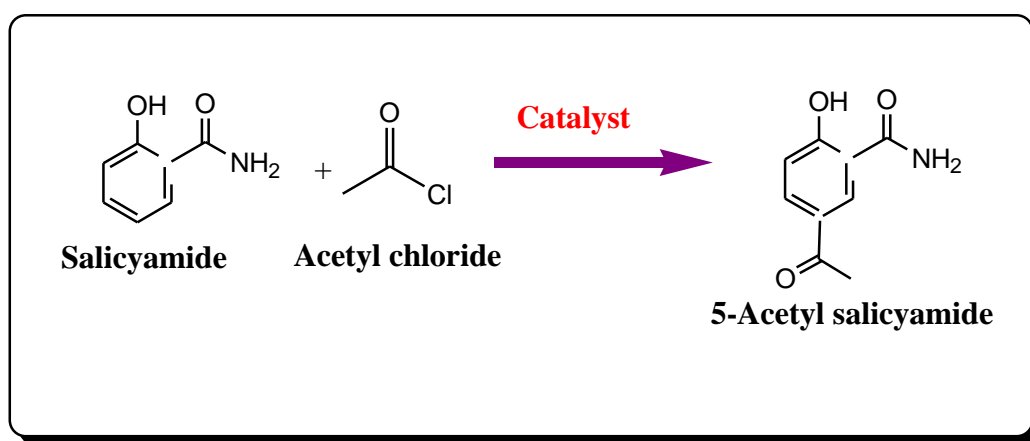


Scheme6.3: Synthesis of FA supported ionic liquid catalyst (*N*-((trimethoxysilyl)propyl)-*N*-(propyl-3-sulfonate) ammonium hydrosulfate /MFA

6.2.3 Characterization techniques

Physicochemical properties of all prepared samples are evaluated using XRD, FTIR, SEM-EDX, TGA, BET surface area, UV-Visible, ^1H NMR techniques, as described in [Annexure-I](#).

6.2.4 Reaction and product analysis



Scheme 6.4 : Simplified reaction pathway of acylation of salicylamide by acetyl chloride to give 5-acetyl salicylamide

In a typical procedure 10 mmol of salicylamide, 20 mmol of acetyl chloride were taken in 10 ml reactor tube covered by intelligent septa cap. The catalyst (acetyl chloride to catalyst weight ratio = 5), activated at 80 °C for 1 h prior to the reaction in vacuum, was added in the reaction mixture. The reaction is carried out in closed vessel system at 50 Psi pressure, by placing the vial in microwave cavity under constant stirring at different time periods, molar ratio, temperatures and power outputs. The pressurized glass vial with continuous stirring checked the vapor loss during the reaction proceeding at desired temperature and time. After completion of the reaction, the mixture was cooled at room temperature through air pump before releasing the pressure of the reactor tube. After filtration, filtered catalyst is washed

with dichloromethane to remove organic impurities and the product was cooled in an ice-water bath, then 50 mL of diluted hydrochloric acid (10%) was added into it. 5-Acetylsalicylamide deposited by acidification and the suspension was kept at room temperature for 24 h. 5-Acetylsalicylamide was filtered and washed with diluted hydrochloric acid and distilled water. Then 5-acetylsalicylamide was dried in a vacuum oven at 70 °C for 24 h.

The filtered catalyst is washed with dichloromethane to remove organic impurities. The reaction conditions were varied to obtain maximum yield and conversion into ester. The reactions were analyzed using a GC with oven temperature range 70-240 °C and N₂ (25 ml/min) as a carrier gas. The conversion % of salicylamide and yield of 5-acetyl salicylamide was calculated by using weight percent method.

$$\text{selectivity(\%)} = \frac{\text{yield}}{\text{conversion}} \times 100$$

6.3 Results and Discussion

6.3.1 Characterization of catalyst

The effect of mechanical activation on surfacial properties of FA as given in chapter 2. The silica percentage is increased marginally after milling for 5 to 40h but the specific surface area is increased from 9 to 36 m²/g. As compared with FA, the crystallite size is reduced from 33 to 17 nm as milling time was increase up to 36h. On grafting of ionic liquid the specific surface area of catalyst decreases progressively due to agglomeration of small particles of fly ash.

Table 6.1 : Characterization of fly ash before and after mechanical activation

Sample	Specific surface area m ² /g
MFA	36
<i>N</i> -(3-(trimethoxysilyl)propyl)- <i>N</i> -(propyl-3-sulfonate) ammonium hydrosulfate/MFA	17

6.3.2 Fourier transform infrared analysis

The FT-IR spectra of MFA-40 as given in chapter 2 shows increment in broadness between 3600-3300 cm⁻¹ evidence for the breaking down of the quartz structure and formation of Si-OH groups[29]. A peak at 1650 cm⁻¹ in the spectra of MFA is attributed to bending mode (δ O-H) of water molecule. However, FT-IR study clearly shows changes in the broadening of IR peaks corresponding to Si-O-Si asymmetric stretching vibrations (1101, 1090 cm⁻¹) indicating structural rearrangement during mechanical milling. After activation of FA, increase in surface roughness, mesopores and concentration of free silanols groups on the surface make it suitable for stabilized ionic liquid layer on MFA-40 via strong covalent bonding.

The FT-IR spectra of *N*-(3-(trimethoxysilyl)propyl)-*N*-(propyl-3-sulfonate) ammonium hydrosulfate/MFA catalyst presented in Figure 6.1 shows characteristic bands at 1650-1550 and 3000-2800 cm⁻¹ which indicate the presence of quaternary ammonium groups and bands at 3400-3300 cm⁻¹ may be caused by a quaternary ammonium salt[30]. The absorption of the S=O stretching modes lies between 1170 and 1060 cm⁻¹ and The S-O stretching mode of the functional group of sulfuric acid lies around 570 cm⁻¹ proving the successful preparation of the catalyst [31].

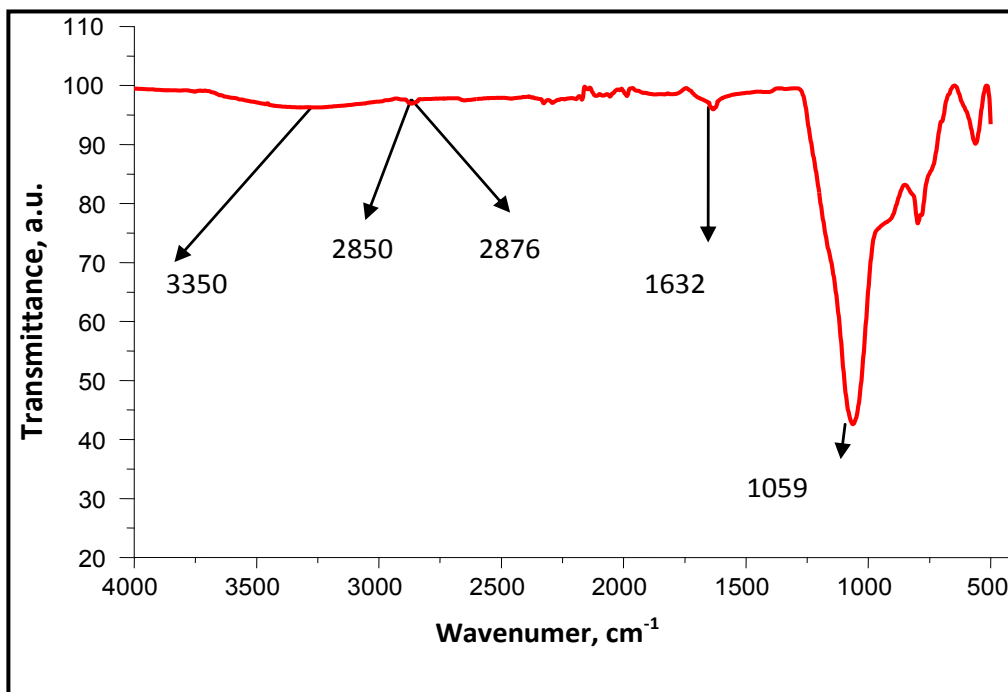


Figure 6.1: FT-IR spectra of *N*-(3-(trimethoxysilyl)propyl)-*N*-(propyl-3-sulfonate) ammonium hydrosulfate/MFA catalyst

6.3.3 Ultra violet Visible spectroscopy

The UV-Vis spectra of the pure ionic liquid *N*-(3-(trimethoxysilyl)propyl)-*N*-(propyl-3-sulfonate) ammonium hydrosulfate in the scanning range 200-800 nm as shown in Figure 6.2 envisions some color impurities through absorption peak at 270 nm.

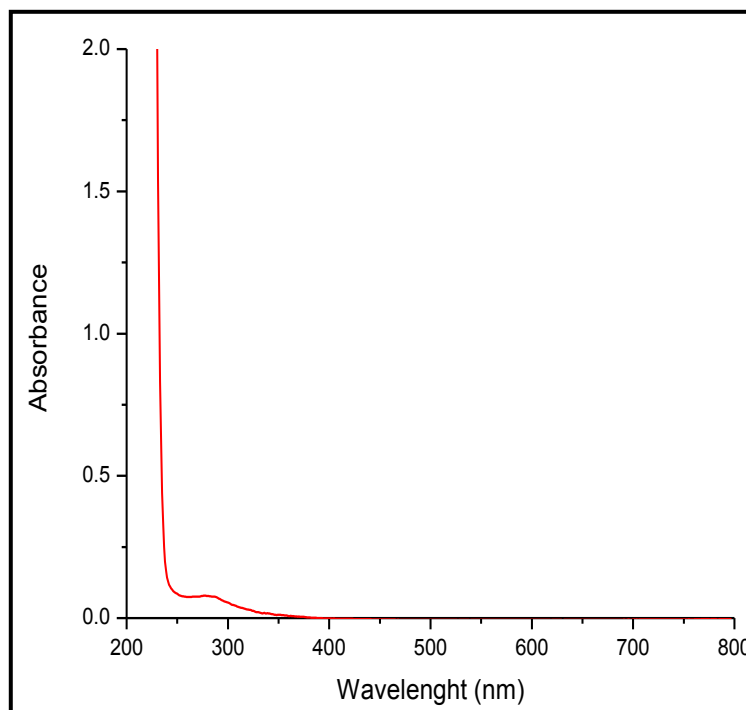


Figure 6.2 : UV-VIS spectrum for purity of *N*-(3-(trimethoxysilyl)propyl)-*N*-(propyl-3-sulfonate) ammonium hydrosulfate

6.4.4 SEM analysis

The SEM photograph of pure fly ash (Figure 6.3A) is observed with hollow cenospheres, irregularly shaped unburned carbon particles, mineral aggregates and agglomerated particles. As a result of mechanical activation the structural break down of larger particles and increased surface roughness are observed (Figure 6.3B).

The primary morphology of MFA is changed after immobilization of ionic liquid on the surface of MFA. Typical SEM images of catalysts show that the resulting particles are aggregated to form the bigger particles. In catalyst all particles are wrapped by IL forming a thin layer over the surface of MFA clearly seen in Figure 6.3 (D).

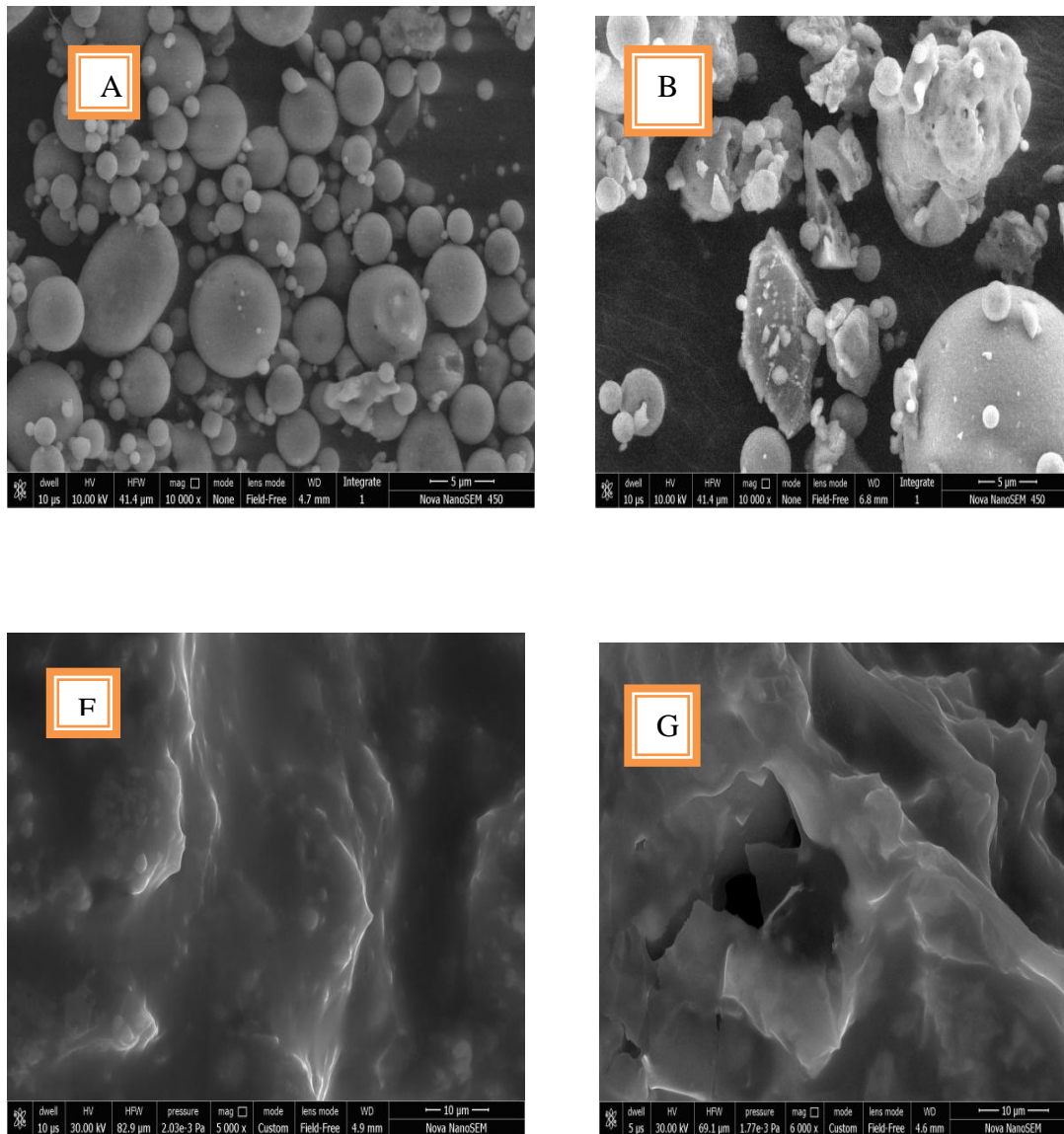


Figure 6.3: SEM micrographs (A) pure FA (B) MFA-40 (C, D) *N*-(3-(trimethoxy silyl)propyl)-*N*-(propyl-3-sulfonate) ammonium hydrosulfate/MFA and magnified image of Catalyst

6.3.5 X-ray diffraction analysis

The X-Ray diffraction patterns of the as received FA as well as MFA are already described in chapter 2. The peaks at 16.4° and 26.2° show mullite (alumino-silicate) phase while quartz (silica) exhibits strong peaks at 20.7° , 26.6° , 40.6° and 49.9° of 2θ values. As a result of ball milling mostly quartz and mullite crystalline phases are reduced.

6.3.6 Thermogravimetric analysis

The thermal stability of the *N*-(3-(trimethoxysilyl)propyl)-*N*-(propyl-3-sulfonate) ammonium hydrosulfate/MFA catalyst was investigated by thermogravimetric analysis (TGA) in which the observed weight loss was associated with the loss of the organic components attached to the Surface of MFA (Figure 6.4). The TGA curve indicated initial weight loss within 200°C mainly attributed to the desorption of physisorbed water and residual solvent. When the temperature further increased to 150°C , the weight loss of *N*-(3-(trimethoxysilyl)propyl)-*N*-(propyl-3-sulfonate) ammonium hydrosulfate/MFA decreased rapidly due to removal of immobilized ionic liquid moieties. Complete loss of all the covalently attached organic structure is seen in the temperature range between 230 and 570°C [30]. These results indicate that the immobilized acid catalyst is apparently stable up to about 230°C .

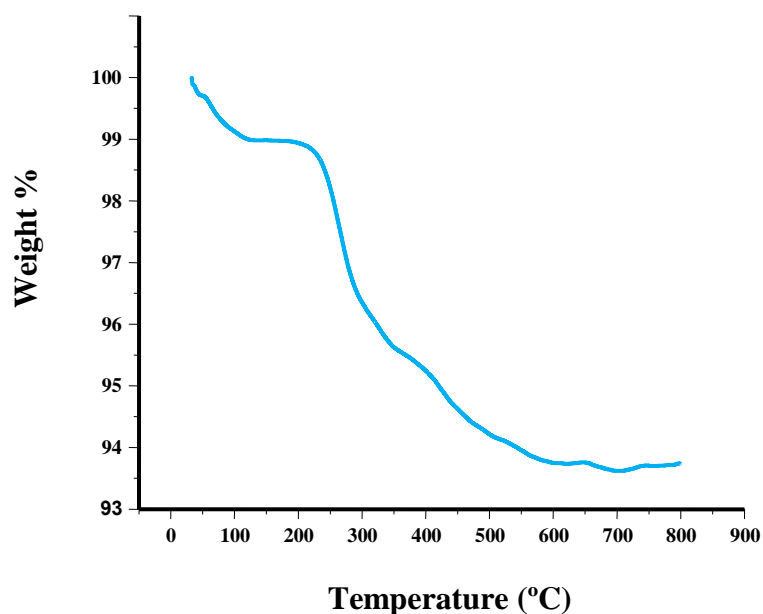


Figure 6.4: TGA pattern of the *N*-(3-(trimethoxysilyl)propyl)-*N*-(propyl-3-sulfonate) ammonium hydrosulfate/MFA

6.3.7 pH analysis of the catalyst

For pH analysis of the catalyst, to 25 mL of an aqueous solution of NaCl (1 M) with a primary pH 5.8, *N*-(3-(trimethoxysilyl) propyl)-*N*-(propyl-3-sulfonate) ammonium hydrosulfate/MFA (0.5 g) was added and the resulting mixture was stirred for 2 h at room temperature, after which the pH of the solution decreased to 1.74. This is equal to a loading of 0.90 mmol H⁺/g [28].

6.4 Catalytic performance

The catalytic performance is tested by Friedel-Crafts acylation reaction of salicylamide reaction and acetyl chloride to give 5-acetyl salicylamide in single step, solvent free conditions. Reaction is performed at 100°C for 10 minutes, taking salicylamide/acetyl chloride molar ratio 1:2 and salicylamide to catalyst weight ratio of 5:1. Results given Table 6.2 show that FA, MFA do not possess any catalytic activity for this reaction. When reaction was carried out in homogeneous medium, *N*-(3-(trimethoxysilyl) propyl)-*N*-(propyl-3-sulfonate) ammonium hydrosulfate showed good catalytic activity but separation of pure product was difficult with no possibility of catalyst reuse. While in the presence of *N*-(3-(trimethoxysilyl)propyl)-*N*-(propyl-3-sulfonate) ammonium hydrosulfate /MFA catalyst the conversion % and yield is obtained highest with no significant loss in the yield of 5-acetyl salicylamide during second cycle confirming the high stability of catalytic sites.

Table 6.2: Catalytic activity of different catalyst for microwave assisted acylation reaction of salicylamide

Catalysts	Conversion%	Yield %
FA	Nil	Nil
MFA	Nil	Nil
<i>N</i> -(3-(trimethoxysilyl)propyl)- <i>N</i> -(propyl-3-sulfonate) ammoniumhydrosulfate	61	58
<i>N</i> -(3-(trimethoxysilyl)propyl)- <i>N</i> -(propyl-3-sulfonate) ammoniumhydrosulfate/MFA	92	90

Reaction conditions: time = 10 minutes; temperature = 100°C; molar ratio(salicylamide/acetyl chloride) = 1:2; substrate/catalyst ratio = 5:1

On basis of above results, *N*-(3-(trimethoxysilyl)propyl)-*N*-(propyl-3-sulfonate) ammonium hydrosulfate/MFA catalyst was selected for further optimization of reaction parameters such effect of reaction temperature and time, molar ratio of reactants, substrate to catalyst ratio, in order to attain maximum conversion and yield %.

6.4.1 Effect of reaction temperature

To optimize the reaction temperature giving maximum conversion and yield % , reaction of salicylamide and acetyl chloride is studied at different temperature ranging from 80°C to 120°C for 10 minutes. The results illustrated that the conversion% of salicylamide gradually increases with increase in temperature as shown in Figure 6.5. The maximum conversion% of salicylamide (92%) is obtained at 100°C within 10 min. along with higher yield (90%) which get decreased on increasing temperature up to 120°C due to formation of side products.

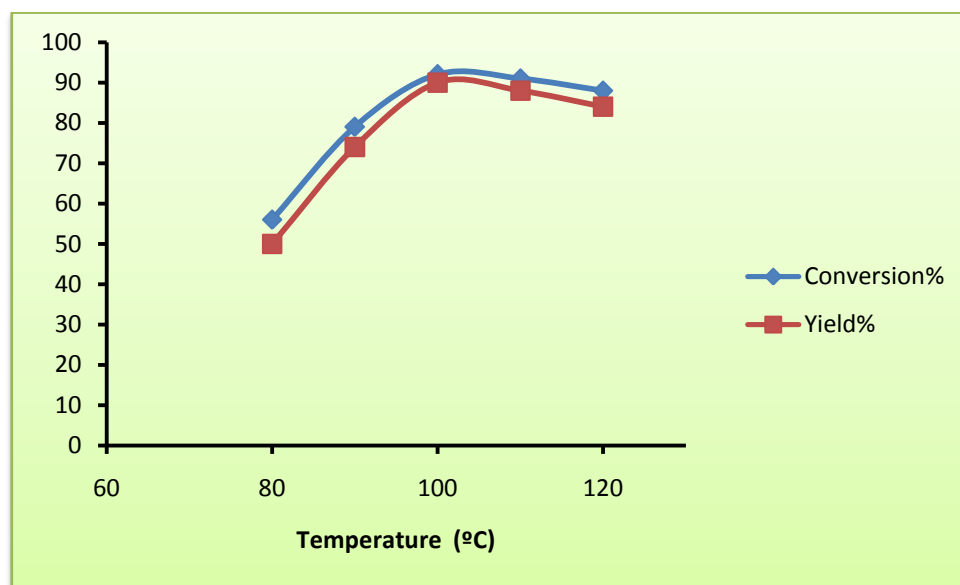


Figure 6.5: Variation of conversion and yield% of salicylamide over *N*-(3-(trimethoxysilyl)propyl)-*N*-(propyl-3-sulfonate)ammonium hydrosulfate/MFA with temperature

6.4.2 Effect of reaction time

The optimization of reaction time is carried out at 100°C to achieve maximum conversion, yield % of desired product in the range of 5 to 20 min as shown in Figure 6.6. It is found that first 10 minutes, the conversion% increases linearly up to 92% which remained constant till 110°C with 90% yield. On further increasing the reaction time, yield of desired product decreases due to formation of side products.

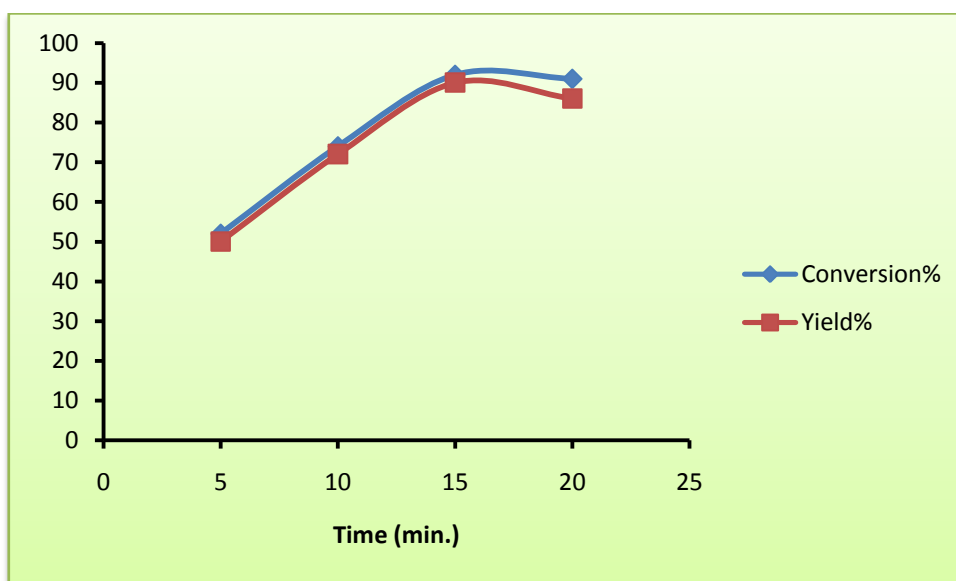


Figure 6.6: Variation of conversion and yield% of salicylamide over *N*-(3-(trimethoxy silyl)propyl)-*N*-(propyl-3-sulfonate) ammonium hydrosulfate/MFA with temperature

6.4.3 Effect of molar ratio reactants

The effect of molar ratio of salicylamide and acetyl chloride on conversion and yield% is monitored at different molar ratios varying from 2:1 to 1:3 as given in Table 6.3. The conversion and yield % of desired product is found maximum (92 and

90%) respectively at 1:2 molar ratio in case of other molar ratios, the amount of reactants was not sufficient to give higher conversion.

Table 6.3: Effect of molar ratio of salicylamide/acetyl chloride on conversion and yield% over *N*- (trimethoxy silyl)propyl)-*N*-(propyl-3-sulfonate) ammonium hydrosulfate/MFA

Molar ratio (salicylamide/acetyl chloride)	Conversion% of salicylamide	Yield%
2:1	58	48
1:1	76	62
1:2	92	90
1:3	60	58

Reaction conditions: Time = 10 minutes; Temperature = 100°C; Substrate/Catalyst ratio = 5:1

6.4.4 Effect of substrate to catalyst weight ratio

The effect of substrate to catalyst weight ratio on conversion of salicylamide and yield% of product is studied by varying the amount of catalyst under optimized reaction conditions. As inferred from Table 6.4, it can be said that on increasing catalytic amount, conversion and yield% increases. It can be attributed due to availability of enhanced number of catalytic active sites. On further increase in the amount of catalyst no significant change is observed.

Table 6.4: Effect of substrate/catalyst weight ratio on conversion and yield% over *N*- (trimethoxy silyl)propyl)-*N*-(propyl-3-sulfonate) ammonium hydrosulfate/MFA

Salicylamide/Catalyst	Conversion% of Salicylamide	Yield %
10:1	60	52
5:1	92	90
2.5:1	90	88

Reaction conditions: Time = 10 minutes: Temperature = 100°C; molar ratio of reactant = 1:2

The maximum conversion (92%) and yield (90%) of product is obtained when reaction is performed at 100°C For 10 minutes, taking salicylamide and acetyl chloride in 1:2 molar ratio and substrate to catalyst ratio of 5:1 over catalyst.

6.4.5 Effect of power output

The effect of power output of microwave instrument on conversion and yield% is studied at different power outputs ranging from 40 to 80W as shown in Figure 6.7. the conversion and yield% of salicylamide is found maximum at 70W suggesting that this much power of microwave irradiations are adequate for occurrence of acylation of salicylamide with highest conversion and yield%. On increasing power output from 60 to 80W no suitable change is seen in term of conversion and yield%.

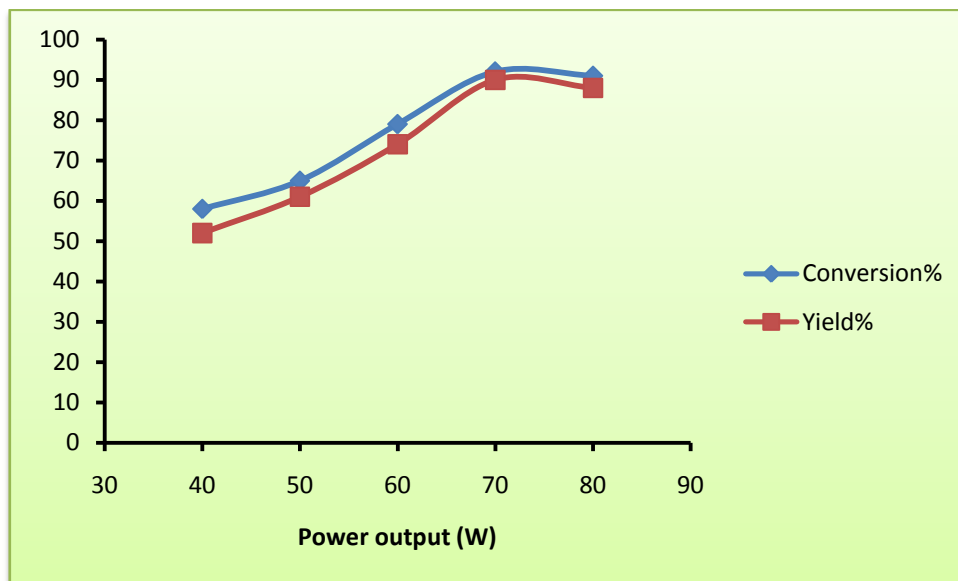
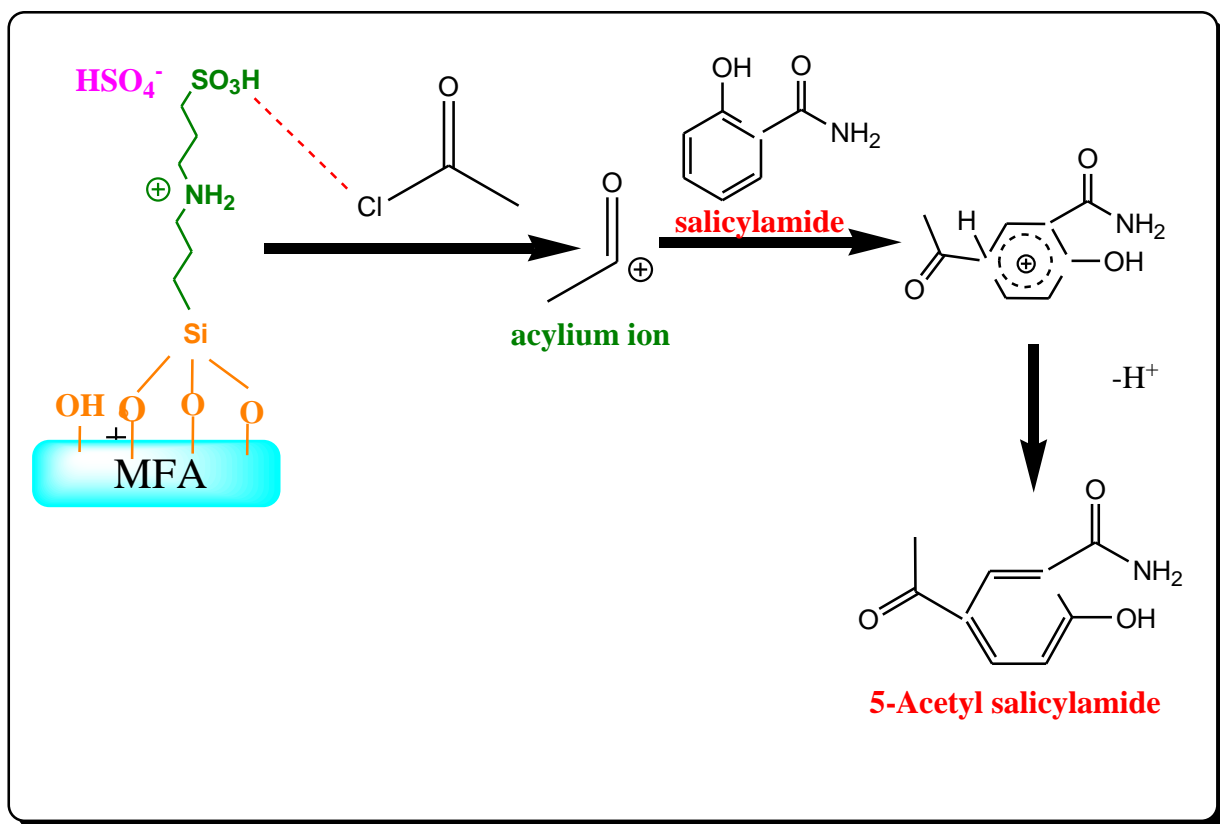


Figure 6.7: Variation of conversion and yield% of salicylamide over *N*-(trimethoxysilyl)propyl)-*N*-(propyl-3-sulfonate)ammonium hydrosulfate/MFA with power output

6.5 Mechanistic aspects

The possible pathway for the production of 5-acetyl salicylamide by acylation of salicylamide and acetyl chloride catalyzed by prepared catalyst is shown in Scheme 6.5. In the first step acidic hydrogen of SO_3H group of *N*-(3-(trimethoxysilyl)propyl)-*N*-(propyl-3-sulfonate)ammonium hydrosulfate/MFA catalyst interact with acetyl chloride and generate acylium ion. The generated acylium ion interacted with salicylamide, forming activated cationic adduct. Finally, the cationic adduct is converted into aromatic ketone by releasing a proton.



Scheme 6.5: The acylation route of salicylamide with acetyl chloride catalyzed by the prepared catalyst

6.6 Regeneration and reusability of catalyst

The catalyst was filtered and washed diethyl ether, dried in vacuum oven at 110°C overnight and uses it in next cycles. The regenerated catalyst show efficient catalytic activity up to consecutive four cycles giving conversion% of salicylamide in the range of 92-82% and yield in the range of 90-82% as shown in Figure 6.8 which indicates the acidic sites are not deactivated during regeneration process and ionic liquid is not washed out in reaction mixture. The conversion% is decreased after four cycle, due to the deposition of carbonaceous materials on the surface of catalyst which could block the surface active sites of catalyst.

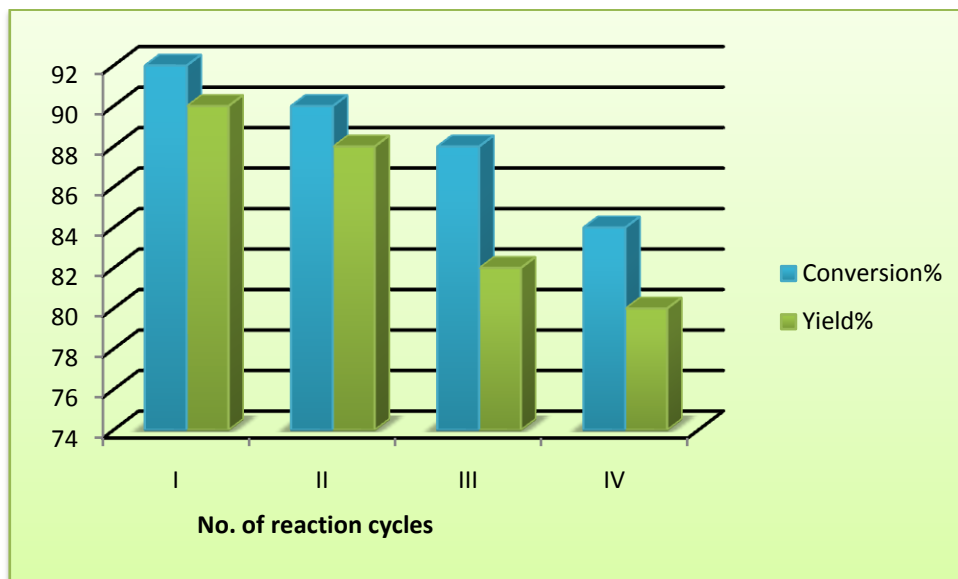


Figure 6.8 The reusability of catalyst in acylation reaction

The data given in Table 6.5 show that there is no considerable change in the catalytic activity of the catalyst even after four reaction cycles. Thus we can say that the prepared catalyst used in our study is considerably stable and can be reused up to minimum four reaction cycles.

Table 6.5: Conversion% of salicylamide with regenerated catalyst

Reaction cycle	% Conversion	% Yield
I	92	90
II	90	88
III	88	82
IV	84	80

6.7 Identification of product

5-Acetyl salicylamide- ^1H NMR spectra of desired product is given in Figure 6.7.

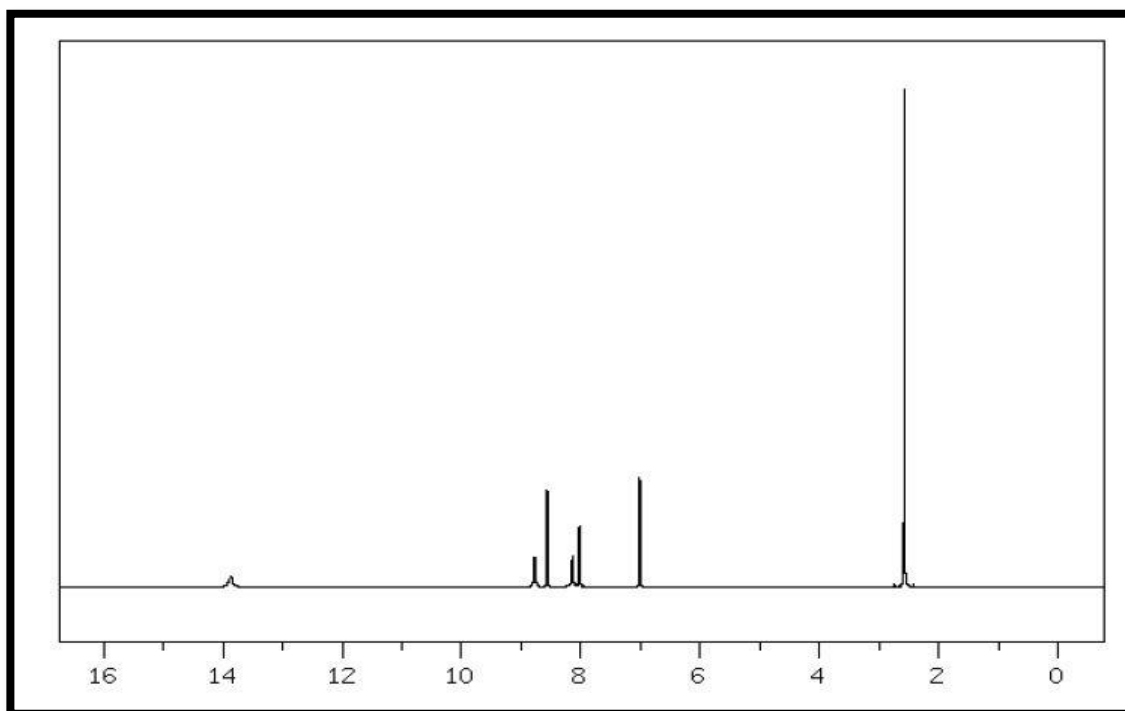
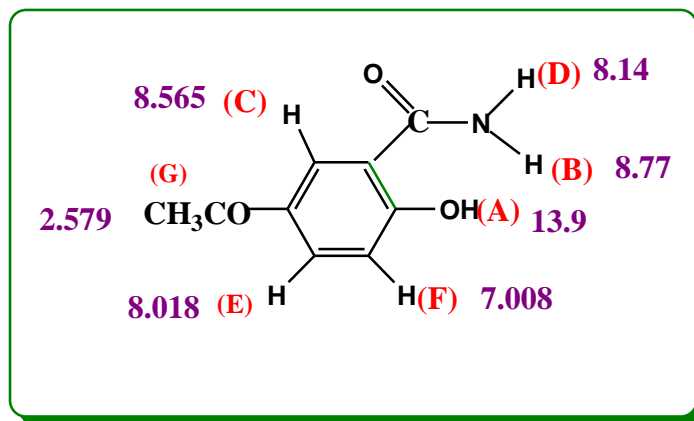


Figure 6.7 : FT-IR spectra of 5-acetyl salicylamide

6.8 Conclusion

The present work provides a novel pathway for the synthesis of fly ash supported *N*-(3-(trimethoxysilyl)propyl)-*N*-(propyl-3-sulfonate) ammonium hydrosulfate heterogeneous acid catalyst possessing significant amount of acidity. The mechanical activation of fly ash results in increased silica content, surface roughness and high concentration of free silanol groups which are responsible for efficient immobilization of ionic liquid on activated fly ash. Fly ash supported sulphonic group functionalized ionic liquid is efficient catalyst for synthesis of 5-acetyl salicylamide via acylation reaction of salicylamide and acetyl chloride under microwave heating. The sulphonic group in ionic liquid cation can greatly accelerate the reactions and showed a synergetic effect with hydrogensulphate anion. The reactions can proceed smoothly, fast under solvent free conditions as compared to conventionally using supported ionic liquids. The catalyst is also recyclable suggesting that acid sites of the catalyst are not lixiviated during the reaction. The novelty of the present work is that low cost renewable waste material, fly ash can replace other commercially available support materials and the organic solvent-free green process presented here could show potential application in industry due to its easy product separation and high efficiency.

6.8 References

1. D.O. Jang, K.S. Moon, D.H. Cho, J. Kim, *Tetrahedron Lett.* 47 (2006) 6063.
2. C.B. Yue, T.F. Yi, C.B. Zhu, G. Liu, *J. Ind. Eng. Chem.* 15 (2009) 653.
3. C. Castro, A. Corma, J. Primo, *J. Mol. Catal. A: Chem.* 177 (2002) 273.
4. H. Li, H. Wang, H. Sun, Y. Liu, K. Liu, S. Peng, *Toxicol. Lett.* 139 (2003) 25.
5. X.Z. Li, W.J. Eli, *J. Mol. Catal. A: Chem.* 279 (2008) 159–164.

6. V.R. Vamsi, V.R. Modukuri, A. Ratnamala, R. Vempati, V.S. Gottumukkala, S. Chava, C.S. Rao, *Org. Process Res. Dev.* 13 (2009) 769–773.
7. J.Z. Gui, X.H. Cong, D. Liu, X.T. Zhang, Z.D. Hu, Z.L. Sun, *Catal. Commun.* 5 (2004) 473–477.
8. J.H. Davis, *Chem. Lett.* 33 (2004) 1072–1077.
9. Z.F. Fei, T.J. Geldbach, D.B. Zhao, P.J. Dyson, *Chem. Eur. J.* 12 (2006) 2122–2130.
10. X. Li, D. Zhao, Z. Fei, L. Wang, *Sci. China Ser. B* 49 (2006) 385–401.
11. H. Olivier-Bourbigou, L. Magna, D. Morvan, *Appl. Catal. A* 373 (2010) 1–56.
12. V. Losetty, B.K. Chennuri, R.L. Gardas, *J Chem Thermodyn* 90 (2015) 251–258.
13. A.B. Pereiro, A. Rodriguez, *J Chem Eng Data* 52 (2007) 600–608.
14. H. Wang, J. Wang, S. Zhang, *J Chem Eng Data* 57 (2012) 1939–1944.
15. Z. Li, Z. Jia, Y. Luan, T. Mu, *Curr. Opin. Solid State Mater. Sci.* 12 (2008) 1.
16. Z. Duan, Y. Gu, J. Zhang, L. Zhu, Y. Deng, *J. Mol. Catal. A: Chem.* 250 (2006) 163.
17. D. Jiang, Y.Y. Wang, L.Y. Dai, *React. Kinet. Catal. Lett.* 93 (2008) 257–263.
18. Y. Zhao, J. Long, F. Deng, X. Liu, Z. Li, C. Xia, J. Peng, *Catal. Commun.* 10 (2009) 732–736.
19. K. Qiao, C. Yokoyama, *Chem. Lett.* 33 (2004) 472–473.
20. K. Qiao, C. Yokoyama, *Chem. Lett.* 33 (2004) 808–809.
21. K. Qiao, Y. Deng, C. Yokoyama, H. Sato, M. Yamashina, *Chem. Lett.* 33 (2004) 1350–1351.
22. Q. Wu, H. Chen, M. Han, D. Wang, J. Wang, *Ind. Eng. Chem. Res.* 46 (2007) 7955–7960.
23. G.A. Olah, T. Mathew, A. Goepfert, B. Török, I. Bucsi, X.Y. Li, Q. Wang, E.R. Marinez, P. Batamack, R. Aniszfeld, *J. Am. Chem. Soc.* 127 (2005) 5964–5969.
24. C. Wang, W. Zhao, H. Li, L. Guo, *Green Chem.* 11 (2009) 843–847.

25. P.K. Chhotaray, S. Jella, R.L. Gardas, *J. Chem. Thermodyn.* 74 (2014) 255–262.
26. W. Ma, W. Wang, Z. Liang, S. Hu, R. Shen, C. Wu, *Kinetics and Cataly.* 55 (2014) 665–670.
27. Y. Shao , H. Wan, J. Miao, G. Guan, *Reac Kinet Mech Cat.* (2013) 109:149–158.
28. J. Miao, H. Wan, Y. Shao, G. Guan, B. Xu, *J. of Mol. Catal. A: Chem.* 348 (2011) 77– 82.
29. A. Sharma, K. Srivastava, V. Devra, A. Rani, *Amer. Chem. Sci. J.* 2(4) (2012) 177-187.
30. W. Maa, W. Wang, Z. Liang, S. Hu, R. Shen, C. Wu, *Kinet. and Catal.* 55 (2014) 665–670.
31. M.N. Sefat, D. Saberi, K. Niknam, *Catal. Lett.* 141 (2011) 1713–1720.



ANNEXURE-

I AND II

CHARACTERIZATION TECHNIQUES

Physico-chemical properties of all catalytic materials are studied by N₂ adsorption-desorption, XRD, FT-IR and pyridine adsorbed FT-IR, SEM, SEM-EDX, TGA, UV-Vis techniques. The reaction products are analyzed by ¹H, ¹³C NMR and gas chromatography.

1. BET analysis

Specific surface area and average pore diameter of samples are determined from N₂ adsorption-desorption, done by using Thermo scientific™ surfer surface area analyzer. The samples are degassed under vacuum at 120°C for 4 h, prior to adsorption in order to evacuate the physisorbed moisture. BET analysis is done at **University of Pune, Pune**.

2. X-ray diffraction analysis

The structural features of samples are analyzed by X-ray diffraction studies. X-ray diffraction at (XRD) patterns are recorded by bruker D8 Advance diffractometer, using Ni-filter and Cu K α radiation (E= 8047.8 eV, λ = 1.5406 Å). The samples are scanned in 2 θ range of 5-75° at a scanning rate of 0.04° s⁻¹. XRD analysis has been done at **UGC-DAE CSR, Indore**.

3. FT-IR analysis

FT-IR study is executed on Bruker FT-IR Spectrophotometer (TENSOR 27) IN DRS (Diffuse Reflectance System) mode by mixing samples with KBr in 1:20 weight ratio. The spectra were recorded in the range of 550-4000 cm⁻¹ with a resolution of 4 cm⁻¹. FT-IR analysis is conducted at **Department of Pure and Applied Chemistry, University of Kota** and **MRC, MNIT, Jaipur**.

4. SEM and SEM-EDX analysis

The detailed imaging information about the morphology and surface topography is studied by scanning electron microscope (Model-JEOL-JSM 5600 and Nova Nano FE-SEM 450) . SEM analysis is done at **UGC-DAE CSR, Indore, MRC, MNIT**, Jaipur.

5. Thermo gravimetric analysis

Thermo gravimetric analysis (TGA) of the samples is carried out using NETZSCH TG 209F1 Libra TGA (209F1D-0105-L), by heating the samples in the range of 33°C to 800°C with a heating rate of 10°C per minute under a dynamic N₂ atmosphere. TGA analysis of samples is done at **CSMCRI, Bhavnagar, Gujarat**.

6. Ultra Violet-Visible spectroscopy

UV-Vis spectra in the range of 200-900 nm were measured with a LAMBDA 750 (Perkin Elmer) UV-Vis NIR Spectrophotometer. UV-Vis analysis is done at **MRC, MNIT, Jaipur**.

7. ¹H and ¹³C NMR analysis

¹H and ¹³C NMR analysis of reaction products is carried out on ECS 400 MHz (JEOL) NMR spectrometer. The analysis is done at **MRC, MNIT**, Jaipur.

8. Mechanical activation

Mechanical activation of fly ash is carried out in a high energy planetary ball mill (Retsch PM-100). As received fly ash is mechanically activated in an agate jar using 5 mm agate balls with 10:1 ball to powder ratio (BPR). The mechanical activation was done at 250 rpm rotation speed for specified time period. Mechanical activation is carried out at **Department of Pure and Applied Chemistry, University of Kota**.

9. Gas Chromatography

The products are analyzed by Gas Chromatograph (Agilent Technologies 7820A) having FID and Agilent J & W Advanced Capillary HP 5 GC Columns of 30 m length and 0.320 mm diameter, programmed oven temperature of 60-325°C and N₂ (1.5 ml/min) as a carrier gas. GC analysis is conducted at **Department of Pure and applied Chemistry, University of Kota.**

10. Rotatory evaporator

A Rotary evaporator (Heidolph G3, Germany) is used for the efficient and gentle removal of solvents from samples by evaporation. Removal of solvents and other liquid materials was carried out at **Department of Pure and applied Chemistry, University of Kota.**

LIST OF PUBLICATIONS

Research papers-

- Supported Imidazolium Based Ionic Liquid as a Green, Highly Effective and Reusable Catalyst for Microwave Assisted Knoevenagel Condensation, *Priyanka Rajoriya*, Ashu Rani, *Chem Sci Rev Lett* 2017, 6(22), 772-778.
- Imidazolium chloride immobilized fly ash as a heterogenized organocatalyst for solvent free esterification reaction using microwave, *Priyanka Rajoriya*, Ashu Rani, *Comptes Rendus Chimie* (Communicated).
- Fly supported ionic liquid [bmim]PF₆: a heterogeneous organocatalyst for benzoylation reactions under microwave irradiation, *Priyanka Rajoriya*, Ashu Rani, *Journal of Molecular Catalysis A: Chemical* (Communicated).
- Immobilization and Characterization of imidazolium based ionic liquid supported on activated fly-ash for microwave assisted esterification reactions, *Priyanka Rajoriya*, Ashu Rani, *Catalysis Today* (Communicated).
- A novel acidic ionic liquid supported on modified fly ash as heterogeneous and recyclable catalyst for acylation reactions under dielectric heating, *Priyanka Rajoriya*, Ashu Rani, *Journal of Molecular Catalysis A: Chemical* (Communicated).
- Fly supported ionic liquid 1-(propyl-3-sulfonate) imidazolium hydrosulfate : an eco approach for Friedel Craft Acylation reactions under microwave irradiations, *Priyanka Rajoriya*, Ashu Rani, *Catalysis Communications* (Communicated).

In international and national conferences/Workshop/symposium-

- Indo-Swedish symposium on **Strategic Knowledge on Climate Change** held at Department of Pure & Applied Chemistry, University of Kota, Kota Oct. 09, 2012.
- Bhabha Atomic Research Centre sponsored **Fifth BRNS-AEACI Winter School on Analytical Chemistry** at Department of Chemistry, IIT Roorkee on 3-10 Dec. 2012.
- Paper entitled **“A Facile and Environmentally Benign synthesis of Acid Activated Fly Ash As Solid Acid Catalyst and Its Catalytic Activity in Green Synthesis”** presented in National Seminar on Chemistry for Economic Growth and Human Held on August 31st, 2013 at Department of Chemistry, University of Rajasthan, Jaipur.
- National Seminar on **Socio-legal Issues and Challenges of female foeticide and Infanticide in India** held at Department of Pure & Applied Chemistry, University of Kota, Kota 4th -5th Oct. 2013.
- Abstract submission on **“A Novel Process for the Synthesis of Pure Precipitated Silica from Perlite”** in National Conference on frontiers in Physical, chemical and Biological Sciences Held during Oct. 4-6, 2013 at at Department of Chemistry, University of Pune.
- Poster presented on **“Mechanical Activation of Fly Ash By High Energy Planetary Ball Mill in** National conference on Global Environment Changes and Disaster Management for Sustainable Life on Earth A Burning Issue organized by Maharishi Arvind. College of Engineering & Technology, Ranpur kota (rajasthan) on October 21st, 2013.
- **Fifth National Academic Workshop on Organic Reaction Mechanisms & Analytical techniques used in Chemical Sciences** held on 21th and 25th Oct.2013 at Department of Pure & Applied Chemistry, University of Kota, Kota(Attended).

- Poster presentation on “ **Enhancing the Surface Properties of Fly Ash : A Solid Waste from Thermal Power Plants, by Mechanical Activation** ” in International Workshop on Green Initiatives in Energy, Environment and Health held at hotel maidens, Dehli from Dec. 2-3, 2013, sponsored by the Royal Society of Chemistry, London.
- Abstract submission on “ **Characterization of Mechanically Activated Fly Ash: A Waste from Thermal Power Plants** ” in National conference on Environment Issue and Social Concerns held during March 21-22, 2014 at Department of Social Sciences & Indian Sociological Society RC-11.
- Paper presented as first author in national conference on **Recent Advancements in Chemical Sciences (RAICS-2015)** on 23-25 August 2015 at Malaviya National Institute of Technology, Jaipur.
- An abstract accepted for oral presentation at **International Conference on Recent Trends in Chemical Science (ICRCS-17)** held on January 12-13, 2017 at P.G Department of Chemistry, Govt. Engineering College, Bikaner.
- Participated in Author Workshop on **How to Write Research Articles and Manuscript by Springer** held on 02 March, 2017 at Department of Pure & Applied Chemistry, University of Kota.
- Participated in workshop on “**LaTeX-An Efficient Documentation Tool**” held on 17-18 March, 2017 at department of computer science & informatics, University of Kota.

Research Article

Supported Imidazolium Based Ionic Liquid as a Green, Highly Effective and Reusable Catalyst for Microwave Assisted Knoevenagel Condensation

Priyanka Rajoriya and Ashu Rani*

Department of Pure and Applied Chemistry, University of Kota, Kota, 324005, Rajasthan, India

Abstract

Imidazolium chloride is synthesized by direct alkylation of 1-methyl imidazole under dielectric heating and grafted on chemically activated fly ash (CFA) using impregnation method to develop an efficient heterogeneous catalyst. The catalyst is characterized with various techniques viz. FTIR, SEM and ¹HNMR and used as environmentally benign catalysts for Knoevenagel condensations of benzaldehyde and ethyl cyanoacetate giving high product yield up to four reaction cycles without any significant loss of its catalytic activity.

Keywords: Imidazolium chloride, Direct alkylation, Knoevenagel Condensation, Impregnation method, CFA

***Correspondence**

Author: Ashu Rani

Email: ashu.uok@gmail.com

Introduction

Knoevenagel condensations of aldehydes with active methylene compounds are extensively used in the synthesis of pharmaceutical and fine chemical intermediates [1]. A wide range of homogeneous bases such as piperidine, amines, ammonia, and ammonium salts [2] and solid bases such as KF/Al₂O₃, hydrotalcite, KNH₂/Al₂O₃ and immines/SiO₂ [3-6] have been reported for catalyzing Knoevenagel condensation although have disadvantages such as difficulty in separation and reuse in case of homogeneous base and high mass transfer resistance and easy to deactivation in case of heterogeneous. Recently, Ionic liquid (IL) technology has become a need of green and sustainable chemistry, due to the remarkable properties of IL viz. nonvolatility, immiscibility with regular organic/inorganic solvents and non inflammability responsible for wide applications [7-8]. In synthetic organic chemistry ionic liquids are used as dual reagent (solvent and catalyst) in various catalytic processes [9-10]. In addition to homogeneous applications of IL, supported ionic liquid (SIL) catalysts in which thin layer of ionic liquid is immobilized on solid support material has been employed in various synthetic applications such as esterification, nitration [11], Baeyer-Villiger reaction [12], Knoevenagel condensation [13] acetalization reaction [14] Friedel-Crafts alkylation reactions [15] carbonylation [16], hydrogenation [17], Heck reactions [18], hydroaminations [19], epoxidation [20], asymmetric aldol condensation [21]. Many mesoporous materials, such as silica [22], polymers [23], and magnetic nano particles [24] etc. are popularly used as support for immobilizing ILs. In continuation, we have synthesized an innovative catalyst by immobilizing 1-butyl-3-methyl imidazolium chloride [bmim]Cl on chemically activated fly ash (FA) and used in microwave assisted Knoevenagel condensation of benzaldehyde and ethyl cyanoacetate giving industrially important product ethyl 2-cyano-3-phenylacrylate up to four reaction cycles. In previous years our laboratory has already reported several fly ash based solid acids [25-29], solid base [30] and oxidation catalysts [31] for organic transformations. This report is novel as firstly presenting chemically activated fly ash based supported ionic liquid catalyst.

Experimental**Materials and Apparatus**

Ionic liquid precursors, 1-methylimidazole (99%), chlorobutane were purchased from Sigma Aldrich. Benzaldehyde and ethyl cyanoacetate were obtained from S.D. Fine Chem. Ltd., India. Coal Fly ash [Class F type (SiO₂ + Al₂O₃) > 70%] was collected from Kota Thermal Power Plant (Rajasthan, India). The Knoevenagel condensation was

carried out in microwave synthesis system CEM, USA (Model-Discover) single mode type, closed Pyrex glass tubes (ca. 10 ml) with Teflon-coated septa. The removal of solvents was performed in rotary evaporator (Heidolph G3, Germany).

Synthesis of [bmim]Cl/CFA

A mixture of 1-methylimidazole (1.23gm, 15mmol) and chlorobutane (1.38 gm, 15mmol) was placed in microwave reactor tube and irradiated at 110 °C for 20 min at 50 psi pressure. After cooling to room temperature, the obtained yellow viscous [bmim]Cl, was thoroughly washed with diethyl ether and the solvent was removed by rotatory evaporator and dried overnight in a vacuum oven at 70 °C. The chemical activation of FA was carried out in a stirred reactor by stirring 5M aqueous solution of H₂SO₄ in the ratio of 1:2 (FA: H₂SO₄) for 24h at 110 °C. Filtered fly ash was then washed with distilled water till complete removal of soluble ionic species (Cl⁻, NO³⁻, SO₄²⁻, ClO₄⁻ further dried at 110 °C for 24h. Prior to the grafting, CFA was activated at 550 °C for 1 h and [bmim]Cl was dried at 70°C under vacuum for 1 h. The pretreated CFA (5gm) was dispersed in 50 ml anhydrous toluene, followed by taking 2gm of [bmim]Cl in a refluxing assembly under vacuum. The mixture was refluxed under N₂ atmosphere at 90 °C for 48 h. After cooling to room temperature the product was filtrated, washed with dry dichloromethane to remove the excess of ionic liquid and dried under vacuum at 70 °C for 24 h to give brown powder. The resultant solid powder is denoted as [bmim]Cl/CFA to be used as a catalyst for Knoevenagel condensation.

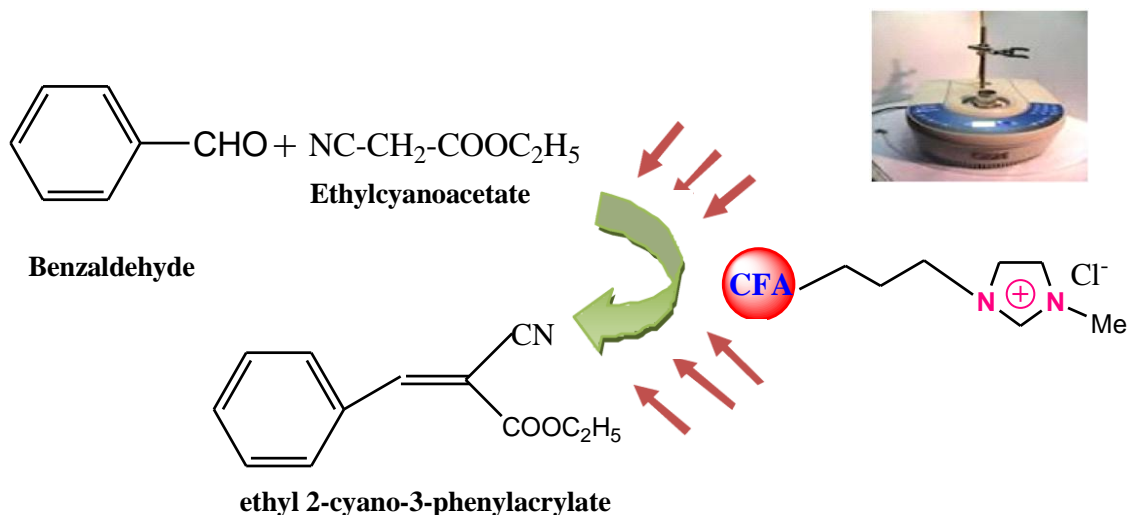
The [bmim]Cl was characterized by ¹H NMR (CDCl₃): δ = 0.71–0.78 (m, 2H), 1.25–1.33 (t, 9H), 1.85–1.91 (m, 2H), 3.40–3.52 (m, 6H), 4.11 (s, 3H), 8.26 (d, 1H), 8.34 (d, 1H), 8.53 (s, 1H)

Characterization Techniques

FTIR spectra of the materials were recorded in the range 550 – 4000 cm⁻¹ with a resolution of 4 cm⁻¹ using FTIR Tensor 27 Bruker with DR (Diffuse Reflectance) accessory. The detailed imaging information about the morphology and surface texture was provided by SEM-EDX (Philips XL30 ESEM TMP). Conversion of benzaldehyde was measured by Gas Chromatograph with an FID detector (Agilent 7820 A, HP-5 capillary column 30m×0.5mm×0.3μm).

Catalytic activity of [bmim]Cl /CFA

The catalytic activity of [bmim]Cl /CFA catalytic system was investigated by microwave assisted solvent free Knoevenagel condensation of benzaldehyde and ethyl cyanoacetate (**Scheme 1**) as a test reaction in microwave reactor. 20 mmol of benzaldehyde and 20 mmol of ethyl cyanoacetate were taken in the reactor tube. The catalyst (benzaldehyde to catalyst weight ratio = 5), activated at 70 °C for 1 h prior to the reaction in vacuum, was added in the reaction mixture and the pressurized glass vial with continuous stirring checked the vapor loss during the reaction proceeding at desired temperature and time. After completion of the reaction, the mixture was cooled at room temperature through air pump before releasing the pressure of the reactor tube.



Scheme 1 The Knoevenagel condensation of benzaldehyde and ethyl cyanoacetate

The filtered catalyst was washed with dichloromethane to remove organic impurities. The product was separated by ether. The reaction conditions were varied to obtain maximum yield and conversion to ester. The reactions were analyzed using a GC with oven temperature range 70-240 °C and N₂ (25 ml/min) as a carrier gas. The conversion of benzaldehyde and yield of product was calculated by using weight percent method [28]

Catalyst regeneration

For catalytic reusability test the spent catalyst was recovered by filtration from the initial run, washed thoroughly with dichloromethane and dried in vacuum oven at 80 °C for 24 h followed by activation at 70 °C for 1 h in vacuum oven. The regenerated catalyst was used in next reaction cycles under the same reaction conditions following the procedure described as above.

Results and Discussion

Characterization of catalyst

After chemical activation the silica content in CFA is significantly enhanced (55% to 81%) showing the loss of other components during the activation with higher concentration of H₂SO₄ [28, 29]. The FT-IR spectra of FA shows broad band in -OH region (3800–2700 cm⁻¹), which is attributed to surface OH groups, particularly of silica and the water molecules adsorbed on the surface (**Figure 1(i)**). The FT-IR spectrum of CFA (**Figure 1(ii)**) shows a significant increase in peak intensity of the band for -OH group due to increased silanol groups and adsorbed water molecules on the surface [29]. The increased amorphous silica in the activated fly ash can be characterized by an intense band in the range 1000–1300 cm⁻¹, corresponding to the valence vibrations of the silicate oxygen skeleton [32]. The main absorption band of the valence oscillations of the groups Si-O-Si in quartz appears with a main absorption maximum at 1100 cm⁻¹ [27]. Increase in silica content results in increase in the surface free silanol groups, enhancing strong hydrogen bonding between anions of IL and surface free silanols groups which stabilized thin layer of IL on the surface of CFA [33].

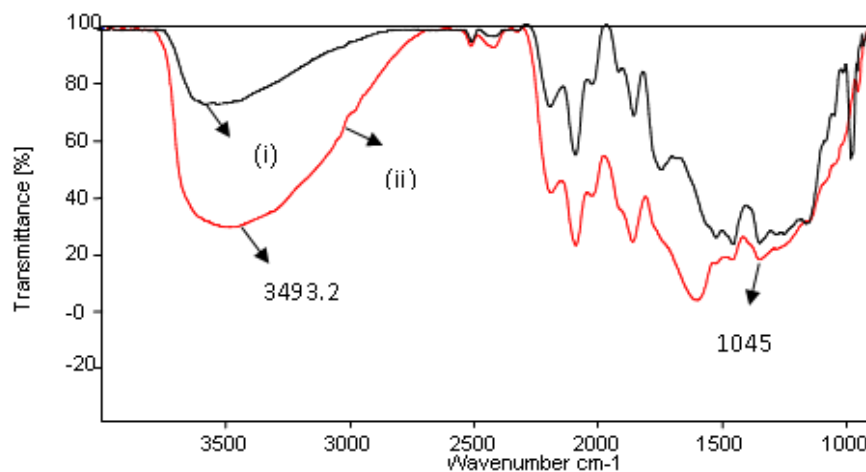


Figure 1 FTIR spectra of (i) FA (ii) CFA

The FT-IR spectrum of [bmim]Cl/CFA in **Figure 2** shows the typical strong peak corresponding to OH stretching frequency centered at about 3410 cm⁻¹, and characteristic bands observed at 1094 cm⁻¹, 1571.7 cm⁻¹, and 1636 cm⁻¹ associated with stretching frequencies of the imidazolium ring [34]. The adsorption band around 2970 cm⁻¹ assigned to C-H stretching vibration which confirms the presence of alkyl groups of ionic liquid [35].

SEM micrographs of raw FA in **Figure 3A** revealed different shaped, relatively smooth hollow cenospheres. In CFA shown in **Figure 3B** the crystalline and spherical particles break down into amorphous ones and get agglomerated. The agglomerated particles are scattered conferring the increase in surface area, which is due to increase in silica content after acid leaching. The SEM images of [bmim]Cl /CFA showed that the resulting particles are represented by irregular structures composed of large blocks with many small particles stacked together to form the bigger particles. All particles are covered by IL forming a thin layer over the surface of CFA clearly seen in **Figure 3 (D)**. The energy dispersive spectrum (EDX) shows the presence of C, Fe, Si, O, and Al and other metals in

FA and CFA samples. However the presence of high carbon (4.96%) and chloride (2.75%) in [bmim]Cl/CFA catalyst confirms immobilization of [bmim]Cl on activated surface of fly ash.

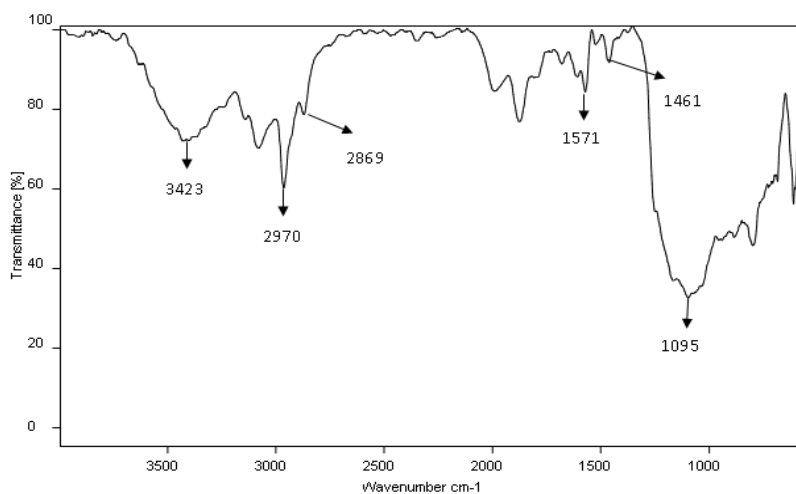


Figure 2 FTIR spectra of [bmim]Cl/CFA

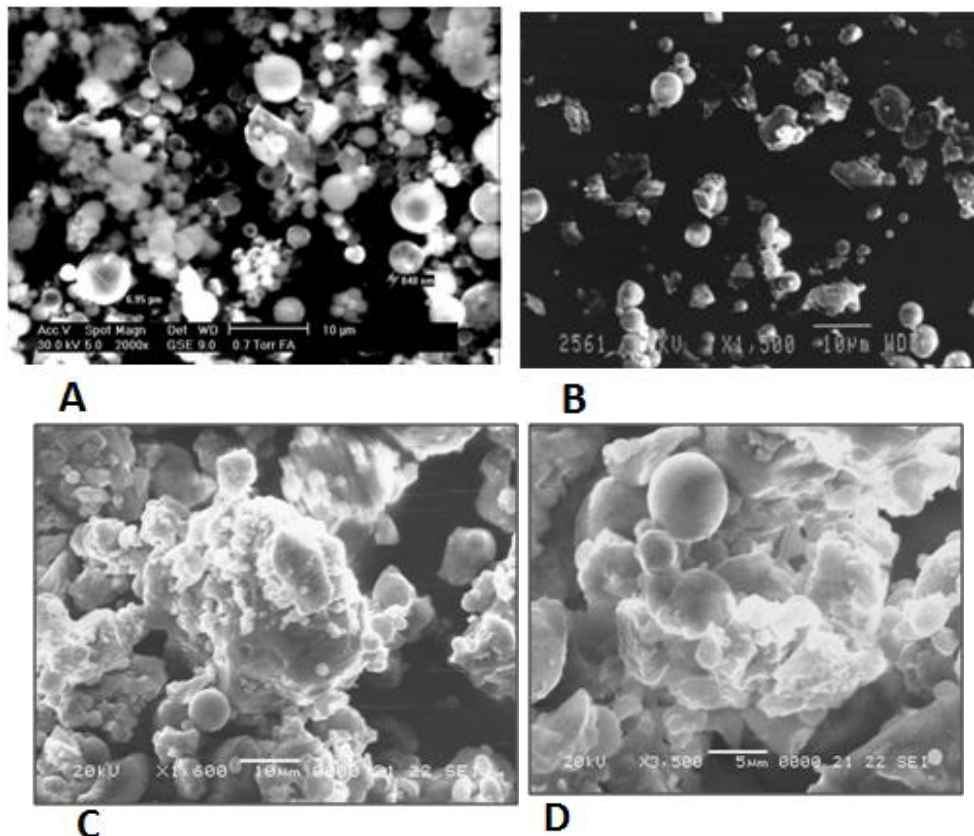


Figure 3 SEM micrographs (A) pure FA (B) CFA (C, D) [bmim]Cl/CFA and magnified image of [bmim]Cl/CFA

To evaluate the catalytic activity of synthesized catalyst, Knoevenagel condensation was performed with pure FA and CFA also, both have not shown any catalytic activity for studied reaction. [bmim]Cl/CFA catalyst showed high catalytic activity for Knoevenagel condensation of benzaldehyde and ethyl cyanoacetate resulting conversion to ethyl 2-cyano-3-phenylacrylate maximum up to 88%.

Microwave assisted Knoevenagel condensation was performed at different temperatures ranging 90 °C to 130 °C for 5 to 20 min. to optimize the reaction temperature, time, catalyst and reactants molar ratio. The results of optimization of reaction conditions for studied reaction are given in **Table 1**. On the basis of table 1 the optimal conditions were; molar ratio, 1:1 ; reactant to catalyst ratio, 5:1 ; reaction temperature, 120°C ; reaction time, 15min.

Table 1 Optimization of reaction conditions for synthesis of ethyl 2-cyano-3-phenylacrylate using [bmim]Cl/CFA as catalyst

S.NO	Molar ratio	Reactant to catalyst weight ratio	Time, min.	T/ °C	Conversion, %	Yield, %
1	1:1	5:1	15	90	61	64
2	1:1	5:1	15	100	75	78
3	1:1	5:1	15	120	88	90
4	1:1	5:1	15	130	87	89
5	1:1.5	5:1	15	120	74	76
6	1:2	5:1	15	120	60	62
8	1:3	5:1	15	120	55	57
9	1:1	5:1	5	120	45	47
10	1:1	5:1	10	120	56	59
11	1:1	5:1	20	130	88	89
12	1:1	10:1	15	120	62	67
13	1:1	2:1	15	120	74	77
14	1:1	2:1	20	130	75	78

Reusability of catalyst

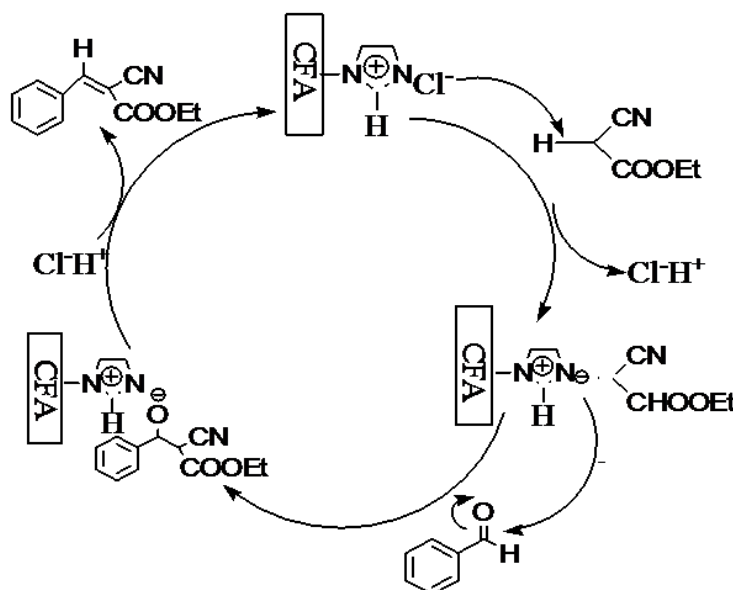
The catalyst [bmim]Cl/CFA could be used up to four reaction cycles to catalyze the reaction in high product yield (**Table 2**). The product yield was slightly decreased with increasing reuse run, which may be due to the deposition of significant amount of carbonaceous material on the surface of used catalyst that may block the catalyst active sites.

Table 2 The reusability test of [bmim]Cl/CFA catalyst

S.No.	Run	Conversion (%)	Yield (%)
1	Fresh catalyst	88	91
2	First cycle	86	88
3	Second cycle	84	86
4	Third cycle	80	84

Proposed mechanism

Reaction mechanism is based on the experimental results with reference to previous findings [36]. The plausible mechanism is schematically presented in **Scheme 2**.

**Scheme 2** Proposed mechanistic pathway of microwave-assisted condensation of benzaldehyde and ethyl cyanoacetate reaction over [bmim]Cl/CFA catalyst

The chloride anion of [bmim]Cl/CFA initiate reaction by accepting a proton from the active methylene group of ethyl cyanoacetate leading to formation of carbanion. The formed carbanion of ethyl cyanoacetate makes nucleophilic attack to the carbonyl carbon atom of aromatic aldehydes, followed by loss of water molecule to form α β unsaturated carbonyl compound.

Conclusion

The present work introduces a new, efficient and recyclable heterogeneous organocatalyst prepared by immobilization of ionic liquid on the active sites of CFA. An energy efficient elegant and fast microwave technology was employed for synthesis of ionic liquid. The resulting heterogeneous catalyst [bmim]Cl/CFA exhibited excellent catalytic activity for microwave assisted condensation reaction at optimized reaction conditions. The CFA posses high silica content and surface roughness and high concentration of free silanol groups, giving an effective solid support for immobilization of ionic liquid. This heterogeneous catalyst can be recovered and reused up to four reaction cycles giving high yield of desired product without significant loss of its catalytic activity.

Acknowledgements

The authors are grateful to Dr. D.D. Phase and Er. V. K. Ahire for SEM-EDX analysis at UGC DAE-CSR Lab Indore. ¹HNMR analyses were conducted at MNIT, Jaipur. The authors are also thankful to UGC, New Delhi, India for awarding Junior Research Fellowship to Priyanka Rajoria.

Reference

- [1] V.S.R. Pullabhotla, A. Rahman, S.B. Jonnalagadda, *Catal. Commun.*, 2009, 10, 365–369.
- [2] S. Saad Al-Shihry, *Molecules*, 2004, 9, 658–665.
- [3] M. Choudary, M.L. Kantam, V. Neeraja, K.K. Rao, F. Figueras, L. Delmotte, *Green Chem.*, 2001, 3, 257–260.
- [4] D. Bi Tian, Z. Jun, J.F. Zhu, Y.X. Shi, J.T. Wang, *Chin. Chem. Lett.*, 2004, 15, 883–884.
- [5] J.M. Clacens, D. Genuit, L. Delmotte, A.G. Ruiz, G.B. Ramon Montiel, J. Lopez, F. Figueras, *J. Catal.*, 2004, 483–490.
- [6] K.A. Utting, D.J. Macquarrie, *New J. Chem.*, 2000, 24, 591–595.
- [7] M. Picquet, D. Poinot, S. Stutzmann, I. Tkatchenko, I. Tommasi, P. Wasserscheid, J. Zimmermann, *Top. Catal.*, 2004, 29, 139–143.
- [8] B.Y. Liu, J. Han, J.F. Dong, F.X. Wei, Y.H. Cheng, *Chin. J. Org. Chem.*, 2007, 27, 1236–1243.
- [9] M.J. Earle, K.R. Seddon, *Pure Appl. Chem.*, 2000, 72, 1391–1398.
- [10] D. Zhao, M. Wu, Y. Kou, E. Min, *Catal. Today*, 2002, 74, 157–189.
- [11] K. Qiao, H. Hagiwarab, G. Yokoyamaa, *J. of Mol. Catal. A: Chem.*, 2000, 246, 65–69.
- [12] A. Chrobok, S. Baj, W. Pudlo, A. Jarzebski, *Appl. Catal. A: Gen.*, 2009, 366, 22–28.
- [13] Y. Liu, J. Peng, S. Zhai, J. Li, J. Mao, M. Li, H. Qiu, G. Lai, *Eur. J. Inorg. Chem.*, 2006, 15, 2947–2949.
- [14] R. Sugimura, K. Qiao, D. Tomida, C. Yokoyama, *Catal. Commun.*, 2007, 8, 770–772.
- [15] M.H. Valkenberg, C. deCastro, W.F. Hölderich, *Top. Catal.*, 2001, 14, 139.
- [16] A. Riisager, R. Fehrmann, Patent Application 2005/00735, 2005 (assigned to DTU).
- [17] C.P. Mehnert, E.J. Mozeleski, R.A. Cook, *Chem. Commun.*, 2002, 3010–3011.
- [18] H. Hagiwara, Y. Sugawara, K. Isobe, T. Hoshi, T. Suzuki, *Org. Lett.*, 2004, 6, 2325–2328.
- [19] S. Breitenlechner, M. Fleck, T.E. Müller, A. Suppan, *J. Mol. Catal. A: Chem.*, 2004, 214, 175–179.
- [20] K. Yamaguchi, C. Yoshida, S. Uchida, N. Mizuno, *J. Am. Chem. Soc.*, 2005, 127, 530–531.
- [21] M. Gruttadauria, S. Riela, P. Lo Meo, F. D'Anna, R. Noto, *Tetrahedron Lett.*, 2004, 45, 6113–6116.
- [22] J. Miao, H. Wan, Y. Shao, G. Guan, B. Xu, *J. of Mol. Catal. A: Chem.*, 2011, 348, 77–82.
- [23] Y. Lin, F. Wang, Z. Zhang, J. Yang, Y. Wei, *Fuel*, 2014, 116, 273–280.
- [24] P. H. Li, B. L. Li, H. C. Hu, X. N. Zhao, Z. H. Zhang, *Catal. Commun.*, 2014, 46, 118–122.
- [25] C. Khatri, A. Rani, *Fuel*, 2008, 87, 2886–2892.
- [26] N. Shringi, K. Srivastava, A. Rani, *Chem. Sci. Rev. Lett.*, 2015, 4, 561–570.
- [27] C. Khatri, M.K. Mishra, A. Rani, *Fuel Process. Technol.*, 2010, 91, 1288–95.
- [28] C. Khatri, D. Jain, A. Rani, *Fuel*, 2010, 89, 3853–3859.
- [29] A. Sharma, A. Rani, *Journal of Nanoscience and Technology.*, 2015, 1, 4–8

- [30] D. Jain, C. Khatri, A. Rani, Fuel Process. Technol., 2010, 91, 1015–1021.
- [31] Srivastava K, Devra V, Rani A, Fuel Process. Technol 2014, 121, 1-8.
- [32] C. Khatri, A. Rani, Green catalytic process for aspirin synthesis using fly ash as heterogeneous solid acid catalyst, Indian Patent No. - 1980/DEL/2007.
- [33] M. Vafaezadeha, A. Fattahi, J. Phys. Org. Chem. 2014, 27 163–167.
- [34] S. Sahoo, P. Kumar, F. Lefebvre, S.B. Halligudi, Appl. Catal. A: Gen., 2009, 354, 17– 25.
- [35] C. Yuan, Z. Huang, J. Chen, Catal. Commun., 2012, 24, 56–60.
- [36] M.N. Parvina, H. Jina, M.B. Ansaria, S.M. Oh, S.E. Park, Appl. Catal. A: Gen., 2012, 413– 414, 205– 212.

© 2017, by the Authors. The articles published from this journal are distributed to the public under “**Creative Commons Attribution License**” (<http://creativecommons.org/licenses/by/3.0/>). Therefore, upon proper citation of the original work, all the articles can be used without any restriction or can be distributed in any medium in any form.

Publication History

Received 24th Mar 2017
Revised 12th Apr 2017
Accepted 14th Apr 2017
Online 30th Apr 2017